Pattern recognition in diagnostic imaging

WORLD HEALTH ORGANIZATION
GENEVA

Pattern recognition in diagnostic imaging

Peter Corr

MBChB, FFRad (D) SA, FRCR
Professor of Radiology
Nelson R Mandela School of Medicine
University of Natal,
Durban
South Africa

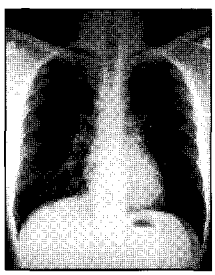

In collaboration with

Wilfred Peh, Wong Siew Kune, Leonie Munro, William Rae, Fei Ling Thoo, Lai Peng Chan, Lesley A. Goh, Lawrence Hadley, Malai Muttarak, Swee Tian Quek.

Medical Artist: Merle Conway

Photography: NV Chetty, S Ezikiel

Diagnostic Imaging and Laboratory Technology
Essential Health Technologies
Health Technology and Pharmaceuticals
WORLD HEALTH ORGANIZATION
GENEVA

WHO Library Cataloguing-in-Publication Data

Pattern recognition in diagnostic imaging / Peter Corr ; in collaboration with Wilfred Peh ... [et al.]

1.Diagnostic imaging - methods 2.Pattern recognition 3.Radiography, Thoracic -methods 4.Musculoskeletal system - radiography. 5.Radiography, Abdominal–methods 6.Manuals I.Corr, Peter II.Peh, Wilfred.

ISBN 92 4 154632 8 (NLM classification: WN 180)

This publication is a reprint of material originally distributed as WHO/DIL/01.2

Reprinted 2003 (Twice)

Designed by minimum graphics in New Zeland
Typeset by Best-set in Hong Kong
Printed in Malta By Interprint Ltd.

Contents

Preface

As modern, high technology based diagnostic imaging is moving increasingly into therapeutic medicine, and molecular imaging is becoming daily routine, it is important to remember that thousands of hospitals and medical institutions worldwide do not even have possibilities to perform the most basic examinations. Today, few other areas of medicine experience such a rapidly growing gap between what might be technically possible, e.g., what can be done in highly developed, rich countries compared to what is the reality in many less fortunate areas of the world.

As the ultimate target for the World Health Organization is to provide *Health For All*, it is with great pleasure and sincere gratitude to Professor Corr, his staff and co-authors that this book on Pattern Recognition in Diagnostic Imaging is now being published and distributed. It aims in a simple, but precise way at assisting medical professionals doing a tremendous work to save lives and reduce suffering in countries where diagnostic imaging has not yet reached the stage of molecular imaging.

We would warmly recommend that this book should not be put on a shelf or into a locker, but be used by everybody whose obligation it is to prescribe, perform, or interpret simple, but often life-saving diagnostic imaging procedures especially in locations where the presence of qualified and fully trained specialists would be a rare exception.

The book is developed and published as a WHO Document under the umbrella of the Global Steering Group for Eduction and Training in Diagnostic Imaging. For further information, please contact:

Team for Diagnostic Imaging and Laboratory Technology,
World Health Organization
20, Avenue Appia
CH-1211 GENEVA 27, SWITZERLAND

Fax: +41 22 791 4836; e-mail: ingolfsdottirg@who.int

Geneva, 30 June 2001
Harald Ostensen, MD

Foreword

Imaging is currently being performed and interpreted by radiographers/technologists and primary care physicians/hospital medical officers in many developing countries. Many primary care physicians have had little or no training in the interpretation of images, both radiographic and sonographic. Radiographers are trained in producing images but often do not have the background in medicine to interpret images with confidence. This book seeks to bridge this gap by providing images of common pathologies seen in many developing countries in a pattern format. The pattern recognition format has been used successfully by both national and international radiographic societies to educate and train radiographers working in regions where radiology advice or services are unavailable.

We hope this book serves you well in your daily work which involves imaging.

Peter Corr
Durban 2001

Authors

Lai Peng Chan MBBS, FRCR
Registrar, Department of Diagnostic Radiology, Singapore General Hospital, Singapore

Peter Corr MBChB, FFRad (D) SA, FRCR
Professor of Radiology, Nelson R Mandela School of Medicine, University of Natal, Durban, South Africa

Lesley A Goh MBBS, FRCR
Registrar, Department of Diagnostic Imaging, Tan Tock Seng Hospital, Singapore

Lawrence Hadley MBChB, FRCS (Edin)
Professor of Paediatric Surgery, Nelson R Mandela School of Medicine, University of Natal, Durban, South Africa

Wong Siew Kune MBChB, FRCR
Associate Consultant, Department of Diagnostic Radiology, Singapore General Hospital, Singapore

Leonie Munro Nat Dip Radiography (D), MA (Unisa), Dip Public Admin-postgrad (UDW), Cert for trainers (Unisa)
Chief Tutor School of Radiography, King Edward VIII Hospital, Durban, South Africa

Malai Muttarak MD
Professor of Radiology, Department of Radiology, Chiang Mai University Medical School, Chiang Mai, Thailand

Wilfred C G Peh MBBS, MD, FRCR, FRCPE, FRCPG
Senior Consultant, Department of Diagnostic Radiology, Singapore General Hospital, Singapore

Swee Tian Quek MBBS, FRCR
Consultant, Department of Diagnostic Imaging, National University of Singapore, Singapore

William Rae MBChB (Wits) PhD (OFS)
Senior Medical Physicist, Addington Hospital, Durban

Fei Ling Thoo MBBS, FRCR
Consultant, Department of Radiology, Changi General Hospital, Singapore

Definitions

ALARA keeping radiation dose 'as low as reasonably achievable'

AP anteroposterior means patient is facing the X-ray tube/beam (see PA)

Atelectasis radiographic pattern to describe (i) incomplete expansion of lungs at birth, or (ii) collapse of adult lung usually with limited re-expansion

Baud number of bytes transmitted in one second in telemedicine

Bit smallest unit of digital information

Byte a group of 8 bits used to transmit a value of character

Collapse radiographic pattern of partially or completely airless lung due to some form of obstruction

Consolidation a region of lung opacification following pneumonia with air bronchograms. Strictly a pathological term for lobar pneumonia.

CTR cardio-thoracic-ratio is the ratio of the measurement of widest transverse diameter of the heart on a chest radiograph versus the widest transverse ratio of the thoracic cage

Decubitus view patient lying on either left or right side and radiograph is taken using a horizontal X-ray beam at right angles to the cassette placed either behind the patient (PA decubitus) or in front of patient (AP decubitus)

DICOM a standard allowing interfacing of digital imaging devices with other digital devices

Digitise process to convert analogue data or images into digital data

Effusion fluid in a cavity, e.g. pleural cavity

FFD focal film distance, i.e. distance from source of X-ray beam to the film

Horizontal beam/shoot-through film taken using horizontal X-ray beam at right angles to the cassette; patient can be supine, prone, semi-erect, lateral

ISDN integrated system digital network

IVU intravenous urography

KUB plain-film-radiograph of abdomen; i.e. kidneys to bladder region

Lossless compression there is no alteration of original image after reconstruction in digital imaging

Osteopaenia decreased bone density on a radiograph.

PA posteroanterior view with X-ray beam entering from behind the patient and emerging through anterior part because patient is positioned facing cassette

Sclerosis increased bone density or opacity on the radiograph

PART 1

TECHNIQUE, QUALITY CONTROL AND RADIATION PROTECTION

CHAPTER 1

Image quality optimisation and control

Leonie Munro

Introduction

What is pattern recognition in imaging and what are the factors that impact on this recognition? Pattern recognition may be defined as being able to recognise normal anatomical and physiological appearances on an image and those variations of appearances, which may indicate pathology. This implies that certain criteria should be met, to be competent in pattern recognition. Firstly a person who performs pattern recognition should have a fair amount of expertise in medical imaging and knowledge of radiographic anatomy and normal variants so as to identify variations that may indicate pathology. This is the overarching aim of this book hence the many aspects of pattern recognition are fleshed out in the other chapters. This chapter concentrates on factors that impact on image quality. It is not easy to clearly define optimal image quality. In theory optimal image quality allows one to make accurate diagnosis. This is an ideal as we also should consider dose to patients in keeping with the ALARA principle (as low as reasonably achievable). There are times when an image is suboptimal but not unacceptable. In other words slight deviations in image quality may not have a significant impact for pattern recognition. Unacceptable images may cause one to miss a fracture or a destructive lesion. To repeat or not to repeat depends on the reasons for the examination and whether one can confidently perform pattern recognition to make a diagnosis. Such a decision is usually based on experience and a set procedure when evaluating images. Examples of unacceptable radiographs are included in this chapter to highlight the importance of optimal image quality. If an image is unacceptable then the radiation received by the patient has no benefit. Thus there are some important factors and/or basic tests that should be considered at all times.

It would be difficult to confidently perform pattern recognition if the image quality of a dynamic image or hard copy is not of an acceptable standard. There is consensus that optimal image quality entails meeting medico-legal requirements, such as each image to contain the patient's details, date of examination, anatomical marker, and adequate visualisation of radiographic anatomy/signs. This means that patient positioning should be correct for each projection, that the images are not blurred and that optimal image density is visualised. Image quality thus depends on correct radiographic techniques being used for each projection, correct selection of exposure factors and use of suitable imaging systems which are of an optimal standard. Just to mention that it is usually necessary to do two projections/views, usually at right angles. The patient/area of interest should be in accordance with recommended projections to ensure that all relevant anatomical parts are visualised (fig 1.1a). For example in skull radiography the patient's head should be straight to allow one to comment of symmetry of the skull bones (fig 1.1b). Chest radiographers should always be exposed on full inspiration to prevent incorrect diagnosis due to unacceptable radiography (fig 1.2). Apart from positioning criteria the following are considered to have an impact on image quality.

Fig 1.1a
Poor radiographic technique. Ankle and knee joints not on film.

Fig 1.1b
Poor patient positioning as skull rotated.

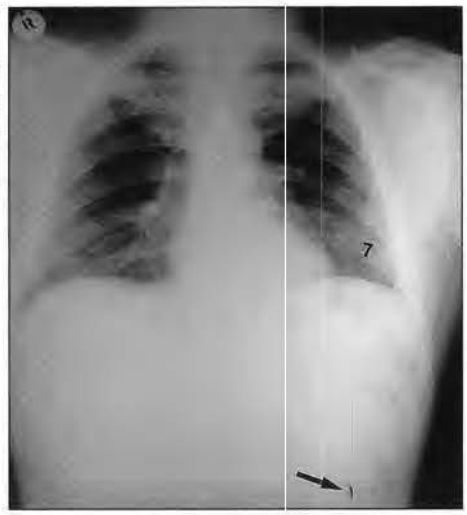

Fig 1.2
Poor inspiration PA chest as only shows 7 ribs. Arrow points to crimp mark caused by poor film handling (fingernail pressure).

Care and maintenance of imaging equipment and accessories, and some QA tests

Care and maintenance of imaging equipment is normally being promoted by national authorities to ensure that staff, patients, and members of the public do not receive unnecessary radiation doses. Well maintained equipment benefits service delivery because repeat radiographs, due to malfunctioning units, poorly calibrated generators, and so forth, decrease. This means that unnecessary dose to patients is also reduced. Many checks can be done by radiographers whilst others require sophisticated test tools which are usually expensive and/or require the expertise of physicists (Borras, 1997). Reject analysis should be carried out regularly to determine reasons for poor quality radiographs. Some basic tests can be done to minimise rejects.

Safelight tests

Unwanted film blackening is fog which reduces radiographic contrast. It is important that darkroom safelighting does not fog unexposed and/or exposed films. Safelight tests should be done at least every six months to ensure that safelights are in proper working order.

Equipment for the tests

An acceptable film/screen light-tight cassette; black paper one-half the size of the cassette (2 sheets of black paper needed), clock/timer with second hand, box of unopened radiographic film, and general X-ray unit capable of selection of low mAs.

Step 1: Switch off all lights in the darkroom and cover lights on the processor. In total darkness place an unexposed film in the light-tight cassette containing intensifying screens.

Step 2: Expose the loaded cassette to radiation to obtain approximately 1 density. Suggested exposure factors—half mAs of finger exposure (see Annexure 2—these factors are appropriate for use with 400 speed system. Should a slower system be used then mAs adjustments to be made.) Working tip: If it is not possible to select low mAs then increase FFD using the inverse square law principle to determine mAs as per FFD changes.

Step 3: In total darkness in the darkroom open the cassette and using the black paper block off half of the exposed film. NB this section of the film to remain covered during the test. The density of the covered part of the film is used to see if the safelights are functioning correctly. Place the other sheet of paper on the other half of the film and move the paper down to uncover part of the unexposed film. Switch on a safelight and expose the uncovered film portion for 60 seconds. Move this sheet of paper off the film and expose the remaining uncovered film half to a further 60 seconds.

Step 4: Process the film which has half exposed to radiation only and the other half to radiation plus light from the safelight.

Step 5: Check the density of the film (fig 1.3). The film- half that was covered throughout the test should have a density of approximately 1. Acceptable density limits when comparing the half not exposed to the safelight and the side exposed to the safelight should not exceed 0,02 for 60 seconds (Barber & Thomas, 1983: 176).

The above steps to be repeated to check each safelight in each darkroom. Should there be unacceptable density/fogging then check safelight position: correct height from working surface should not be less than 120 centimeters. Safelight filters and wattage of safelight bulbs to be checked so that the fault is then corrected. The indicator light on the processor should be checked as per the above steps. Indicator light to be uncovered and safelights switched on. Density should not exceed 0,05 for a 2 minute exposure to indicator light plus safelights.

Fig 1.3
Safelight test: 1 = film-half only exposed to radiation to obtain approximately density 1. Sections 2 & 3 = film exposed to safelight plus radiation. Section 2 exposed to safelight for 2 × 60 seconds, section 3 for 60 seconds. Both also exposed to radiation. Obvious increased density due to safelight; this exceeds 0,02 density limit compared to 1.

Careful film-handling and film storage

Note that exposed film is more sensitive to light thus care should be taken when handling film. Crimp marks from excessive handling may be of concern. A problem that has recently surfaced is that of darkroom personnel/radiographers using cell phones whilst handling film in the darkroom (fig 1.4).

Film should always be handled with clean hands and in a dust free environment. Film to

Fig 1.4 *Example of film-fogging caused by LED of cell phone in a darkroom.*

be stored in boxes in cool room with good air circulation. Boxes of film must never to be stacked on top of each other as this will cause marks on the films.

Processor control

This quality control method should be done for all processors to reduce unnecessary repeats caused by processing factors, such as exhausted chemistry, incorrectly mixed chemistry, and incorrect replenishment. Monitoring film quality due to processing factors means that assessment of film contrast, film speed and base fog is done based on an objective method.

Equipment required

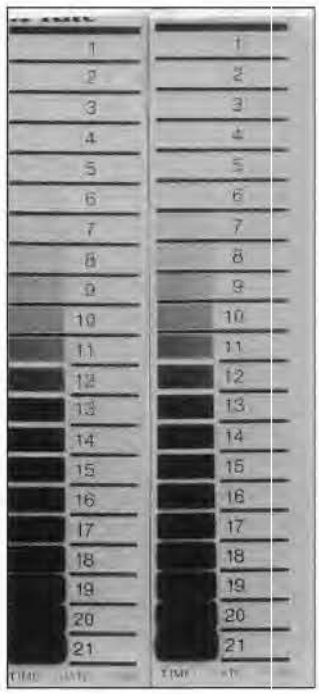

Fig 1.5 *Sensitometric strips showing steps 1 to 21.*

A sensitometer to expose film to different light intensities in steps (fig 1.5); a densitometer to measure optical density of selected sensitometric steps, a non-mercury thermometer to manually check the temperature of the chemistry, and a box of unexposed film and sheets of processing control charts or graph paper.

Step 1: Under safelight conditions expose one film to the sensitometer. It is important that blue light be used for monochromatic (blue sensitive film) and green light for orthochromatic film. Select appropriate switch on the sensitometer. Note that some sensitometer only produce blue light thus can only be used with blue sensitive film. Process film after checking temperature of chemistry as per step 2.

Step 2: Temperature of chemistry to be taken using the thermometer. Temperature gauge readings to be recorded to check with thermometer readings. This is done to ensure that the gauge is accurate.

Step 3: Process exposed film.

Step 4: Using a densitometer read densities of each step.

Step 5: The sensitometric step with the density closest to 1, 20 (mid-density) to be used to determine speed index. If sensitometric step 9 has density closest to 1,20 (including base fog) then all subsequent readings for speed index to be at this sensitometric step (ie step 9) for all future films used for processor control.

Step 6: On chart record temperature, date and base fog reading.

Step 7: Plot position for speed index obtained in the above step.

Step 8: For 5 consecutive days repeat the preceding steps to obtain average density at sensitometric step 9. This value will be the control speed index against which all future sensitometric films will be compared.

Step 9: Plot average speed index on chart/graph paper as obtained over the five days.

Step 10: Draw 2 lines above and below the speed index. One parallel line to be +0,15 of speed index and the other to be at –0, 15 from the speed index. Deviations outside these 2 lines means that there is an unacceptable processor problem. For example replenishment may have been decreased, the temperature may have decreased/ increased, and so forth.

NB: Base fog reading of each film, the date the test was done, and temperature of chemistry to be recorded on the chart. Working tip: Always do processor control at the same time.

Some firms supply pre-exposed sensitometric films but it is important to only use the film within a given period because with time film fog increases. If a densitometer is not available then do visual checks by placing the strips on an illuminator but ensure that all extraneous light is masked off and ambient (overhead) light switched off. Visual comparisons are a crude method but preferable to no checks at all. Some film suppliers have facilities to read film for customers. Suggestion: find out from film supplier whether such facilities are available. Arrangements could be made to post batches of film strips to the supplier. Recommendations: density readings to be written next to each sensitometric step on each film then this should allow one to compared with visual comparisons. However the proper method of processor control should where possible be used for valid objective testing to enhance processor control results which enables speedy problem solving (fig 1.6a, 1.6b).

- ***Film-screen contact test***

It is essential that images be obtained with good film-screen contact. Poor film-screen causes loss of information which may cause inaccurate pattern recognition. The film-screen contact test tool is readily available but a bit expensive. To perform the test place the contact mesh tool (wire mesh encased in perspex) on the top of the suspect cassette containing an unexposed film. Centre to center of cassette, collimate to cover cassette. Make sure that table on which the cassette is placed and the central ray are at right angles. Expose the test tool using approximately 55–60 kVp and 4 mAs (for 200 speed system) and 100 cms Focal film distance. Process the film and view at a distance of 150–180 cms to evaluate the sharpness of the wire mesh. Poor contact is seen as a "blurred" outline (fig 1.7). Poor film-screen contact usually occurs when a cassette gets dropped when excessive force is used during handling.

- ***Collimator-beam alignment test***

This test should be done at least every month to check proper alignment of collimator and primary beam as daily use of the collimator contributes to poor alignment of the light beam and primary beam. This in turn causes suboptimal positioning as it may be difficult to accurately centre as per routine techniques.

Equipment for the test

35 × 43 cassette or smaller l loaded with unexposed film. Four coins/steel washers and metal clips/allan keys. Lead markers (L & R).

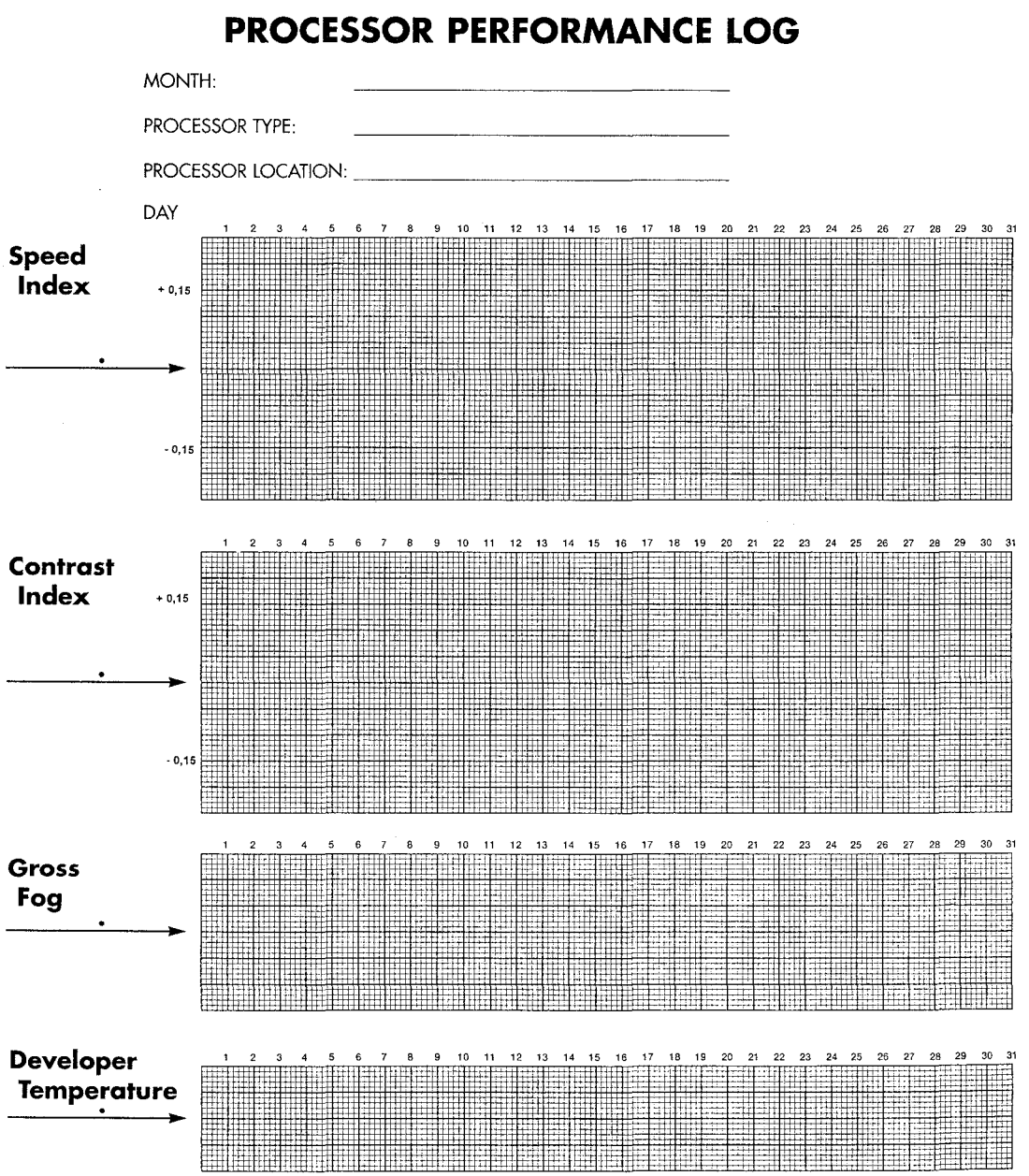

Fig 1.6a
Example of blank graph paper for processor monitoring.

Steps for the test

Place the cassette on the table and centre primary beam to center of cassette. Open light-beam diaphragms to set measurements—suggest 30 × 30 cms (note readings on the scale). Ensure FFD is at 100 cms or higher. Record this measurement. Place a coin in each corner of the light square and place a metal corner clip/allan key exactly at the edge of each corner. Position L or R marker at center of beam. Expose the cassette: suggest 50 kVp and 4 mAs for 200 speed system. Process the film (fig 1.8). The suggested performance criterion is –+2% of source to image distance. If FFD is 100 cms then upper limits of difference between light field edges and edges of primary beam radiation visualised on the film should not exceed 2% of 100 cms .ie 2 cms (Borras, 1997: 253). This will entail measuring the area of light beam based on position of the

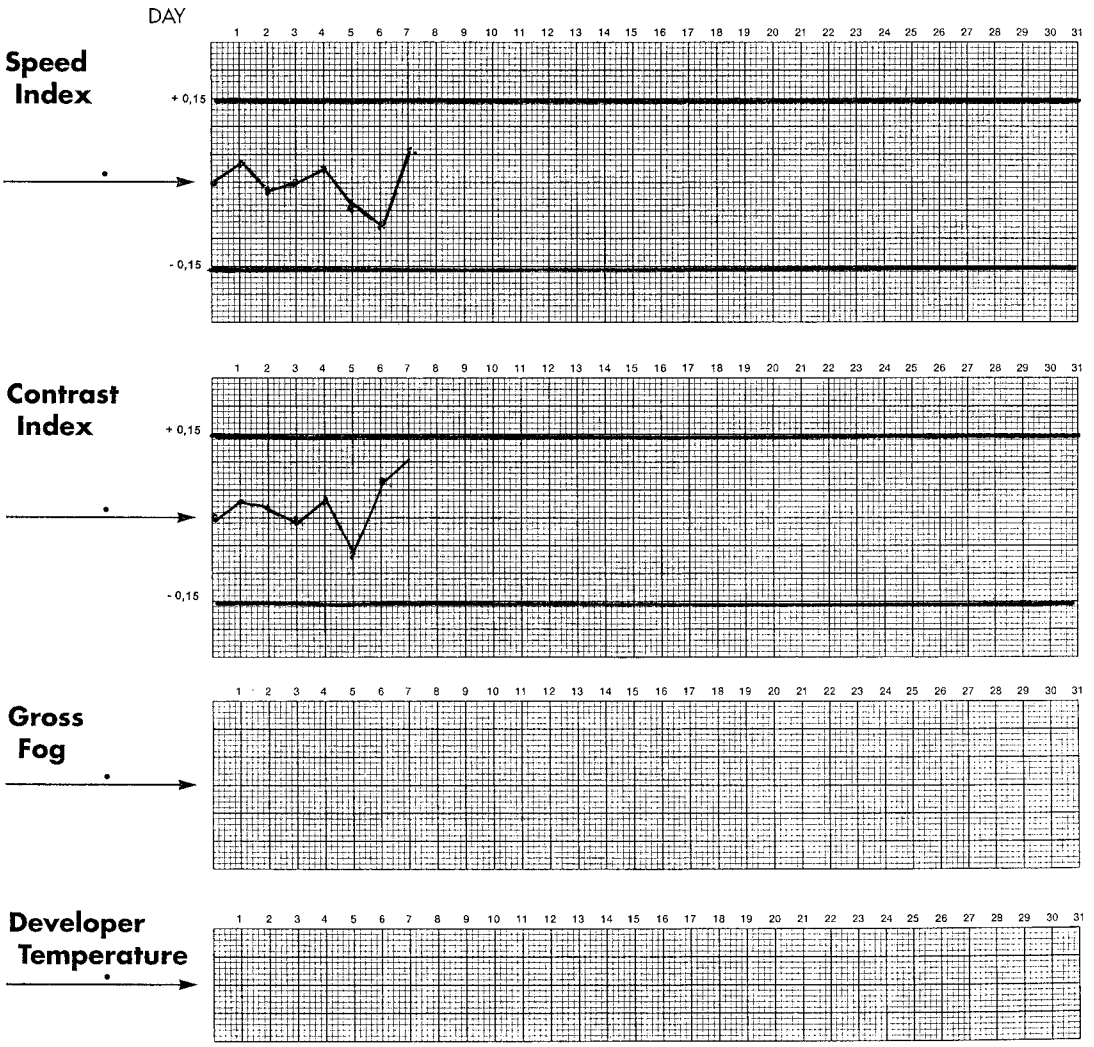

Fig 1.6b
Parallel lines above and below speed and contrast indices.

coins and metal clips and then comparing this measurement with total area of film-blackening to establish performance criteria.

- ***Test to check alignment of beam***

This simple test can be done by placing a cassette loaded with an unexposed film on the table. Reduce lateral diaphragms to a slit. Close the other diaphragms. Centre to cassette and expose using 60 kVp and 4 mAs. Close these diaphragms and open the others to a slit and expose again. Process the film and bend in half to check that exposed "cross" (fig 1.9) is in the middle of the film. If there is not proper alignment check that the tube is straight so that the primary beam is vertical at 90 degrees to the cassette/table top. This test can also be used alignment of central ray to the bucky tray.

Factors relating to contrast and sharpness of the image

Contrast refers to the difference in density (film blackening) of two areas. To put it simply an image that only has two densities/tones will have high contrast as it only has a short scale such as a black/white image. Long scale contrast occurs when the

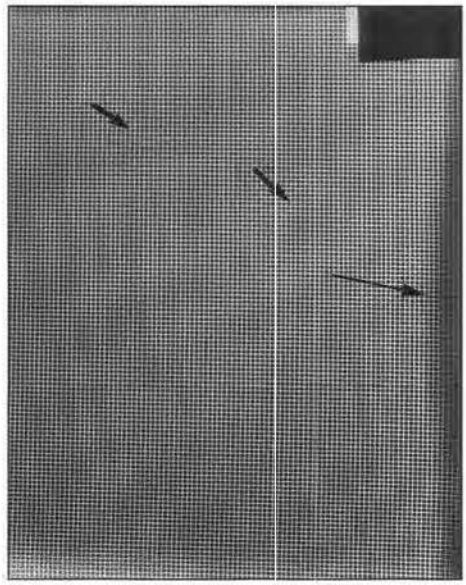

Fig 1.7
Film-screen contact test: arrows show areas of poor contact.

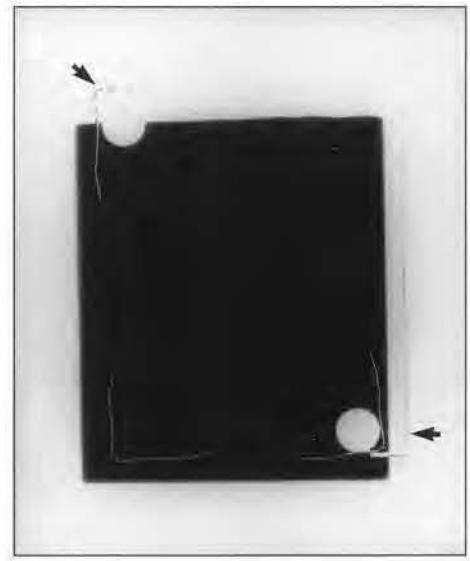

Fig 1.8
Two fields do not match; arrows show actual light-beam edges. Difference within the acceptable range of not more that 2% of FFD.

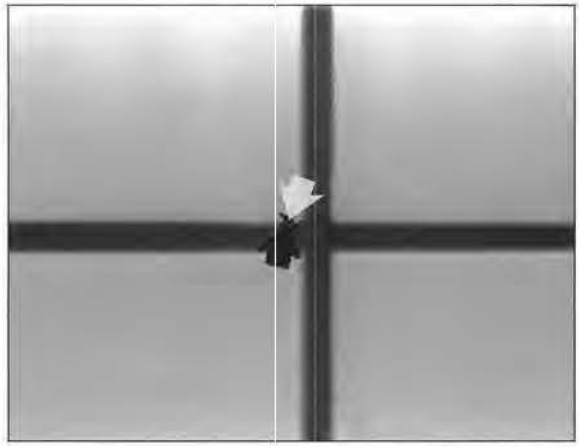

Fig 1.9
Arrows indicate middle of film; cross and film-centre not aligned.

difference in densities is not very marked; we perceive shades of grey. This means that at times a short scale contrast image may be needed for diagnostic purposes. A typical example is soft tissue thighs to visualise low density calcification for query cysticercosis. Kilovoltage selection of approximately 65–75 is usually recommended for visualisation of renal size, shape, and position. On the other hand >110 kVp is required to adequately visualise the gastric-intestinal-tract when doing contrast studies. Chest radiography should always be performed using moderately high to high kVp (fig 1.10a–1.10g).

Image sharpness refers to the amount of detail that we can see when viewing an image. Good film-screen contact enables high image sharpness. Detail screens are used to visualise fine detail but this results in additional dose to the patient due to mAs adjustments (fig 1.11 and fig 1.12).

- There are several factors that effect contrast and sharpness. Image contrast is broadly divided into three categories: subjective, subject/patient, and objective. Image sharpness is dependent upon geometric factors, movement factors, and systems factors. The most important factor influencing contrast is kilovoltage. Some radiographers make use of a fixed Kv and adjust mAs to suit different types of patients and/or pathology. Most modern units have automatic exposure devices which are programmed for the various anatomical regions. What one has to consider is dose to patients thus it should be borne in mind that high mAs selections result in the patient receiving additional radiation. Selection of the fastest film-screen

Fig 1.10a
Lateral view of femur a bit over-penetrated for visualisation of soft tissue but image acceptable.

Fig 1.10b
AP supine abdomen (control) of 10 year male patient for barium enema. Note lack of gonad protection. Exposure selection not based on ALARA as low kV and high mAs (70kVp, 40mAs) used.

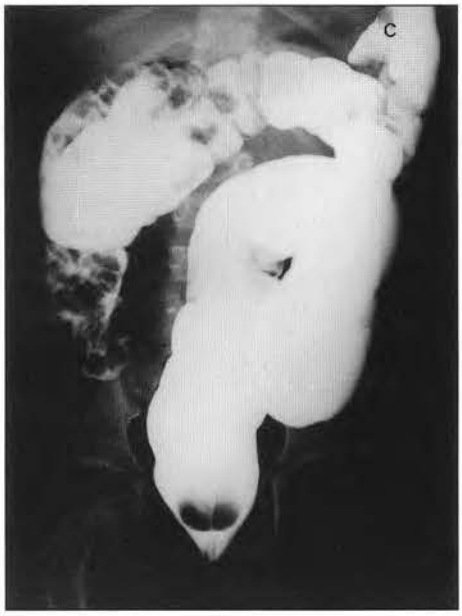

Fig 1.10c
AE film of same patient; again no gonad protection and inappropriate exposure selection.

Fig 1.10d
Delayed AE of same patient. Radiograph taken by different radiographer who applied ALARA principles, gonad protection, 88 kV used and mAs decreased accordingly to 5 mAs. Note improved visualisation of large bowel patterns due to long-scale contrast image.

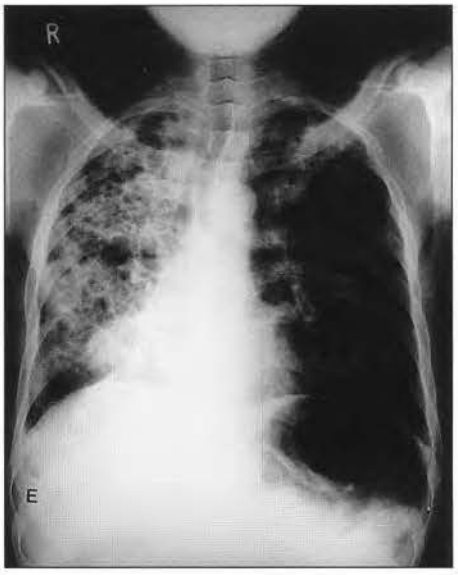

Fig 1.10e
Too much mAs used for the chest hence lung markings not demonstrated.

Fig 1.10f, g
PA chest of same patient. Film (f) taken using 75 kV. Film (g) taken using 110 kV and 4 mAs. Note improved visualisation of entire lung-field's and good inspiration.

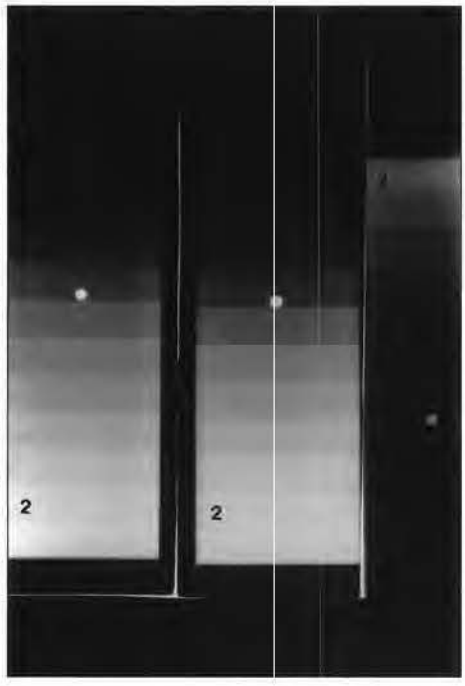

Fig 1.11
Example of different densities of calibrated step-wedge. Step-wedge of Right not same as the other two. Note ball-bearing taped on step 8 to make it easy to align similar density steps. On right step 4/5 aligned to match steps of the other two. Right step-wedge of a fast system thus if system on Left is used then mAs has to be adjusted as per scale in Figure 1.13.

combinations will reduce dose but one may not see fine detail. The deciding factor should be the reason for the examination paying attention to ALARA. Careful positioning should be practiced with appropriate exposure factors to produce an image with film blackening within the useful density range. A dark image is unacceptable as is a pale image (fig 1.12).

Factors influencing mAs selection include: FFD as per the inverse square law, speed of imaging system, collimation of the primary which reduces scatter/secondary radiation thus contrast is improved, and use of secondary radiation grids. It is necessary to increase mAs when reducing the area of the primary beam (coning) to compensate for loss of film blackening caused by scatter. Grid exposures require an increase in mAs based on the grid ration. For example a 8:1 grid ratio has a grid factor of 4 (half of 8) thus the mAs has to multiplied by 4 when moving from non-grid to grid technique. Grids improve contrast but reduce image sharpness as the distance between the patient and film is increased. The output of the generator also influences mAs selection, eg single phase unit requires more mAs than a high output generator. A simple method to establish difference is to perform a stepwedge test as described in this chapter (see page 14). Contrast is high when images are produced using single phase units as the overall kV is less than the selected kV. The benefits of higher output generators far outweigh the loss of contrast as such units enable use of low mAs settings, short exposure times, and a range of kV selections allowing the use of moderately high to high kv techniques to reduce dose to patients in keeping with the ALARA principle.

Fig 1.12a, b, c
Range of unacceptable images. Insufficient kV used for lateral spine (a); poor patient positioning for peg view as C1/2 not demonstrated due to overlying occiput (b); not true lateral view for scapula plus insufficient kV used (d).

NUMBER FOR EXPOSURE (mAs) ADJUSTMENT

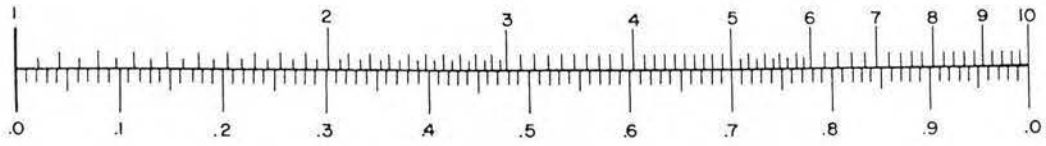

MANTISSA OF LOGARITHM

Practical use of a stepwedge to determine mAs adjustment when comparing 2 different speed systems. Note if 4 step difference then log = 0,304 then antilog = 2.

Fig 1.13
Scale for determining logarithms to calculate adjustments to mAs for different speed systems.

- Subjective contrast includes how tired one is when viewing an image, the brightness of the illuminator (viewing box), and the brightness of surrounding light. Where possible illuminators should be kept clean and have the same intensity and light colour. Images should be viewed in a room which has subdued lighting.
- Subject/patient contrast includes selection of kVp (exposure factors), the thickness of the part being imaged, use of contrast media, and scatter-secondary radiation. If we require an image with high contrast/short scale then low kVp factors are selected but when a long scale image is important then high kVp should be used.

Determining mAs adjustments: stepwedge tool

A calibrated aluminium stepwedge is a basic useful tool as it can be used to establish mAs adjustments when using different speed systems.

• *Method*

Expose each system with same film type if determining different speed of intensifying screens. The same factors should always be used. For example 70 kVp and 5 mAs at 120 cms FFD. NB never use less than 0,1 second exposure time to allow the screens to respond to the quanta to emit light (ie to minimise reciprocity failure). Process the films. Place the films edge to edge on a horizontal view box and mask all unwanted light areas. Visually compare the steps and adjust to align with a selected step. It makes it easier to do if a metal ball-bearing is taped to the middle step of the wedge (see fig 1.11). If there are 4 step differences obtained when using a calibrated step-wedge with a calibration factor of 0,076 at 70 kVp, 5 mAs and at 120 centimetres FFD. then the logarithm value is $4 \times 0{,}076 = 0{,}304$ (fig 1.13) The exposure factor for mAs adjustment can be determined by reference to a table of logarithms, by use of a slide rule (D and L scales) or by reference to the scale at the back of the step-wedge (if supplied) or by the above figure. Note that the antilogarithm of 0,3 is 2. The mAs would have to be halved if moving from a slow to faster system or vice versa.

The step wedge method may be used to check output of units. ideally the resultant stepwedges should be the same density for a specific unit. Should there be differences and if the processing factors are optimal then this information could be useful when communicating with the firm/repair technician. Making use of a calibrated stepwedge to regularly check output of units saves money and time. This tool produces crude results but is inexpensive.

Optimal image quality requires careful positioning, regular maintenance and care of equipment, and careful selection of exposure factors. The acid test being that one is confident when engaged in pattern recognition.

References

1. Ballinger PW. 1998. Merrill's atlas of radiographic positions and radiologic procedures. St Louis: Mosby Year Book.
2. Bontrager KL & Anthony BT. *Textbook of radiographic positioning and related pathology.* Second Edition. St Louis: CV Mosby Company.
3. Clifford MA & Drummond AE. *Radiographic techniques related to pathology.* Third Edition. London: Wright PSG.
4. Freeman M. 1988. Clinical imaging: an introduction to the role of imaging in clinical practice. New York: Churchill Livingstone.
5. Goldman M & Cope D. *Radiographic index.* Eighth Edition, London: Wright PSG.

6. Swallow RA, Naylor E, Roebuck EJ & Whitley AS. *Clark's positioning in radiography.* Eleventh Edition. London: William Heinemann Medical Books, Ltd.

7. Barber TC & Thomas JM. 1983. *Radiologic quality control manual.* Reston: Prentice-Hall Company.

8. Bluth EI, Havrilla M & Blakeman C. 1993. Quality improvement techniques: value to improve the timeliness of the preoperative chest radiographic report. *AJR*, 160: 995–998.

9. Borras C. Editor. 1997. Organisation, development, quality assurance and radiation protection in radiology services: imaging and radiation therapy. Washington DC: PAHO/ WHO.

10. Gould R & Boone JM. 1996. Syllabus: categorical course in physics: technology update and quality improvement of diagnostic imaging equipment. Oak Brook: RSNA Learning Center.

11. Pizzutiello RJ & Cullinan JE. 1993. *Introduction to medical radiographic imaging.* Rochester: Eastman Kodak Company.

12. Smit KJ. 1996. *Proposed regulations and the role of quality control in diagnostic radiology.* Bellville: Directorate Radiation Control, Department of Health, South Africa.

13. Thornhill PJ. 1987. Quality assurance in diagnostic radiography: are we using it correctly and what is the future? *Radiography*, Vol 53, No 609: 161–163.

14. Ball J & Price T. 1990. *Chesneys' radiographic imaging.* Oxford: Blackwell Scientific Publications.

15. Burns EF. 1992. *Radiographic imaging: a guide for producing quality radiographs.* Philadelphia: WE Saunders Company.

16. Curry TS 111, Dowdey JE & Murry RC. 1993. *Christensen's introduction to the physics of diagnostic radiology.* Philadelphia: Lea & Fabiger.

17. Stockley SM. 1988. *A manual of radiographic equipment.* London: Churchill Livingstone.

18. Wilkes R. 1985. *Principles of radiological physics.* London: Churchill Livingstone.

CHAPTER 2

Radiation protection in radiological practice

William Rae

X-ray production

The radiation emitted from X-ray units while taking X-rays is photon radiation, and these photons are known as X-rays. They are generated when high energy electrons, accelerated by a high voltage potential difference, strike a target in the X-ray tube and their energy is converted to photons which radiate out from the target. The energy of the electrons, and hence the resultant photons, is expressed in terms of thousands of electron volts (keV). Photon energies used in diagnostic radiology are in the range 20 keV to 150 keV. These photons have enough energy to cause ionisation, resulting in deposition of energy in the irradiated material. This energy deposition results in a reduction in the number of photons in the beam, and the beam is said to be "attenuated" by the absorbing material. The amount of energy absorbed differs for materials of different density or atomic composition. The differential absorption of X-rays between different structures, allows the creation of the contrast that is seen on X-ray films, and is diagnostically useful.

When a patient is exposed to an X-ray beam a large amount of radiation is also produced in other directions. Much of the radiation entering the patient is scattered and exits the patient in all directions. Some of the photon energy is lost during the scattering process, so the scattered photons are of a lower energy than the primary photons. For most radiographic procedures only about 1 to 10% of the primary beam emitted from the X-ray tube actually interacts with the detector system. (This excludes the photons absorbed by the casing and collimators of the X-ray tube). The rest of the energy is lost due to scatter or absorption in the patient. With newer, and more efficient, detector systems, less radiation is required to produce diagnostic quality images. This reduces exposure to the patient.

Biological effects of X-ray radiation

The damaging (negative) effects of X-rays were noticed soon after their discovery. Early workers were initially unaware of the associated risks and thus took no precautions against being exposed to the X-ray beam whilst imaging patients. Skin damage and induced cancers were soon attributed to the extreme overexposures experienced by early radiation workers. As a result, efforts to understand and limit the negative biological effects have been made since the very early years of diagnostic radiology. Most of the information about the negative effects of radiation comes from nuclear power plant accidents, atomic explosions, radiotherapy patients, and radiation workers.

The biological effects of X-ray radiation are due to the ionisation that occurs when photon energy is deposited in living tissue. Intracellular water is ionised producing free radicals that can damage either the genetic material of the cell in the DNA of the chromosomes, or the intracellular organelles. The resultant effects are related to the amount of radiation absorbed by the tissues.

Negative effects associated with X-ray radiation

The intracellular damage that takes place after exposure results in two main categories of effects. Either the damage to the cells results in immediate effects, which may result in progressively worsening function and eventually cell death, or the damage to the cell's genetic content allows it to live and reproduce, but ultimately result in cancer after some delay period. The risk of seeing both these types of effects increases with increasing radiation exposure to the individual. The direct damage effects are only seen above some relatively high threshold level of exposure and they worsen as the dose increases. The chance of getting cancer though is low, but can be induced by low amounts of radiation. Cancer induction is an all or nothing effect, and there is a statistical chance that it will occur. The chance of occurrence is proportional to the amount of exposure.

Rapidly dividing cells are more sensitive to radiation effects, and the most sensitive tissues are thus gastrointestinal tract, gonads, bone marrow, and skin. The tissues most susceptible to radiation induced malignancy are bone marrow, bowel mucosa, breast tissue, gonads and lymphatic tissues.

The foetus is most susceptible to radiation at about 20 to 40 days post conception, and microcephaly and mental retardation are the most likely effects, followed by an increased incidence of cancer in childhood.

Quantification of radiation dose

The amount of radiation delivered to an object (or person, or tissue) can be quantified as the energy (joules), deposited per unit mass (kilogram), of whatever is being exposed to the radiation. The specific SI unit for radiation dose is the gray (Gy), which is defined as one joule per kilogram. Different biological tissues respond differently to different types of radiation and to account for this a biological weighting factor is used. The SI unit of biologically effective dose is the sievert (Sv). This is also measured in terms of joules per kilogram, but accounts for the biological response of the particular tissue being irradiated.

Radiation protection regulations

Regulations have been developed internationally over many years to control the amount of exposure that is allowed, and thus to minimise the incidence of radiation effects. The latest relevant publications are ICRP Publication 60, printed in 1990, and titled *1990 Recommendations of the International Commission on Radiological Protection,* and the *International Basic Safety Standards for Protection Against Ionizing Radiation and for Safety of Radiation Sources* jointly published in 1996 by the WHO, IAEA and other international Organizations.

The "Alara" principle

The guiding principle used in all these documents is that radiation doses to the public, and to people who work with radiation, must be kept As Low As Reasonably Achievable (ALARA principle). The effect of radiation at very low doses is still debated and the ALARA principle is adopted to avoid radiation exposure as much as possible, knowing that the risk of negative effects from small amounts of radiation approach those seen in the general public for those same negative effects.

Protection regulations

Equivalent dose is the sum of all doses from different types of radiation to an organ in an exposed person. Effective dose is the sum of the weighted equivalent doses, and is the

Table I. *Occupational dose limits*

Application	Occupation dose limit	Public dose limit
Effective Dose	20 mSv per year, averaged over 5 yrs, and not more than 50 mSv in any year.	1 mSv per year.
Equivalent Dose: Eyes	150 mSv per year	15 mSv per year
Equivalent Dose: Skin	500 mSv per year	50 mSv per year
Equivalent Dose: Hands	500 mSv per year	–
Pregnant Women Workers	2 mSv to the surface of the woman's abdomen for remainder of pregnancy	As for members of the public

dose that gives an indication of the overall effect of the exposure to the person. This is the dose that is limited by the regulations. A radiation worker is defined as a person who works with radiation, and may potentially exceed 30% of the prescribed dose limits.

The regulations impose limits on the radiation doses that may be received by radiation workers and the general public. The dose limits are all set to a level that will reduce the risk of effects to below some arbitrary acceptable level. This level is conservative and the result is that the radiation profession is one of the safest fields of work, if the rules are properly followed.

Dose monitoring of radiation workers

Radiation workers should be monitored at all times when working. The reason for monitoring is to ensure that the practices being followed by the workers in their daily routine are safe and do not result in high doses being received. If monitoring is not done then unsafe practices will not be noticed and excessive exposures to staff may result.

Personnel monitoring is normally the responsibility of national authorities. They should supply pre-packed thermoluminescent dosimeters, which are returned for automatic readout on a monthly cycle. The dosimeter should be worn on the torso and under any protective lead clothing being worn. All radiation workers should wear their own dosimeter at all times during working hours. If the monthly limit exceeded, the responsible radiation protection officer should be informed and a report should be required.

It is good practice to set a local action limit at some lower level then the national level so that the practices in the department are appropriate to the local conditions. Doses above the allowed local limit could be followed up in an attempt to rectify any practices resulting in increased doses to staff. A record should be kept of all radiation doses recorded for all radiation workers.

Recommendations for pregnant radiation workers

Pregnant radiation workers should not work in areas where there is a risk of getting more than 30% of the allowed whole body limits for radiation workers. They should wear an alarm radiation monitor at all times. They should not be allowed to work with fluoroscopy, theatre radiography, mobile X-ray units, or interventional radiography.

X-ray doses to patients

The skin dose delivered during X-ray investigations has been reduced over the years with the introduction of newer technology equipment using more sensitive detectors and better shielding, but the ability to deliver large doses of radiation very quickly and easily during examinations has also increased. Generally the doses given are lower than

Table 2. *Typical effective dose equivalent values for radiological examinations*

Procedure	Effective dose equivalent in mSv
PA chest X-ray	0.01-0.05
Skull X-ray	0.1-0.2
Abdominal X-ray	0.6-1.7
Barium enema	3-8
Head CT	2-4
Body CT	5-15
Nuclear Medicine	2-10

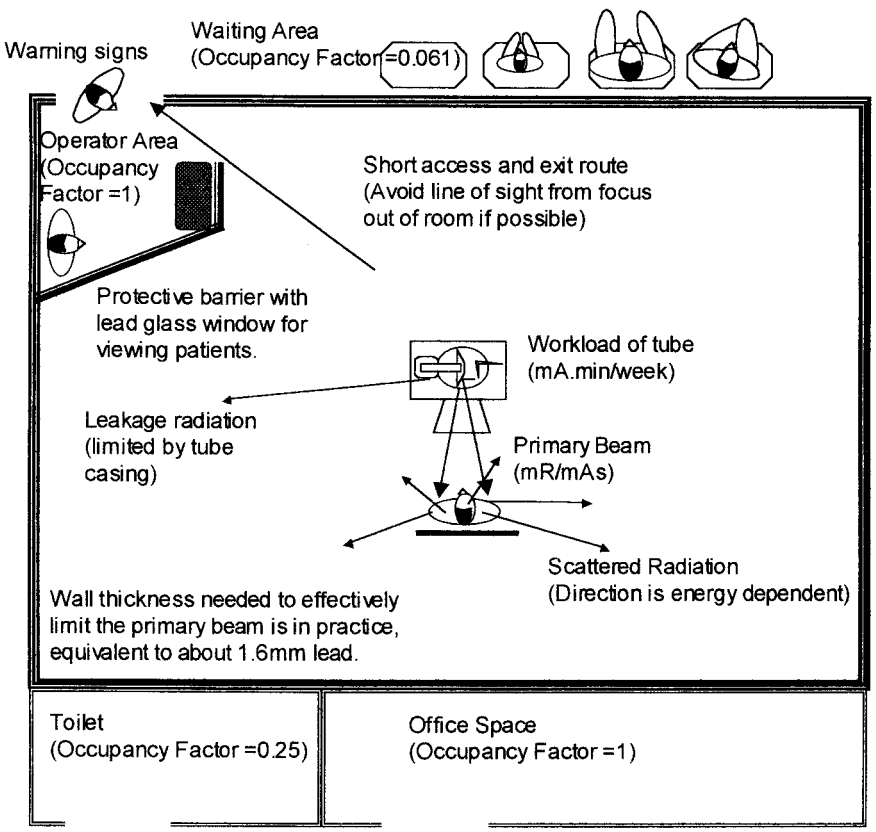

Fig 2.1
A typical layout of a X-ray suite, showing some of the safety aspects that must be considered when designing a room to be used for taking X-rays. Barrier thicknesses are designed to ensure that exposures are within acceptable limits. Workloads and occupancy factors are used in the calculation of the required thickness of the protective barriers.

the threshold for deterministic effects, but interventional radiology, and similar long procedures, can result in epilation (>3000 mSv), and erythema (>5000 mSv). The doses to patients should be minimised wherever possible, and the following good practices are advised:

1. Only image patients if there are good clinical grounds for doing the procedure.

2. Only image the area required. Proper collimation minimises risk.

3. Gonadal shielding should be used in people of reproductive age.
4. Imaging of pregnant patients should be avoided when medically possible. If the last menstrual period has been missed then the patient should be assumed pregnant.
5. Minimise repeat examinations by using good radiographic practice.
6. Increase the focus skin distance to reduce the entrance dose.

In general the risk of radiation injury from X-ray examinations is far less important than the clinical benefit being derived from doing the examination. The availability of X-ray units has resulted in a marked increase in the medical radiation dose being delivered to the population as a whole. This medical exposure should be limited if possible.

X-ray suite design

The design of a X-ray room takes into account the expected doses in the room and surrounding areas. The dose calculation takes into account occupancy, workload, X-ray energy, beam direction, shielding materials used, and other relevant factors.

Practical ways to minimise radiation doses

Radiation dose increases with decreasing distance from the source ($\propto 1/\text{distance}^2$), time of exposure ($\propto$time), intensity of the radiation beam ($\propto$intensity), and the inverse of the thickness of any absorbers between the source and the exposed person ($\propto \exp^{-\mu.\text{thickness}}$).

To reduce the dose to radiation workers the following practices should be adhered to:

1. The distance from the source of the radiation must be increased as much as possible. One way to encourage this is to mark distances from the source on the floor of the X-ray room.
2. The time of exposure should be decreased, and workloads should be shared as much as possible. If it is not required to be present during exposure then leave the room.
3. Protective shields should be used and worn by workers during exposure. Standard lead aprons, lead gloves and thyroid shields substantially reduce the effective dose for most diagnostic examinations. Lead glass shields can also be used to protect the eyes.
4. The primary source of radiation should be collimated as much as possible. For example the smallest fields possible should be viewed when doing fluoroscopy.
5. Controlled access to areas where radiation exposure may be taking place is required. Suitable radiation warning signs should be displayed at entrances to rooms and on any radiation source.

If the above simple principles are applied and all attempts are made to keep the radiation doses to staff and patients "as low as reasonably achievable" (ALARA), then the risks from exposure to radiation in an X-ray department should be minimal.

CHAPTER 3

Contrast media in imaging

Peter Corr

Purpose of contrast media

Contrast media are used in imaging to opacify normal structures including the vascular system, collecting system of the kidneys and the lumen of the gastrointestinal system to obtain further diagnostic information about focal lesions in the body.

How do they work?

Vascular contrast media contain 50% by weight of molecular iodine which absorbs X-rays via the photoelectric effect and appears white on X-ray film. Oral agents consisting mainly of barium works on the same principle.

What are they?

Vascular contrast agents are iodinated organic compounds that are very hydrophilic and have a low lipid solubility and low binding affinity for proteins and membranes. Most agents have a molecular weight of less than 2000 (*1*). On intravascular injection they are rapidly distributed into the extravascular space but do not enter the intracellular spaces. They are rapidly excreted by normal kidneys some 90% within two hours. They do not cross the blood brain barrier.

What do I need to know to use them safely?

Vascular contrast media are not drugs like antibiotics and are pharmacologically inert. However even though they are very safe when injected intravenously or intraarterially, they can have side effects and complications. Before you use them you must be familiar with their side effects and how to manage them.

Side effects can be classified into allergic idiosyncratic reactions and non idiosyncratic reactions (*1*). Allergic reactions are the most serious and unpredictable reactions to contrast media. Reactions occur immediately or within 5 minutes of contrast injection. Patients with a history of allergy and atopy, for example hay fever or asthma, are 8 times more likely to have allergic reactions than non-allergic patients. These reactions are not dose dependent and are due to a release of vasoactive molecules such as histamine and kinins.

Non idiosyncratic contrast reactions are due to direct contrast toxicity which is dose dependent. Patients with renal failure or renal impairment from dehydration, diabetes or multiple myeloma are especially susceptible. Newborns and elderly patients are less able to excrete contrast media hence are more likely to have nephrotoxic complications.

Complications of contrast media

Although idiosyncratic reactions are unpredictable, prevention is the best policy. Whenever a contrast injection is performed a resuscitation trolley should be close by in the same room. It must have an "Ambu bag" for ventilation, airways, ECG monitor, oxygen cylinder as well as the following drugs: adrenaline, hydrocortisone, IV fluids,

chlorpheniramine and bronchodilator spray. It is mandatory that the trolley is checked weekly and that all the drugs are in stock. **Do not use intravenous contrast agents without being fully trained in cardiorespiratory resuscitation.**

Complications

Complications are divided into: minor, intermediate, major or life threatening and death.

- **Minor complications** include nausea, facial flushing or a warm sensation and urticaria. These complications usually disappear within 15 minutes and only require reassurance. It the symptoms persist an injection of 10 mg of an antihistamine intramuscularly, such as chlorpheniramine, should cure the allergic effects.
- **Intermediate complications** include bronchospasm and hypotension. These complications respond to reassurance and an inhaled bronchodilator such as salbutamol, intravenous hydrocortisone 100 mg bolus and **intramuscular** adrenaline 0.3–1.0 mls of 1 in 1000 solution.
- **Severe life threatening reactions** include seizures, severe bronchospasm and laryngeal oedema, pulmonary oedema and cardiovascular collapse. These reactions require urgent treatment. The airway must be secure and intravenous access established. Adrenaline 0.3–1.0 ml of a 1 in a 1000 solution by intravenous injection is the most effective drug to treat anaphylaxis. Death following contrast injection is extremely rare.

Reference

1. Grainger R. Intravascular Contrast Media. In: *Diagnostic Radiology: A textbook of medical imaging*. 1997. Eds Grainger R, Allison D. Churchill Livingstone, Edinburgh.

CHAPTER 4

Digital imaging and telemedicine

Peter Corr

Digital imaging

A digital image consists of a matrix of numbers or digits that when processed by a computer will produce an image on a monitor. Digital information is stored as bits, with 8 bits forming a byte that represents a value or character.

Digitization is the process of acquiring or converting analogue images into a digital format. Many imaging modalities acquire the image initially in this format, for example with CT, MR and ultrasound. All images today can be converted into digital format. The advantages of digital imaging are the ease of storing images and the ease of transmitting images and manipulating the images during image interpretation. You no longer have to rely on finding the radiographs! It is important to be aware of the disadvantages. Digital imaging hardware is expensive to purchase and to maintain. Long term storage of digital images is especially expensive. Given these challenges, there is no doubt that as computer processors and storage devices become less expensive, many hospitals in developing countries will use digital imaging in the future. Each medical image is stored as a file on the computer. The file can be compared to the X-ray packet of a conventional radiograph. The files vary greatly in their size or number of bytes they contain. Chest radiographs when in digital format consist of 2 Mbytes (2 million bytes) while an ultrasound or CT scan may be 10 times smaller at 200 Kbytes in size. Generally plain analogue radiographs when in digital format have much larger files than more modern imaging investigations, such as ultrasound or CT imaging.

Teleradiology and telemedicine

Telemedicine is the electronic transmission of medical images from one site to another for interpretation and consultation. The concept of telemedicine is not new and was first used in the 1950s. However with the development of more reliable and cheaper electronic communication and computers, telemedicine is becoming more accessible to many developing countries.

Goals of telemedicine

The goals are threefold:

i. to provide consultation and interpretation of images in regions of need,

ii. to provide specialist services in hospitals without specialist support

iii. to promote educational opportunities for doctors working in rural hospitals.

Advantages and disadvantages

There are many advantages. Specialist advice is available without the patient having to travel to the regional or city hospital. Better utilization of specialist resources is made at the regional hospital. Travel and accommodation costs are reduced for patients who are less likely to be referred to the regional hospital after telemedical consultation.

Telemedicine can be used to provide continual medical education programmes to doctors working in rural areas. Disadvantages of telemedicine include: high initial capital costs of hardware, staff training, requires a good telecommunication network, and patient confidentiality is more difficult to maintain.

Applications in telemedicine

Telemedicine has been successfully used in radiology, ultrasound, surgery, opthalmology, pathology and dermatology. In imaging it has been used for plain radiographs, CT, MR, ultrasound, angiograms and nuclear medicine.

Image acquisition

Analogue images such as radiographs have to be digitised using a digitiser which currently is the most expensive component of the system. Most radiographs such as a chest radiograph produce large files of up to 2 MB in size which takes a few minutes to digitise. The data are usually compressed using a lossless algorithm to reduce the transmission time.

Image transmission

Conventional telephone lines found in many developing countries have very slow transmission rates however but are inexpensive to transmit data (around 12 kb/sec). This means that a chest radiograph will take 3 minutes to transmit. Integrated services digital network (ISDN) lines which are available in certain countries are twenty times faster than conventional copper telephone lines, in the region of 256 kb/sec. Satellite communication is obviously wireless technology and is very fast but very expensive and not freely available in many countries.

Image display

To read images at the receiving station high resolution monitors are recommended. The American College of Radiology recommends 2000 × 2000 × 12 bit resolution as a standard (*1*). These monitors are very expensive and not freely available. The monitors must be sufficiently bright to see all levels of grey scale in medical images. Most images can be interpreted using 1000 × 1000 × 8 bit resolution which are much cheaper.

Image files

Each image is kept in its own file. Static ultrasound, CT and MR images are relatively small compared to radiographs: 100 kilobytes versus 2 megabytes. The larger the file the longer transmission time.

Problems with teleradiology

Most teleradiology systems will have limited spatial resolution and subtle lesions in the lungs and fine bone fractures can easily be missed unless the original radiographs are reviewed later (*2*). As faster computer systems and digital telephone lines become available limited spatial resolution should become less of a problem. The high capital costs of equipment and limited opportunities to train health professionals in some countries are a barrier to the development of telemedicine services in some developing countries (*3*). WHO is looking into the development of telemedicine services as a way of providing imaging services to rural clinics and hospitals in developing countries.

LEARNING POINTS: DIGITAL IMAGING AND TELEMEDICINE

- Digital imaging is the process of acquiring, storing, transmitting and interpreting medical images in a digital format
- A digital format is when images are stored as a matrix of numbers or digits and can be processed by a computer to produce a medical image on the image
- Files contain an image in digital format
- Files are measured in the amount of digital data they contain in bytes
- Plain radiographs contain the largest amount of data while CT and ultrasound contain the least data
- Transmission of digital images depends on the transmission rate of the communication system used (in bauds)
- Good spatial resolution of the monitors is necessary to interpret images is extremely important

References

1. American College of Radiology: *Telemedicine Standards*, 1994. Reston, Virginia.
2. Corr P. Teleradiology in KwaZulu Natal: a pilot project. *SAMJ*, 1998;88:48–49.
3. Blignault I, Kennedy C. Training in Telemedicine. *J Telemed Telecare*, 1999;5:S112–4.

PART 2

CHEST IMAGING PATTERNS

CHAPTER 5

The normal chest radiograph

Peter Corr

Understanding the anatomy of the chest is critical in interpreting chest radiographs. Only by reading many normal chests will you be able to detect abnormalities. It is important to develop a routine system and to keep to it.

Soft tissues

The soft tissues of the chest consist of the skin, muscle, fat and fascial planes of the chest wall. There are a number of "companion" shadows to bones such as the clavicles. The breast shadows and axillary folds should be symmetrical (figs 5.1a, 5.1b & 5.2).

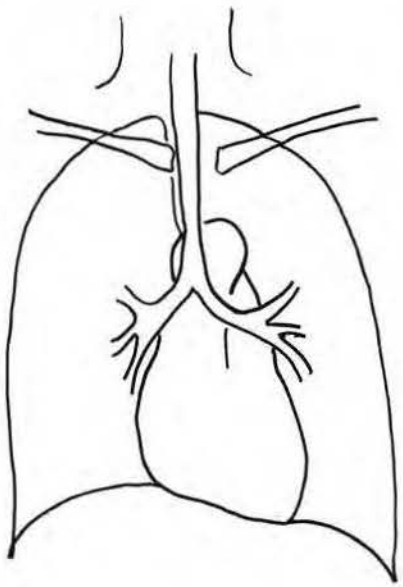

Fig 5.1a
Normal adult male chest.

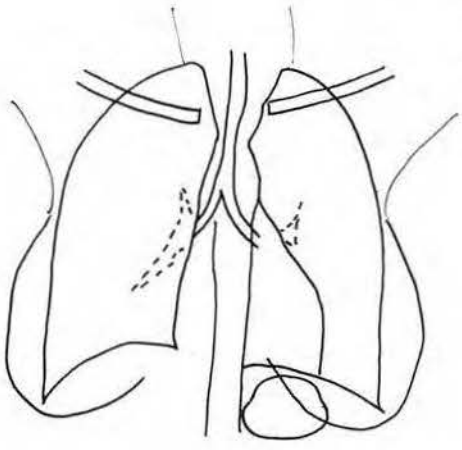

Fig 5.1b
Normal adult female chest.

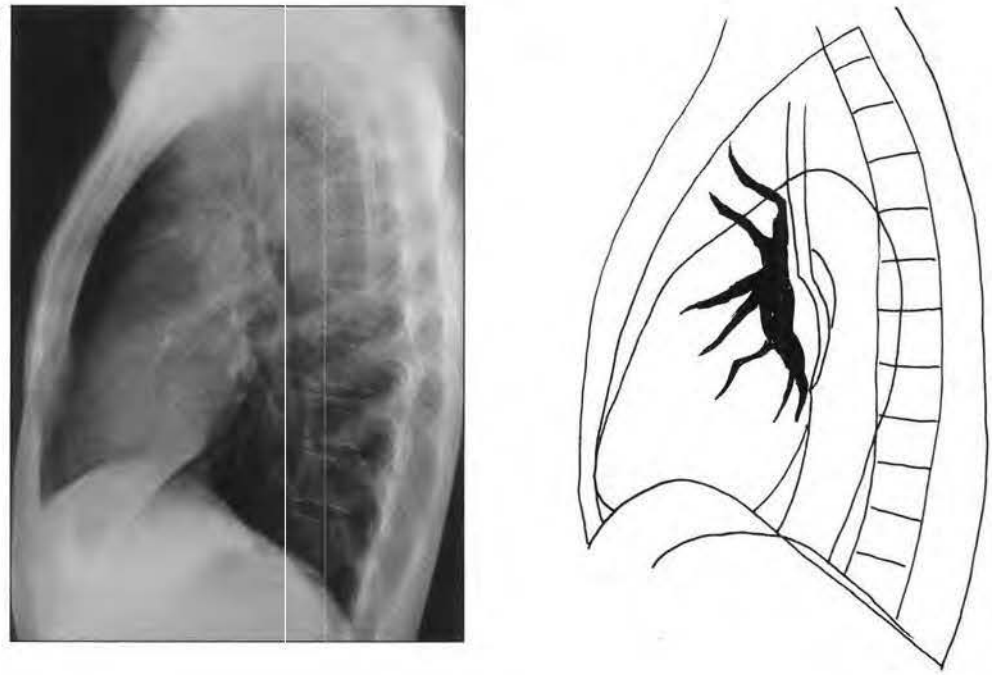

Fig 5.2
Lateral adult chest.

Skeleton

There are 12 ribs which can be traced from their posterior attachment to the spine to their anterior costochondral junctions. The anterior cartilaginous region ossifies especially in women and must not be confused with calcified lung lesions. The 11th and 12th ribs are shorter and do not articulate anteriorly with the sternum. Imaging of ribs requires both PA or AP chest views plus localised oblique views. The clavicles articulate medially at the sternoclavicular junction. This joint is difficult to visualise on PA films. Dislocation or subluxation can therefore be easily missed. Laterally the clavicle articulates with the acromion of the scapula. The sternum consists of two bones; the manubrium superiorly and the body of the sternum which articulate at the manubriosternal junction. The sternum is best imaged obliquely or laterally (fig 5.3).

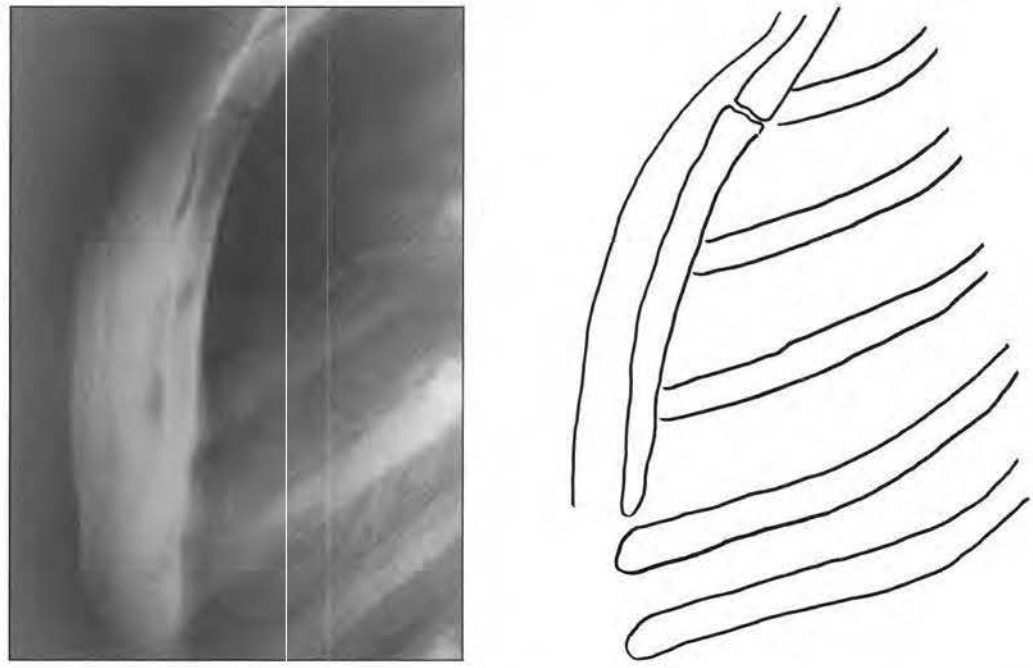

Fig 5.3
Lateral sternum.

The cervical spine normally has 7 vertebrae, the thoracic 12 vertebrae. Normally the spine has a slight thoracic kyphosis and cervical lordosis. The lower cervical and thoracic spine is visualised best using a high Kvp technique (>120 Kvp).

Mediastinum

To understand the anatomy it is best to think of the mediastinum in the following compartments:

Superior mediastinum

This is the compartment superior to a horizontal plane passing through the aortic arch. It includes the trachea, oesophagus, lymph nodes, superior vena cava and brachicephalic artery on the right, left subclavian artery, recurrent laryngeal, phrenic and vagal nerves. With age there is widening of the superior mediastinum as the arteries dilate, however the contour is maintained.

Anterior mediastinum

This region is bounded superiorly by the superior mediastinum and posteriorly by the middle mediastinum. It is best visualised on the lateral chest radiograph. It includes the thymus in infants which appears like a sail, lymph nodes and mediastinal fat. The thymus is important to recognise and not to confuse with a pathological lesion.

Middle mediastinum

This region contains the heart, pericardium, lymph nodes, tracheobronchial tree and carina, and the hila regions. The right atrium and right ventricle comprise the anterior half of the heart, with the posterior half composed of the left atrium and ventricle. The carina is where the trachea bifurcates into the left and right main bronchi with the right main bronchus being much steeper than the left. Surrounding the carina and in the hila are numerous lymph nodes which have a maximum diameter of 10 mm. The hila are slightly different on each side. The left hilum is located 2 cm superior to the right. The reason for this is the left main pulmonary artery ascends and curves over the superior border of the left main bronchus while on the right, the right main pulmonary artery is located anterior to the right main bronchus. The pulmonary veins enter the hila posteriorly. It is important to understand the hila anatomy so as not to be confused between pulmonary aneurysms and tumours in this region.

Posterior mediastinum

This compartment contains the descending thoracic aorta, the oesophagus, nerves, lymph nodes and paraspinal fascia. The descending aorta is located anterior and to the left of the thoracic spine with the oseophagus situated between them.

Heart (figs 5.1a, 5.1b & 5.2)

The heart is situated within the middle mediastinum with in the pericardium. On PA and AP chest radiograph one third of the heart is to the right of the thoracic spine, two thirds to the left of the spine. On a lateral chest the anterior border of the heart is comprised of the right atrium and right ventricle; the posterior border is comprised of the left atrium and ventricle. It is important to be able to recognize the normal frontal contour of the heart.

Lungs

It is important to remember than the right lung with its three lobes, is different from the left with two lobes. The greater or oblique fissures separate the right upper and middle lobe from the lower lobe and the left upper from the lower lobe. The fissures are best seen on a lateral chest radiograph as thin white lines, the right fissure being steeper than the left. The lesser or horizontal fissure separates the right upper from the right middle lobe and extends from the right hilum to the chest wall. The pulmonary arteries and veins extend out from the hila and are visible to the outer one third of the lungs. The veins tend to be more lateral than the arteries but often cannot be distinguished apart on plain radiographs.

Diaphragm

The diaphragm consists of three parts: the right hemidiaphragm, the central tendon, and the left hemidiaphragm. The right hemidiaphragm is 3 cm superior to the left due to the presence of the liver inferiorly. The hemidiaphragms are muscles under control of the phrenic nerves. The diaphragm inserts peripherally into the costal margin and thoracic wall at the costophrenic angles. The diaphragm may be scalloped as a normal variant.

Pleura

The pleura is a thick fibrous layer consisting of a parietal pleura and visceral pleura. The visceral pleura covers the lungs while the parietal pleura covers the inner surface of the chest wall. Usually the pleural space is a potential space only. The normal pleural surface cannot be visualised using radiographs.

Chest radiography

Good radiographic technique is critical for producing diagnostic chest X-rays. **Important points to remember are:**

- **Exposure factors**—a high kV >120 technique is important to improve visualization of the soft tissue planes of the mediastinum and tracheobronchial tree. The pulmonary vessels are well visualised with this technique.
- **Size and shape of the chest**—exposures will vary depending on the size and shape of the chest.
- **Good inspiration is critical.** You should aim to visualise at least 11 ribs posteriorly above the diaphragm. Poor inspiration will result in difficulties in measuring heart size and assessing the lungs.
- **Patient positioning**—the PA position is best. AP and supine films will result in difficulties in assessing cardiac size and pulmonary vasculature. Check that the patient is not rotated by checking that the medial edges of the clavicles and the spine are equidistant.

Technique

The patient should stand erect with the anterior chest wall flat against the bucky/cassettte with the hands on the hips and the elbows rotated forwards, The X-ray tube should be more than 1 m from the cassette and centred at the T3 level.

How to read a chest radiograph

Try to develop a systematic method and keep to it. Start peripherally and read towards the centre of the chest

1. Soft tissues: compare both sides. In females check both breasts shadows are present. Look for focal soft tissue calcification and subcutaneous gas.
2. Skeleton: count all ribs. Check for focal lesions such as metastases (lytic or sclerotic) and fractures. Check clavicles, shoulders, cervical and thoracic spines.
3. Lungs: compare both sides. Divide the lungs into three zones: upper, middle and lower and compare both sides.
4. Diaphragm: the right hemidiaphragm is 2 cm superior to the left. Compare the shape and position. Look for free air beneath the diaphragm.
5. Hilar regions: the left is 2 cm superior to the right. Check position, contour and density
6. Mediastinum: check the position with two thirds of the transverse diameter of the heart to the left of the spine and one third to the right. In the superior mediastinum the trachea should be central anterior to the thoracic spine.
7. Heart: check size (normally <50% CTR), position and contour.
8. Pleura: normally invisible. Check costophrenic angles for pleural fluid and pneumothorax.

Chest patterns

Clinical information

To improve diagnostic specificity always take a relevant history from the patient. Ask the following questions:

How long have there been symptoms, such as cough?

Is there haemoptysis?

Is there chest pain?

Is there shortness of breath?

Important clinical information includes:

Does the patient have a fever?

Is the patient immunosuppressed or HIV positive?

Is the patient taking any drugs? eg. antibiotics or chemotherapy?

Is the patient exposed to any occupational dusts?

CHAPTER 6

Pulmonary infection

Peter Corr

Most pathological processes involving the lungs will cause increased density of the lung and appear white or appear as focal opacities.

Pneumonia patterns

Pneumonia is air space consolidation in which the alveolar air space is filled with inflammatory exudate from the infection. Pneumonias can be classified both anatomically and by aetiology. Anatomical classification is useful as certain patterns have specific causes, for example lobar pneumonia is often due to streptococcal pneumoniae. Age is also important to consider as childhood pneumonias have a different appearance and cause from adult infections. The presence of immuno-suppression from human immunodeficiency virus (HIV) infection has complicated these patterns in many developing countries.

Lobar pneumonia pattern

Pneumonia is airspace opacification of a lung lobe. The alveolar air spaces are filled with inflammatory exudate while the bronchi and bronchioles remain patent. The cause is often strep. pneumoniae. The pattern to identify is opacification of the pulmonary lobe with the presence of air bronchograms which appear like the branches of a leafless tree (fig 6.1). Air bronchograms are the patent air containing bronchial tree, which is surrounded by airspace opacification. Once you see bronchograms these are diagnostic of lobar pneumonia. The important differential diagnosis is lobar atelectasis where there are no air bronchograms as the bronchus is usually obstructed and the air in the distal bronchus is reabsorbed (fig 6.2).

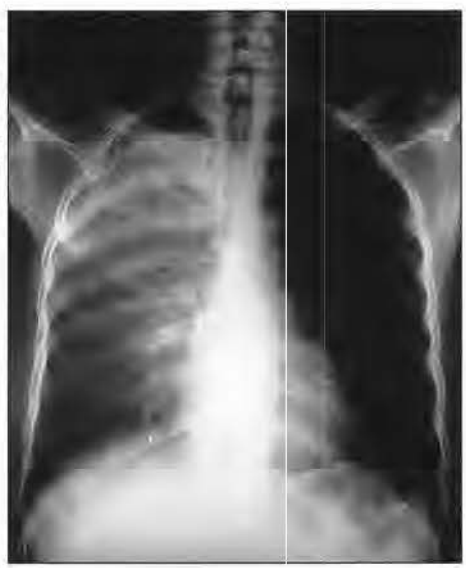

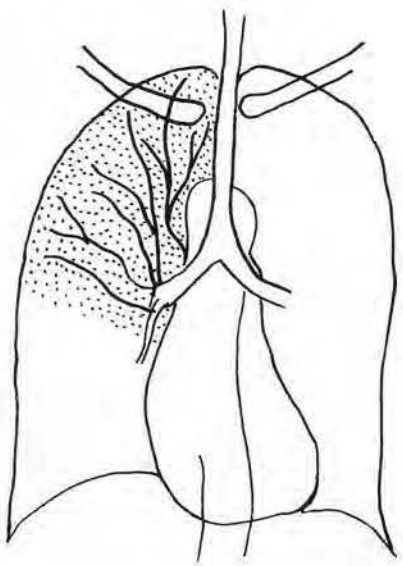

Fig 6.1
Right upper lobe pneumonia from strep. pneumoniae infection with lobar opacification and air bronchograms (arrow).

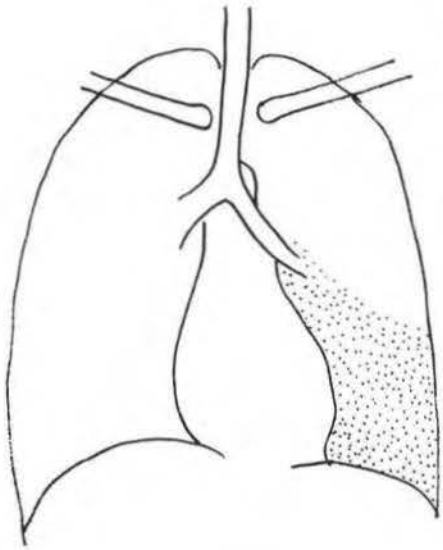

Fig 6.2
Left lower lobe atelectasis from obstruction of the left lower lobe bronchus. Note absent air bronchograms and slight volume loss.

Fig 6.3a
Right middle lobe pneumonia demonstrates loss of the right heart border (arrow). This is called "loss of the silhouette" sign.

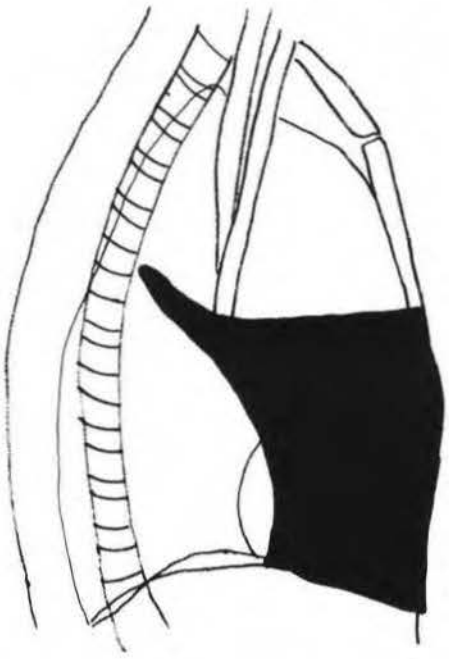

Fig 6.3b
Lateral chest demonstrates the right middle lobe pneumonia.

To localize a lobar pneumonia anatomically, the loss of the silhouette sign can be used. Right middle lobe pneumonias will cause the right heart border to disappear (figs 6.3a, 6.3b) and lingula left upper lobe pneumonias result in loss of visualisation of the left heart border. In lower lobe pneumonias either hemidiaphragm will be not be visualised.

Bronchopneumonia pattern

In this pattern there is multifocal peribronchial opacification bilaterally. This pattern is common in childhood infections. The cause of the infection is often viral or following mycoplasm infection.

Cavitating or necrotising pneumonia (fig 6.4)

Necrotising pneumonia pattern occurs when there is extensive necrosis of lung tissue. Cavities form, which may have multiple fluid levels. Common causes are infections from klebsiella, bacteroides and pseudomonas bacteria. The clue to this pattern is the presence of a cavity within the pneumonia. The differential diagnosis includes cavitating cancer (usually a squamous primary or secondary) and tuberculosis.

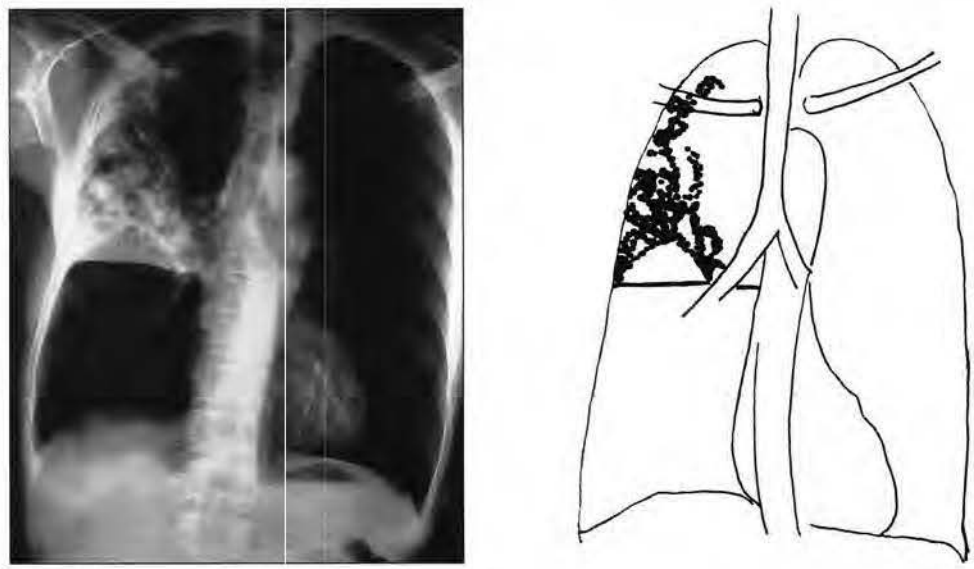

Fig 6.4 *Cavitating right upper lobe pneumonia from klebsiella infection.*

"Ground glass" pneumonia pattern (fig 6.5)

This pattern is often difficult to recognize initially, however the clue is the pulmonary vessels appear ill defined or "fuzzy" and the lung appears slightly opaque. No air

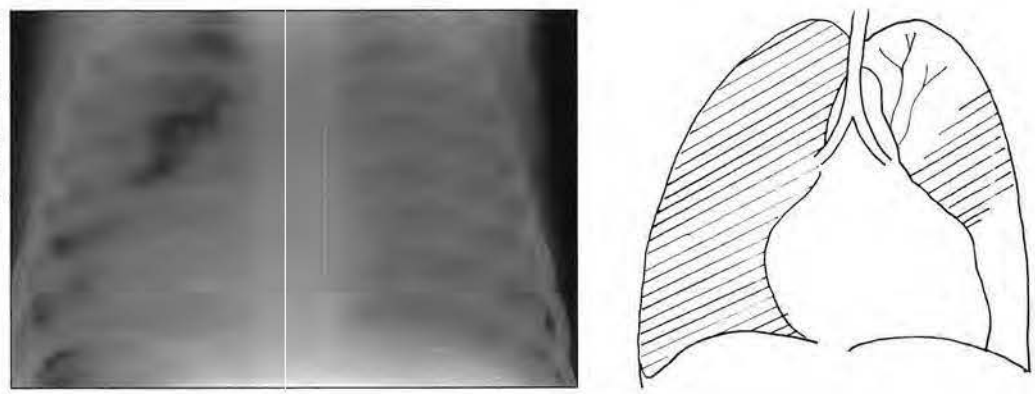

Fig 6.5 *Chest radiograph demonstrates "ground glass" opacification in an HIV positive child with pneumocystis carinii infection.*

bronchograms are found. This pattern is found in pneumocystis carinii pneumonia infections in patients who are immunosuppressed especially from AIDS, mycoplasma infection and, viral infections.

Pulmonary tuberculosis patterns

The appearance of pulmonary tuberculosis is changing in many developing countries with the spread of HIV/AIDS. It is therefore very important to establish whether the patient is immunosuppressed.

Primary pulmonary TB pattern (fig 6.6)

This is usually a small focus of opacification in the lung (Ghon focus) with hilar adenopathy and mediastinal adenopathy on the same side. Often the primary pulmonary focus is not detected only the hilar or mediastinal adenopathy which may cause tracheobronchial airway compression in young children.

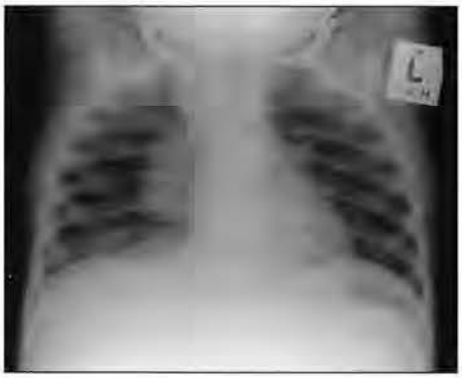

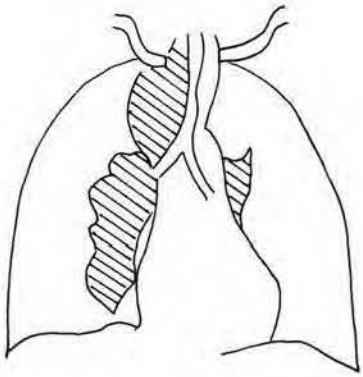

Fig 6.6
Chest radiograph of a child with primary tuberculosis. Note right hilar and paratracheal lymphadenopathy.

Secondary or post primary TB pattern (figs 6.7, 6.8)

In patients with normal immunity this pattern is:

cavitation—usually in the upper lobes or lung apices;

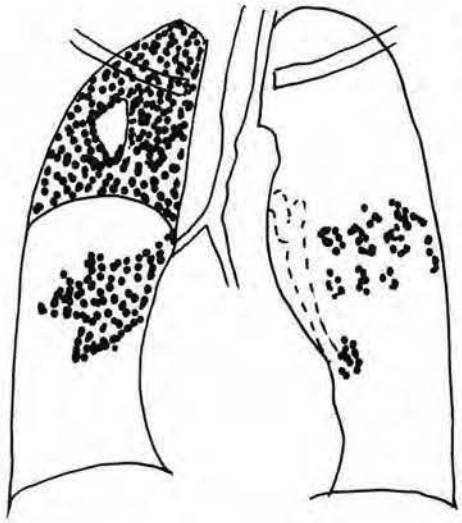

Fig 6.7
Chest radiograph in an adult with post primary or secondary tuberculosis demonstrates right upper lobe infiltrates with cavities which have spread to the right and left lower lobes.

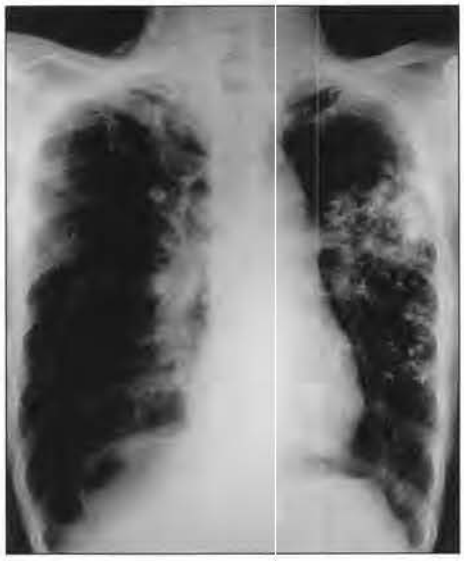

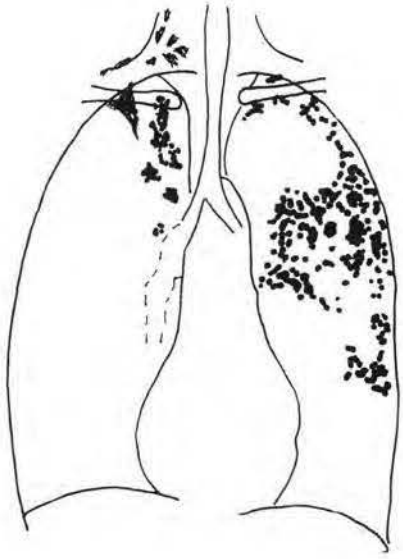

Fig 6.8 *Chest radiograph demonstrates healed tuberculosis with focal calcification in the left mid zone and scarring in the right apex.*

small nodules/infiltrates in the upper lobes. The lesions heal by calcifying with fibrosis of the surrounding lung.

Miliary TB pattern (fig 6.9)

This is a very important pattern to detect as the disease is fatal if untreated. Patients often have non-specific symptoms and signs. Multiple small nodules 2–5 mm in size are detected throughout both lungs from blood borne spread of TB. It is therefore extremely important to exclude miliary tuberculosis in any patient with a miliary infiltrate pattern. The differential diagnosis includes metastates in adults from melanoma, carcinoma of the prostate, pancreas and thyroid, pneumoconioses, sarcoid and lymphoma.

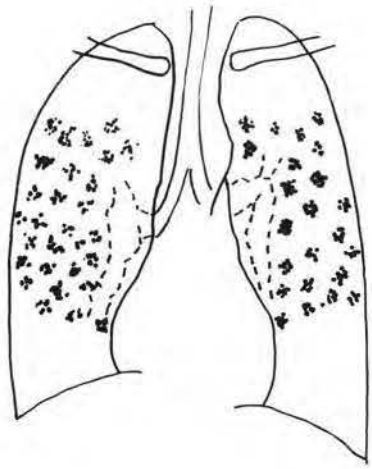

Fig 6.9 *Chest radiograph of a patient with miliary tuberculosis demonstrates a micronodular infiltrate in both lungs.*

LEARNING POINTS: PULMONARY INFECTIONS

- Lobar pneumonia: air bronchograms in the presence of lobar opacification.
- Broncho pneumonia: diffuse peribronchial opacification.
- Necrotising pneumonia: cavitation in the presence of pneumonia; can progress to a lung abscess.
- Ground glass opacification: in pneumocystis carinii pneumonia, mycoplasma, CMV infection.
- Primary PTB: focal pulmonary opacification and unilateral hilar adenopathy (Ghon focus).
- Secondary TB: upper lobe cavitation, nodular(acinar) infiltrates.

Reference

1. Chapman S, Nakielny R. (eds). In: *Aids to Radiological Differential Diagnosis.* 1995, Saunders, London.

CHAPTER 7

Lung cancer

Peter Corr

Lung cancer is a serious public health problem in many developing countries due to increasing cigarette smoking especially amongst young women (*1*). Chest radiographs are important to establish the diagnosis. **The common patterns are:**

solitary pulmonary nodule

hilar mass

lobar atelectasis

multiple pulmonary nodules.

Solitary pulmonary nodule pattern (fig 7.1)

The commonest cause of a solitary pulmonary mass over 3 cm diameter is a carcinoma. There are usually no specific features to suggest cancer apart from the size of the lesion. The presence of focal "pop corn" type calcification suggests a benign cause such as a hamartoma. The differential diagnosis includes granulomas such as tuberculomas and fungal infections, such as cryptococcoma, benign tumours; and a solitary metastasis. The diagnosis can be confirmed by percutaneous fine needle biopsy using fluoroscopy or bronchoscopic biopsy.

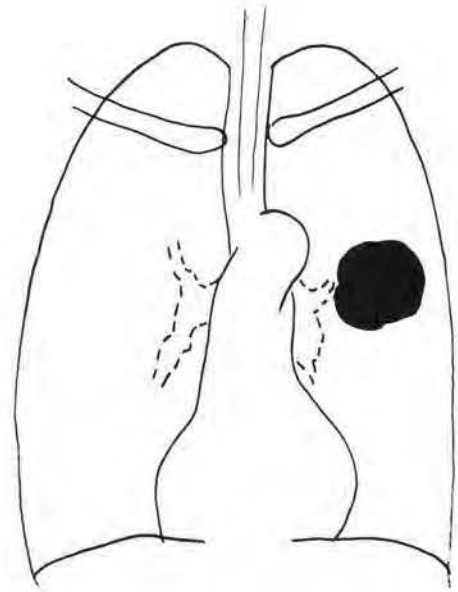

Fig 7.1 *Chest radiograph in a patient presenting with haemoptysis demonstrates a left mid zone solitary bronchial carcinoma.*

Hilar mass pattern (fig 7.2)

A hilar mass is a common presentation as many cancers involve the proximal bronchi with associated tracheobronchial lymphadenopathy. They present as masses distorting the normal contour of the hilum or causing increased density to the hilum.

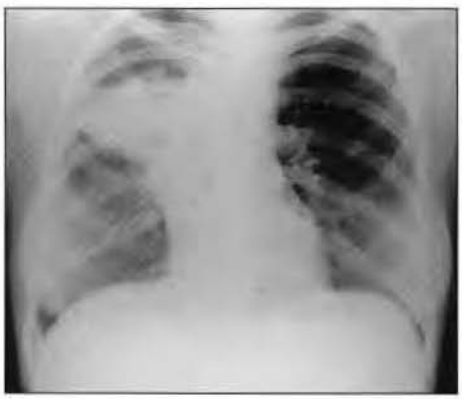

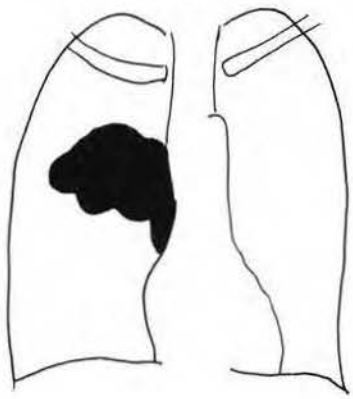

Fig 7.2
Chest radiograph of a patient with haemoptysis demonstrates a large right hilar mass with volume loss of the right lung.

Pancoast's tumour (apical sulcus tumour) (figs 7.3a, 7.3b)

This tumour involving the apex of the lung is often difficult to detect and may often be confused with pleural thickening at the lung apex. Clues to the diagnosis are presence of erosion or destruction of the first three ribs and the presence of a bulging convex inferior to the border to the mass. An apical or lordotic projection is extremely useful to demonstrate this region. The patient may present with pain down the arm from brachial plexus involvement and or involvement of the sympathetic chain with a Horner's syndrome on clinical examination.

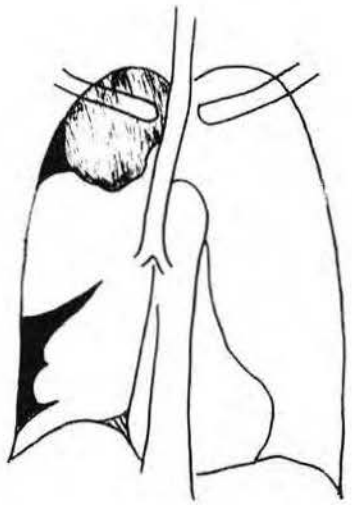

a

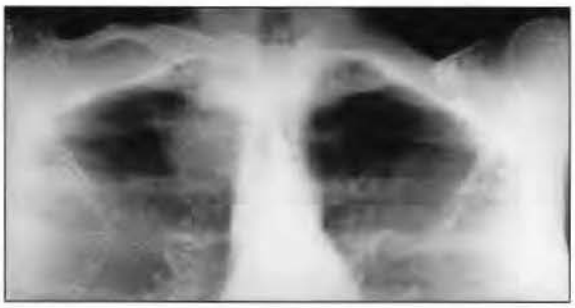

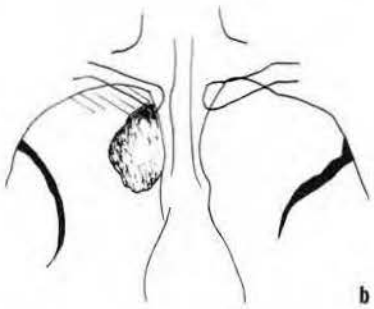

b

Fig 7.3a, 7.3b
Chest radiograph of a Pancoast tumour in the right apex. Note the elevated right hemidiaphragm from right phrenic nerve palsy from tumour infiltration of the right phrenic nerve. The apical view demonstrates the tumour better (3b).

Pulmonary atelectasis pattern (figs 7.4a, 7.4b)

There is a common presentation where there is opacification of a lobe or segment of a lobe with volume loss with no air bronchogram as the airway is obstructed by the tumour with reabsorption of the air distal to the obstruction. This pattern must be differentiated from segmental or lobar pneumonia where there is minimal or no volume loss and air bronchograms are usually present. Where chest infections or pneumonias do not resolve after two weeks of treatment, a follow up chest radiograph is recommended to exclude the possibility of endobronchial obstruction from a tumour or foreign body (in a child).

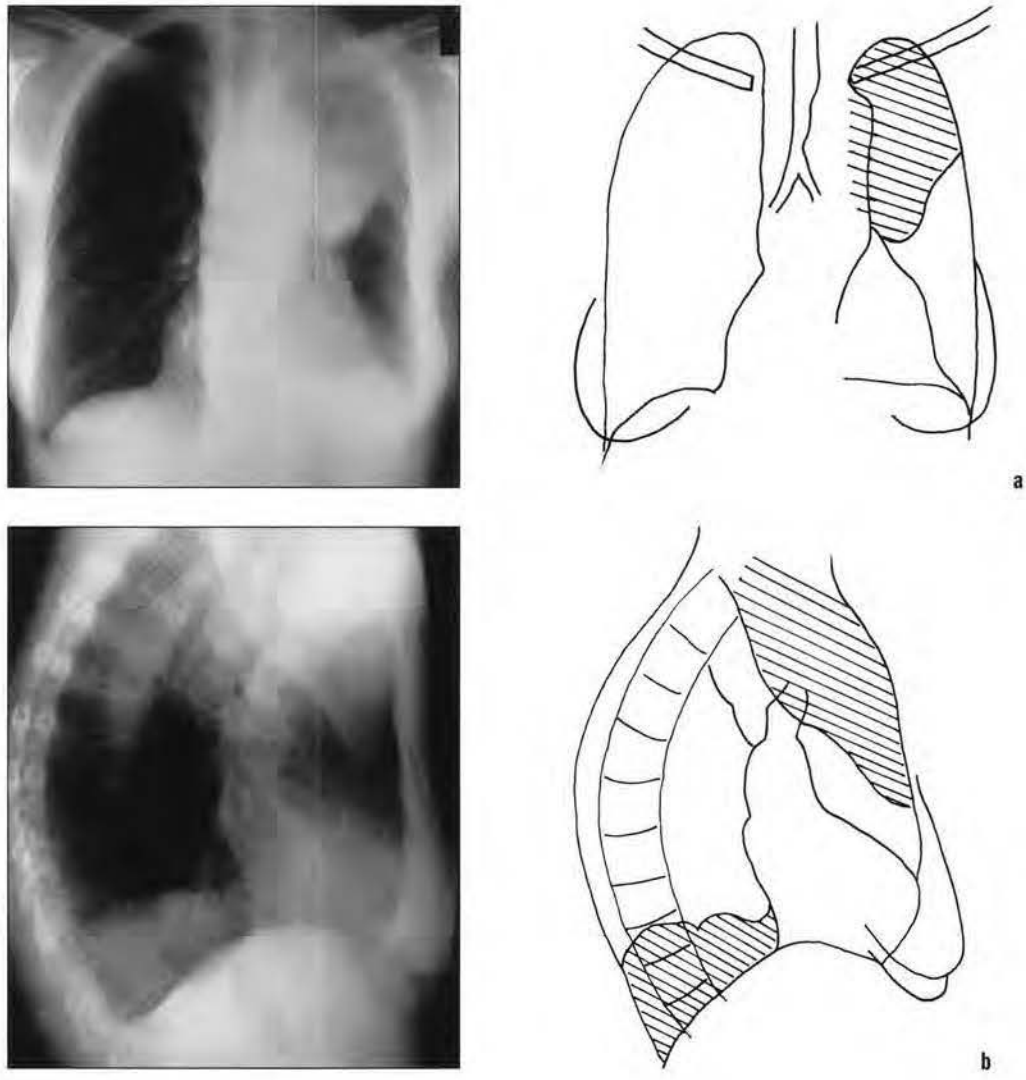

Fig 7.4a, 7.4b *Chest radiograph demonstrates a left hilar mass and left upper lobe opacification and volume loss caused by a left main bronchus obstruction from a carcinoma.*

Multiple masses pattern (figs 7.5a, 7.5b)

Multiple lung masses or nodules >2 cm diameter are most likely due to metastases or granulomas such as tuberculomas or sarcoid. Metastases commonly originate from the breast, primary lung cancer, colon, kidney, pancreas, thyroid, testis or sarcomas from bone or soft tissue. It is often impossible to differentiate between metastasis and

granulomas, although metastases are of variable sizes and have smooth borders while granulomas are the same size and have irregular borders.

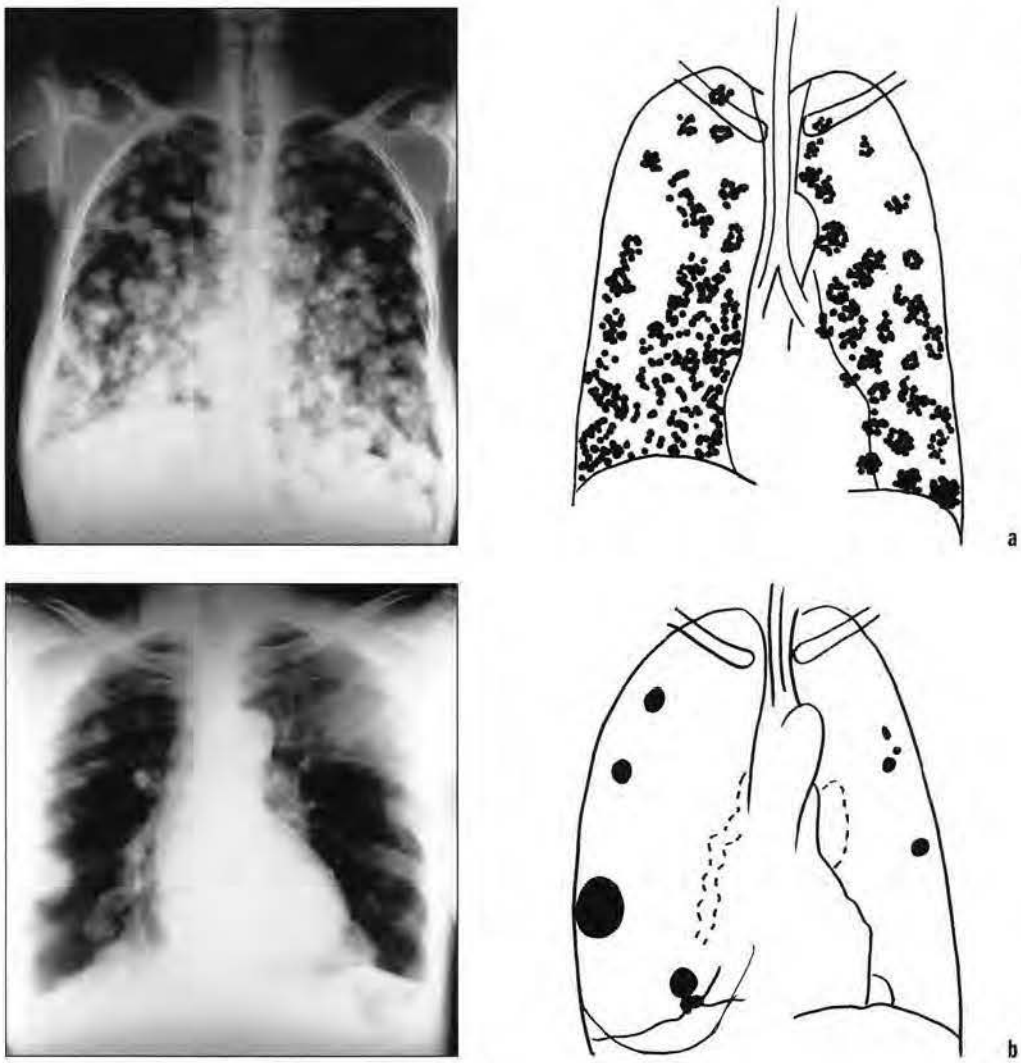

Fig 7.5a, 7.5b
Chest radiographs of two patients with multiple pulmonary metastases. In 5a from choriocarcinoma, in 5b from carcinoma of the breast. Note absent left breast following a mastectomy and destoyed left 5th rib from metastatic disease.

Multiple micronodular or miliary pattern (fig 7.6)

This is a very important pattern to recognise. These small pulmonary nodules are easy to miss if the radiograph is too dark (over-penetrated film). Patient's symptoms are often non-specific especially with miliary tuberculosis: loss of weight and cough (*2*). The correct diagnosis is only suspected once the chest radiograph is reviewed. Micronodules are less than 1 cm in diameter. This pattern is also called the "miliary" pattern and is found in metastatic lung disease, lymphoma, miliary tuberculosis, and pulmonary sarcoid. Causes of "miliary" pulmonary metastases include: thyroid, prostate, breast, pancreas, bronchial carcinomas. Miliary tuberculosis micronodules are usually very discrete without associated hilar lymphadenopathy and are distributed diffusely throughout both lungs. On treatment the pattern resolves very slowly compared to the patient's rapid clinical improvement. A common cause in children with AIDS is lymphoproliferative pneumonitis. This is a peribronchial lymphoid reaction to the HIV virus and is common in seropositive children and young adults.

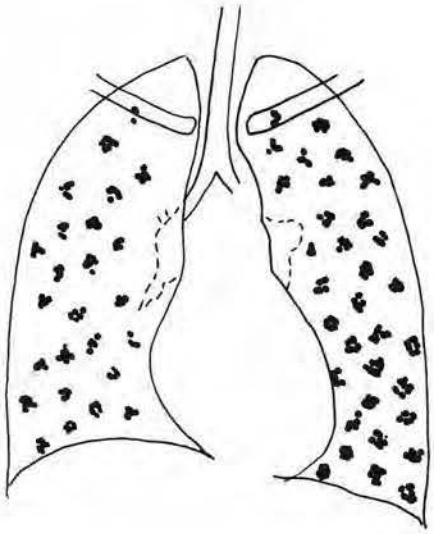

Fig 7.6
Chest radiograph of a patient with multiple micronodular metastases.

LEARNING POINTS: LUNG CANCER

- Solitary pulmonary nodule >3 cm is most likely cancer. Other causes are tuberculomas, benign tumours
- Hilar mass is a common presentation for cancer.
- Pulmonary atelectasis is a common presentation; there is opacification of a segment or lobe with volume loss and absent bronchograms.
- Multiple masses: metastases and granulomas are commonest cause. Cancers are from breast, lung, thyroid, colon, kidney, pancreas, testis and soft tissue sarcoma.
- Micronodular or miliary infiltrates: metastatic disease and TB are common causes. Cancers originate from the thyroid, stomach, prostate, and melanomas.

References

1. Combating the tobacco epidemic. In: *World Health Report* 1999. Geneva WHO.
2. Chapman S, Nakielny R. In: *Aids to Radiological Differential Diagnosis.* 1995. Saunders, London.
3. Hussey G, Chisholm T, Kibel M. Miliary tuberculosis in children: a review of 94 cases, *Pediatr Infect Dis J*, 1991;10:832–6.

CHAPTER 8

Pulmonary hypertranslucency and cystic lungs

Peter Corr

Hyperinflated lung pattern (figs 8.1 & 8.2)

Assessment of lung hyperinflation on chest radiograph is often difficult. Hyperinflation is present if the posterior margins of at least 11 ribs are detected above the diaphragm, which is flattened. An accurate assessment of airways obstruction requires lung

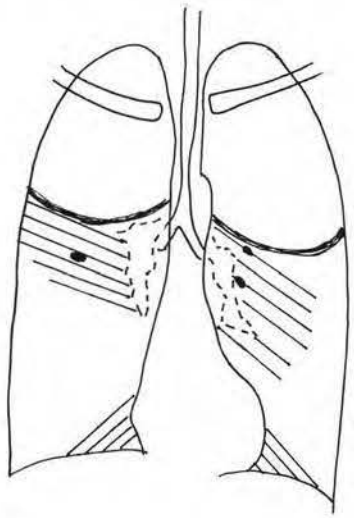

Fig 8.1
Chest radiograph of a patient with hyperinflation and upper lobe bulla from emphysema.

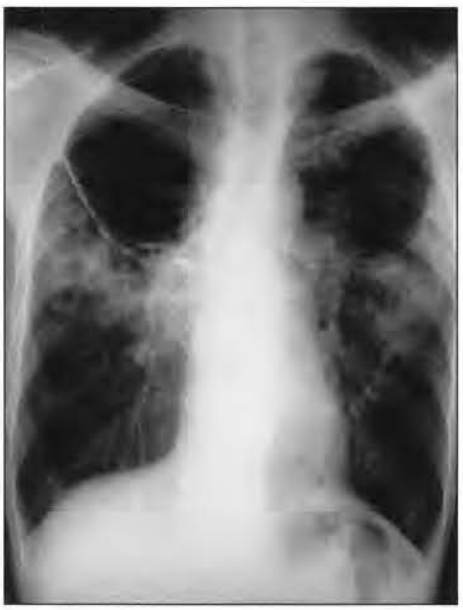

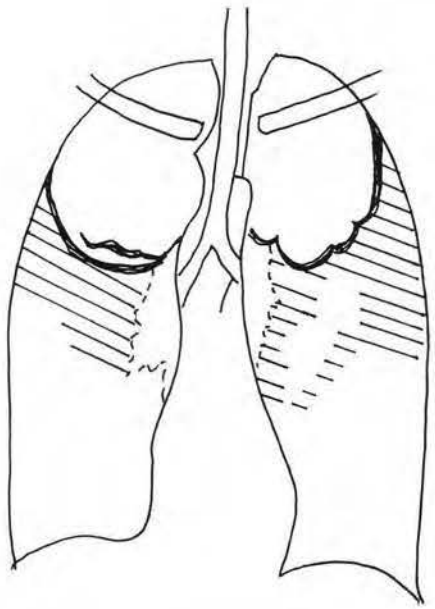

Fig 8.2
Chest radiograph in a patient with emphysema with recurrent chest infection. Note upper lobe bulla with mid zone opacification from pulmonary infection.

function tests, not chest radiographs. Hyperinflation is found in airway obstruction from asthma and chronic obstructive airways disease following cigarette smoking. The presence of focal thin walled cysts in the lung (called bulla) and hyperinflation are seen in emphysema. Patients may have radiographic signs of pulmonary hypertension with prominent central arteries and thin peripheral arteries.

Cystic lung pattern (figs 8.3 & 8.4)

Lung cysts appear as focal translucencies in the lung contained by thin cyst walls which are usually 2 mm or less in thickness. The most common cause is cystic bronchiectasis where there is cystic dilatation of the bronchi usually appearing as multiple basal ring shadows. Often air fluid levels are present if there is superimposed infection. The diagnosis is best made on high resolution CT of the lungs where the bronchial dilatation is better defined. Lung cysts must be differentiated from cavities. Hydatid disease can appear "cystic" if the fluid drains into the bronchi.

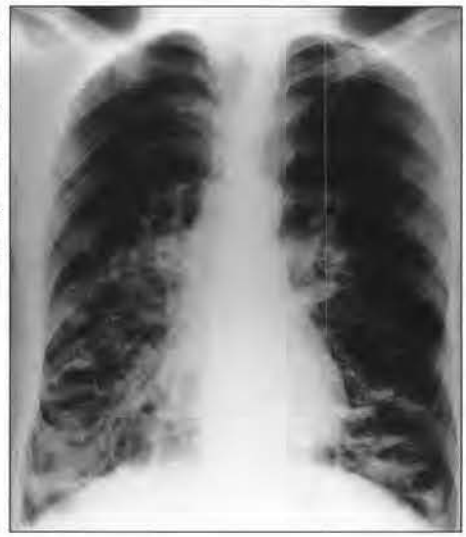

Fig 8.3
Chest radiograph of a patient with chronic cystic bronchiectasis demonstrates multiple cysts in the lower lobes many of which containing fluid levels from infected fluid.

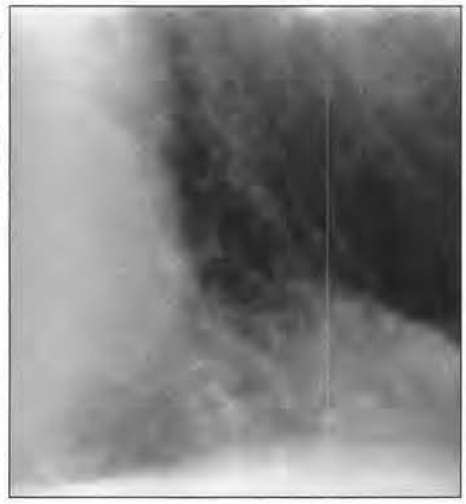

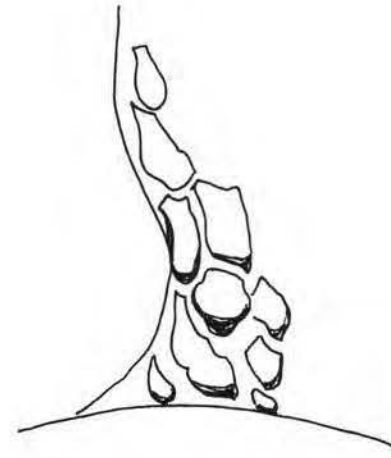

Fig 8.4
Localised view of the left lower lobe of a patient with bronchiectasis demonstrating the multiple dilated bronchi.

Cavities (figs 8.5-8.7)

Cavitities occur commonly in pulmonary tuberculosis, necrotising pneumonias or abscesses and cavitating tumours. With cavities the wall of the cavity is irregular and much thicker than 2 mm, usually in the region of 1 cm thick. In necrotising pneumonias or lung abscesses there is often an associated air fluid level within the cavity.

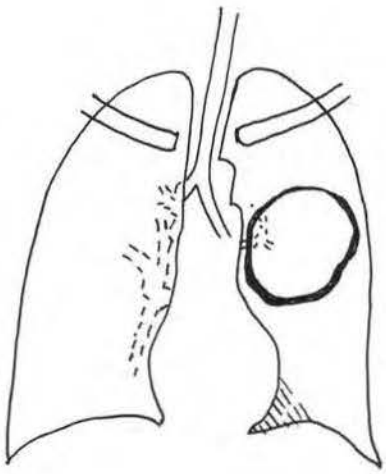

Fig 8.5
Chest radiograph of a patient with active pulmonary TB with a large left mid zone cavity. Note the wall is much thicker than a bulla.

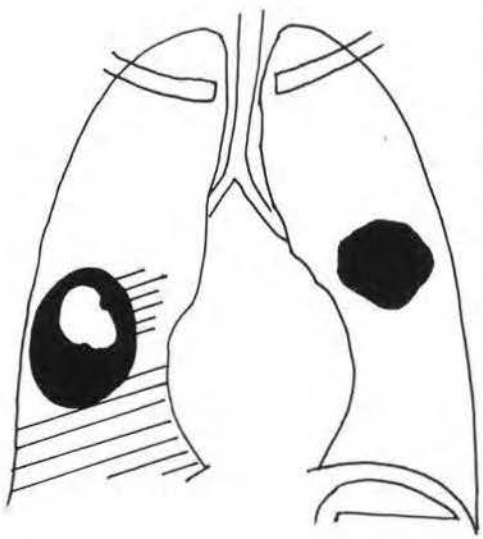

Fig 8.6
Chest radiograph of a patient with pulmonary hydatid disease. The right lower hydatid cyst contents have drained into the bronchial tree leaving a thicked walled cyst with a nodular border.

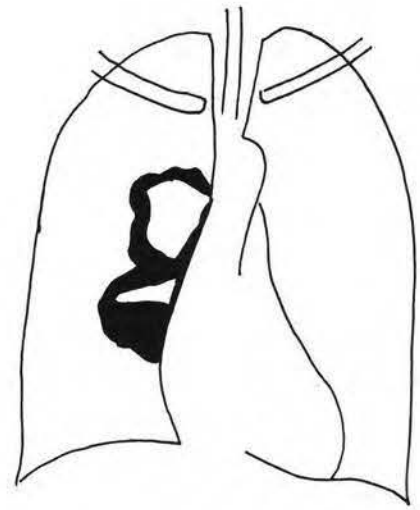

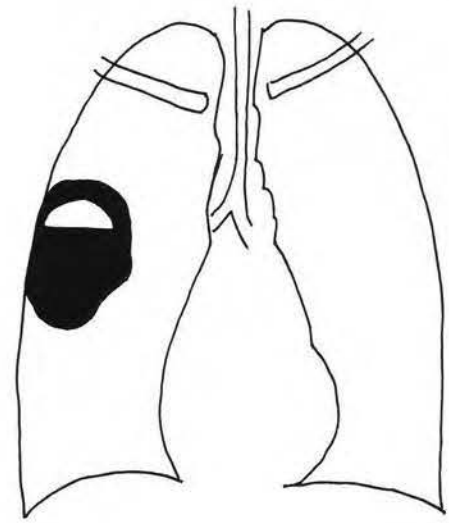

Fig 8.7
Chest radiographs of an epileptic patient who developed two abscesses in the right lung folowing aspiration during a seizure.

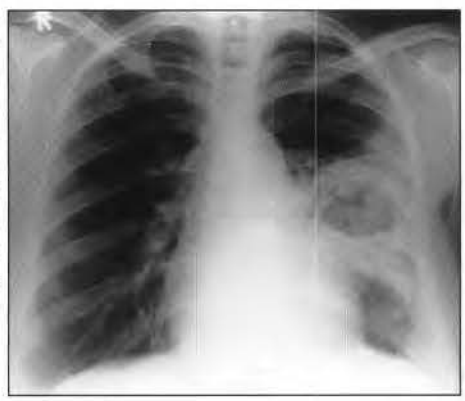

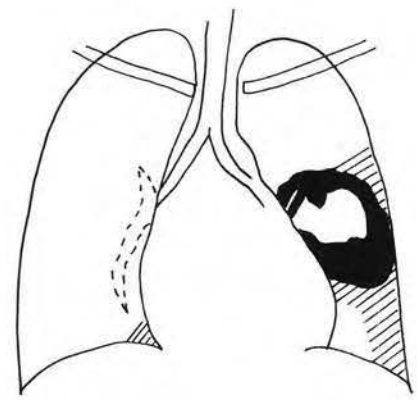

Fig 8.8a & 8.8b
Chest radiograph of a left mid zone cavity containing a mycetoma which moves to the dependent region of the cavity on positioning the patient in the left decubitus position (fig 8.9).

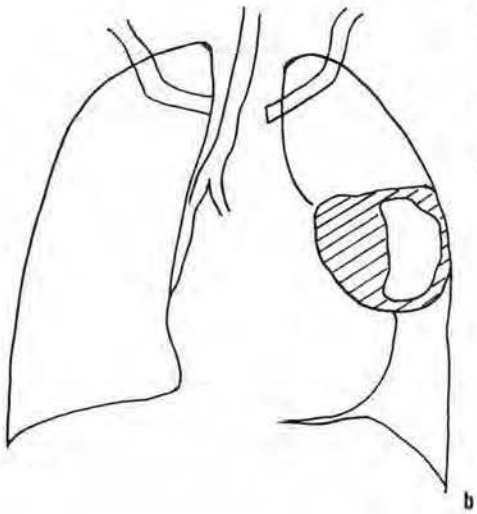

Fig 8.9a & 8.9b
Chest radiograph of the same patient as shown in fig. 8.8, but taken in the left decubitus position.

Mycetomas (figs 8.8 & 8.9)

These are inflammatory masses within prior lung cavities usually from chronic TB. They are due to fungal infections, especially aspergillosis (so called "aspergillomas"). They are not attached to the cavity wall and move on changing the patient's position to the most dependent position within the cavity. These masses are important to detect as they are an important cause of haemoptysis. Thickening of the lateral wall of the cavity is a good predictor of the presence of a mycetoma. The main differential diagnosis is an intracavitatory haematoma. Surgical resection is the treatment of choice.

LEARNING POINTS: HYPERTRANSLUCENCY & LUNG CYST PATTERNS

- Hyperinflated lungs are found in airways obstruction from asthma and chronic obstructive airways disease following cigarette smoking.
- The presence of a bulla and hyperinflation is found in pulmonary emphysema.
- Unilateral hyperlucent lung may be due to technical factors such as chest rotation, a previous mastectomy, or a hyperinflated lung from Swyer James syndrome (bronchiolitis obliterans) or a "ball valve" effect from partial bronchial obstruction by a foreign body especially in young children or rarely an endobronchial tumour.
- Hydatid cysts can mimic bulla.
- A cavity has a thick wall >2 mm which is irregular and may contain an air fluid level if there is a communication with the bronchial tree.
- Cavities are found in lung abscess/necrotising pneumonia, tumours especially squamous cancers and pulmonary tuberculosis.
- Mycetomas are intracavitatory inflammatory masses of aspergillus. They cause haemoptysis.

References

1. Chapman S, Nakielny R. eds. In: *Aids to Radiological Differential Diagnosis*. 1995, Saunders. London.
2. Sansom HE, Baque-Juston M, Wells AU, Hansell DM. Lateral cavity wall thickening as an early radiographic sign of mycetoma formation. *Eur Radiol* 2000;10:387–90.

CHAPTER 9

Pleural and extra pleural disease

Peter Corr

Pleural effusions (figs 9.1–9.3)

Pleural fluid is first detected in the costophrenic angles and subpulmonic pleural spaces (fig 9.1a). There may be actually 250 mls of fluid present before it is detected radiologically. Subpulmonic fluid collections are common particularly in trauma where

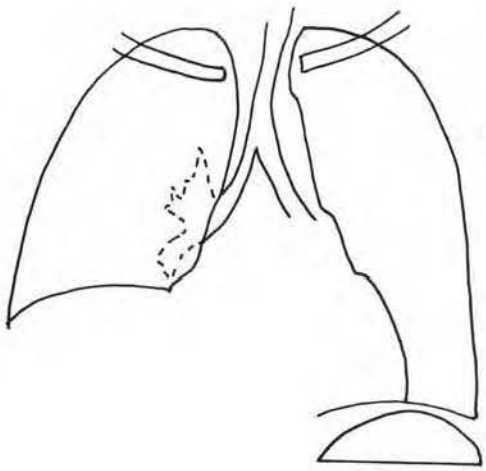

a

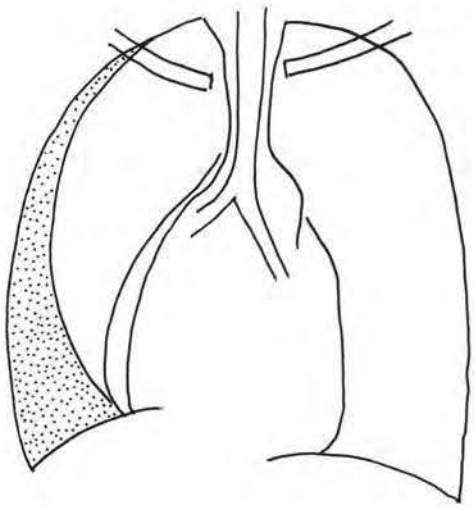

b

Fig 9.1a, 9.1b
Chest radiograph of a patient with a right subpulmonic pleural collection. Note the pseudo elevated hemidiaphragm with a more lateral apex than normal. On the right side down decubitus film the pleural fluid is now demonstrated laterally. Note the presence of a small medial pneumothorax.

the apparent hemidiaphragm appears elevated and the apex is displaced laterally. To confirm the diagnosis a decubitus chest radiograph will detect the subpulmonic collection (fig 9.1b). Encysted collections are common due to pleural adhesions and can appear like masses on radiograph. Fluid encysts in the fissures and can also appear as a pseudo mass (fig 9.2). The diagnosis becomes more evident on the lateral chest film where the fluid loculates in a "aeroplane propeller" configuration. **Common causes of pleural effusions are**:

tuberculosis

malignancy (either primary or secondary cancer).

Ultrasound using a high frequency transducer (>5 MHz) will confirm the presence of fluid as opposed to a mass. Ultrasound is very useful to direct aspiration of encysted effusions.

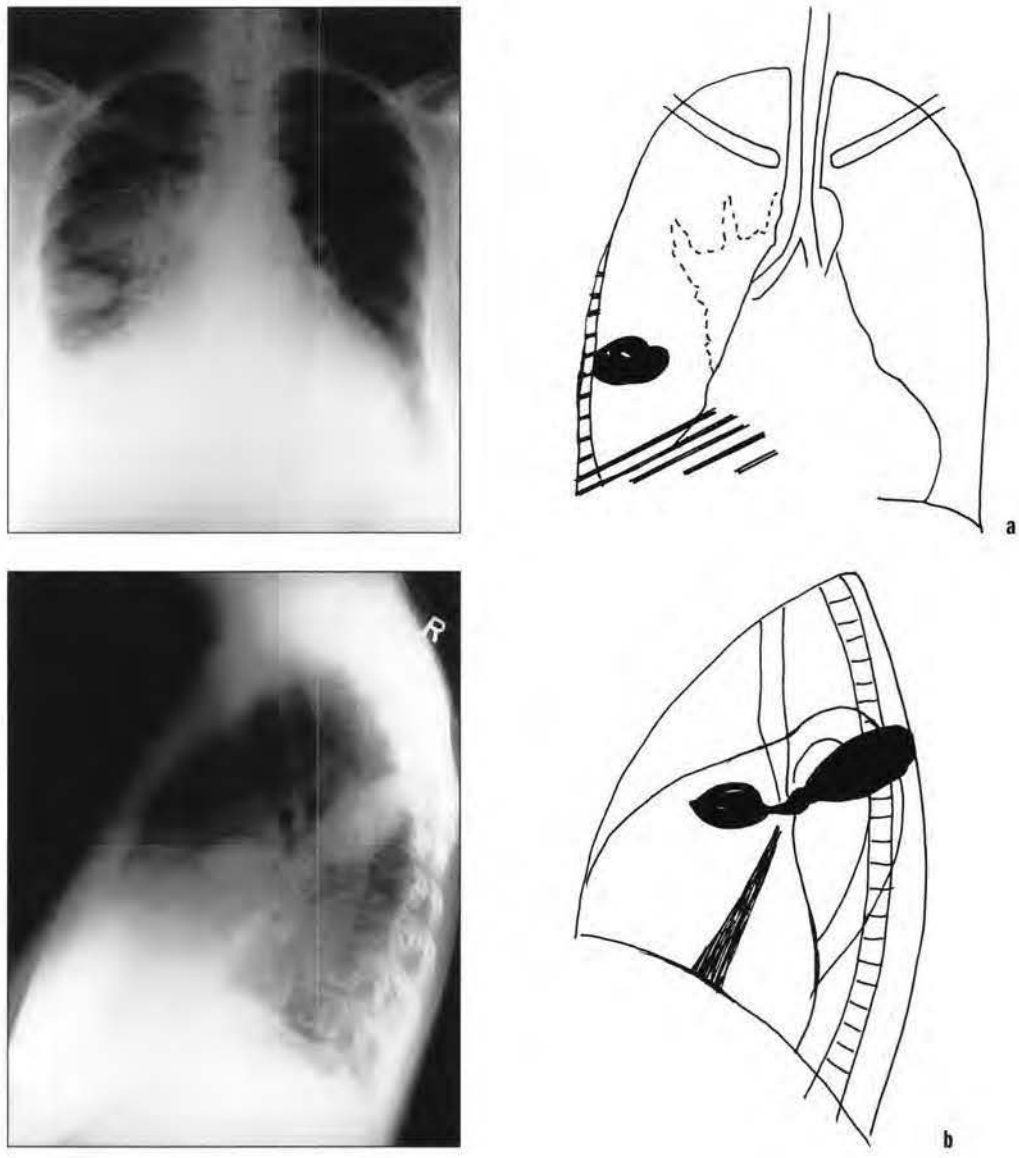

Fig 9.2a, 9.2b *Chest radiograph of a patient in cardiac failure demonstrating a "pseudomass" in greater and lesser right fissures from encysted pleural fluid.*

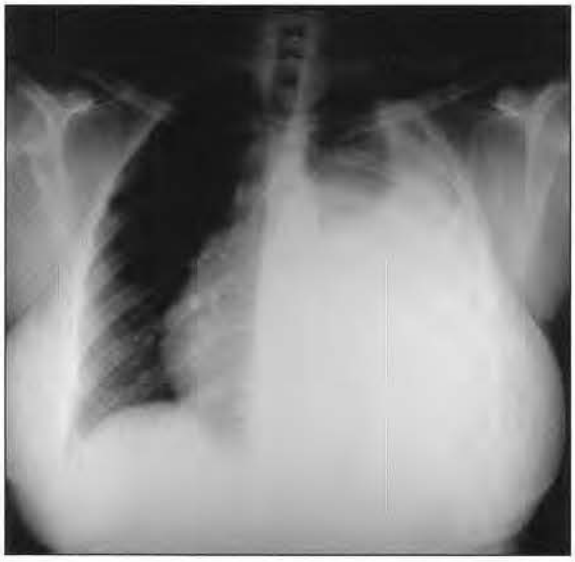

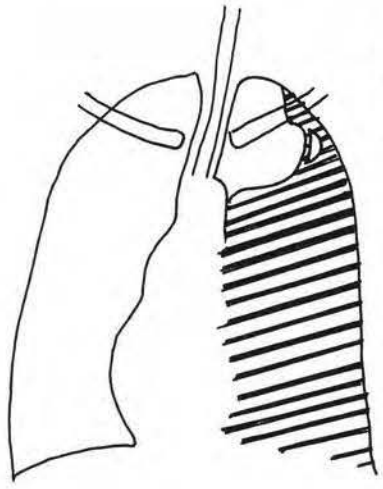

Fig 9.3
Chest radiograph demonstrates a large left pleural effusion with mediastinal shift to the right.

Empyema (figs 9.4a & 9.4b)

Empyema is a collection of pus in the pleural space. The pleura is thickened and bulges outwards. It may not be possible to differentiate between a pleural effusion and empyema on the chest radiograph alone. Empyemas appear echogenic on ultrasound. Ultrasound is excellent in guiding a needle into the the collection for aspiration.

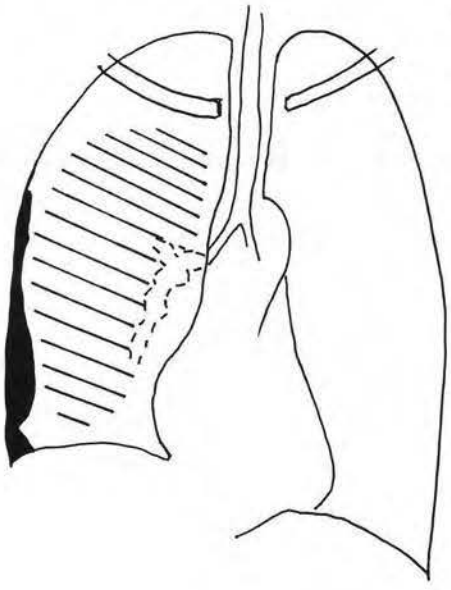

a

Fig 9.4a, 9.4b
Chest radiograph of a patient with a right empyema. Note the anterior convex margin of the pleural collection suggesting the pus in the pleural space is under pressure.

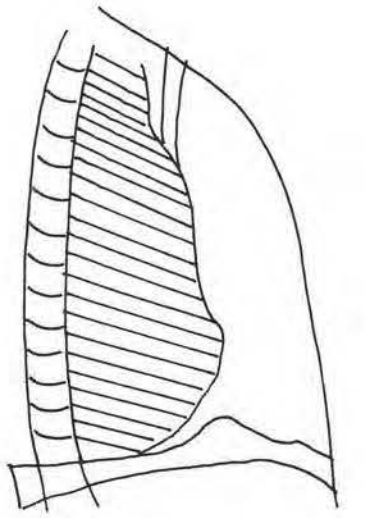

b

Pleural mass (figs 9.5-9.7)

Pleural masses are either benign or malignant. **Malignant pleural masses** include metastases from adenocarcinoma often from breast cancer, lung primary, bowel, ovary or a primary cancer such as a mesothelioma from asbestosis exposure. **Benign masses** include inflammatory masses, fibrosis, benign fibromas and pleural plaques from asbestos exposure. Inflammatory lesions include tuberculosis. It is not possible to differentiate benign from malignant masses. Rib destruction is more common with malignant tumours but is also detected with granulomatous infections such as tuberculosis.

Extra pleural masses

Extrapleural masses which may be associated with rib destruction. Metastatic involvement of the ribs often has an associated soft tissue mass. Similarly chronic infections of the rib such as TB, actinomycosis can be associated with an abscess or granulomatous mass. Plasmacytomas causes localised rib expansion and a soft tissue mass. To differentiate an extrapleural mass from a pleural mass, look at the medial border of the mass. If it is convex medially it is probably extrapleural while if it is concave medially it is probably pleural in origin.

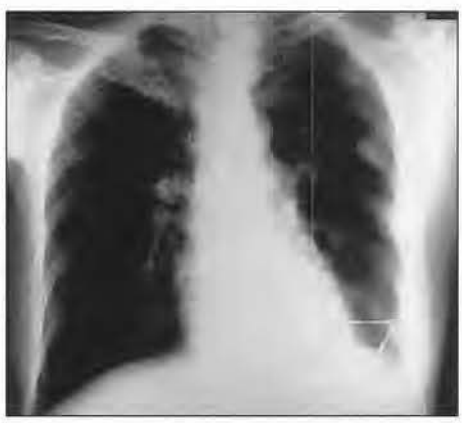

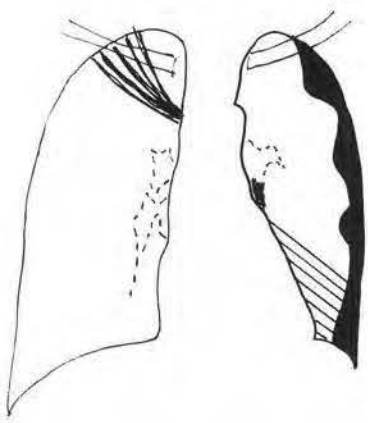

Fig 9.5
Chest radiograph of a patient with breast cancer and pleural metastases. Note right mastectomy from the absent breast shadow and the left peripheral pleural metastases.

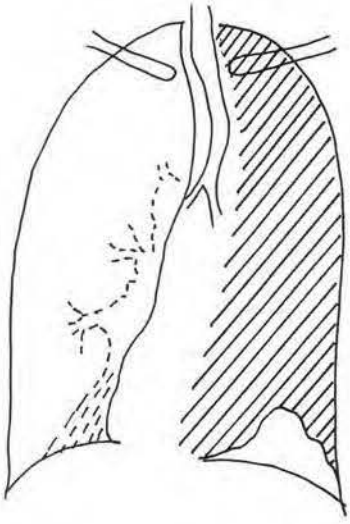

Fig 9.6
Chest radiograph of a patient with a left pleural mesothelioma. Note mediastinal shift to the left and opacification of the left pleural space.

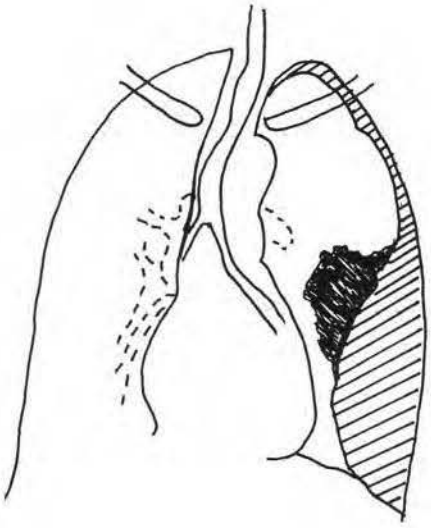

Fig 9.7
Chest radiograph of a patient with left lower zone pleural fibrosis following a haemothorax. Note the crowding of the left lower ribs and the pleural calcification.

LEARNING POINTS: PLEURAL DISEASE

- Subpulmonic effusions result in an apparent elevation of the hemidiaphragm, the diagnosis can be confirmed on an ipsilateral decubitus chest radiograph.
- Common causes of unilateral pleural effusions are malignancy (primary and secondary) and tuberculosis.
- Encysted pleural collections resemble pleural masses; ultrasound can differentiate between a mass and fluid.
- Pleural masses are most commonly adenocarcinoma metastases, mesothelioma, inflammatory masses or benign fibromas.
- Extrapleural masses often have associated rib destruction.

Reference

1. Chapman S, Nakielny R. *Aids to Radiological Differential Diagnosis*. 1995 Saunders, London

CHAPTER 10

Rib lesions

Peter Corr

It is always important to scan the bones of the chest for both focal and diffuse abnormalities. Often the presence of bone lesions will suggest the correct diagnosis of the pulmonary abnormality.

Focal rib lesions

Lytic lesions are usually due to tumours especially metastases or myeloma. They can be difficult to detect initially if the individual rib contours are not carefully traced out from posterior to anterior. The patterns of these lesions appear as if the ribs have been "erased" with a rubber eraser with an associated extrapleural soft tissue mass (fig 10.1). Bronchial carcinoma, especially Pancoast's tumour at the apical sulcus of the lung, invades the pleura and overlying brachial plexus to cause early lytic destruction of the first and second ribs. Occasionaly pleural tuberculosis involves the overlying ribs. With myeloma it is particularly useful to assess other flat bones such as the clavicles and scapulae for similar lesions as the presence of such lesions will suggest the diagnosis.

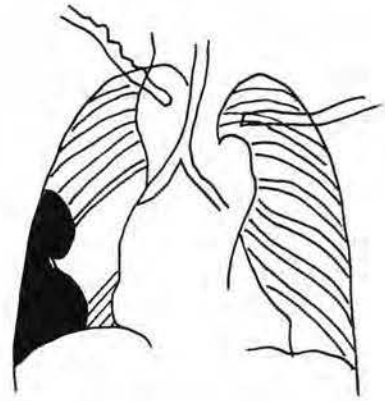

Fig 10.1
Chest radiograph of a patient with multiple myeloma. There is a soft tissue mass in the right lower zone with destruction of the lower right ribs. A lytic lesion in the right clavicle is noted.

Sclerotic rib lesions in which bone density is increased are especially common with prostate and breast metastases. Occasionally all the ribs become diffusely sclerotic (fig 10.2).

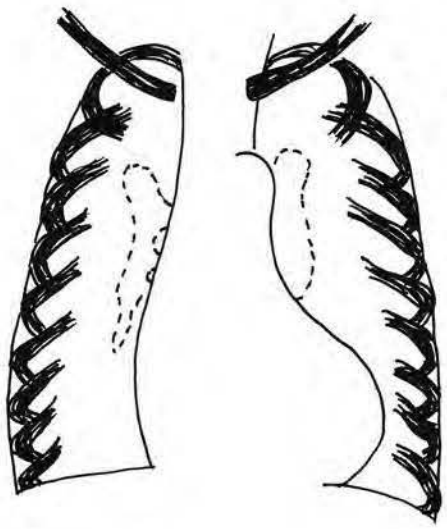

Fig 10.2
Chest radiograph of a patient with diffuse sclerotic metastases in the ribs from carcinoma of the prostate.

Rib erosions usually destroy the superior or inferior rib cortex. Inferior rib notching or erosions are often due to erosion from neurofibromas or collateral vessels in aortic coarctation (fig 10.3). In neurofibromatosis the ribs may appear thin and gracile because of the associated mesodermal dysplasia. Superior cortical erosions are detected in collagen vascular disorders such as rheumatoid arthritis, systemic lupus erythrematosis and scleroderma. Erosions of the lateral margins of the clavicles are common in advanced rheumatoid arthritis.

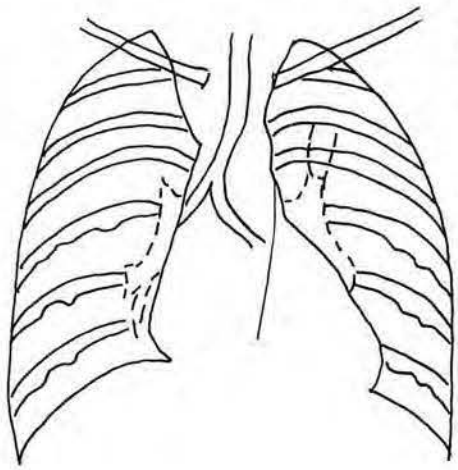

Fig 10.3
Chest radiograph of a patient with coarctation of the aorta. Note left ventricular hypertrophy, small aortic arch and bilateral inferior rib notching of the ribs.

Diffuse rib lesions

Metabolic bone disease, such as osteomalacia, hyperparathyroidism, Paget's disease and rickets in children, may demonstrate bone softening and rib deformity. Microfractures with exuberant callus may be detected in osteomalacia, Cushing's syndrome and Paget's disease.

Diffuse osteopenia or decreased bone density occurs in osteoporosis, osteomalacia, and Cushing's syndrome. Diffuse bony sclerosis occurs in Paget's disease, sclerotic metastases from breast and prostate cancer.

LEARNING POINTS: RIB LESIONS

- Common cause of focal lytic rib lesions are lytic metastases for breast and lung carcinoma, and multiple myeloma
- Common cause of focal and diffuse sclerotic rib lesions are sclerotic metastases from prostate and breast carcinoma, and Paget's disease
- Common causes of rib notching and erosion include coarctation of the aorta, collagen vascular disorders, and neurofibromatosis
- Common causes of decreased bone density are osteoporosis, hyperparathyroidism, osteomalacia, and rickets in children

Reference

1. Chest wall, pleura and diaphragm. Wilson AG, Flower CDR, Verschakelen JA. In: *Diagnostic Radiology: a textbook of medical imaging*. 1997. Eds Grainger RG, Allison DJ. Churchil Livingstone, Edinburgh

CHAPTER 11

Chest trauma

Peter Corr

Good quality radiographs are critical for evaluation of chest trauma patients. An erect chest radiograph is important to detect pneumothorax and haemothorax. If the patient is unable to sit or stand a decubitus chest is useful to detect a pneumothorax and or subpulmonic haemothorax.

Blunt trauma

Bony injury (fig 11.1)

Ribs usually fracture laterally after blunt trauma; the lower six are commonly involved. Fractures in two places may lead to a flail chest. Fractures of the upper four ribs are usually associated with severe blunt injury and vascular injury must be excluded if there is widening of the superior mediastinum. Sternal injuries are detected on lateral coned views of the sternum. It is important to check the thoracic spine carefully for associated fractures in these patients.

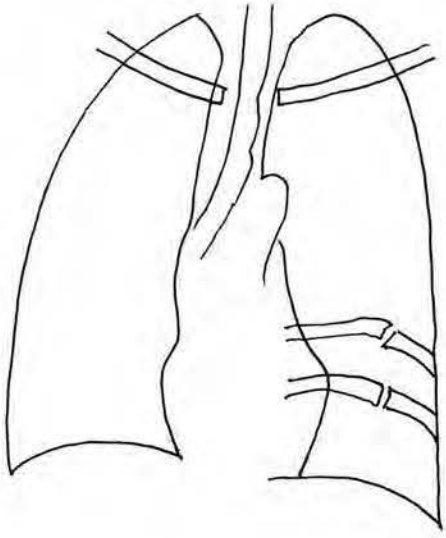

Fig 11.1
Chest radiograph of a patient following chest trauma. Note fractures of the left 8th and 9th ribs.

Pneumothorax (figs 11.2a, 11.2b)

This is an important diagnosis and can be detected as a fine white line of the visceral pleura with absent peripheral lung markings. Pneumothoraces can also be medial or subpulmonic in position. A decubitus chest radiograph will identify a shallow pneumothorax. If the pneumothorax is large and there is mediastinal shift away from

the side of the injury, the pneumothorax is considered to be under tension. This is extremely important to recognise because if left undetected this can be rapidly fatal. A clue to the presence of a pneumothorax is gas in the soft tissues, which appears as low density streaks (surgical emphysema).

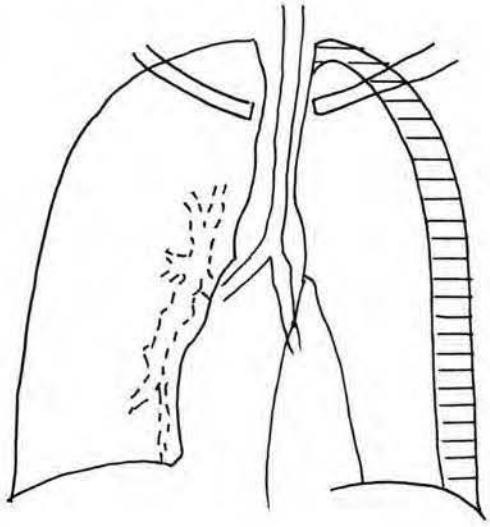

Fig 11.2a *Chest radiograph of a patient who sustained a penetrating chest wound. Note the shallow left pneumothorax.*

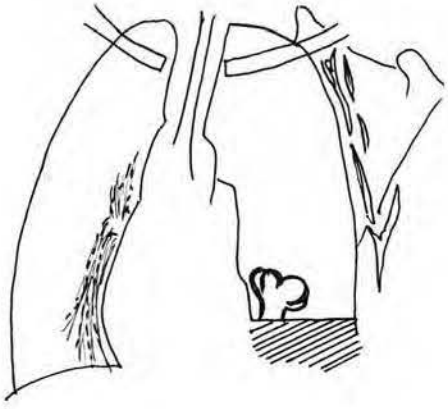

Fig 11.2b *Chest radiograph of a patient with a large left haemopneumothorax, with mediastinal shift to the right and surgical emphysema in the chest wall.*

Haemothorax (fig 11.3)

Blood collects inferiorly in the pleural spaces beneath the lung to form a subpulmonic haemothorax. The hemidiaphragm appears elevated with the apex of the dome displaced more laterally than normal. A decubitus chest radiograph with the affected side dependent will confirm the presence of blood in the pleural space.

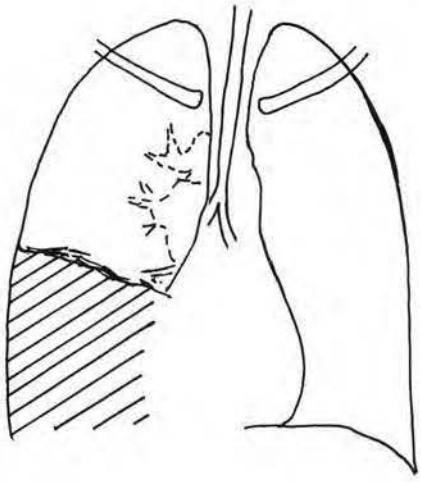

Fig 11.3
Chest radiograph of a patient with a right subpulmonic haemothorax. Note the "pseudo elevated" right hemidiaphragm.

Pulmonary lesions (fig 11.4)

Haematomas within the lungs appear as pulmonary masses that resolve over days. They can be differentiated from other masses by reviewing serial radiographs. Contusion appears as opacification of the lungs.

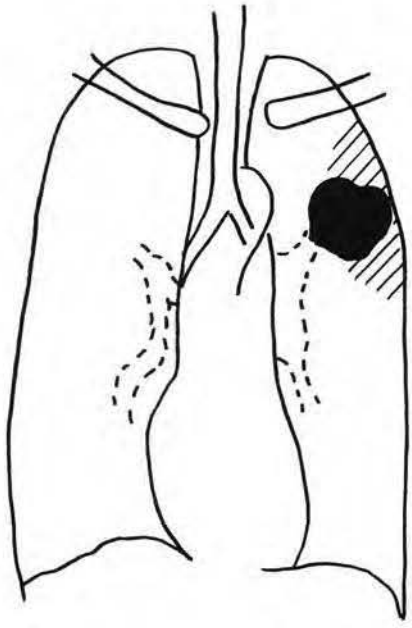

Fig 11.4
Chest radiograph of a patient with a left upper lobe pulmonary haematoma following blunt trauma.

Vascular injuries (figs 11.5a, 11.5b)

Aortic arch injuries are important to detect especially after deceleration injuries to the chest and mediastinum. The aorta tears transversely at the level of the ductus arteriosus. The important signs on the chest radiograph are:

- A widened mediastinum >8 cm wide on an erect film
- Loss of the normal mediastinal outline

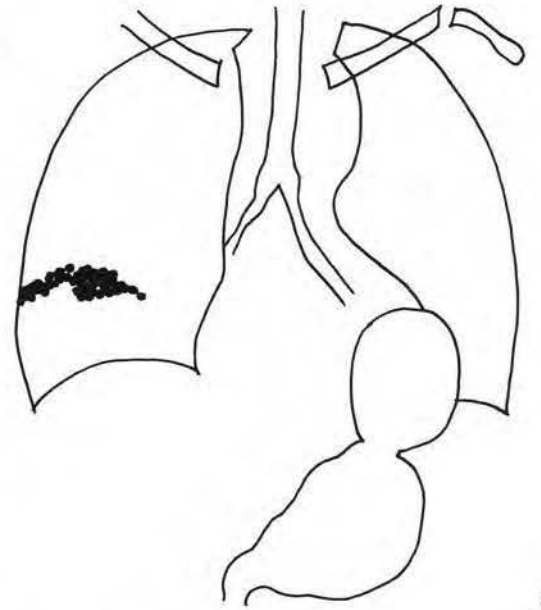

a

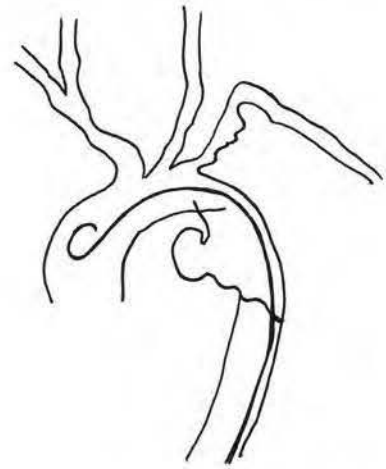

b

Fig 11.5 *Chest radiograph of a patient following blunt trauma to the sternum, demonstrates a markedly widened superior mediastinum with loss of the normal aortic arch outline from a false aneurysm of the aortic arch and a rupture of the left hemidiaphragm and herniation of the stomach in the chest. Fig 11.5b demonstrates the false aneurysm of the proximal descending aorta.*

- Fracture of the upper ribs
- Apical cap from haematoma

If these signs are present the patient should be transferred for aortography to confirm the diagnosis. It is important to measure the superior mediastinum on an erect chest radiograph if possible. Note a supine radiograph may falsely suggest a wide mediastinum.

Trauma to the tracheobronchial tree

Injury to the trachea or bronchi leads to a pneumomediastinum and pneumothorax and often a collapsed lung.

Diaphragmatic injury (fig 11.6)

Rupture of the diaphragm usually involves the left hemidiaphragm. Diaphragmatic tears can often be asymptomatic untill bowel herniation and incarceration occur. The diagnosis is easily missed and this can be fatal. Contrast studies of the stomach and left colon demonstrate the position of these structures in relation to the diaphragm and, to detect herniation.

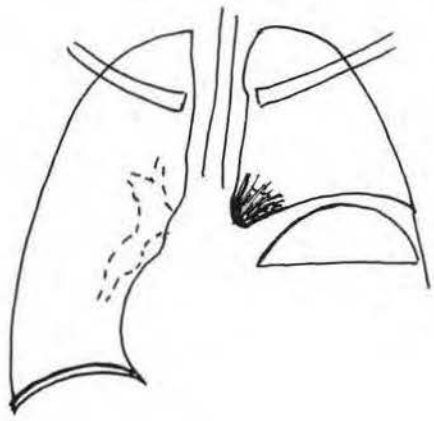

Fig 11.6
Chest radiograph of a patient following blunt trauma demonstrates a large left traumatic diaphragmatic hernia and free intraperitoneal air below the right hemidiaphragm.

Penetrating trauma

Penetrating trauma often causes haemopneumothorax and pneumomediastinum. Vascular injury will be detected by a widened mediastinum; the patient will require arteriography to confirm the diagnosis. Injuries may involve the oesophagus with perforation (fig 11.7) A swallow using water-soluble contrast will detect the leak.

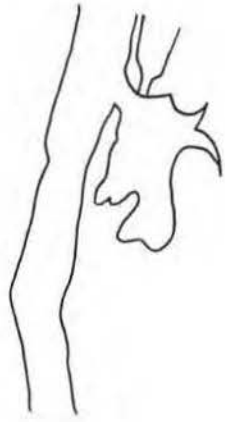

Fig 11.7
Barium swallow of a patient who sustained a knife wound to the superior mediastinum demonstrates an oesophageal perforation and leak of contrast into the mediastinum.
***Important**: Use water-soluble contrast medium when perforation is suspected!*

Injuries of the lower chest may cause a defect in the diaphragm with the possibility of bowel herniation and incarceration. This is very dangerous and needs to be detected early when asymptomatic by checking the diaphragm carefully in a patient with a history of penetrating injury.

LEARNING POINTS

- Pneumothorax is best detected on erect chest or decubitus chest radiograph.
- Mediastinal shift away from the injured side indicates a tension pneumothorax
- Subpulmonic haemothorax causes apparent elevation of the hemidiaphragm with a laterally displaced dome. Diagnosis confirmed on a decubitus chest radiograph.
- Aortic injury sugested by a wide mediastinum >8 cm dianmeter, loss of normal mediastinal outline, apical cap. Requires aortography to confirm the diagnosis.
- Diaphragmatic injury is often missed, it commonly involves the left hemidiaphragm. Requires contrast study of stomach and left colon to confirm the diagnosis.
- Always attempt to assess mediastinal widening on an **erect chest radiograph** if possible.

Reference

1. Chest trauma Flower CDR. In: *Diagnostic Radiology—a textbook of medical imaging.* Eds Grainger RG, Allison DJ, 1997, Churchill Livingstone, Edinburgh.

CHAPTER 12

Pulmonary AIDS

Peter Corr

There has been a rapid increase in AIDS in many countries in Africa and Asia over the last ten years. An understanding of common presentations of pulmonary opportunistic infections and AIDS related neoplasms is important as 80% of AIDS patients will have respiratory disease (*1*).

Tuberculosis patterns in AIDS (fig 12.1)

The human immunodeficiency virus is synergistic with tuberculosis (*2*). Tuberculosis infection is progressive, often extrapulmonary and multifocal in patients with AIDS (*2*). Adults present with a pattern similar to primary TB in children with unilateral hilar or mediastinal adenopathy and lower lobe opacification. Cavities are uncommon. Progressive disease follows spread along the bronchial tree in addition to blood borne spread. Patients often have skeletal or abdominal tuberculosis as well (*2*).

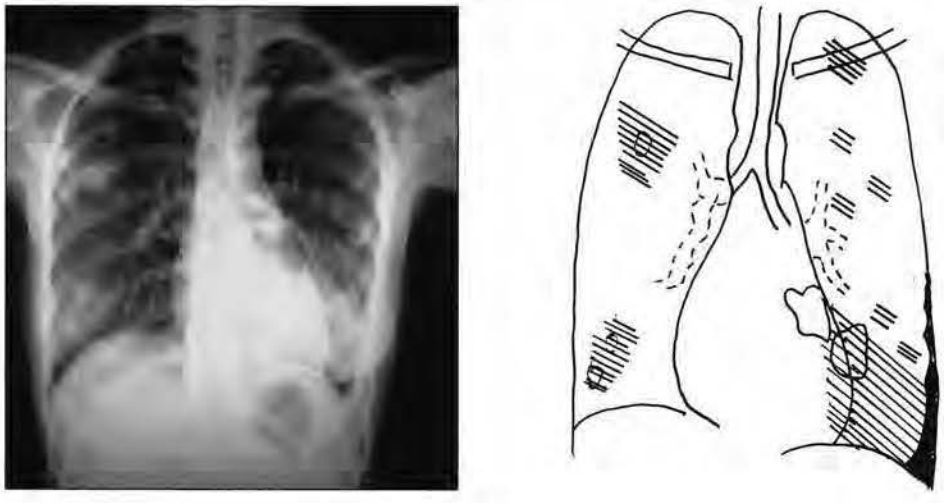

Fig 12.1
Chest radiograph of an AIDS patient with pulmonary TB. Note the predominantly lower lobe distribution of the opacification with perihilar cavities.

Ground glass pattern (fig 12.2)

The cause is pneumocystis carinii and or cytomegalovirus infection. Patients have a "ground glass" opacification of the lungs that obscures the pulmonary vessels. It starts around the hila and spreads outwards. It is easy to miss in early cases but the clue is the lung vessels appear blurred and ill defined. Lymphadenopathy is rare in pneumocystis infection. However not all patients have the typical "ground glass" pattern, a large number also have consolidation, nodules, cavitating masses, subpleural cysts and spontaneous pneumothorax (*3*).

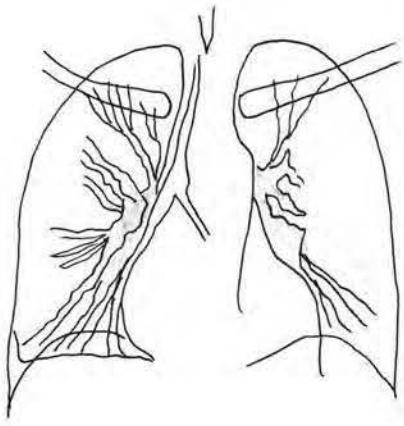

Fig 12.2 *Chest radiograph of a patient with pneumocystis carinii infection. Note the perihilar "ground glass" opacification.*

Bacterial infection patterns

Bacterial pneumonias are very common in AIDS patients especially streptococcus pneumoniae, haemophilus influenza, pseudomonas infection because the HIV infected lymphocytes cannot destroy bacteria with capsules. A destructive pneumonia or bronchiectasis often results from inadequate treatment especially in children.

Viral infection patterns

Cytomegalovirus infection and herpes simplex cause a bronchioloitis and pneumonitis with a "ground glass" pattern identical to pneumocystis carinii infection.

Neoplasm patterns (fig 12.3)

Kaposi's sarcoma is a vascular tumour that occurs in up to 25% of all patients with AIDS. It is caused by the herpes type 8 virus and causes masses in the skin, bowel and lungs (*4*). In the chest, nodules are noted spreading from the hila peripherally along the pulmonary vessels and bronchi in "tongue" like projections.

Non Hodgkin's lymphoma presents in the lungs of these patients with pulmonary nodules or cavitating masses, however lymph node involvement in the hila and mediastinum is uncommon.

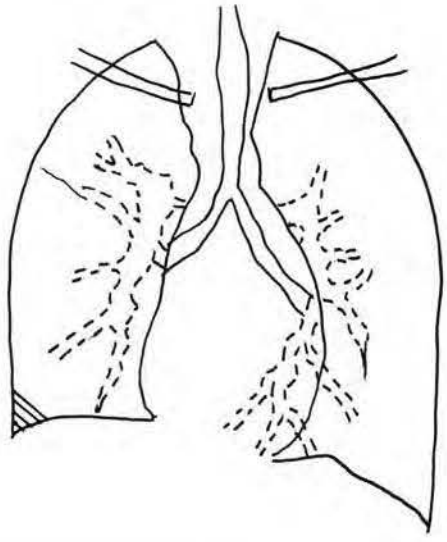

Fig 12.3 *Chest radiograph of an AIDS patient with pulmonary Kaposi's sarcoma. Note the hilar lymphadenopathy and the thickened bronchovascular markings in the perihilar regions.*

Lymphoproliferative interstitial pneumonia (LIP) pattern (fig 12.4)

Benign lymphocyte proliferation is a common cause of the miliary or small nodular pattern in AIDS patients (5). It is a benign response by lymphocytes to the HIV virus and is found in children and young adults. It is important to consider this pattern in the differential diagnosis of miliary tuberculosis.

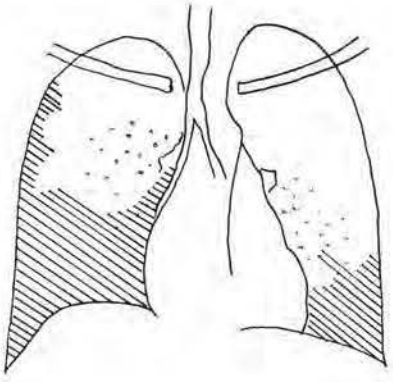

Fig 12.4
Chest radiograph of an AIDS patient with lympocytic interstitial pneumonitis. Note the miliary nodules in the lungs.

LEARNING POINTS: PULMONARY AIDS

- Tuberculosis is progressive, multifocal and often extrapulmonary in AIDS patients. Cavities are uncommon in severe immunosuppression. Lower lobe infiltrates and hilar adenopathy are common in adults.
- Pneumocystis pneumonia is common in severe immunosuppression. Ground glass opacification is common in both pneumocystis and cytomegalovirus infections.
- Bacterial infection is very common, and leads to destructive pneumonia and bronchiectasis.
- Viral infections especially cytomegalovirus and herpes simplex infections are common.
- Kaposi's sarcoma is the commonest neoplasm. Multiple nodules along the bronchovascular bundles are noted on chest radiographs and CT.
- Lymphocytic interstitial pneumonia (LIP) is a benign lymphocytic response to HIV. It causes multiple small pulmonary nodules. Main differential is miliary TB.

References

1. Fauci A. The AIDS epidemic-considerations for the 21st century. *NEJM* 1999;341:1046–1050.
2. Havlir D, Barnes P. Current concepts: Tuberculosis in patients with the human immunodeficiency virus infection. *NEJM* 1999;340:367–373.
3. Boiselle PM, Crans CA, Kaplan MA. The changing face of pneumocystis carinii pneumonia in AIDS patients. *AJR* 1999;172:1301–1309.
4. Antman K, Chang Y. Kaposi's sarcoma-review article. *NEJM* 2000;342:1027–1033.
5. Berdon WE, Mellins RB, Abramson SJ, Ruzal-Shapiro C. pediatric HIV infection in its second decade-the changing pattern of lung involvement. Clinical, plain film, and CT findings. *Rad Clin N America* 1993;31:453–463.

CHAPTER 13

Paediatric chest

Peter Corr

Children present challenges for the radiographer. The child will often not keep still for the radiograph so immobilization is important. This requires an assistant wearing a lead rubber apron and gloves to hold the child by the outstretched arms. Chests are taken in the AP position. You must be aware of the radiation exposure to the gonads of the child, and a lead strip must be placed over the gonadal area.

NEONATAL CHEST PATTERNS

Ground glass pattern in premature babies (fig 13.1)

A bilateral "ground glass" appearance to the lungs is found in premature babies with hyaline membrane disease and viral infections. Hyaline membrane disease is due to insufficient surfactant. Lung volumes are small and air bronchograms are commonly detected.

Fig 13.1
Chest radiograph of a premature infant with hyaline membrane disease. Note the pulmonary opacification and small volume lungs.

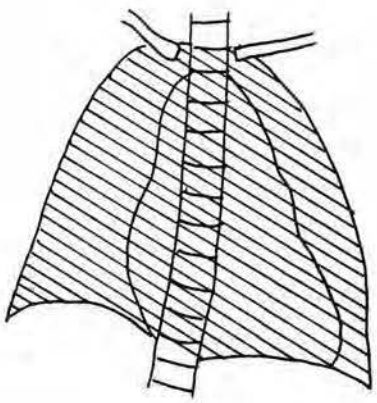

"Bubbly" or cystic lungs

Cystic lesions in the lungs of a neonate may be due to congenital diaphragmatic herniation of bowel that requires urgent surgery. This is due to a congenital defect in the left hemidiaphragm (fig 13.2). There is usually mediastinal shift to the opposite side. Usually both the compressed lung and contralateral lung are hypoplastic. Cystic adenomatoid malformation of the lung is a congenital malformation of the lung that usually presents as a cystic mass. There is usually no mediastinal shift away from the lesion.

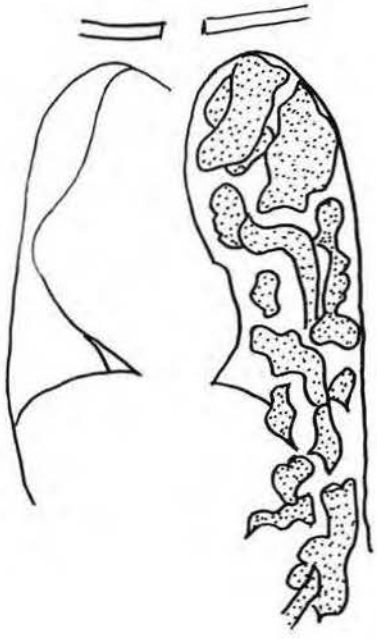

Fig 13.2
Chest radiograph of an infant with respiratory distress from a congenital diaphragmatic hernia in the left hemithorax.

Meconium aspiration pattern (fig 13.3)

The lungs are hyperinflated with perihilar opacities in these full term babies who have aspirated meconium into their lungs during labour. There are streaky linear opacities in both lungs.

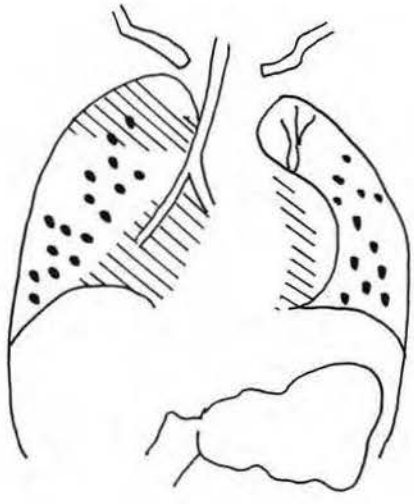

Fig 13.3
Chest radiograph of a neonate with respiratory following meconium aspiration. Lungs are hyperinflated with perihilar infiltrates.

INFANT CHEST PATTERNS

Bilateral air trapping pattern

Hyperinflated lungs with peribronchial infiltrates are found in bronchiolitis from viral infections especially the respiratory syncytial virus and adenovirus infections. It is important to exclude pneumonia, which may require antibiotic treatment.

Unilateral lung hyperinflation pattern

Unilateral lobar or segmental hyperinflation should suggest a foreign body in the bronchus causing a "ball valve" effect with air trapping in the lobe. By taking chest radiographs in inspiration and expiration the hyperinflation can be accentuated. Similarly lobar atelectasis in a child is due to an impacted foreign body until proven otherwise (fig 13.4).

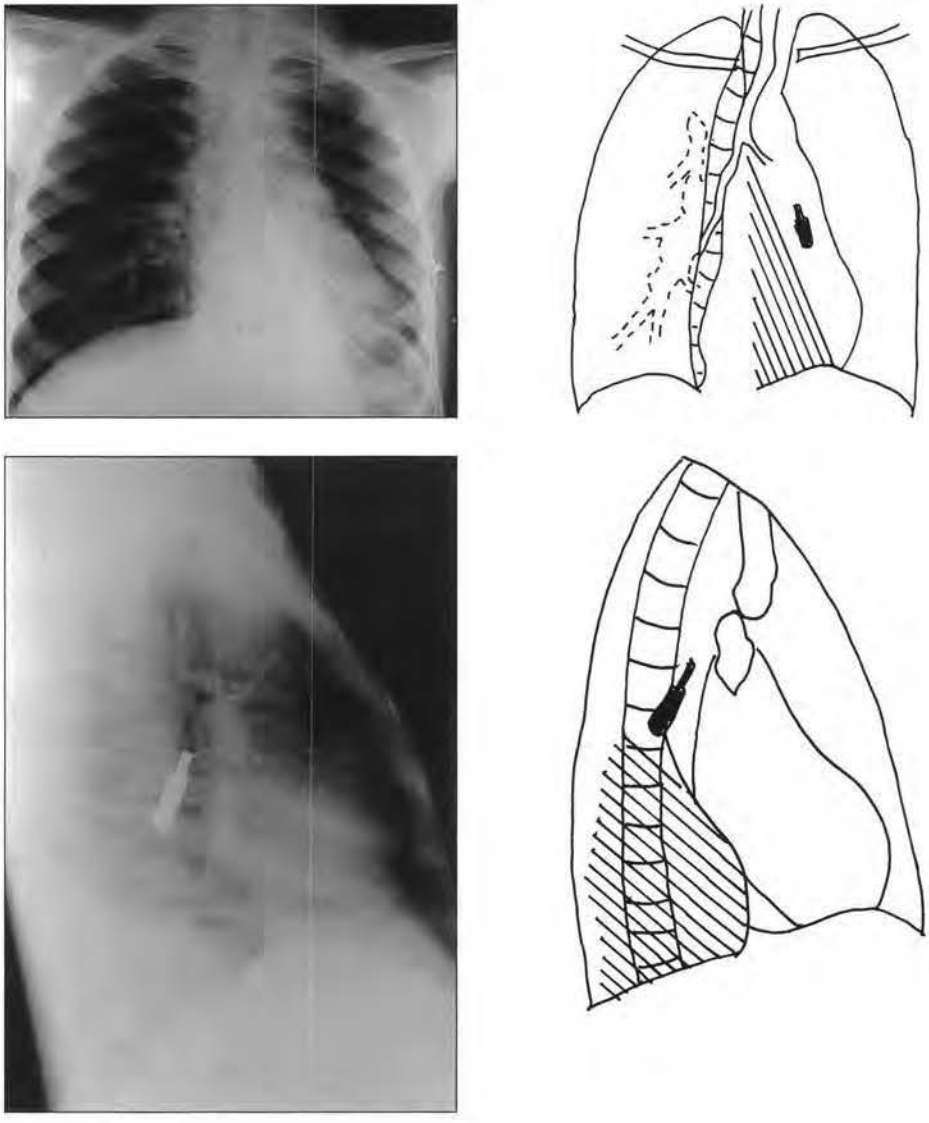

Fig 13.4
Chest radiograph of a child who aspirated a ball point pen tip (foreign body) into his left lower lobe bronchus causing lower lobe atelectasis.

Bronchopneumonia pattern

This is a very common pattern of peribronchial opacification of both lungs from viral and or bacterial infection. It is important not to confuse this pattern with cardiac failure where the heart is enlarged and there are often pleural effusions.

Pulmonary atelectasis pattern (figs 13.4a & 13.4b)

Unilateral volume loss and opacification of a lobe or segment of the lung may be due to bronchial obstruction from a foreign body, mucus plug as seen in pertussis, asthma, or enlarged hilar nodes in tuberculosis.

CHILDHOOD PNEUMONIA PATTERNS

Round pneumonia (fig 13.5)

This pattern is common in childhood infection and can mimic a mass in the lung. The key to this pattern is the presence of air bronchograms within the opacification. Round pneumonias occur because infection spreads easily through the interalveolar foramina.

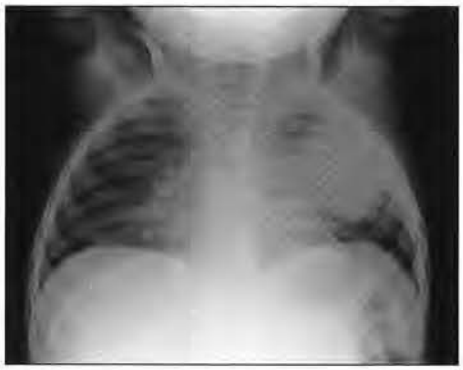

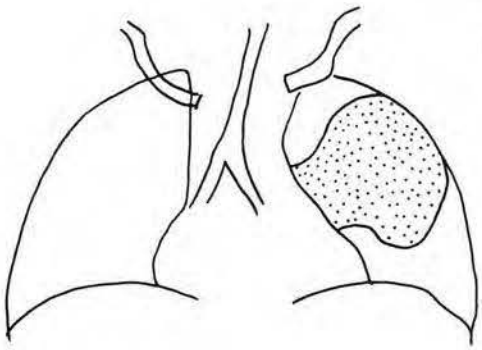

Fig 13.5
Round pneumonia.

Staphylococcal pneumonia pattern (figs 13.6a & 13.6b)

This is a serious pneumonia in children. There are features of a bronchopneumonia with multiple cavities or cysts. It is important to recognise this pattern because untreated or treated with the incorrect antibiotic will lead to very serious complications such as pneumothorax and empyema.

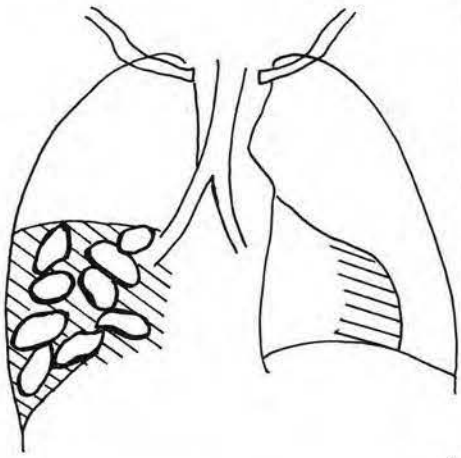

a

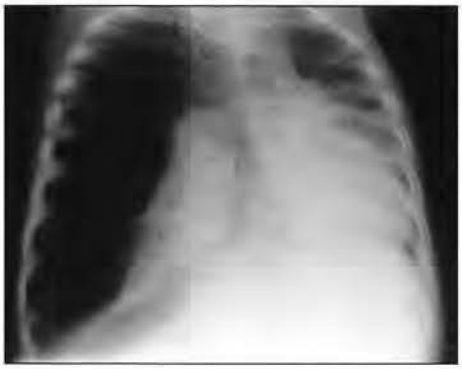

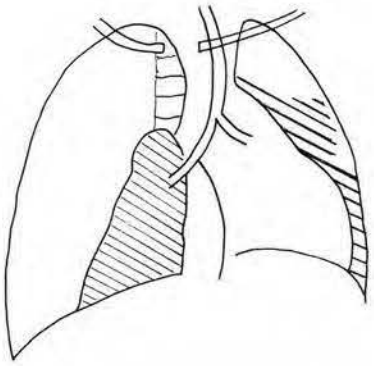

b

Fig 13.6a, 13.6b
Chest radiograph of an infant with staphylococcal pneumonia in the right lower zone with cavitation. A tension pneumothorax with collapse of the right lung is a recognised complication ***6b****.*

Primary TB pattern (figs 13.7a & 13.7b)

This pattern is detected in primary tuberculosis where there are large unilateral hilar and mediastinal lymph nodes which may cause bronchial obstruction and lobar atelectasis. The primary lung lesion is often not detected as an area of focal pulmonary opacification (Ghon focus).

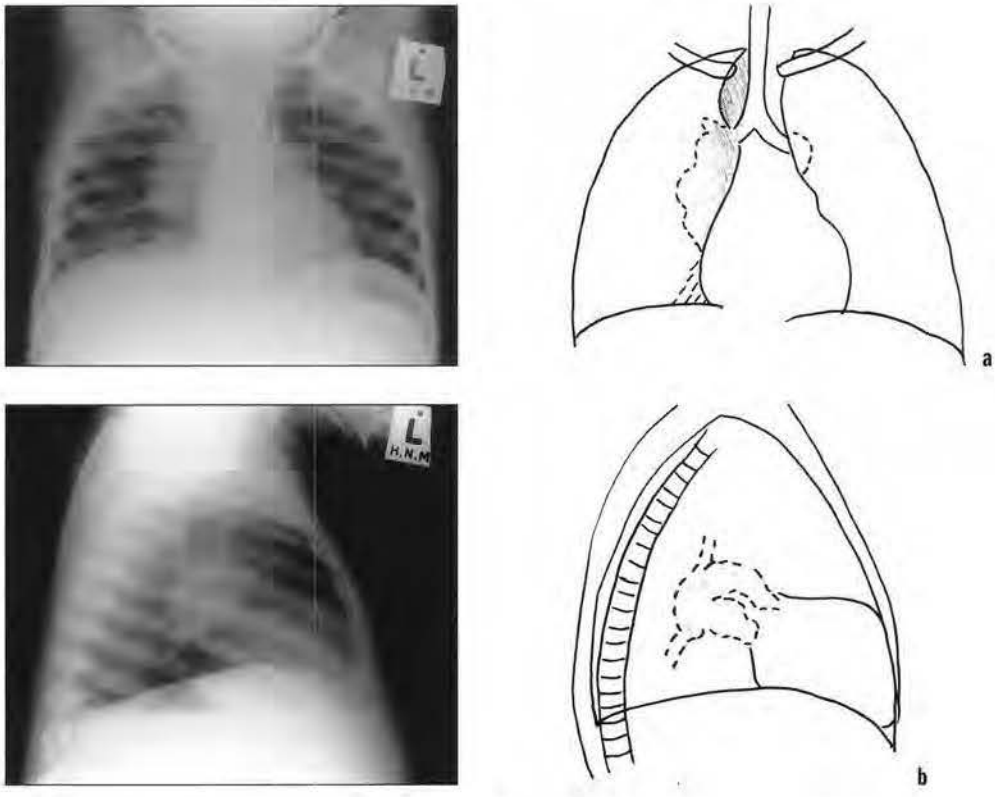

Fig 13.7
Chest radiograph of an infant with primary TB demonstrates right hilar and paratracheal lymphadenopathy.

LEARNING POINTS: PAEDIATRIC LUNG PATTERNS

- Hyaline membrane disease presents in premature babies with small volume lungs and ground glass opacification.
- Bubbly lungs in a neonate must suggest congenital diaphragmatic herniation if there is mediastinal shift to the opposite side.
- Meconium aspiration syndrome results in hyperinflated lungs with a streaky appearance in full term infants following meconium aspiration.
- Bilateral air trapping in infants should suggest bronchiolitis.
- Unilateral hyperinflation or lobar atelectasis of a lung or lobe should suggest an impacted foreign body in the bronchial tree.
- Round pneumonias in children can mimic lung masses but they often have bronchograms.
- Staphylococcal pneumonia presents with cavitating bronchopneumonia or cyst formation. Serious complications of pneumothorax and empyema can occur if not recognized early and treated.

CHAPTER 14

Cardiac disease

Peter Corr

Cardiac size (fig 14.1)

The heart size is normally 50% or less of the thoracic diameter in adults as measured from the inner borders of the lower ribs. It is important to use an erect chest film, preferably a PA film, with a good inspiration. A film focal distance of 180 cm is important for cardiac assessment. A poor inspiration and or a supine film is suboptimal as it results in the heart having an apparently increased transverse diameter and apparent cardiomegaly. In children up to 12 years of age the maximum heart size is 60% or less of the internal thoracic diameter.

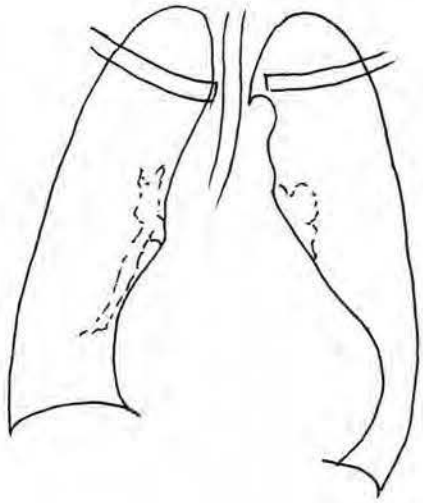

Fig 14.1
Chest radiograph of a patient with cardiomegaly.

Cardiac silhouette enlargement (fig 14.2)

Enlargement of the cardiac silhouette may be due to cardiomegaly or pericardial effusion. Pericardial effusion gives the heart a globular appearance with loss of the normal cardiac contour (fig 14.3). The diagnosis of pericardial effusion can be made by ultrasound examination using a 2 MHz transducer. There is a hypoechoic fluid collection in the preicardium surrounding the heart. **Common causes of pericardial effusions are:**

- **infection**—viral, pyogenic and tuberculous
- **neoplastic**—metastatic disease and direct invasion from breast and lung cancer
- **trauma**—haemopericardium or sympathetic effusion

Tuberculous pericarditis can be identified by detecting strands of fibrin in the pericardial effusion. As the effusion resolves pericardial constriction may occur. This can be identified as faint calcification of the pericardial lining on the PA chest radiograph.

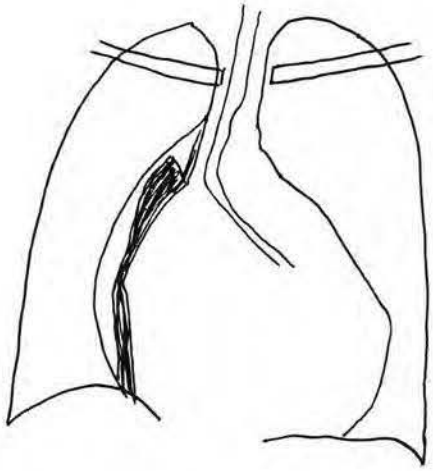

Fig 14.2
Chest radiograph of a patient with a pericardial effusion. Note the globular contour of the cardiac shadow.

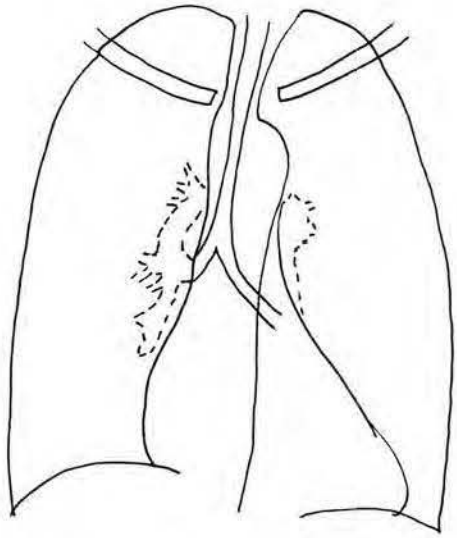

Fig 14.3
Chest radiograph of a patient with hypertension with left ventricular cardiomegaly. Note how the left cardiac border slopes towards the left costophrenic angle.

Mitral valve disease

Mitral valve disease causes enlargement of the left atrium and right ventricle following either mitral valve stenosis or incompetence as the end result of rheumatic heart disease. Enlargement of the left atrium is detected as a double shadow behind the right atrium on the PA chest radiograph with splaying of the carina of the trachea and posterior displacement of the oesophagus on barium swallow.

Aortic valve disease

Aortic valve stenosis causes left ventricular hypertrophy that is recognized as left displacement of the cardiac apex on the PA chest radiograph. Aortic valve incomptence, usually following rheumatic fever or infective endocarditis leads to left ventricular dilatation.

Cardiac failure pattern (figs 14.4 & 14.5)

Left ventricular failure initially causes pulmonary venous distension in the upper lobes and constriction of the pulmonary veins in the lower lobes. As the venous pressure

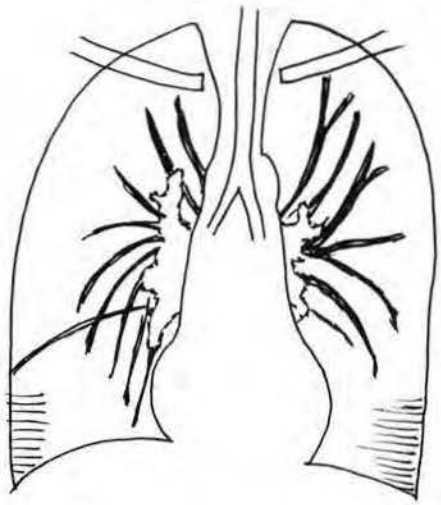

Fig 14.4
Chest radiograph of a patient with interstitial pulmonary oedema. Note the septal lines and prominent upper lobe pulmonary veins.

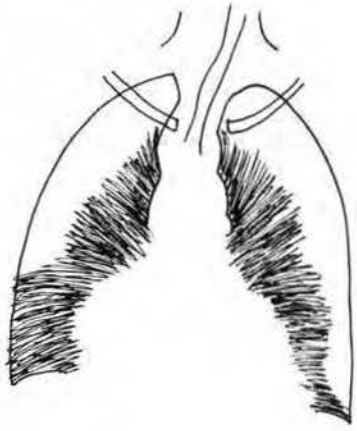

Fig 14.5
Patient in acute pulmonary oedema demonstrates pulmonary opacification and dilated upper lobe veins.

rises, there is perihilar oedema, detected as blurring of the hilar vessels and perihilar opacification. Pleural effusions develop at the costophrenic angles, then septal lines form at the CP angles.

Septal lines are 1–2 cm long and 1 mm thick in the region of the costophrenic angles. They represent distended lymphatics and are an early sign of **interstitial pulmonary oedema**. As the cardiac failure progresses there is perihilar opacification ("bats wing" distribution) which represents **alveolar pulmonary oedema**. Pulmonary oedema usually resolves rapidly over hours with diuretic and anti failure treatment. This pattern can be used to differentiate alveolar oedema from other air space opacification from pneumonia or pulmonary haemorrhage.

Pulmonary plethora pattern

Plethora means increased blood flow and is usually due to left to right intracardiac shunts such as an atrial septal defect, ventricular septal defect and patent ductus arteriosus. Pulmonary arteries are dilated from the hila out to the periphery of the lungs. This pattern should not be confused with pulmonary venous dilatation that involves only the upper lobes.

Pulmonary oligaemia pattern

This pattern is often difficult to recognise unless you have a history of cyanotic heart disease to suggest the correct diagnosis. The lungs have diminished pulmonary blood

flow however the bronchial arteries often enlarge to compensate for the pulmonary oligaemia and the lungs may appear plethoric. Pulmonary oligaemia is detected in the "3 T's": Tetralogy of Fallot, truncus arteriosus, and transposition of the great vessels. It is also seen in reversed left to right intracardiac shunts (ASD with pulmonary hypertension: Eisenmenger's syndrome fig 14.6).

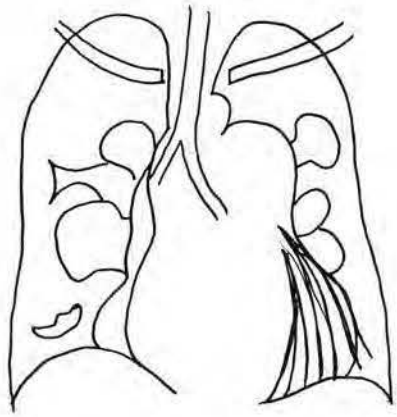

Fig 14.6 *Patient with pulmonary hypertension from an atrial septal defect (Eisenmenger syndrome). Note cardiomegaly, with dilated pulmonary arteries centrally and peripheral pruning.*

LEARNING POINTS: CARDIAC DISEASE

- Cardiomegaly >50% cardio thoracic ratio in adults, >60% in children less than 12 years.
- Remember cardiac silhouette enlargement may be due to cardiac dilatation, hypertrophy and pericardial effusion (globular contour). Pericardial effusion can easily be diagnosed by ultrasound.
- Signs of cardiac failure are upper lobe pulmonary vein distention, blurring of the perihilar vessels and pleural effusions and septal lines.
- Signs of pulmonary oedema are septal lines and perihilar opacities that often resolve within hours on anti-failure treatment.

CHAPTER 15

Mediastinal masses

Peter Corr

The mediastinum can be divided into superior, anterior, middle, and posterior compartments.

Superior mediastinum

The superior mediastinum is superior to the level of the aortic arch. Masses in this region include retrosternal thyroid masses and aneurysms of the ascending aorta and great vessels. Retrosternal goitres cause displacement of the trachea, extend inferiorly from the neck, and may have focal calcification within them. The diagnosis can be confirmed by ultrasound of the neck or by using A common cause of a superior mediastinal mass on the right is a dilated brachiocephalic artery in an elderly patient. Here the diagnosis can be easily confirmed by ultrasound. The important point to remember is that this is a normal aging phenomenon and not to do any further investigations on these patients.

Anterior mediastinum

This region is between the heart and ascending aorta and the sternum and inferior to the aortic arch. It is best visualized on a well penetrated lateral chest radiograph. The region contains lymph nodes, the thymus in children and the thymic remnant in adults, and the pericardium. Masses include: enlarged lymph nodes, thymic masses, teratomas or dermoids, and aneurysms of the ascending aorta. Often it is not possible to differentiate between these masses on radiographs however if the mass has a lobulated contour it suggests enlarged lymph nodes. Focal calcification is detected in dermoids and teratomas. Linear calcification may be detected in aortic aneurysms from syphilis or Takayashu's disease.

Middle mediastinum

This region is between the anterior and posterior mediastinum and contains the heart, great vessels, pulmonary vessels and lymph nodes. Masses in this region include: enlarged hilar and tracheobronchial lymph nodes, bronchogenic cysts, aortic arch aneurysms, and bronchial carcinomas.

Posterior mediastinum

The posterior mediastinum extends from the middle mediastinum to the spine and paraspinal gutters. It includes the descending thoracic aorta, lymph nodes, nerves and the oesophagus. Masses in this region: neurogenic tumours, paravertebral masses, tuberculous abscesses, oesophageal tumours, hiatus hernia, and dilated oesophagus. It is very important when a posterior mediastinal mass is detected to clearly visualise the spine, so as to detect early bony destruction or erosion from tuberculosis or bony metastases.

LEARNING POINTS: MEDIASTINAL MASSES

- Common superior mediastinum masses: retrosternal thyroid goitre, aneurysms of great vessels
- Common anterior mediastinum masses: 3T's teratomas or dermoids, retrosternal thyroid, thymoma and ascending aortic aneurysm
- Common middle mediastinum masses: lymphadenopathy, bronchogenic cysts, bronchial carcinoma
- Common posterior mediastinum masses: lymphadenopathy, neurogenic tumours, paraspinal abscess especially TB, oesophageal tumours

References

1. Chapman S, Nakielny R. *Aids to Radiological Differential Diagnosis*. 1995, Saunders, London.
2. Armstrong P. The Mediastinum. *In: Diagnostic Radiology—Textbook of Medical Imaging*. Grainger RG, Allison DJ. 3rd edition 1997 Churchill Livingstone, Edinburgh.

CHAPTER 16

Diaphragm lesions

Peter Corr

Diaphragmatic elevation

Eventration is a congenital deficiency of the muscle in the hemidiaphragm usually the left, resulting in non-function and resultant elevation. The diagnosis is confirmed on fluoroscopy/screening when there is limited or no movement on deep inspiration and expiration. If fluoroscopy is unavailable perform one chest film using a double exposure in inspiration and an expiration at 50% normal mas, this will show movement of the diaphragm. Eventration must be distiguished from phrenic nerve palsy.

Phrenic nerve palsy results in paralysis of diaphragmatic movement on one side resulting in elevation of the hemidiaphragm and limited or paradoxical movement on deep inspiration and expiration. There are many causes, however the commonest causes is carcinoma of the bronchus.

Subphrenic masses, liver enlargement and abscesses will elevate the hemidiaphragm. On the chest radiograph with a liver or right subphrenic abscess, the right hemidiaphragm is elevated and its outline becomes "fuzzy" or ill-defined with associated linear atelectasis in the right lower lobe. This is a very important pattern to recognise as you need to perform an ultrasound examination of the right subphrenic space and liver to detect an abscess. Pseudo elevation is seen with **subpulmonic pleural effusions** and haemothoraces. The apex of the "elevated hemidiaphragm" is usually displaced more laterally that what is normally seen. A decubitus chest film with the affected side dependent will confirm the diagnosis.

Diaphragmatic injury is commonly missed especially following penetrating trauma. Injury is nine times more common on the left. The diagnosis can be difficult to make. On the left, detection of bowel loops above the hemidiaphragm or a soft tissue mass contiguous to the diaphragm is suspicious. A contrast study of the stomach and colon will confirm the diagnosis. If there is incarcerated bowel present is will be opacified by contrast above the diaphragm.

CHAPTER 17

Pneumoconiosis

Peter Corr

Occupational dust exposure is a common cause of lung disease in many developing countries. You must always ask whether the patient has been exposed to dust at work.

Small nodules

This is the commonest occupational dust exposure pattern and results from inorganic dust exposure such as silica. The nodules are around 1–2 mm size and dense compared to the granulomas of tuberculosis (fig 17.1). Hilar nodes may be enlarged and have peripheral calcification ("egg shell" calcification). A complication of silicosis is conglomeration of the nodules into large masses of fibrosis called progressive massive fibrosis (fig 17.2).

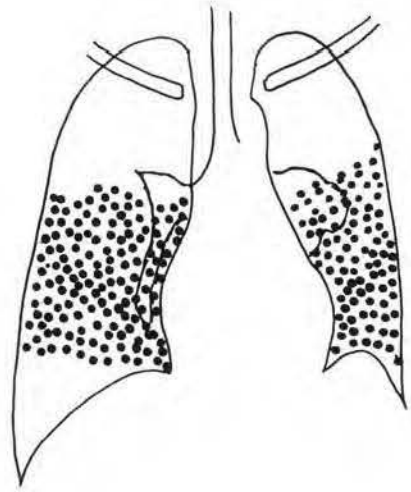

Fig 17.1 *Patient with silicosis. Note dense bilateral pulmonary nodules in mid zones of the lungs.*

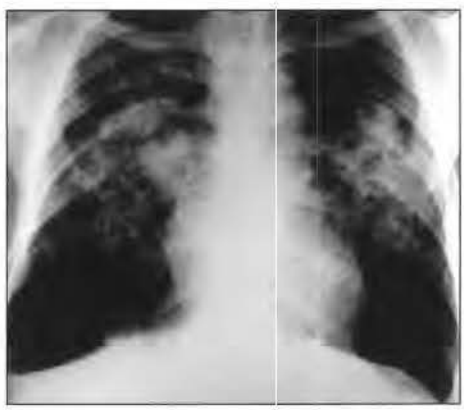

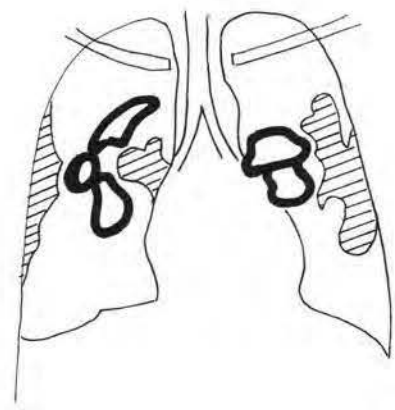

Fig 17.2 *Patient with progressive massive fibrosis with bilateral perihilar masses centrally.*

Asbestos exposure

The most common appearance are pleural plaques which become easier to see once they calcify giving a "holly leaf" appearance. Diaphragmatic calcification is also common. These findings indicate asbestos exposure (fig 17.3). Pulmonary asbestosis presents with a linear or reticular fibrosis of the lower lobes and represents pulmonary fibrosis from asbestos exposure. Mesothelioma is a pleural malignancy that spreads circumferentially along the pleura. The diagnosis is usually made by biopsy. The differential diagnosis is encysted pleural fluid that can be detected by using a 5 MHz ultrasound transducer on the chest wall.

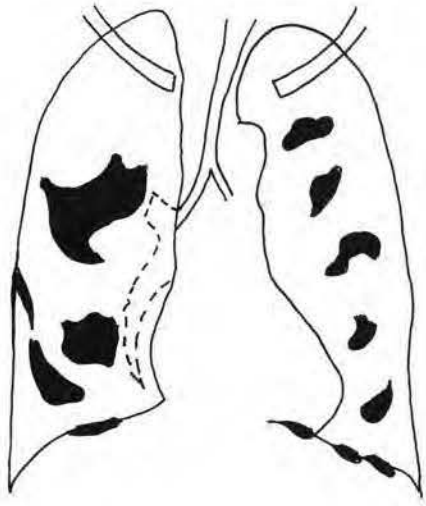

Fig 17.3
Patient with asbestos dust exposure demonstrates multiple calcified plaques on the paritetal pleural surface.

LEARNING POINTS: PNEUMOCONIOSIS

- Always ask the patient about dust exposure
- Consider silicosis in the small nodular lung pattern especially when the nodules appear very white or dense
- Consider asbestosis esposure when there are calcified pleural plaques and or calcification of the diaphragm

PART 3

MUSCULOSKELETAL PATTERNS

CHAPTER 18

Approach to focal bone lesions

Fei-Ling Thoo & Wilfred C.G. Peh

Focal bone lesions can generally be divided into benign and malignant bone lesions. The malignant group can be further subclassified into primary and secondary tumours. The secondary tumours can arise from transformation of benign conditions or from metastatic lesions.

Clinical information

The patient's age and determination of whether a lesion is solitary or multiple are important approaches in the diagnosis of bone tumours. Aneurysmal bone cysts rarely occur beyond 20 years of age. Giant cell tumour usually occurs after the closure of the growth plate. Metastases tend to be multi-focal and are more common in the older age group. The rate of tumour growth may be an additional factor in differentiating malignant tumours (usually rapid growing) from benign lesions (slower growing). It is also important to know if a lesion is an incidental finding or is symptomatic. If painful, the lesion requires attention regardless of its imaging appearance. Some benign osseous tumours may undergo sarcomatous transformation and this should also be considered in a patient who presents with pain and a lesion that appears benign.

Imaging modalities

In the evaluation of bone tumours, plain radiographs are the standard imaging study. The choice of the imaging technique is dictated by the type of the suspected tumour and also by equipment available. Imaging modalities for bone tumours include bone scintigraphy, CT scan, MRI and angiography. CT is superior to MR for the detection of calcification in the tumour matrix, cortical erosions and periosteal reaction. If the radiographs suggest cortical destruction and soft tissue mass, MRI would be the preferred as it provides excellent soft tissue contrast and can determine the extraosseous extent of tumour much better than CT.

Site of the lesion

The bone tumour can be epiphyseal, metaphyseal or diaphyseal in location. There is predilection of some bone tumours for specific sites in the bone.

Skeletal predilection of benign osseous neoplasms include

Enchondroma—short tubular bones (fig. 18.1)

chondroblastoma—epiphyses

giant cell tumour—articular ends of the femur, tibia and radius chondromyxoid

fibroma—tibial metaphyses

simple bone cyst—proximal humerus and femur

osteoid osteoma—femur and tibia

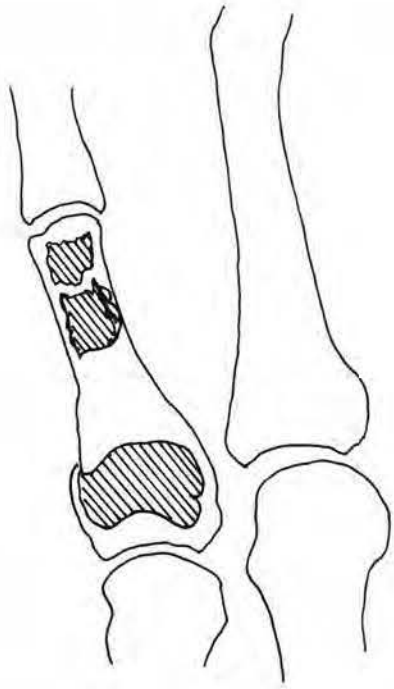

Fig 18.1 *Shows fracture through an enchondroma located in the proximal phalanx of the little finger. The tubular bones of the fingers are typical sites for enchondroma.*

Skeletal predilections for malignant osseous tumours include

chordoma—sacrum, clivus, C2

multiple myeloma—pelvis, spine and skull

parosteal osteosarcoma—posterior cortex of posterior femur

chondrosarcoma—epiphyseal lesion of femur and humerus

adamantinoma—tibia, fibula

Lesions that have a predilection for flat bones such as the scapula body and the iliac wing or the diaphyses of long bones include Ewing sarcoma, lymphoma and Langerhans cell histiocytosis (eosinophilic granuloma). Ewing sarcoma would be more likely in a younger age group. Lymphoma can be seen in any age but peaks later in life. Langerhans cell histiocytosis can be seen at any age.

Borders of the lesion

Slow growing lesions are usually benign and have sharply outlined sclerotic borders (narrow zone of transition). An example of a benign lesion (non ossifying fibroma) is shown in fig 18.2. Aggressive or malignant lesions typically have indistinct borders (a wide zone of transition) with either minimal or no reactive sclerosis (fig 18.3). This is seen in fig 18.4 of a child with osteogenic sarcoma. Treatment can alter the appearance of malignant bone tumours; they may exhibit sclerosis as well as a narrow zone of transition.

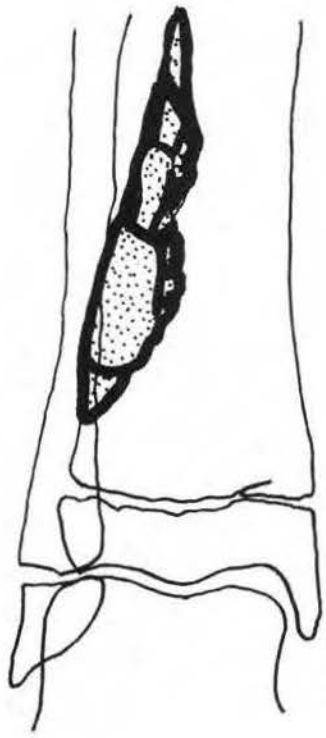

Fig 18.2
Well defined osteolytic lesion with sharply outlined sclerotic border and a narrow zone of transition in the distal right tibia due to a non-ossifying fibroma.

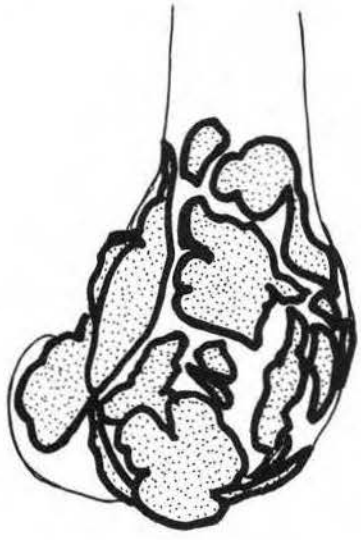

Fig 18.3
Expansive osteolytic lesion in the subarticular region of the distal femur in keeping with a giant cell tumour.

Fig 18.4
Plain radiograph of an osteogenic sarcoma in the proximal left humerus of a child. There is an osteolytic lesion in the diametaphyseal region which shows a poor zone of transition. Adjacent sunburst periosteal reaction and soft tissue mass are present.

Type of matrix

Osteoblastic and cartilaginous matrix can be recognized radiographically. Osteogenic sarcomas can form cloud-like dense osteogenic matrix. Cartilaginous tumours can be identified by popcorn-like, punctate, annular or comma-shaped calcifications. Cartilage tumours tend to grow in lobules and can be identified by their lobulated growth (fig 18.5).

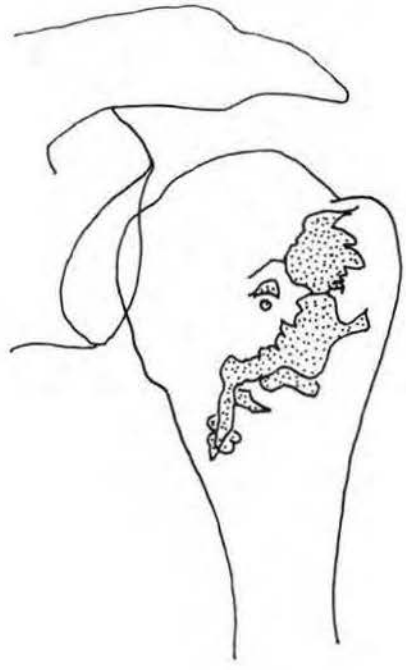

Fig 18.5
Plain radiograph shows calcification within the medullary cavity from a chondroid tumour.

Type of bone destruction

The type of bone destruction can be described as geographic, moth-eaten or permeative. A benign process tends to show a geographic—uniformly destroyed area with sharply

defined border. A likely malignant process shows moth-eaten areas of destruction with ragged borders. It should be kept in mind that non-neoplastic lesions like osteomyelitis may also appear as an aggressive destructive bone lesion with moth eaten areas. The clinical presentation, radiographic findings of cloaca and sequestrum and uninterrupted periosteal reaction would be helpful in the diagnosis of osteomyelitis. The permeative bone destruction is indicative of a more aggressive (malignant) process with ill-defined area spreading through the bone marrow. This is seen in Ewing's sarcoma and bone lymphoma.

Periosteal reaction

The type of periosteal reaction is one of the most important features in determining the aggressiveness of the bone lesion. Periosteal reactions are discussed in the next chapter.

Soft tissue extension

Benign tumours do not exhibit soft tissue extension. Few exceptions are giant cell tumours, aneursysmal bone cysts, osteoblastomas and desmoplastic fibromas. It should be kept in mind that non-neoplastic conditions such as osteomyelitis also show a soft tisssue component, the involvement of the soft tissue is usually poorly defined, with obliteration of the soft tissue layers. In a malignant process, the soft tissue component is sharply defined, extending through the destroyed cortex.

If a bone lesion is associated with a large soft tissue mass, round cell tumours should be a consideration. These include metastatic neuroblastoma (seen in infancy), Ewing's sarcoma, primitive neuroectodermal tumour (paediatric patients), lymphoma (most common in adults) and plasmacytoma (seen in the middle-aged to elderly population).

Multiplicity of lesions

i) Multiple malignant appearing lesions usually indicate metastatic disease, multiple myeloma or lymphoma.

ii) Benign lesions with multifocal presentations include polyostotic fibrous dysplasia, multiple enchondromas, enchondromatosis, histiocytosis, haemangiomatosis, and Paget's disease.

Management: biopsy versus "do not touch lesions"

There are certain features of a bone lesion on a radiograph, which help distinguish between benign and malignant lesions. Benign lesions usually have well defined sclerotic borders, a geographic type of bone destruction, an uninterrupted solid periosteal reaction and no soft tissue mass. Malignant lesions have poorly defined borders with a wide zone of transition, a "moth eaten" or permeative pattern of bone destruction, an interrupted periosteal reaction of a "sun burst" or "onion skin" type and an adjacent soft tissue mass. The analysis of a lesion involves clinical and radiological information. A decision must be made whether the lesion is definitely benign and not to be biopsied ("a do not touch" lesion) but rather monitored or whether a biopsy is required.

The following is a list of "do not touch" lesions

Tumour and tumour-like lesions

Fibrous cortical defect

Non ossifying fibroma

Cortical desmoid

Solitary fibrous dysplasia

Pseudotumour of haemophilia

Intraosseus ganglion

Enchondroma of a short tubular bone

Non neoplastic processes

Stress fracture

Avulsion fracture

Bone infarct

Bone island

Myositis ossificans

Degenerative or post traumatic cysts

Brown tumour of hyperparathyroidism

Discogenic vertebral sclerosis

LEARNING POINTS: FOCAL BONE LESIONS

- Helpful clinical data are:
  (a) age of the patient
  (b) duration of symptoms and
  (c) growth rate of the tumour
- Key radiographic features:
  (a) site of tumour
  (b) border of the lesion
  (c) type of matrix
  (d) type of bone destruction
  (e) type of periosteal reaction
  (f) the presence of absence of soft tissue extension
- A lesion is slow growing (likely to be benign) when it shows:
  (a) geographic bone destruction
  (b) sclerotic margin
  (c) solid, uninterrrupted periosteal reaction, or no periosteal response
  (d) no soft tissue mass
- A lesion is aggressive (likely to be malignant) when it shows:
  (a) poorly defined margins
  (b) moth-eaten or permeative type of bone destruction
  (c) interrupted periosteal reaction
  (d) soft tissue mass
- A lesion is likely to represent a cartilage tumour when it shows:
  (a) lobulation (endosteal scalloping)
  (b) calcifications in the matrix

CHAPTER 19

Periosteal reactions

Lai-Ping Chan & Wilfred C.G. Peh

The periosteum is a thick layer of fibrous tissue that covers the surface of the bone. The periosteum has abundant neurovascular supply and the cells in the deeper layers are able to form bone. The periosteum is not normally seen on imaging but when it responds to various bony insults, the resultant periosteal reaction is seen as projections of bone arising from the bony cortex. There are several patterns of periosteal reaction, and they can be due to benign or malignant conditions. Careful perusal of the underlying bone will give important clues about the etiology of the periosteal reaction.

Patterns of periosteal reactions

Periosteal reactions can be solid or interrupted. Four types are described:

SOLID PERIOSTEAL REACTIONS

Thin undulating periosteal reaction (diagram 19A)

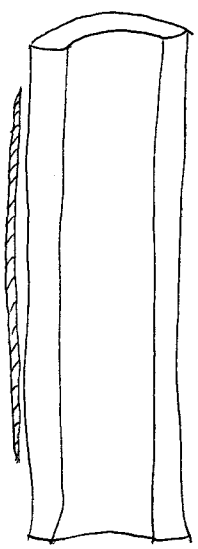

Diagram 19A

This appears as an undulating bony margin around the shafts of the bone, sparing the epiphysis. This type of periosteal reaction tends to be bilateral and symmetrical and is commonly due to systemic disease rather than a localized process. This pattern, when due to vascular insufficiency (either arterial, venous or lymphatic) is usually found in the legs with soft tissue swelling. Another cause of an undulating periosteal reaction is hypertrophic pulmonary osteoarthropathy (HPOA). In these patients, the underlying bone may appear osteoporotic. Patients with HPOA have painful swelling of the joints, especially the wrists and ankles. They may also have clubbing of the fingers. HPOA is often secondary to chronic pulmonary disease, heart disease, inflammatory bowel disease, liver disease and malignancy. It is important to do a chest X-ray to exclude thoracic causes of the disease.

Thick solid periosteal reaction (diagram 19B)

This periosteal reaction tends to merge with the cortex of the bone. The cortex of the bone can appear sclerotic and thickened. This can be due to an osteoid osteoma, a benign neoplasm of the bone. This occurs in young patients who usually present with pain. The lesion tends to occur in the long bones such as the femoral neck, the proximal tibia, fibula, and humerus. The lesion appears as a radiolucent area within the

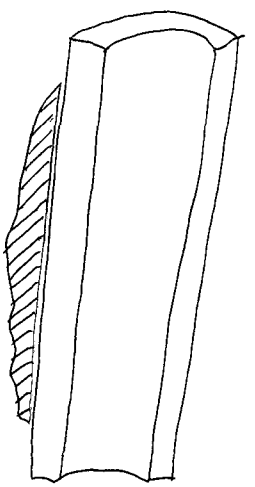

Diagram 19B

defined border. A likely malignant process shows moth-eaten areas of destruction with ragged borders. It should be kept in mind that non-neoplastic lesions like osteomyelitis may also appear as an aggressive destructive bone lesion with moth eaten areas. The clinical presentation, radiographic findings of cloaca and sequestrum and uninterrupted periosteal reaction would be helpful in the diagnosis of osteomyelitis. The permeative bone destruction is indicative of a more aggressive (malignant) process with ill-defined area spreading through the bone marrow. This is seen in Ewing's sarcoma and bone lymphoma.

Periosteal reaction

The type of periosteal reaction is one of the most important features in determining the aggressiveness of the bone lesion. Periosteal reactions are discussed in the next chapter.

Soft tissue extension

Benign tumours do not exhibit soft tissue extension. Few exceptions are giant cell tumours, aneursysmal bone cysts, osteoblastomas and desmoplastic fibromas. It should be kept in mind that non-neoplastic conditions such as osteomyelitis also show a soft tisssue component, the involvement of the soft tissue is usually poorly defined, with obliteration of the soft tissue layers. In a malignant process, the soft tissue component is sharply defined, extending through the destroyed cortex.

If a bone lesion is associated with a large soft tissue mass, round cell tumours should be a consideration. These include metastatic neuroblastoma (seen in infancy), Ewing's sarcoma, primitive neuroectodermal tumour (paediatric patients), lymphoma (most common in adults) and plasmacytoma (seen in the middle-aged to elderly population).

Multiplicity of lesions

i) Multiple malignant appearing lesions usually indicate metastatic disease, multiple myeloma or lymphoma.

ii) Benign lesions with multifocal presentations include polyostotic fibrous dysplasia, multiple enchondromas, enchondromatosis, histiocytosis, haemangiomatosis, and Paget's disease.

Management: biopsy versus "do not touch lesions"

There are certain features of a bone lesion on a radiograph, which help distinguish between benign and malignant lesions. Benign lesions usually have well defined sclerotic borders, a geographic type of bone destruction, an uninterrupted solid periosteal reaction and no soft tissue mass. Malignant lesions have poorly defined borders with a wide zone of transition, a "moth eaten" or permeative pattern of bone destruction, an interrupted periosteal reaction of a "sun burst" or "onion skin" type and an adjacent soft tissue mass. The analysis of a lesion involves clinical and radiological information. A decision must be made whether the lesion is definitely benign and not to be biopsied ("a do not touch" lesion) but rather monitored or whether a biopsy is required.

The following is a list of "do not touch" lesions

Tumour and tumour-like lesions

Fibrous cortical defect

Non ossifying fibroma

Cortical desmoid

Solitary fibrous dysplasia

Pseudotumour of haemophilia

Intraosseus ganglion

Enchondroma of a short tubular bone

Non neoplastic processes

Stress fracture

Avulsion fracture

Bone infarct

Bone island

Myositis ossificans

Degenerative or post traumatic cysts

Brown tumour of hyperparathyroidism

Discogenic vertebral sclerosis

LEARNING POINTS: FOCAL BONE LESIONS

- Helpful clinical data are:
  - (a) age of the patient
  - (b) duration of symptoms and
  - (c) growth rate of the tumour
- Key radiographic features:
  - (a) site of tumour
  - (b) border of the lesion
  - (c) type of matrix
  - (d) type of bone destruction
  - (e) type of periosteal reaction
  - (f) the presence of absence of soft tissue extension
- A lesion is slow growing (likely to be benign) when it shows:
  - (a) geographic bone destruction
  - (b) sclerotic margin
  - (c) solid, uninterrrupted periosteal reaction, or no periosteal response
  - (d) no soft tissue mass
- A lesion is aggressive (likely to be malignant) when it shows:
  - (a) poorly defined margins
  - (b) moth-eaten or permeative type of bone destruction
  - (c) interrupted periosteal reaction
  - (d) soft tissue mass
- A lesion is likely to represent a cartilage tumour when it shows:
  - (a) lobulation (endosteal scalloping)
  - (b) calcifications in the matrix

CHAPTER 19

Periosteal reactions

Lai-Ping Chan & Wilfred C.G. Peh

The periosteum is a thick layer of fibrous tissue that covers the surface of the bone. The periosteum has abundant neurovascular supply and the cells in the deeper layers are able to form bone. The periosteum is not normally seen on imaging but when it responds to various bony insults, the resultant periosteal reaction is seen as projections of bone arising from the bony cortex. There are several patterns of periosteal reaction, and they can be due to benign or malignant conditions. Careful perusal of the underlying bone will give important clues about the etiology of the periosteal reaction.

Patterns of periosteal reactions

Periosteal reactions can be solid or interrupted. Four types are described:

SOLID PERIOSTEAL REACTIONS

Thin undulating periosteal reaction (diagram 19A)

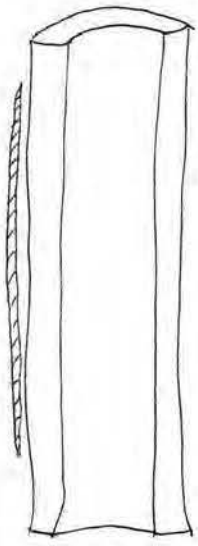

Diagram 19A

This appears as an undulating bony margin around the shafts of the bone, sparing the epiphysis. This type of periosteal reaction tends to be bilateral and symmetrical and is commonly due to systemic disease rather than a localized process. This pattern, when due to vascular insufficiency (either arterial, venous or lymphatic) is usually found in the legs with soft tissue swelling. Another cause of an undulating periosteal reaction is hypertrophic pulmonary osteoarthropathy (HPOA). In these patients, the underlying bone may appear osteoporotic. Patients with HPOA have painful swelling of the joints, especially the wrists and ankles. They may also have clubbing of the fingers. HPOA is often secondary to chronic pulmonary disease, heart disease, inflammatory bowel disease, liver disease and malignancy. It is important to do a chest X-ray to exclude thoracic causes of the disease.

Thick solid periosteal reaction (diagram 19B)

This periosteal reaction tends to merge with the cortex of the bone. The cortex of the bone can appear sclerotic and thickened. This can be due to an osteoid osteoma, a benign neoplasm of the bone. This occurs in young patients who usually present with pain. The lesion tends to occur in the long bones such as the femoral neck, the proximal tibia, fibula, and humerus. The lesion appears as a radiolucent area within the

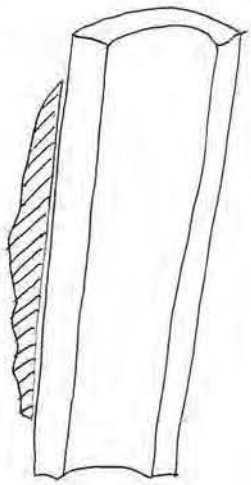

Diagram 19B

thickened bony cortex with a central sclerotic nidus (fig 19.1). A Brodie's abscess can have a similar appearance (fig 19.2). This is a subacute osteomyelitis that is most commonly due to staphylococcus aureus. The tibial metaphysis is the most common site and the lesion appears as a lucent area surrounded by dense sclerosis. The bony cortex may be thickened. The lesion can be cortical or intra-medullary in location. A Brodie's abscess can be differentiated from an osteoid osteoma if a sinus track or channel can be detected.

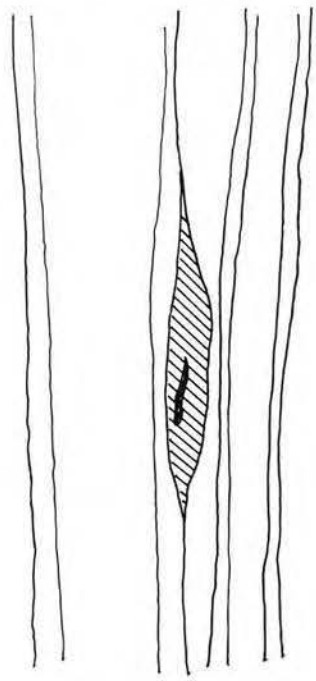

Fig 19.1
Osteoid osteoma of the shaft of the tibia with a thick solid periosteal reaction and thickened cortex. Note the small radiolucent nidus.

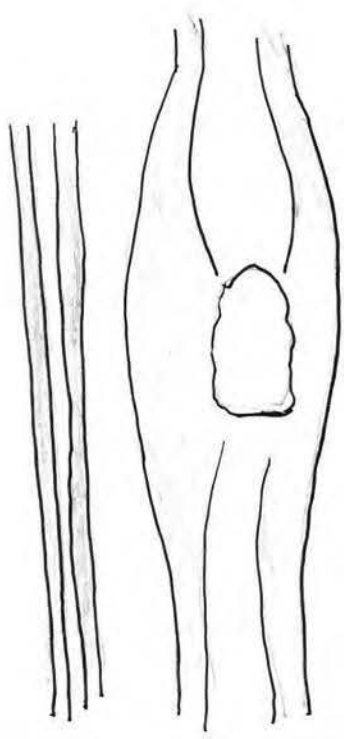

Fig 19.2
Brodie's abscess of the proximal tibia demonstrates a thick periosteal reaction with surrounding sclerosis.

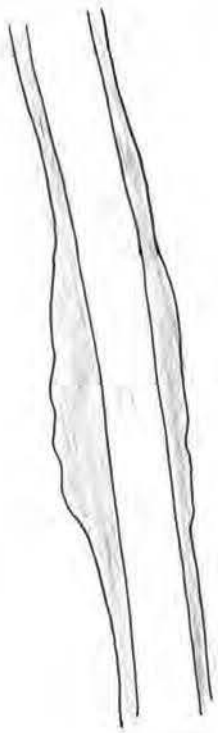

Fig 19.3
Chronic osteomyelitis of the humerus demonstrates marked cortical thickening with a thick periosteal reaction.

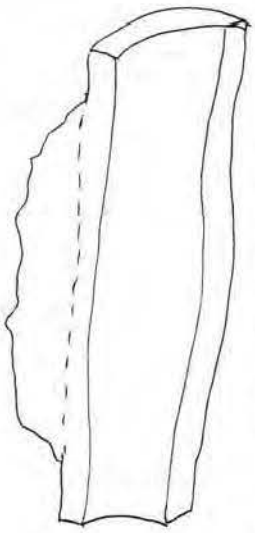

Diagram 19C

Cloaking periosteal reaction (diagram 19C)

This type of periosteal reaction is very abundant and covers almost the entire bone. If it occurs in a single bone, this is usually due to chronic osteomyelitis. There is usually associated thickening and sclerosis of the underlying bone (fig 19.3). There may be underlying radiolucent areas present due to involuted bone and also dead detached cortical bone, which appears very dense (sequestrum). There is often underlying bone destruction and new bone formation. There may be soft tissue swelling present. A sinus track leading to the skin may be present within the soft tissue. If this type of periosteal reaction occurs in multiple bones in young infants, the diagnosis can be congenital syphilis whose hallmark is a bilateral symmetrical osteomyelitis involving multiple bones (fig 19.4). The underlying bone will show evidence of bony destructionin the metaphysis, which appears as lucent bands adjacent to a widened epiphyseal plate. The metaphysis may also appear frayed. Bilateral and symmetrical focal bone destruction in the medial aspects of the proximal tibial metaphyses is known as Wimberger's sign and is almost pathognomonic of congenital syphilis.

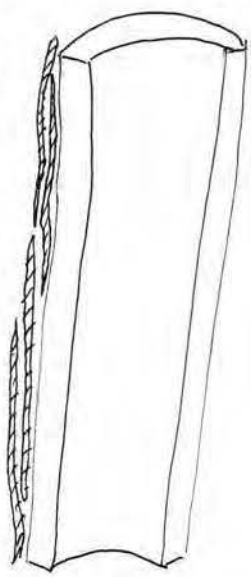

Diagram 19D

Lamellated periosteal reaction (diagram 19D)

In this pattern, the periosteum has an appearance like an "onion skin" with many layers around the shaft of the bone. This can

Fig 19.4
Cloaking periosteal reaction along the shaft of the tibia in keeping with congenital syphilis.

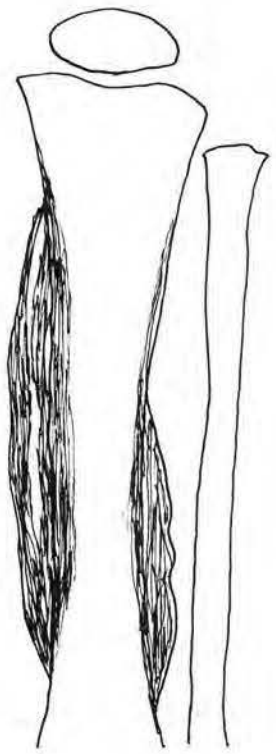

Fig 19.5
"Onion skin' periosteal reaction in Ewing's sarcoma of the clavicle.

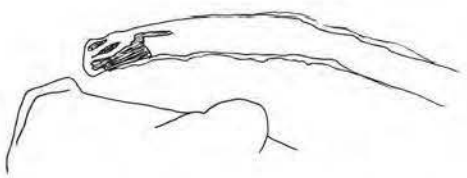

be due to tumours such as osteosarcoma and Ewing's sarcoma (fig 19.5), or chronic osteomyelitis.

In children, rickets can also give this appearance as uncalcified subperiosteal osteoid separates the periosteum and the ossified cortex of the bone. The underlying bone appears poorly mineralised and there may be deformities such as bowing. The epiphyseal appears widened due to an abundance of unossified osteoid and there may be cupping and fraying of the metaphysis. In scurvy, subperiosteal haemorrhages can occur and during healing, the periosteum can calcify, giving the appearance of lamellae around the bone (fig 19.6).

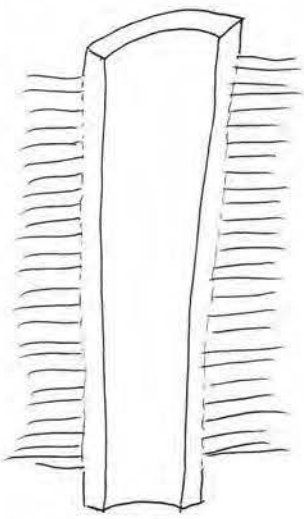

Diagram 19E

INTERRUPTED PERIOSTEAL REACTIONS

Four types are discussed:

"Hair-on-end" periosteal reaction (diagram 19E)

These appear as straight projections of bone that are parallel to the bony cortex, like hairs standing on-end.

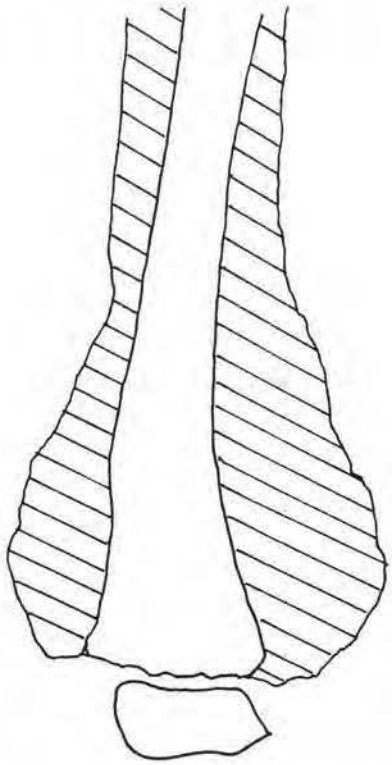

Fig 19.6
Large calcified subperiosteal haematoma around the distal femur in a patient with scury.

This is usually due to an aggressive process such as a bone tumour or acute osteomyelitis. Ewing's sarcoma is a tumour that typically causes this appearance. There is usually associated destruction of the bony cortex. Ewing's sarcoma occurs in the young, with most cases occuring in patients less than 20 years of age. The long bones are affected in 60% of patients and the flat bones in the other 40%. This tumour tends to involve the diaphysis and there are mottled "moth-eaten" destructive changes in the underlying bone. There may also be soft tissue swelling but unlike osteomyelitis, the soft tissue planes are usually preserved. The radiographic changes of acute osteomyelitis begin usually after a few days (initial radiographs tend to be normal). There is soft tissue swelling adjacent to the bone and the fat planes are obliterated. There may be elevation of the periosteum associated with the periosteal reaction (especially in children). The underlying bone will show destructive changes. In children, the common site to be affected is the bony metaphysis. As the disease progresses, involucrum and sequestrum can develop. Growth disturbances to the bone may occur, either shortening of the bone due to epiphyseal destruction or premature maturation of the epiphysis due to hyperemia. A "hair-on end" appearance can also be seen in the skull vault (sparing the occipital bone) and this is usually due to chronic haemolytic anaemias such as sickle cell anaemia and thalassaemia (fig 19.7). In these patients, the bone marrow expansion within the skull causes this appearance.

"Sunray" periosteal reaction (diagram 19F)

In this pattern, spicules of bone radiate from the bone in a divergent manner, just like the rays of the sun (fig 19.8). This type of periosteal reaction typically occurs in osteosarcoma. This common malignant primary bone tumour has a peak age of involvement from 10 to 25 years of age, and another peak after 60 years. The tumour tends to involve the metadiaphyseal region of long bones and is especially common around the knee. The tumour can be seen usually expanding and destroying the

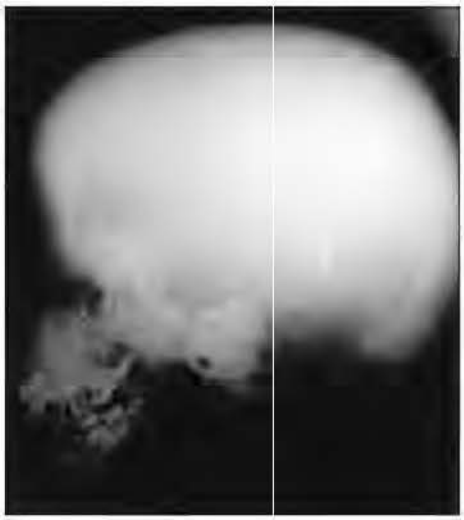

Fig 19.7 *"Hair on end" periosteal reaction of the skull in a child with thalasemia major.*

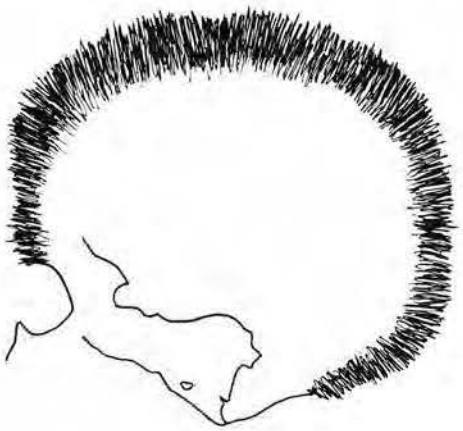

underlying bone. At the margins of the lesion, periosteum is lifted up by the tumour and this elevation is termed a "Codman's triangle". There is usually a soft tissue mass and abnormal tumourous new bone formation is a prominent feature. A pathological fracture may also be present. Codman's triangle is not pathognomonic of osteosarcoma, and can occur in any condition that elevates the periosteum. At the periphery of the lesion, the elevated periosteum calcifies, forming a triangle with the cortex of the bone. Though not specific, Codman's triangle does tend to occur in more aggressive lesions such as tumour or infection. Bony metastases, especially those from colonic tumours, can also cause a sunray periosteal reaction.

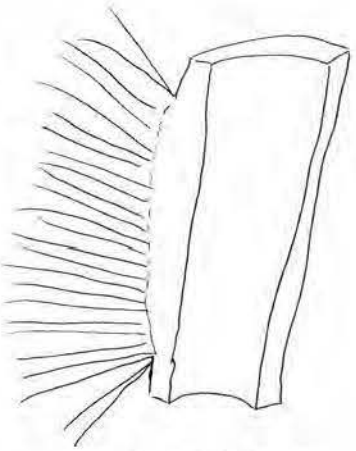

Diagram 19F

Interrupted amorphous periosteal reaction (diagram 19G)

This type of periosteal reaction is discontinuous and appears irregular. It is usually a result of reaction to a localised process. A healing fracture is a common cause of this pattern and careful study of the underlying bone will show a fracture line. There may also be thickening of the cortex of the bone. In some instances, the periosteal reaction is due to stress fracture and common sites being the postero-medial cortex of the proximal tibia and in the 2nd metatarsal. There is usually associated cortical thickening (fig 19.9).

This pattern of periosteal reaction can sometimes be seen in early acute osteomyelitis and there will be associated destructive lytic changes in the adjacent bone. At later stages, the periosteal reaction may become more lamellar in appearance and extend parallel to the shaft of the bone (fig 19.10).

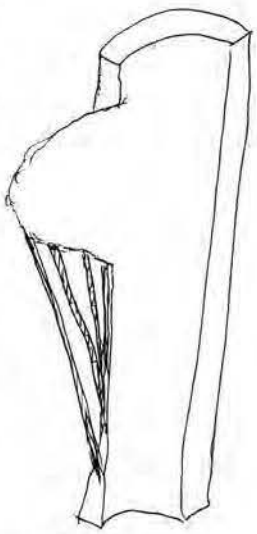

Diagram 19G

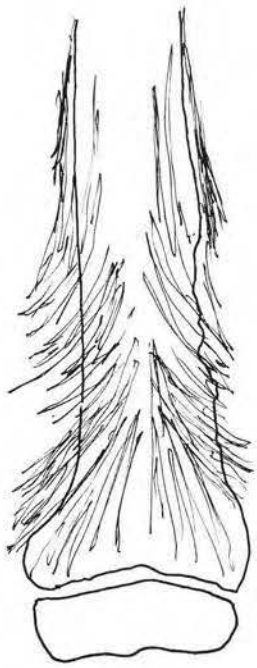

Fig 19.8
"Sun burst" periosteal reaction due to osteosarcoma of the distal femoral metaphysis.

Fig 19.9
Healing fracture of the 2nd metatarsal with surrounding callus.

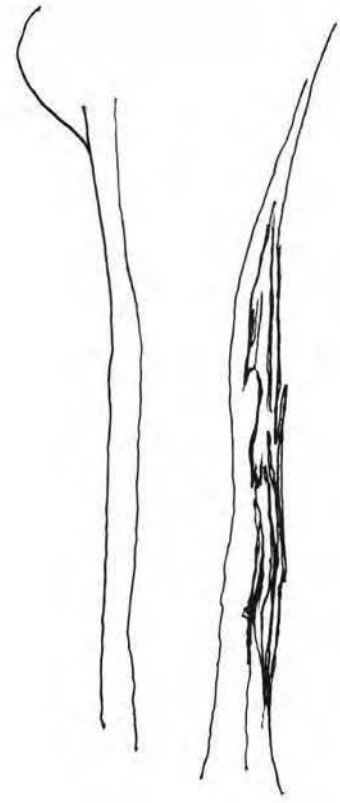

Fig 19.10
Patient with acute osteomyelitis of the proximal femur demonstrates a fluffy irregular periosteal reaction.

LEARNING POINTS: PERIOSTEAL REACTIONS

- Periosteal reactions are result of bone reacting to various insults. The same disease may produce several patterns of periosteal reaction.
- An aggressive lesion will usually be associated with destruction of the adjacent bone.
- Bilateral periosteal reactions are usually due to systemic diseases or syndromes.
- Obliteration of the soft tissue planes tends to favour an infective process.
- Looking at the underlying bone for an expansile mass, destruction, bone mineralisation and fracture will give important clues for diagnosis

CHAPTER 20

Extremities trauma

Siew-Kune Wong & Wilfred C.G. Peh

Introduction

Importance of radiographs

The primary aim is to diagnose the presence of a fracture or dislocation. It is also important to assess the position of the bone ends before and after treatment. Follow-up radiographs are subsequently needed for bony union and complications.

Principles of radiographic examination

a. It is essential to take radiographs in at least 2 planes, preferably at right angles to each other. This will ensure that a fracture will not be missed and the bony alignment can be accurately assessed.

b. The joint above and below the fracture should be included in the radiograph. This is to assess for associated dislocation especially in paired bones such as those in the forearm and leg.

c. Due to bone resorption, a fracture line will become more visible about 2 weeks after an injury. Callus formation may also be present. Hence serial examinations may be required if a fracture is clinically suspected but is not visible immediately after injury (fig 20.1).

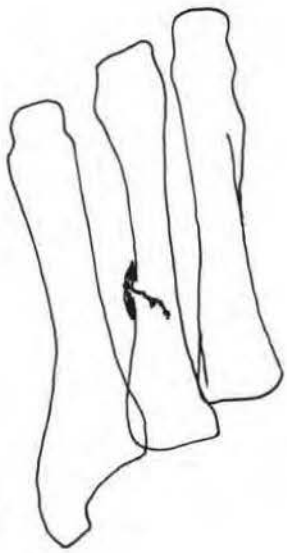

Fig 20.1
Callus formation is seen around a stress fracture of the 4th metatarsal bone.

d. Comparison views of the opposite limb may be required in the immature skeleton before epiplyseal closure. This will help to confirm if a bony fragment is an accessory ossicle, unfused ossified epiphysis, or a fracture.

e. Stress views are useful to assess for ligamentous injury, especially to the ankle and knees. These views help to accentuate the abnormal widening of the joint space associated with laxity or injury to the supporting ligaments (figs 20.2a & 20.2b).

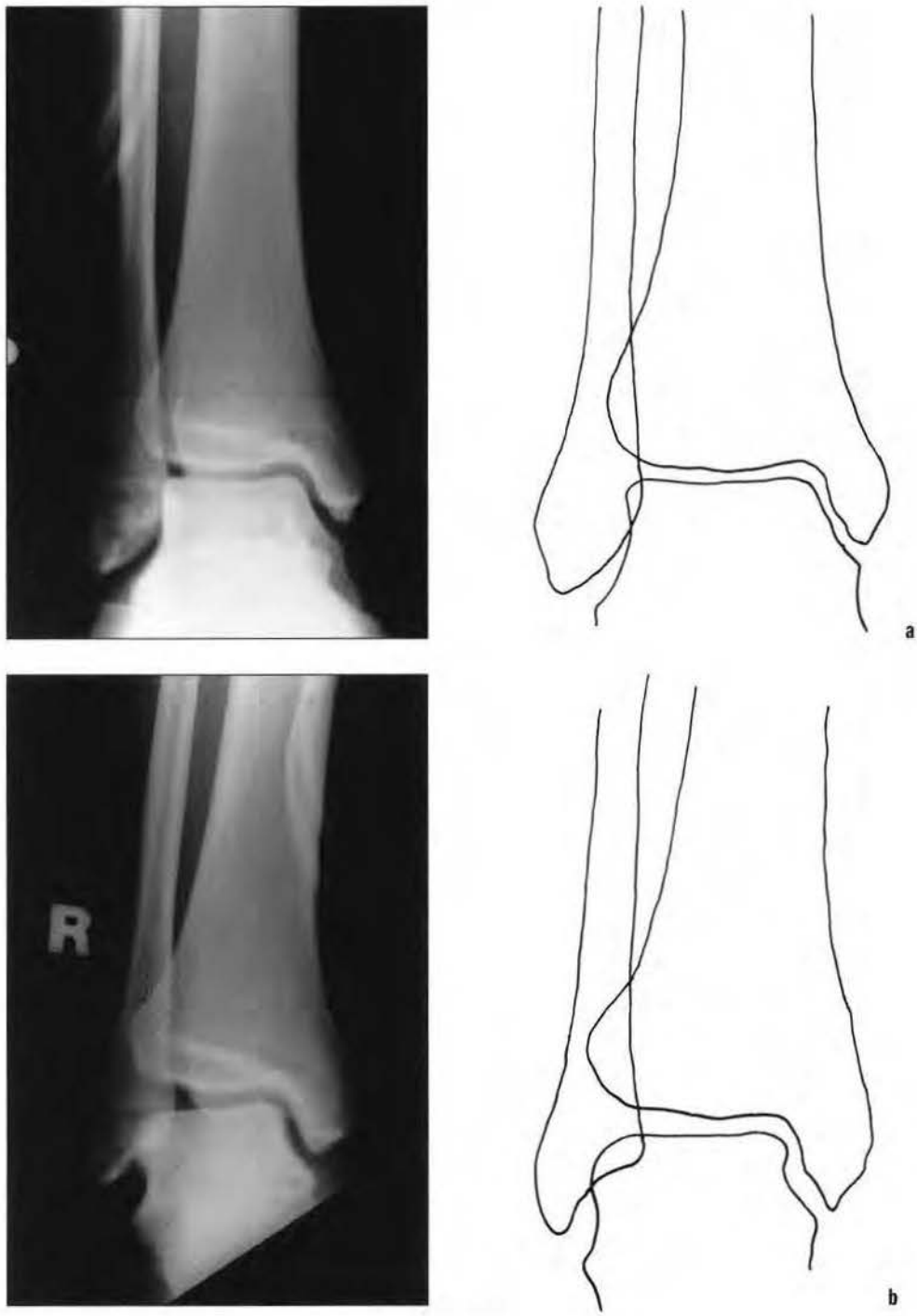

Fig 20.2 *Neutral (a) and inversion (b) views of the ankle demonstrate a lateral ligament injury.*

Indirect signs of trauma

a. Soft tissue swelling due to haemorrhage is commonly associated with fractures or ligamentous injury.

b. Joint effusion due to haemorrhage or fluid displaces the extracapsular fat pads away from the bone creating what is known as the "fat pad" sign. This is useful for assessing trauma involving the wrist and elbow (fig 20.3).

c. Free fat within a joint capsule is indicative of bony injury. It is best demonstrated on a horizontal beam radiograph and appears as a fluid-fluid level due to free fat floating on top of synovial fluid or blood (fig 20.4).

Fig 20.3
Note displaced fat pad posterior to the elbow joint following a supracondylar fracture.

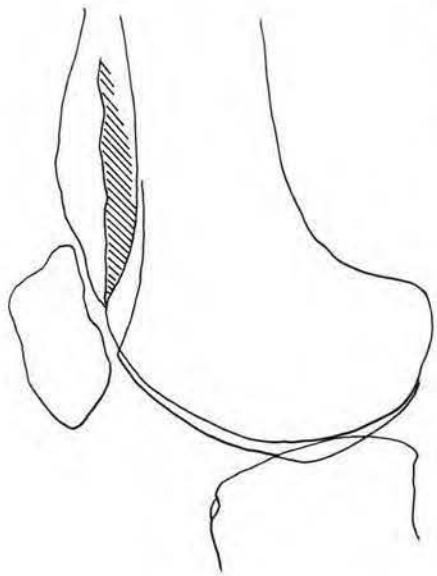

Fig 20.4
Horizontal beam lateral knee view shows a fat fluid level following a fracture.

Pitfalls in imaging

a. Nutrient arteries appear as radiolucent lines and can be mistaken for crack fractures. This is commonly seen in tubular bones.

b. Prior to bony maturation, the epiphyseal plate can appear irregular with sclerosis. The periphery of the epiphyses is usually the last to fuse and should not be mistaken for a fracture.

c. Bony grooves or notches can be misinterpreted as a linear fracture. This is not uncommonly seen in the bicipital groove with the humerus in internal rotation.

d. Accessory ossicles can mimic small avulsed bony fragments. Comparison views and the presence of any indirect signs of trauma, such as soft tissue swelling or joint effusion, will help to confirm or exclude a fracture.

Stress fractures (fatigue)

This is due to abnormal stress upon bones of normal mineralisation. It is commonly seen in the tibia and the metatarsal bones. The fracture line usually runs transversely across the bone. In the early stage, the fracture may appear as a lucent line or a dense shadow due to trabecular compression and interval callus across the fracture. Lamellar periosteal and endosteal reaction can be seen at a later stage (fig 20.5). The diagnosis can be made on bone scans and serial radiographs. A positive isotope bone scan may be obtained 3–4 weeks prior to appearance of the radiographic abnormality.

Fig 20.5
Stress fracture of the tibial shaft demonstrates the fracture line and surrounding sclerosis.

Special extremity fractures

INTRA-ARTICULAR FRACTURE

Bennett fracture

This is due to forced abduction of the thumb and appears as an oblique fracture involving the proximal articulating surface of the first metacarpal bone (fig 20.6). A small fragment of the first metacarpal bone continues to articulate with the trapezium, while the rest of the bone is dorsally and radially dislocated due to the pull of the abductor pollicis longus muscle. Failure to diagnose and treat intra-articular metacarpal fractures may lead to protracted pain, stiffness, and post-traumatic arthritis due to incongruity of the articular surface.

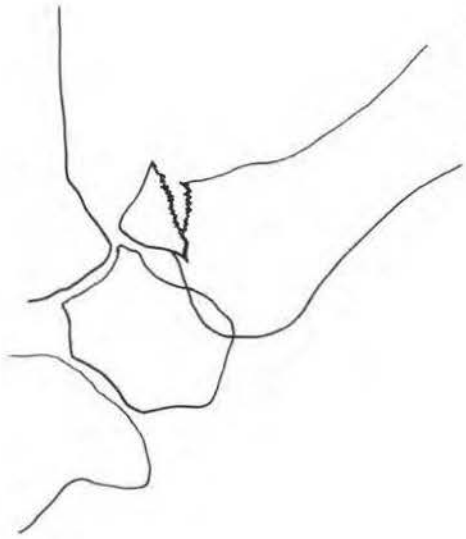

Fig 20.6
Bennett's fracture of the 1st metacarpal bone.

Barton fracture

This is due to a fall on the outstretched hand. The intra-articular oblique fracture involves the dorsal margin of the distal radius. Occasionally, there may be an associated dislocation of the wrist joint. If the fracture involves the volar surface of the distal radius, it is known as a reverse Barton's fracture. Both varieties are best seen in the lateral projection due to the coronal orientation of the fracture line.

Tibial plateau fracture

Majority of these fractures involve the lateral tibial plateau. Mechanism of injury is due to a twisting or valgus force. The fracture may occasionally not be obvious on the standard AP and lateral projections. Hence, oblique views, or tomography, may be needed to reveal the fracture and to assess its severity (fig 20.7). About 10% of the fractures are associated with ligamentous injury of the knee joint.

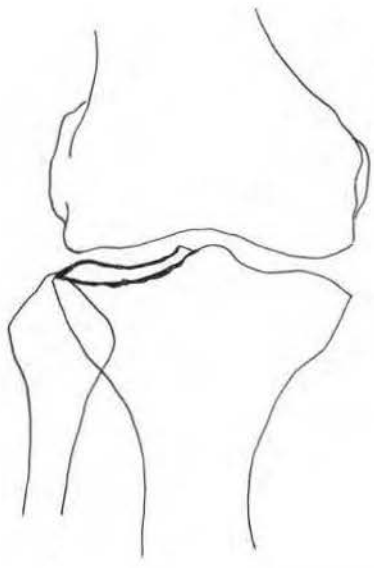

Fig 20.7
Depressed fracture of the lateral tibial plateau

Ankle fracture

This fracture is due to either inversion or eversion injuries, or a combination of both mechanisms. The variety of fractures can be classified based on the types of injury or the types of fractures involved. The latter would include an unimalleolar fracture (either the medial or lateral malleolus), bimalleolar fracture, trimalleolar fracture if the posterior tubercle of the distal tibia is involved, or a complex fracture when comminuted fractures of the distal tibia and fibula occur (fig 20.8). Fracture-dislocation can occur when the ankle mortise is disrupted due to associated bone and ligamentous injury (fig 20.9).

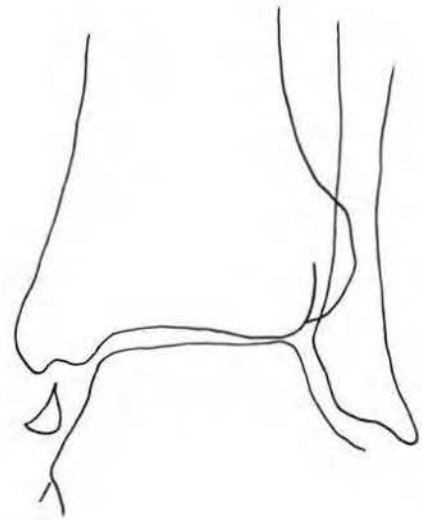

Fig 20.8 *Medial malleolar fracture with a displaced fragment.*

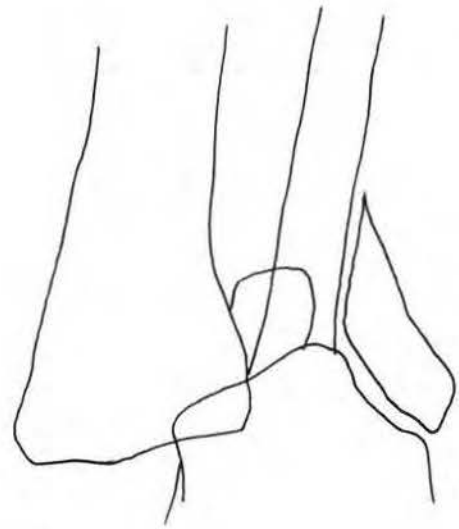

Fig 20.9 *Fracture dislocation of the ankle.*

Calcaneal fracture

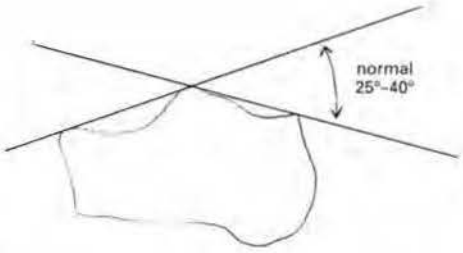

Diagram 20.1

This is the most commonly fractured tarsal bone. The injury is due to a fall from a height and is commonly bilateral. May be associated with spinal fractures, especially of the second lumbar vertebra. The fracture can be classified as extra-articular or intra-articular if it involves the subtalar or calcaneocuboid joint. In an intra-articular fracture, it is important to assess the degree of depression of the posterior facet of the subtalar joint. Measuring the Bohler's angle (diagram 20.1) from the lateral radiograph helps to evaluate depression. However a CT scan can precisely demonstrate the position of the bony fragment and the extent of the depression at the posterior facet of the subtalar joint (fig 20.10).

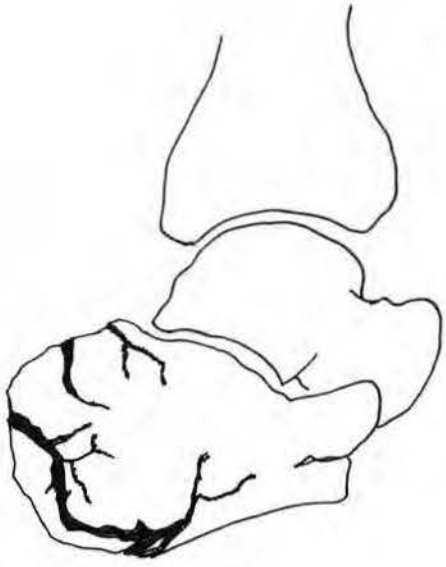

Fig 20.10
Comminuted fracture of the calcaneus.

NON-ARTICULAR FRACTURE

Four types are discussed:

Colles fracture

This is due to a fall on the outstretched hand. The radial fracture occurs in the distal shaft, usually about 2 cm from the articular surface. The distal fragment displaces dorsally and proximally, giving a "dinner-fork" deformity. There may be an associated fracture of the ulnar styloid process (figs 20.11a & 20.11b).

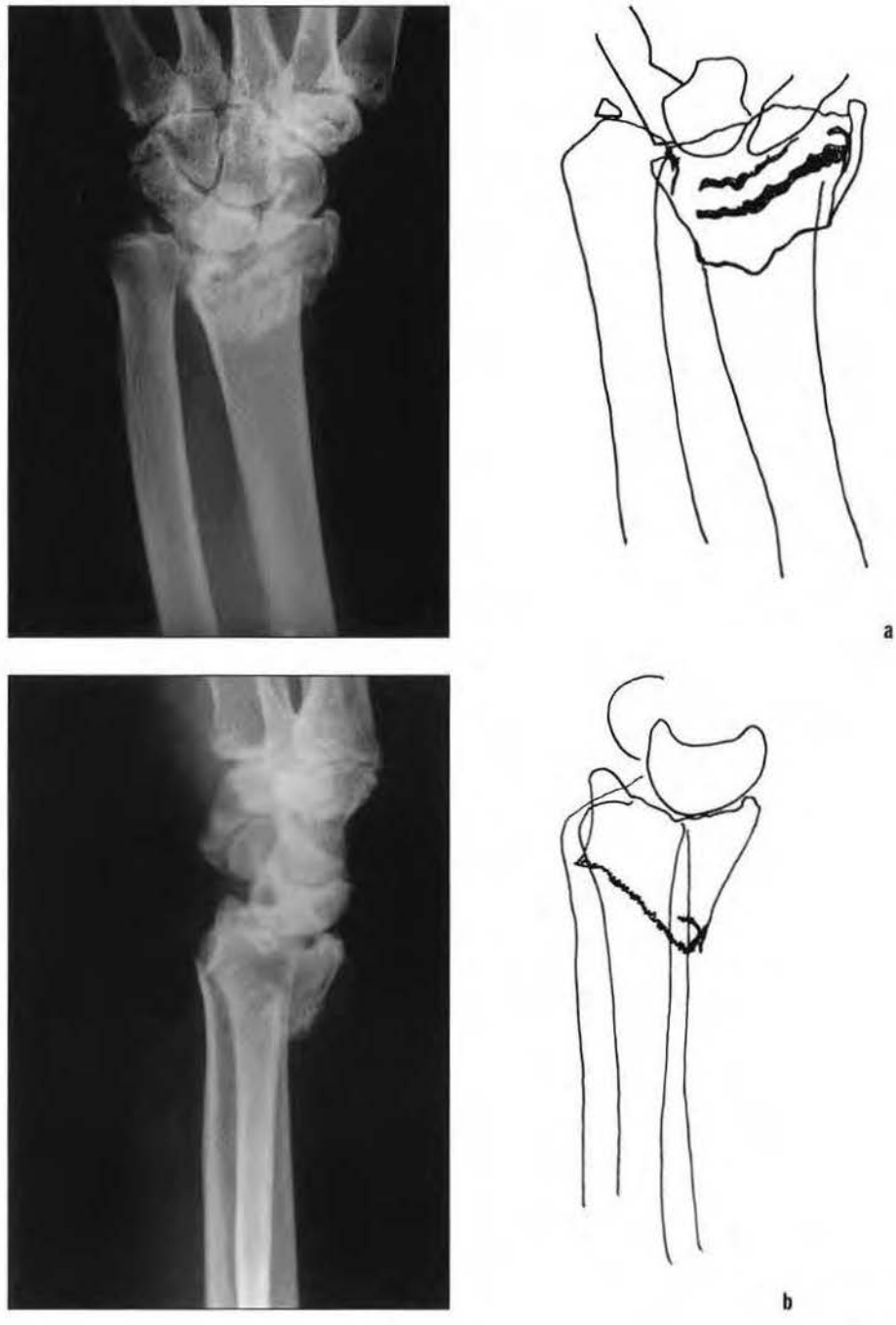

Figs 20.11a & 20.11b
Colles fracture of the wrist in AP and lateral views.

Smith's fracture

This is usually due to a fall on the back of the hand or a direct blow to the dorsum of the hand. The distal fragment is displaced ventrally with radial deviation of the hand giving a "garden spade" deformity (fig 20.12).

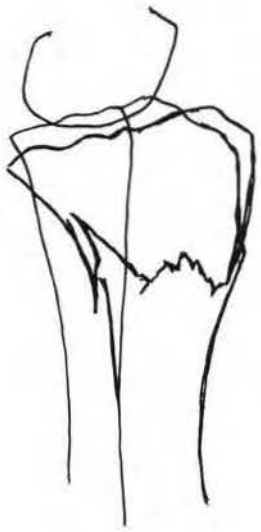

Fig 20.12
Lateral view of the wrist demonstrates a Smith's fracture (reversed Colles fracture).

Supracondylar fracture

This is the most common type of elbow fracture in children between the ages of 3 and 10 years. Majority of fractures are due to a fall on the outstretched hand with the elbow hyperextended. The distal fragment is posteriorly displaced (fig 20.13).

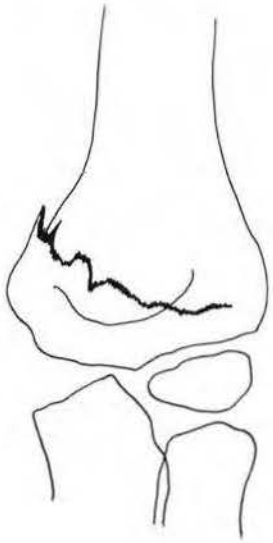

Fig 20.13
Supracondylar fracture of the distal humerus in a child.

Jones fracture

This is a fracture involving the base of the 5th metatarsal bone. The fracture line is transversely oriented as compared to the ossification centre, which is obliquely oriented.

FRACTURES ASSOCIATED WITH INCREASED RISK OF AVASCULAR NECROSIS (AVN)

Scaphoid bone

This is the most common carpal bone to be fractured. The majority occur in the waist followed by the proximal pole and the tuberosity. Associated injuries include perilunate dislocation and radial fracture. Complications of delayed union or non-union increase the risk of osteonecrosis, which commonly affects the proximal fragment (fig 20.14).

Fig 20.14 *Displaced scaphoid fracture with a fracture of the distal radius.*

Neck of femur

These are intracapsular fractures, which may be subcapital, transcervical or basicervical. Non-union is a common complication of such injury, which can result in osteonecrosis (fig 20.15).

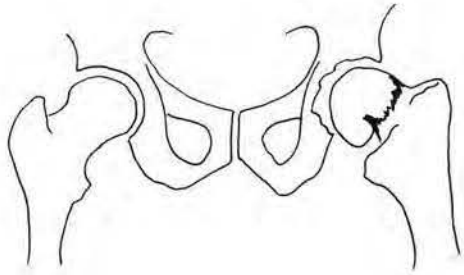

Fig 20.15 *Displaced fracture of the left femoral neck.*

FRACTURE/DISLOCATION

Galeazzi

This results from a fall on the outstretched hand with the forearm in pronation, or a direct blow to the dorsolateral aspect of the wrist. It consists of a fracture of the distal third of the radius with associated dislocation of the distal radioulnar joint. The distal fragment is dorsally displaced and angulated. The ulna is both dorsally and medially dislocated (fig 20.16).

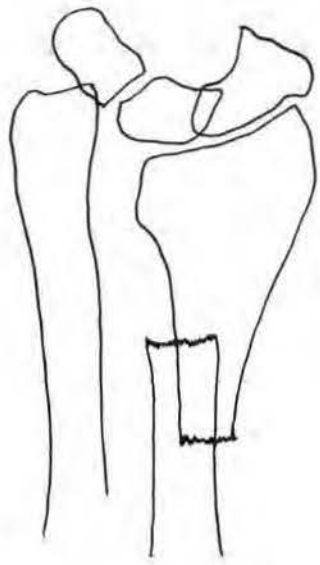

Fig 20.16
Galeazzi fracture of the radius with dislocation of the distal radioulnar joint.

Monteggia

This is due to forced pronation of the forearm during a fall or a direct blow to the dorsal aspect of the proximal third of the forearm. It consists of an anteriorly-angulated proximal ulnar fracture associated with anterior dislocation of the radial head.

Transcaphoid perilunate dislocation

This is the most common fracture associated with carpal dislocation. The frontal (AP) projection clearly demonstrates the scaphoid fracture but the lateral view shows the dorsally displaced capitate in relation to the lunate, which remains in articulation with the distal radius—hence the name perilunate dislocation (fig 20.17).

Maisonneuve fracture

There is a fracture of the proximal fibula associated with a tear of the interosseous membrane and the distal tibia fibula syndesmosis. There may also be an associated tear of the deltoid ligament or a fracture of the medial malleolus resulting in widening of the medial joint compartment.

Lisfranc fracture

This commonly occurs after a fall from height or down a flight of stairs. The Lisfranc ligament between the 1st cuneiform bone and the base of the 2nd metatarsal bone is disrupted or avulsed at the site of insertion. There are 2 varieties of injuries, namely, homolateral dislocation of the 1st to 5th metatarsal and divergent lateral displacement of the 2nd to the 5th metatarsal with medial or dorsal shift of the 1st metatarsal bones.

Associated fractures include those of the base of the 2nd metatarsal and less commonly, those of the 3rd metatarsal, 1st cuneiform or the cuboid bones (fig 20.18).

Fig 20.17 *AP and lateral views of the wrist demonstrate a displaced transcaphoid fracture with perilunate dislocation.*

a

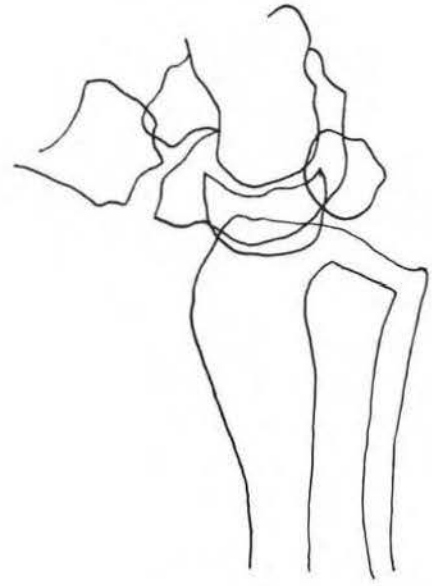

b

Fig 20.18 *Lisfranc fracture dislocation of the foot.*

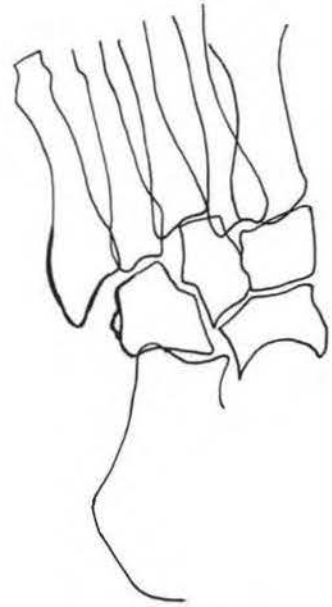

JOINT SUBLUXATION/DISLOCATION

Joint injuries are commonly seen in the shoulder, wrist, knee and ankle. They can be divided into contusion, sprain, subluxation or dislocation.

The joint is subluxed if the articular surface is partially displaced as apposed to complete displacement in dislocation. If a fracture is associated with either dislocation or subluxation, it is classified as a fracture-dislocation/subluxation.

Shoulder dislocation

Anterior dislocation is the most common type of glenohumeral dislocation. This is easily diagnosed on the AP and lateral shoulder views (fig 20.19).

Associated fracture of the posterolateral aspect of the humeral head produces a "hatchet" defect known as the Hill-Sachs lesion. The Bankart lesion which is a fracture of the anterior aspect of the inferior rim of the glenoid is less commonly seen on radiographs. Posterior dislocation is less common but is easily missed on the standard AP radiograph of the shoulder. The humeral head however has a "light-bulb" appearance due to forced internal rotation. Overlapping of the humeral head with the glenoid in a radiograph taken with the glenoid in profile is also diagnostic. Associated compression fracture of the humeral head, giving a double cortical density to the humeral head, can also be demonstrated (fig 20.20).

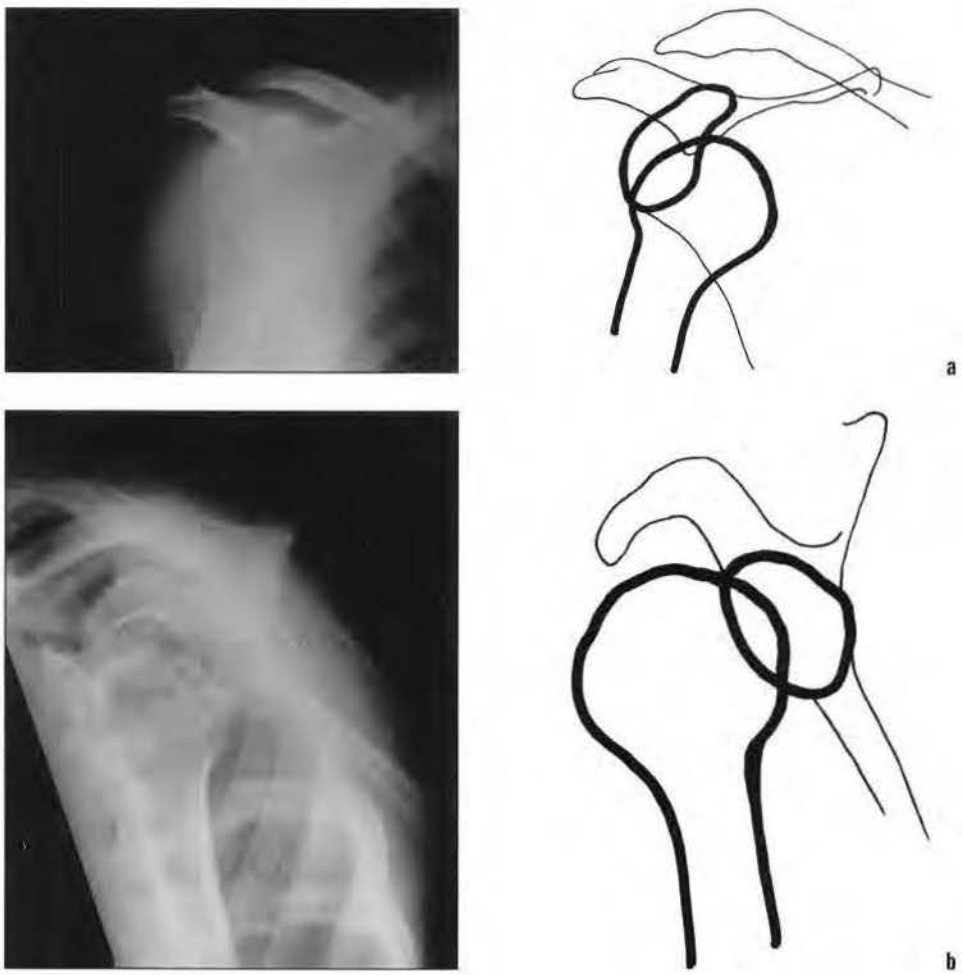

Fig 20.19
Anteroinferior dislocation of the right shoulder.

Fig 20.20 *Compression fracture of the medial humeral head.*

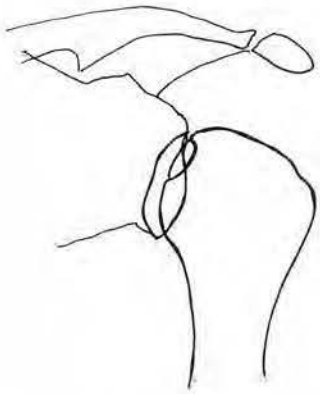

Wrist dislocation

This is due to a fall on the outstretched hand. Common types are lunate dislocation, perilunate dislocation and transcaphoid perilunate dislocation. The normal alignment of the carpal bones can be demonstrated in the standard AP and lateral views. On the frontal view, Gilula has described 3 arcs outlining the carpal bones. Arc I outlines the proximal articular surfaces of the scaphoid, lunate and triquetrum. Arc II outlines the distal concavities of the same bones. Arc III outlines the proximal convexity of the capitate and lunate (diagram 20.2). In the lateral radiograph, the longitudinal axes of the radius, lunate, capitate and the 3rd metacarpal bone form a straight line (diagram 20.3).

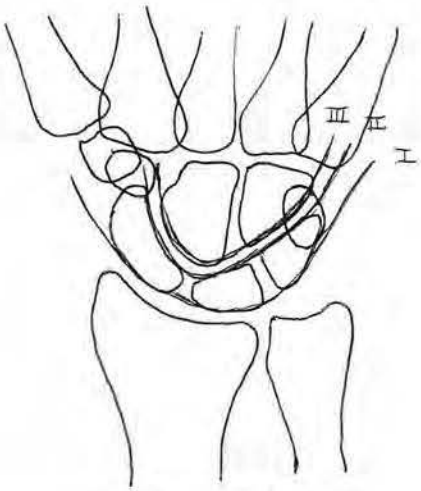

Diagram 20.2

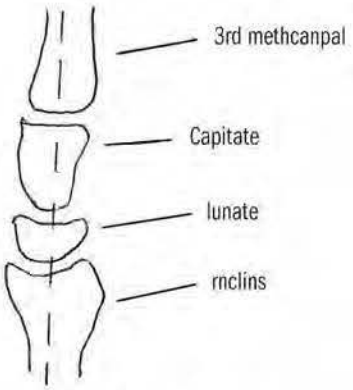

Diagram 20.3

Epiphyseal plate injury

This injury is seen in the immature skeleton prior to the fusion of the epiphysis. It can be divided into 5 types based on the Salter-Harris classification.

Type 1: Fracture through the growth plate due to shearing force separating epiphysis from physis. The periosteum is usually intact.

Type 2: Fracture through the growth plate extending into the metaphysis.

Type 3: Fracture through the growth plate extending into the epiphysis.

Type 4: Fracture through the growth plate involving the metaphysis and epiphysis.

Type 5: Compression fracture through the growth plate due to a crush injury (diagram 20.4).

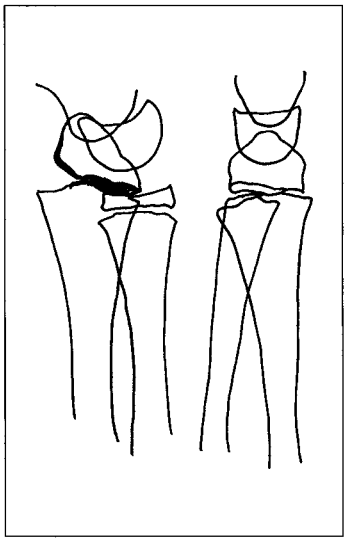

Diagram 20.4

CHAPTER 21

Fractures–classification, union, complications

Lesley A. Goh & Wilfred C.G. Peh

Classification of fractures

A fracture refers to a break in the structural continuity of the bone. The fractured bone heals by a complex process of bone repair. Complications can arise both as a result of the inciting trauma, as well as during the healing process Fractures may be broadly classified into **complete** and **incomplete fractures**. In a complete fracture, the bone is completely broken into two or more fragments. An incomplete fracture is one where only one side of the bone is broken. Complete fractures may be subdivided into transverse, oblique/spiral, impacted, comminuted and intra-articular fractures. Incomplete fractures may be divided into greenstick fractures, which are typically seen in children, and compression fractures, which are usually seen in adults. An avulsion fracture occurs when a fragment of bone is torn away from the rest of the bone due to the pull of a strong ligamentous or tendinous attachment and is commonly seen as a result of forcible muscular contractions (fig 21.1). The pattern of some typical fractures are illustrated in the diagrams 21.1a–21.2g.

Fig 21.1
Fracture of the anterior tibial spine resulting from an avulsion injury to the anterior cruciate ligament.

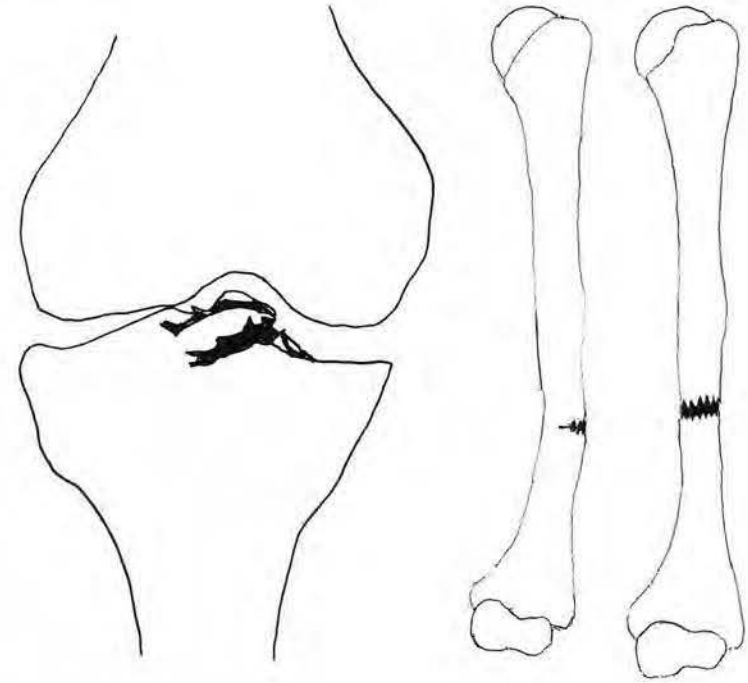

Diagram 21.1
Complete and incomplete fractures:
a. *Incomplete fracture–greenstick.*
b. *Complete fracture.*

Diagram 21.2
Types of complete fracture

21.2a
Transverse

21.2b
Oblique

21.2c
Spiral

21.2d
Impacted

21.2e
Comminuted

21.2f
Intra-articular fracture–fracture of capitellum

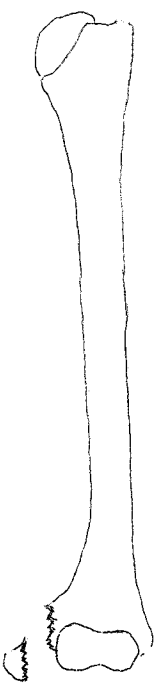

21.2g
Avulsion fracture–avulsion of medical epicondyle

Complete fractures

Complete fractures may be further subdivided by the orientation of the fracture line. Types of complete fractures:

a. Transverse fracture

b. Oblique/spiral: typically due to rotational stress (fig 21.2)

c. Impacted: fracture fragments are jammed tightly together (fig 21.3).

d. Comminuted: more than two fracture fragments which are usually poorly apposed.

e. Intra-articular: fracture involves a joint surface (fig 21.4).

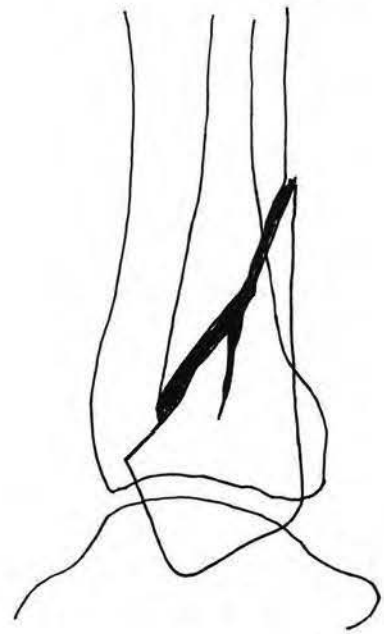

Fig 21.2 *Spiral fracture of the distal fibula.*

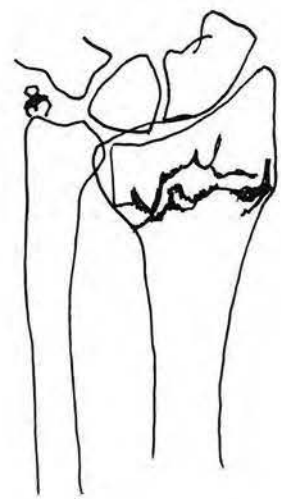

Fig 21.3 *Imapacted Colles fracture of the wrist joint.*

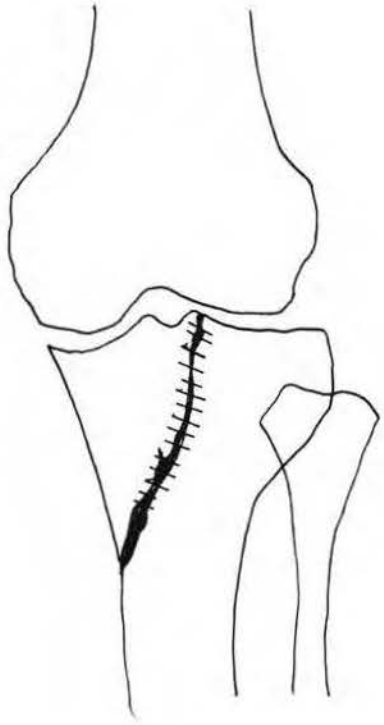

Fig 21.4
Intra-articular fracture of the proximal tibia extending to the lateral tibial condyle.

Incomplete fractures

The bone is incompletely divided in these fractures. Types of incomplete fractures are:

Greenstick fractures (fig 21.5)
This type of fracture is commonly seen in children where the bone buckles due to its springy consistency. The periosteum is intact. These fractures are usually easy to reduce and heal well.

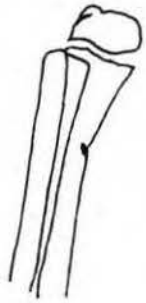

Fig 21.5
Greenstick fracture of the distal radius in a child. Note the fracture is incomplete and does not extend to the dorsal cortex.

Compression fractures (fig 21.6)

These fractures are usually seen in adults and typically involve the vertebral bodies or the calcaneum. Complete reduction is seldom possible and the patient is likely to have a residual deformity.

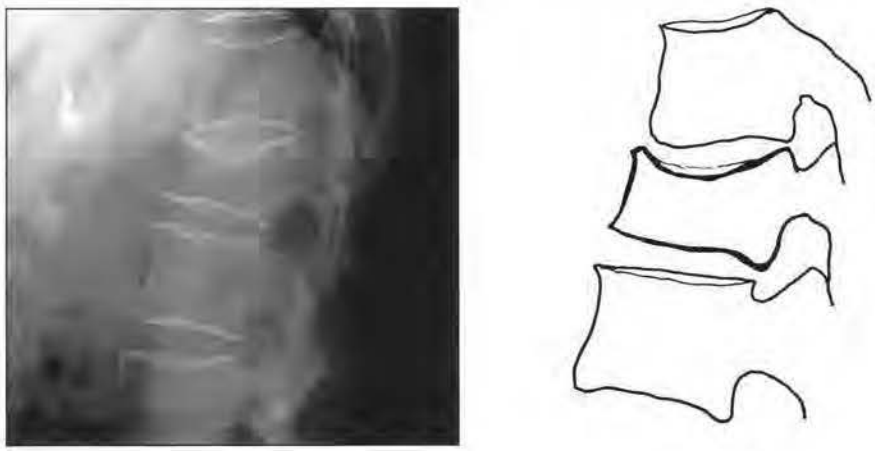

Fig 21.6 *Anterior wedge compression of T12 vertebral body.*

Clinical importance of classification

It is important to classify fractures correctly. This is helpful in determining the likely prognosis and choosing the correct treatment. Fractures can be treated conservatively in a plaster cast or surgically using internal or external fixation. Surgical fixation is usually undertaken when there is failure of reduction, failure to maintain reduction, in open fractures and intra-articular fractures. External fixation is usually done for open fractures with gross contamination.

If the fracture is incomplete as in a greenstick fracture, reduction is usually easy and the child can be reassured that healing is usually quick. In contrast, compression fractures are seldom completely reducible.

Certain fractures are also less stable and correct classification can alert the clinician to fractures at risk of complications of union. Among the complete fractures, transverse fractures are more likely to remain in place following reduction unlike oblique and spiral fractures that have a tendency to displace. Displacement after reduction may give rise to delayed union, malunion or even nonunion. Similarly, comminuted fractures are usually unstable and are less likely to heal in a optimal position as reduction of the fracture fragments is often difficult to maintain. Finally, healing time tends to be longer in certain types of fractures although most fractures should unite by 16 to 18 weeks (table I). For example transverse fractures take a longer time than spiral fractures to heal. Fractures involving children and the upper limbs (rather than the lower limbs) tend to heal more quickly. Such knowledge is useful when following up a fracture.

Table I. *Healing times in tubular bones in adults*

	Upper limb	Lower limb
Early callus	2-3 weeks	2-3 weeks
Late consolidation	6-8 weeks	12-16 weeks

Special types of fractures

Stress fractures may be divided into insufficiency and fatigue fractures. The main difference is that insufficiency fractures occur in abnormal bone exposed to normal stress while fatigue fractures are seen in normal bone that has been subjected to abnormal repetitive stress. An example of insufficiency fracture would be of that typically seen in elderly patients with osteoporosis. Common fracture sites include the upper tibia, sacrum, ilium and pubic bones. Fatigue fractures occur in people with normal bones and are often seen in a younger age group. The fracture site is related to the nature of the activity producing the abnormal stress (fig 21.7).

Pathologic fractures occur secondary to pre-existing abnormality in the bone, most commonly a bone tumour. The bone is weakened by abnormalilty and a fracture may follow acute trauma or even normal stress (fig 21.8).

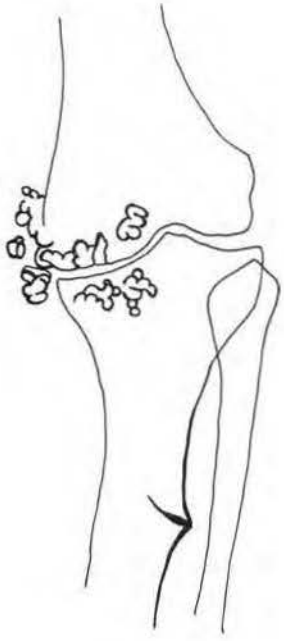

Fig 21.7
Fatigue fracture of the proximal tibia in a patient with severe osteoarthrosis of the knee joint.

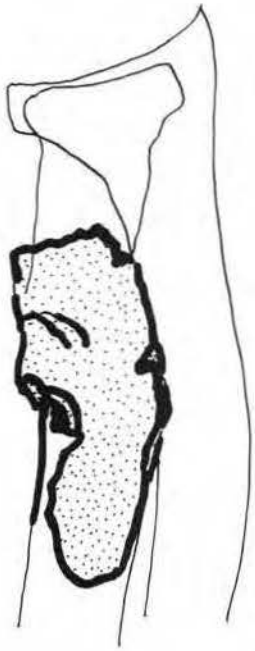

Fig 21.8
Pathological fracture through a fibrous dysplasia lesion in the proximal radius.

Union

Bony union occurs as result of a complex process of bony repair that is seen radiographically as callus formation.

Early callus formation

At the early stages, the callus only contains radiolucent fibrous tissue and the fracture line would be seen radiologically. At a slightly later stage, immature callus forms. This typically forms "a soft cotton-wool appearance". The callus may be seen to bridge the fracture though the fracture line remains visible even when clinical union has occurred. There is no motion at the fracture site under stress.

Late consolidation

The soft callus is gradually converted into hard mature bone. This is the late consolidation stage and radiographic consolidation is said to have occurred when the bony callus is seen to bridge the fracture and obliterate the fracture line. Bone remodelling follows. The marrow cavity eventually becomes continuous and the cortices are reformed.

Complications

Complications arising from fractures may be **systemic** or **localised** to the fractured bone, adjacent soft tissue or joints. Local complications involving bone include: complications of union, infection, avascular necrosis, reflex sympathetic dystrophy and growth disturbances in children when the growth plate is involved.

Non-bony local complications may involve the soft tissue and adjacent joints. Among the soft tissue injuries, trauma to the vessels adjacent to the fracture site, compartment syndrome as well as injury to nerves and adjacent viscera are among the more commonly encountered conditions.

Complications involving the joints include haemarthrosis and joint stiffness due to oedema and fibrosis. Post-traumatic osteoarthritis can result from damage to the articular cartilage and joint surface or to abnormal stress subsequent to malunion of a shaft fracture.

Complications of bony union

Bony union usually occurs within 16 to 18 weeks depending on the age of the patient, the fracture site and the type of fracture. Complications of union are delayed union, non-union and malunion. Certain fractures such as oblique fractures and comminuted fractures are less stable. Therefore correct classification is important. Early diagnosis allows the cause to be determined and correct treatment to be instituted before there is permanent disability.

- **Delayed union**
  The fracture fails to unite within a reasonable amount of time (16–18 weeks). Possible causes are inadequate blood supply, infection, insufficient splintage and excessive traction. Failure to diagnose and treat delayed union at its early stages may lead to non-union.

- **Non-union**
  The fracture fails to unite. Causes of delayed union may also cause non-union. Interposition of soft tissue between the fracture fragments may also prevent bone union. Radiographically, the fracture ends are separated by a gap. Motion between the two ends may be demonstrated under fluoroscopy or between consecutive stress films.

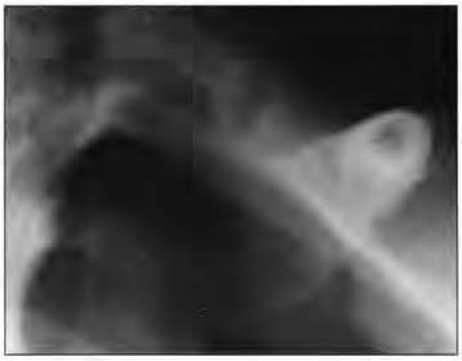

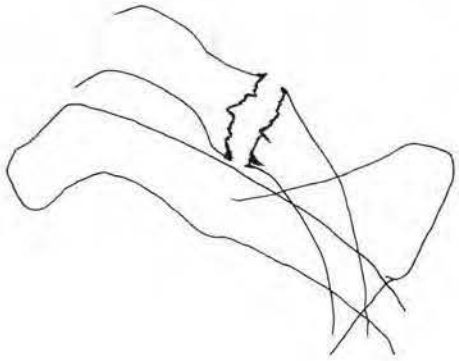

Fig 21.9
Hypertrophic non-union of a rib fracture.

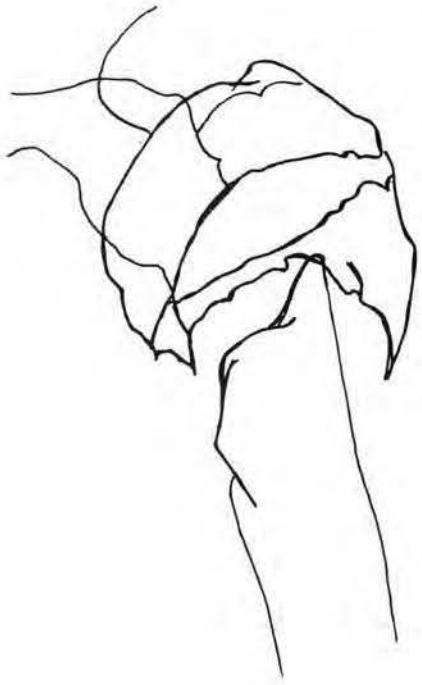

Fig 21.10
Atrophic non-union following a fracture of the humeral neck.

There are two main types of non-union: reactive and nonreactive.

- **Reactive/hypertrophic:** exuberant bone reaction with hypertrophy and sclerosis of the bone ends, and abundant callus is present (fig 21.9).
- **Nonreactive/atrophic:** bone ends are atrophic, have a tapered appearance and there is a lack of surrounding callus (fig 21.10).

Conservative treatment may not produce union and surgical fixation is therefore needed. In a hypertrophic pseudarthrosis, stabilization of the fracture is often all that is required as potential for healing is still present, while in an atrophic nonunion, stabilization in combination with additional bone grafting is required to stimulate bone healing.

- **Malunion** (fig 21.11)
  The fracture fragments join in an unsatisfactory position. This may occur when the fracture is not reduced adequately or if the fracture reduction is not maintained during healing. Angulation in a long bone may result in obvious deformity, limb shortening and osteoarthritis of the adjacent joints. An osteotomy can be performed in cases of malunion to prevent premature deterioration of the joint and subsequent osteoarthritis but this only possible if malunion is recognised and treated early.

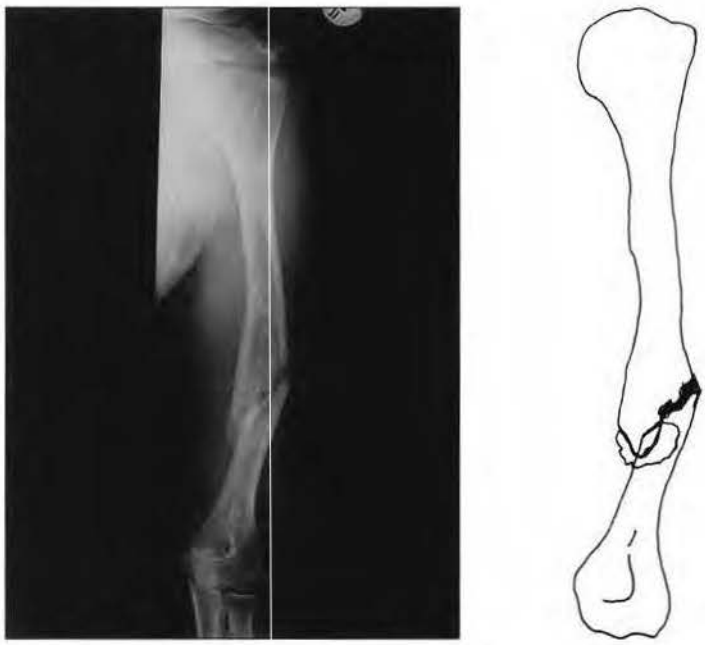

Fig 21.11 *Malunion of a humeral shaft fracture with resultant angulation.*

Infection

Wound infection may complicate open fractures or surgically treated fractures. Osteomyelitis needs to be recognised and treated early as it can lead to inadequate healing. This results in delayed union or non-union. Radiographically there is soft tissue swelling, bony destruction associated with periosteal new bone formation, rarefaction and sequestration of non-viable bony fragments.

Avascular necrosis (fig 21.12)

Avascular necrosis occurs when the bone dies due to lack of blood supply. The fracture fails to unite and the ischaemic bone may collapse. This typically manifests radiographically as areas of rarefaction and sclerosis. Certain fractures are particularly associated with avascular necrosis. Careful follow-up of these fractures enables early diagnosis and treatment.These fractures are listed below:

Fig 21.12 *Avascular necrosis of the proximal fragment of a scaphoid fracture as well as the lunate bone.*

Site of fracture	Site of avascular necrosis
Femur–neck	Femur–head
Scaphoid–waist	Scaphoid–proximal fracture fragment
Talus–neck	Talus–body
Humerus–neck	Humerus–head

Growth disturbances

This is seen in children. Fractures which cross the epiphyseal growth plate may lead to abnormal growth. If only part of the growth plate is damaged then this may lead to asymmetrical growth, resulting in angulation. If the entire growth plate is involved, there may be premature fusion and cessation of growth resulting in limb length discrepancy.

LEARNING POINTS: FRACTURES

- **Fractures**–may be treated conservatively or surgically depends on the type of fracture, hence need for correct radiological classification
- **Fracture**–complete-transverse, oblique, spiral, impacted, comminuted
  –incomplete-greenstick, compression
- **Complications**–systemic
  –local-bone, soft tissue, joints
- **Complications of union**–delayed union (bone fails to unite in 16-18 weeks)
  –non-union (fails to unite)
  –malunion

  Important to identify abnormal union and its cause (mechanical, blood supply, infection) and institute appropriate treatment promptly.
- **Other local complications** involving bone also benefit from early diagnosis and treatment.

–infection	–bony destruction, sequestra, soft tissue swelling
–avascular necrosis	–areas of patchy rarefaction and sclerosis
	–typical sites –femoral head, scaphoid, talus
–reflex sympathetic dystrophy	–patchy, rapidly progressive rarefaction
–growth disturbances	–angulation, cessation of growth

CHAPTER 22

Spinal trauma

Wilfred C.G. Peh

Biomechanics and classification

Spinal trauma is conventionally classified based on the mechanism of injury. These mechanisms include flexion, extension, rotation, compression, distraction and shear forces and often, a combination of these forces. In general, the vertebral end-plates are vulnerable to compression forces while supporting ligaments are prone to damage by rotation and shear forces. The resulting injuries produced by these forces may be further classified into stable and unstable categories.

The concept of stability is controversial with the definition of clinical instability being generally accepted as being the inability of the vertebrae to maintain their relationships such that spinal cord and nerve root damage are avoided, and deformity and excessive pain do not develop. Although instability is regarded as a clinical concept, radiological imaging has a useful role in demonstrating signs that support the clinical diagnosis of spinal instability. In the "three-column theory", disruption of two out of three columns is highly suggestive of instability. The anterior column consists of the anterior longitudinal ligament, anterior disc annulus and anterior vertebral body. The middle column consists of the posterior vertebral body, posterior disc annulus and posterior longitudinal ligament while the posterior column comprises all the bony and ligamentous structures posterior to the vertebral body (diagram 22.1).

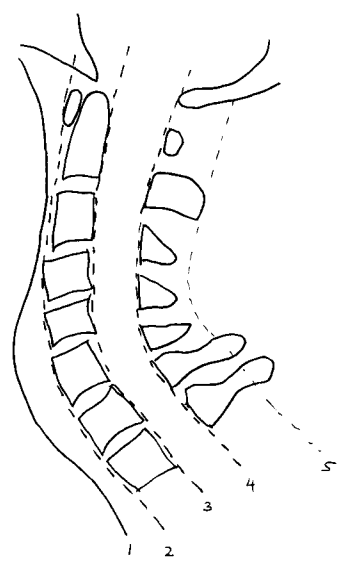

Diagram 22.1

Radiographic projections

The initial routine examination for the traumatised spine consists of conventional radiographs in the anteroposterior and lateral projections. The lateral projection is done at a FFD of 180 cms. An open-mouth radiograph to show the C1/2 vertebrae should be added for symptomatic patients with neurological signs or symptoms of cervical injury or for patients with impeded consciousness or head injury. It is essential not to move the patients head or neck to avoid inadvertent spinal injury. All seven cervical vertebrae should be included on the lateral radiograph. Special projections such as a swimmer's view should be performed if the C7/T1 junction cannot be visualised (figs 22.1a & 22.1b). Flexion and extension radiographs are useful in symptomatic patients in which ligamentous injury is suspected and where standard radiographs are normal. Radiographs may be supplemented by specialised modalities such as tomography, computed tomography (CT), myelography, CT myelography and magnetic resonance imaging.

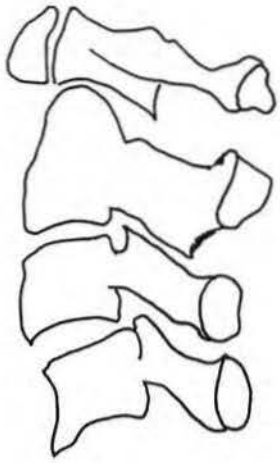

a

b

Fig 22.1
Inadequate coverage of the cervical spine. Initial lateral radiograph demonstrates C1-6 only (a). Repeat radiograph with the shoulders pulled down reveals a C6/7 bilateral facet dislocation. A C6 clay shoveller's fracture is also present (b).

Interpretation of cervical spine radiographs

The lateral cervical spine radiograph is the single most useful projection. Obvious fractures or dislocation may need further characterisation by CT or tomography if available. More subtle injuries may be detected by systematic radiographic evaluation, enhanced by knowledge of the mechanism of injury. The 5 spinal "lines" to be assessed (diagram 22.2) are as follows:

Line 1: Pre-vertebral soft tissue line.
Pre-vertebral haematoma resulting from vertebral body or ligamentous injuries may produce a soft tissue swelling. Anterior to the upper four cervical vertebrae, the maximum pre-vertebral soft tissue width is 5 mm while in the lower cervical spine, the soft tissue width should not exceed the anteroposterior width of the adjacent vertebral body.

Line 2: Anterior spinal line.
This line links the anterior cortices of the cervical vertebral bodies, and should form a smooth gently curved line.

Line 3: Posterior spinal line.
This links the posterior cortices from the cervical vertebral bodies, and should form a smooth gently curved line.

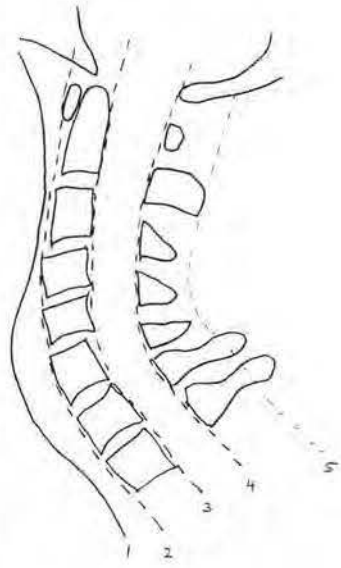

Diagram 22.2

Line 4: Spinolaminar line.
The line links the junctions between the laminae and base of the spinous processes of the cervical vertebrae. It should form a smooth curved line.

Line 5: Spinous process.
The spinous process should be examined for the presence of fractures.

Spinal trauma patterns

These may be classified according to anatomical region, mechanism of injury and stability. A few distinctive types of fractures are listed and illustrated.

Cervical spine: Jefferson fracture

This fracture results from axial loading of C1 vertebra. Jefferson fracture consists of ipsilateral disruption of both the anterior and posterior C1 arches. The injury may be unilateral or bilateral. This injury is best seen on the open mouth radiograph where there is lateral displacernent of the lateral masses of the atlas (C1) relative to those of the axis (C2) (fig 22.2). CT is useful for confirming the fracture.

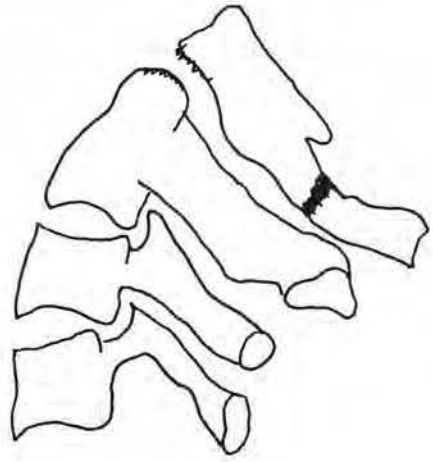

Fig 22.2 *Jefferson fracture. Lateral radiograph shows fractures of the C1 lateral masses. There is posterior displacement of the C1 spinolaminar line. The odontoid peg is also fractured.*

Cervical spine: Odontoid fracture

The mechanism of injury of the odontoid fracture is not well understood. There are three types:

Type 1 odontoid tip fracture (stable)

Type 2 fracture at junction of the odontoid peg and C2 body (unstable)

Type 3 fracture through C2 body extending into cancellous bone (stable)

Type 2 fractures are associated with non-union hence the importance of recognising the odontoid fracture types. Fractures of the odontoid are best demonstrated on the open mouth radiograph. This fracture may be difficult to see on the lateral radiograph if it is undisplaced. Tomography is useful for detection and characterisation of odontoid fractures (fig 22.3).

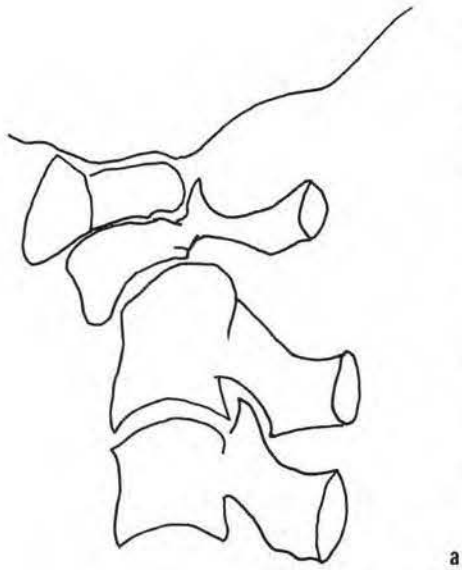

a

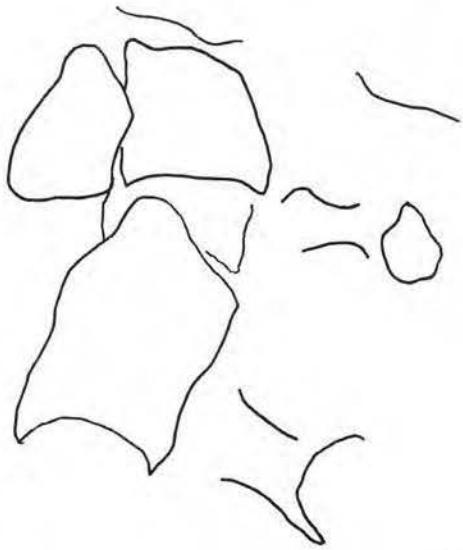

b

Fig 22.3
Odontoid peg fracture. Lateral radiograph shows forward displacement of the odontoid peg with disruption of the anterior and posterior spinal lines and spinolaminar line (a). Lateral tomogram shows a type 2 fracture optimally (b).

Cervical spine: Hangman's fracture

This fracture is due to vertical compression and hyperextension. It consists of bilateral avulsions of the neural arches from the vertebral body, and is also known as traumatic spondylolisthesis (fig 22.4). This injury is best seen on the lateral radiograph, particularly if there is fracture displacement. Associated C2/C3 posterior element retrolisthesis is often present.

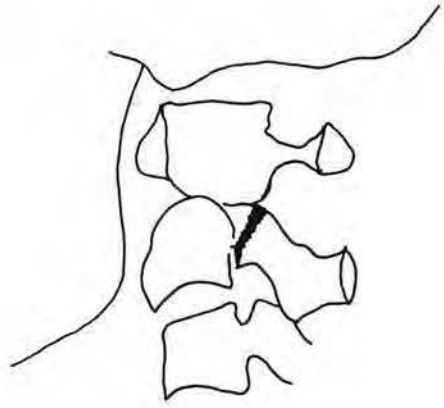

Fig 22.4 *Lateral spine demonstrates a Hangman's fracture.*

Cervical spine: Clay shoveler's fracture

This fracture results from avulsion by the infraspinatus ligament due to hyperflexion. It refers to an oblique fracture of the C6 or C7 spinous process. This injury is stable and is of no clinical significance (fig 22.5).

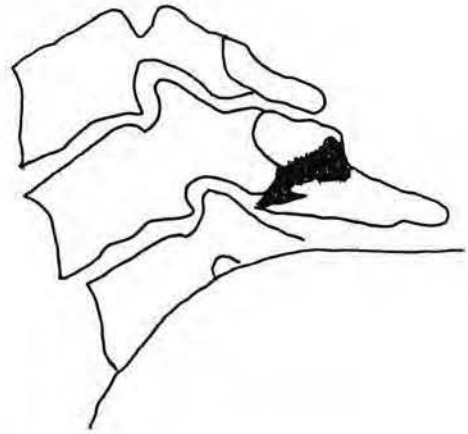

Fig 22.5 *Lateral spine shows a clay shoveler's fracture of C6 spinous process.*

Cervical spine: Flexion teardrop fracture

This fracture is due to combined flexion and axial loading. It typically involves the lower cervical spine. The affected vertebral body is divided into a smaller anteroinferior fragment (teardrop) and a larger posterior fragment. The teardrop fragment remains aligned with the vertebral body below while the posterior fragment is displaced posteriorly but remains aligned with the upper cervical vertebrae. Associated posterior structural injuries may be seen as interspinous widening, facet widening and lumbar fractures (fig 22.6). This unstable injury produces the anterior cord syndrome.

Fig 22.6
Flexion tear drop fracture of C5 vertebra.

Cervical spine: Bilateral facet dislocation (or lock)

This injury occurs secondary to severe hyperflexion. The inferior articular processes of the superior vertebra are dislocated and locked anterior to the superior articular processes of the inferior vertebra. On the lateral radiograph, the superior vertebra is anteriorly displaced greater than half the width of the vertebral body (fig 22.7).

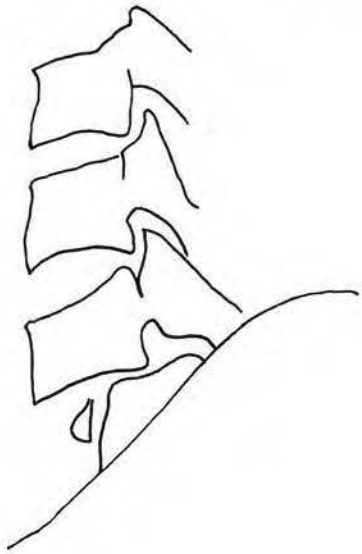

Fig 22.7
C6/7 bilateral facet dislocation.

Cervical spine: Unilateral facet dislocation (or lock)

This injury results from a combination of flexion and rotation. Due to interspinous ligament and facet joint capsule rupture, the inferior articular process of the superior vertebra dislocates and locks anterior to the superior articular process of the ipsilateral

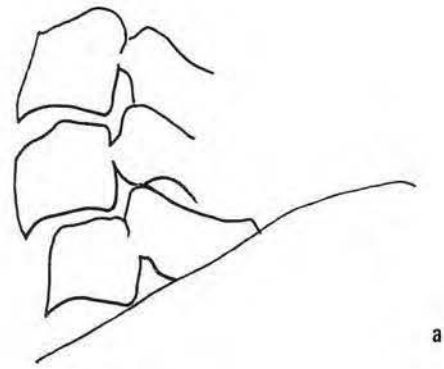

a

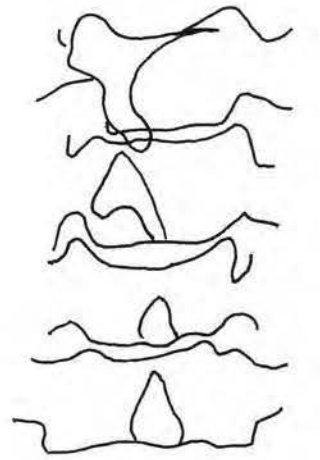

b

Fig 22.8 *C5/6 unilateral facet dislocation with anterior displacement of C5 by one third of a vertebral body width (a). AP radiograph shows deviation to the right of the spinous process of the vertebra superior to the dislocation (b).*

inferior vertebra. On the lateral radiograph, the superior vertebral body is anteriorly displaced, typically one third or less than the width of the vertebral body width. There is abrupt rotation of the facet joints at the level of the injury, producing the "bow-tie" sign. The antroposterior radiograph may show rotation of spinous processes at the site of the dislocation. Oblique radiographs are useful in confirming the fracture dislocation (figs 22.8a & 22.8b).

Upper thoracic fractures

Fractures affecting the upper 4 thoracic vertebrae are uncommon but when they occur, are usually due to major traumatic forces. The characteristic injury is a fracture-dislocation involving two adjacent vertebrae. There is typically an associated facet joint disruption, anterior displacement of the superior vertebra and a compression fracture of the superior end-plate. The components of these complex injuries, namely: malalignment, degree of displacement and spinal canal compromise, is best assessed on CT.

Thoraco-lumbar spine: Chance fracture

This fracture (also known as seatbelt fracture) is due to a hyperflexion force with the fulcrum of motion located anteriorly at the level of the anterior abdominal wall. This force results in compression of the vertebral body and distraction of the posterior body and ligamentous structures, typically at the thoraco-lumbar junction. On radiography, a horizontal fracture extending transversely through the body, pedicles and posterior elements is seen. As all three columns are disrupted, this fracture is unstable (figs 22.9a & 22.9b).

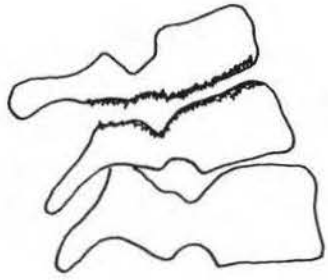

a

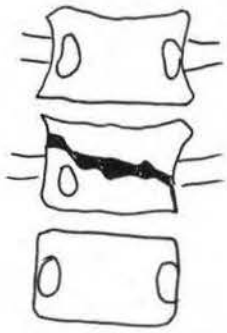

b

Fig 22.9a & 22.9b *Chance fracture through L2 vertebra (arrows).*

Burst fracture

This fracture results from axial loading of the vertebral body combined with flexion. Centripetal vertebral body disruption produces posterior displacement of the posterior vertebral margin and loss in height of the posterior vertebral body. There may be associated fractures of the posterior elements. The fractures typically occur at the thoracolumbar junction and are often associated with deficit. CT is the best method for showing the presence of posterior element fractures and retropulsed bony fragments.

Wedge compression fracture

This may occur anywhere in the spine and is due to a flexion force with the fulcrum located within the vertebral body. The typical simple wedge compression fracture results in loss of anterior vertebral body height with preservation of the middle and posterior columns. These fractures are stable and are commonly encountered in the osteoporotic spine (fig 22.10).

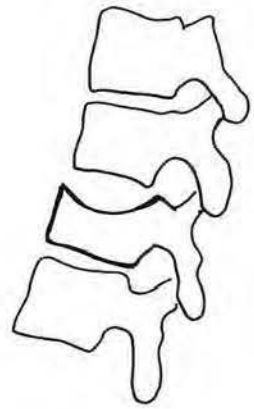

Fig 22.10
Wedge compression fracture of the L2 vertebral body.

LEARNING POINTS

- Spine trauma may result in spinal cord and nerve root damage and should be diagnosed promptly.
- Radiological imaging is useful in demonstrating signs that support the concept of instability.
- Radiographs, especially those of the lateral cervical spine, should be interpreted in a systematic manner.
- The types of spinal fractures or dislocations are generally classified according to the predominant mechanism of injury.

CHAPTER 23

Facial and pelvic trauma

Swee-Tian Quek & Wilfred C.G. Peh

Introduction

Facial and pelvic injuries are commonly encountered with patients with multiple injuries. Due to the complex anatomy of these areas, there is often superimposition of the bony structures on the radiographs rendering radiographic assessment challenging. As a result of this, cross-sectional imaging by CT is often useful in the further evaluation of these injuries.

Facial trauma

Radiographic assessment of facial trauma can be daunting due to the complex anatomy of this region as well as the number of different projections available for evaluation. The projections employed depend largely on the suspected pathology although routinely this usually includes at least an occipitomental (OM) or (Waters) and a lateral view. Of particular importance is the OM view (fig 23.1) where a number of lines have been described to aid assessment of the bony structures (diagram 23.1).

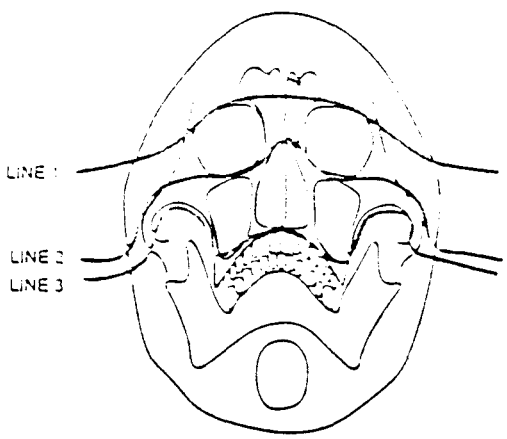

Diagram 23.1
OM view.

Trace McGrigor's lines
Line 1 *crosses the zygomaticofrontal suture to run along the superior orbital margin and across the frontal sinus to the opposite side.*
Line 2 *runs along the superior border of the zygomatic arch and follows the inferior orbital margin and superior contour of the nose to the other side.*
Line 3 *follows the inferior border of the zygomatic arch down the lateral wall of he maxillary sinus and across the maxilla to the opposite side.*
Look for breaks in the continuity of these lines or opacification of the sinuses where they cross as clues to facial fractures.

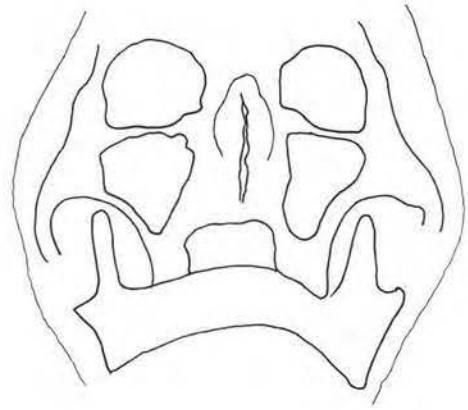

Fig 23.1
Normal OM view.

Nasal fracture

This is the most common facial fracture. Imaging is however not required for routine clinical management. Where indicated, the lateral nasal and OM views are helpful. It is important to specifically request for the lateral nasal view (figs 23.2a & 23.2b) rather than rely solely on the routine lateral skull radiograph as the latter tends to be too overpenetrated for proper assessment of nasal fractures.

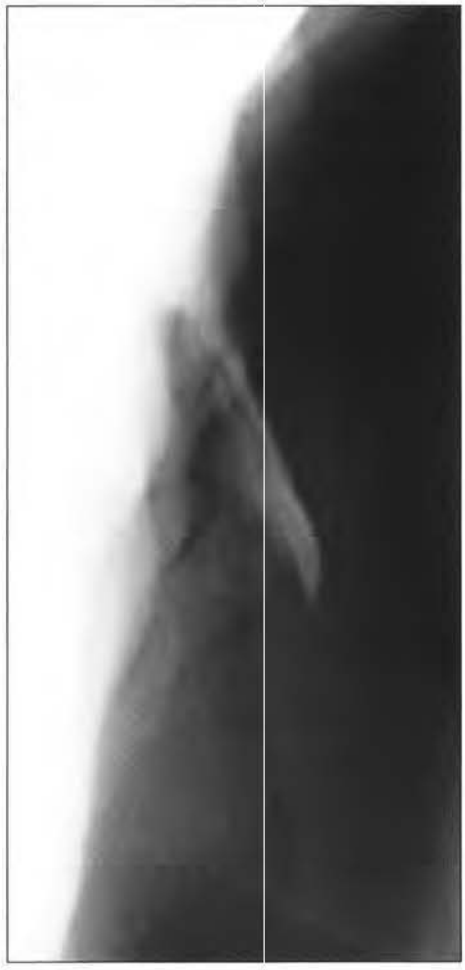

Fig 23.2
Lateral nasal views showing (a) normal nasal bone and (b) fracture. Note the break in the cortex and bony displacement in the fig 23.2b.

a

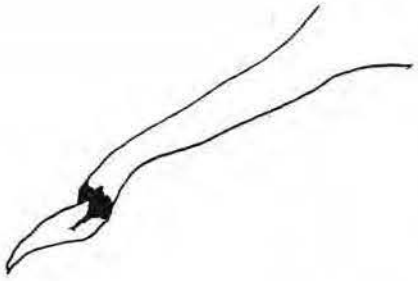

b

Fig 23.2
Lateral nasal views showing (a) normal nasal bone and (b) fracture. Note the break in the cortex and bony displacement in the fig 23.2b.

Fractures are clearly seen as a break in the bony cortex. Sometimes however, suture lines or vascular markings may be confused with a fracture. In general, fracture lines tend to be more radiolucent and more clearly defined than suture or vascular grooves. Furthermore the latter do not extend into the nasal ridge.

Mandibular fracture

Radiographic evaluation for mandibular fractures may include PA (postero-anterior) and lateral oblique views, reverse Towne's view and a pantomography. Although the latter is often regarded as the best view in the assessment of mandibular injuries, it has its limitations in the emergency setting. It requires the patient to sit or stand still during the exposure and hence cannot be used for the unconscious or the critically ill patient who cannot keep still. Furthermore, the equipment required for the examination may not be available in the emergency department. Fractures of the mandibular body and symphysis are often easily diagnosed on the PA view while fractures of the ramus and mandibular angle are usually better seen on the lateral oblique view. Condylar or subcondylar fractures which not uncommonly occur in combination with fractures of the body and symphysis (fig 23.3) may be difficult to detect on routine PA and lateral oblique views especially if undisplaced and are often better assessed on the reverse Towne's or panoramic views. In addition to identification of the fracture, it is also important to assess displacement of the fractured segments and note possible involvement of the teeth and inferior alveolar canal by the fracture as these factors have bearing on the clinical management.

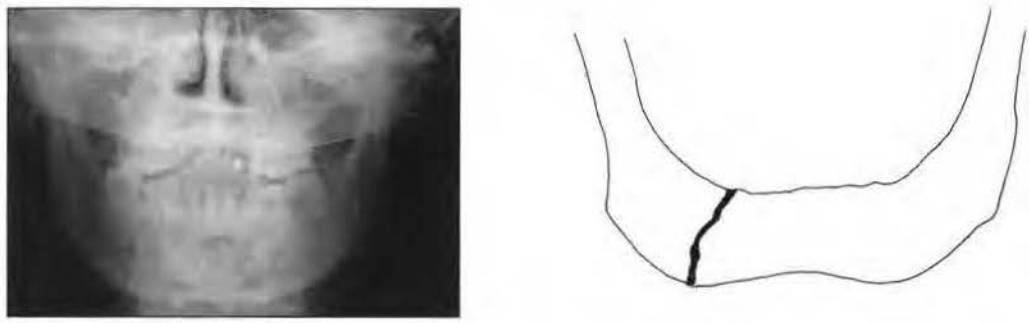

Fig 23.3
Mandibular fractures. The fracture of the body is well visualised on the PA view but the left condylar fracture is more subtle and may be better demonstrated on a panoramic or reversed Towne's view.

Zygomatic and malar fractures

The classical malar or tripod fracture involves the zygomatic arch and the orbital process of the zygoma. It extends to the lateral wall of the orbit, the orbital floor and the lateral maxillary wall (fig 23.4). This is again best assessed on the OM view where the findings include fracture of the zygomatic arch, diastasis of the zygomaticofrontal suture, a step deformity of the infraorbital margin and opacification or an air-fluid level in the maxillary sinus due to haemorrhage within it. Isolated zygomatic arch fractures can also occur and are usually the result of a direct blow posterior to the malar prominence. This is usually seen on the OM or submento-vertical (SMV) view (fig 23.5).

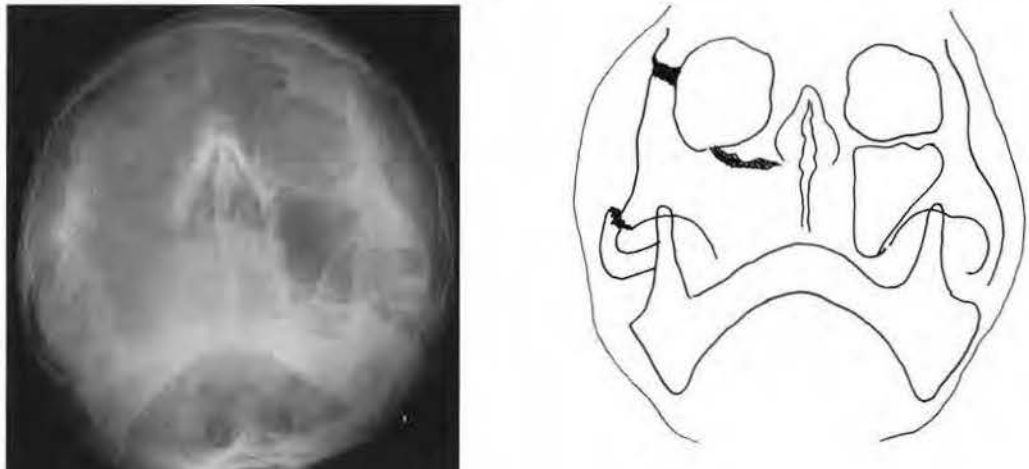

Fig 23.4
Tripod fracture. Note the fracture lines. The orbital floor fracture is not as well seen but there is secondary evidence of the fracture with opacification of the right maxillary sinus.

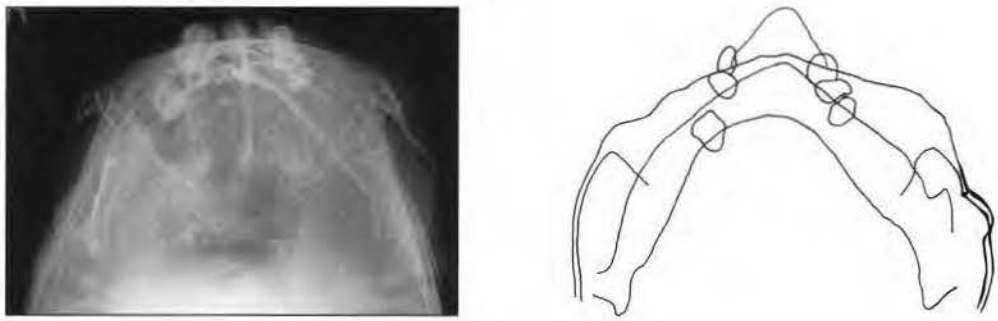

Fig 23.5
SMV view of a left zygomatic arch fracture.

Maxillary fracture

Maxillary fractures have been traditionally divided according to the level of the fracture for convenience and classified by the Le Fort system (diagram 23.2):

- **Le Fort I** (low transverse) fractures are horizontal fractures through the maxilla that separate the alveolar segment of both maxillae and leave the orbits and nose intact.
- **Le Fort II** (pyramidal) fracture are fractures that cross the nasal bridge and extends across the orbits and lateral maxillary walls to the pterygoid plates.
- **Le Fort III** (high transverse) fractures are fractures that extend from the orbital floor to the lateral maxillary wall and separates the facial skeleton from the cranium.

Although these fractures can be assessed on the OM and OF (occipital-frontal) views, further imaging by CT is often helpful in the preoperative evaluation.

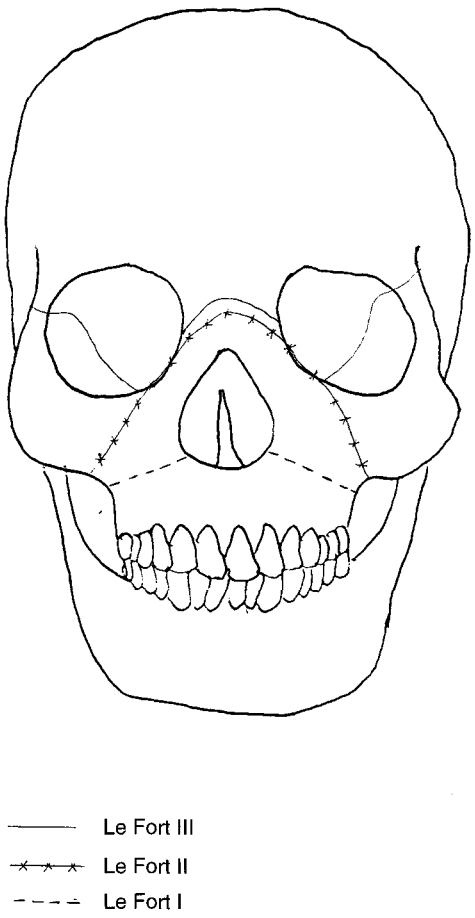

Diagram 23.2
Le Fort fractures.

Orbital fracture

These may represent isolated orbital injuries or be associated with other more complex fractures e.g. tripod or Le Fort fractures.

Blow-out fractures are the result of direct trauma to the orbit causing it to fracture at its weakest points namely the thin orbital floor and its medial wall. The OM view is useful in detecting these fractures.

Radiographic findings include:

1) a break in the cortex of the orbital floor or rim,
2) herniation of the orbital contents e.g. inferior rectus muscle through the orbital floor fracture into the roof of the maxillary sinus (teardrop sign),
3) opacification or an air-fluid level in the maxillary sinus, and
4) intra-orbital emphysema due to air entering the orbit through the maxillary or ethmoid sinus (fig 23.6).

Fractures of the superior orbital rim require a significant amount of force as these involve thick cortical bone. They are therefore frequently associated with other injuries such as fractures of the frontal sinus or anterior cranial fossa. While they may be visualised on the standard OM, PA and lateral views, they sometimes require additional views such as oblique or tangential view to better demonstrate the injury. As with maxillary fractures, the true extent of the injury may be difficult to assess on radiographs alone and further evaluation with CT may be required.

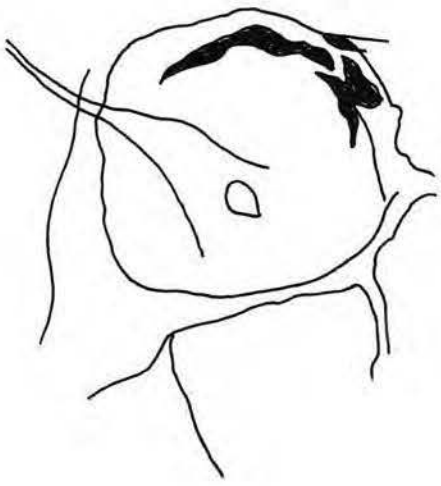

Fig 23.6
Orbital emphysema due to a fracture of the medial wall of the right orbit.

Pelvic fractures

The spectrum of pelvic fractures ranges from avulsion injuries to more severe life-threatening ones. They can be broadly classified into stable and unstable injuries. Identification of the type of injury is important as the key issue in their management revolves around the stability of the fracture. The routine radiographic projection for assessment is the AP view.

- **Stable fractures** are those which:

  1) do not involve the pelvic ring e.g. avulsion fractures (fig 23.7), isolated fractures of the iliac wing (fig 23.8) or

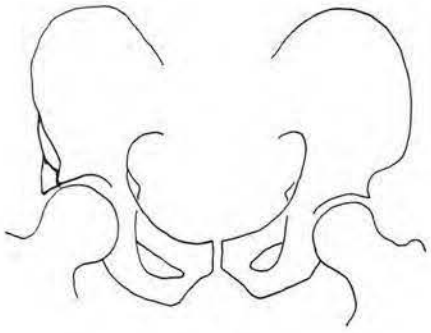

Fig 23.7
Stable pelvic fracture. Avulsion fracture of the right anterior inferior iliac spine is seen.

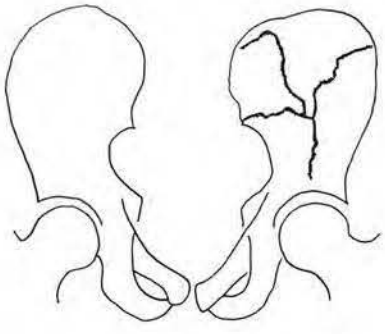

Fig 23.8
Stable pelvic fracture. Stellate fracture of the left iliac blade is present (Courtesy of L.A. Goh).

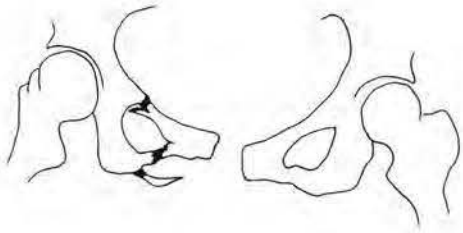

Fig 23.9
An unstable pelvic ring fracture involving the right pubic rami, as well as both sacral ala. The public symphysis is disrupted. There is also mild diastasis of the left SI joint, which was better demonstrated on CT scans (not shown).

2) involve the ring but result in little bony displacement (fig 23.8) leaving the soft tissues largely intact. Usually these fractures involve the pelvic ring in only one place.

- **Unstable fractures** are generally those which involve the pelvic ring in two or more sites. Depending on whether there is significant disruption of the posterior sacroiliac ligamentous complex, these can be further subdivided into fractures which are rotationally unstable but vertically stable (partially stable fractures) or those which are both rotationally and vertically unstable (fig 23.9).

Pelvic fractures are an important group of injuries to diagnose and manage both in terms of mortality and morbidity. It is pertinent to remember that the pelvis does not merely comprise of a number of bones but also contains many major vessels as well as a number of important viscera and damage to these structures may be as important as or even more important than the bony injuries sustained. These associated injuries should be therefore carefully sought for and managed.

Acetabular fractures

Several classification systems have been proposed. Whichever system is used, proper fracture assessment requires good quality radiographs with AP and two oblique (Judet) views. CT is also often employed to better demonstrate the fracture pattern as well as look for intra-articular involvement or loose bodies. Accurate classification is important in determining which patients will benefit from surgical intervention (fig 23.10).

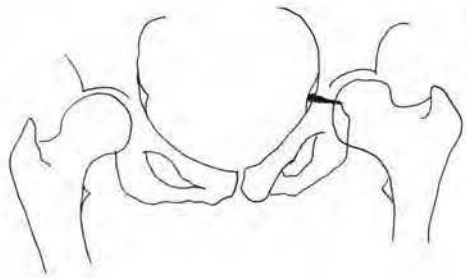

Fig 23.10
Left acetabular fracture.

KEY LEARNING POINTS: FACIAL AND PELVIC FRACTURES

Facial fractures

- A number of projections are available. In general, the OM view is particularly useful.
- In the OM view, follow McGrigor's lines. Also look for fluid/opacification of the sinuses and for intra-orbital emphysema.
- Imaging nasal fractures is not usually required for clinical management
- CT is often useful in the further evaluation of the more complex fractures Remember the review areas on the OM skull radiograph.

Pelvic fractures

- Often associated with other injuries which must be actively sought for and managed
- Recognise stable fractures; everything else is unstable!

CHAPTER 24

Bone infections

Peter Corr

Bone infection is a common cause of morbidity in many developing countries. Diagnosis of osteomyelitis is often delayed resulting in persistent infection and disability especially in children. For effective treatment early diagnosis is essential. Plain film radiography is usually normal in early acute bone infection. Over-reliance on radiography without examining the patient carefully can lead to a delay in diagnosis.

Osteomyelitis

Bone infection is particularly common in the 5–15 year age group. Infection usually follows blood borne spread from a focus of infection elsewhere especially from the skin or lung. In childhood a long bone, such as the femur, is the commonest site of infection, while in adults the spine is more commonly involved. Staphylococcus aureus is the most common organism in children, followed by streptococcal and haemophilius influenzae. In neonates streptococcal and E coli infection are common. With patients who are immunosuppressed gram negative organisms, tuberculosis and fungal infection can occur. Osteomyelitis is more common in children because of the excellent blood supply to the metaphyseal regions of long bones. In the metaphysis infection starts in the bone contiguous to the growth plate where blood flow is slow. Abscess formation and bone marrow oedema causes the infection to penetrate the cortex and elevate the adjacent periosteum. Bone necrosis follows thrombosis of the metaphyseal arteries and stripping of the periosteum by the abscess.

The first radiographic signs are soft tissue swelling and effacement of tissue planes adjacent to the focus of bone infection that appears after 3 days. Periosteal reaction and bone destruction is detected as lytic "holes" (permeative pattern) in the bone appear after 10 days. Necrotic cortex forms sequestra that are bony debris detached from the live bone. The dead bone is a culture medium for infection (fig 24.1). With bone necrosis, there is an attempt at healing and new bone formation from the periosteum. This is called involucrum (fig 24.2). It is important to remember that osteomyelitis may mimic malignant long bone sarcomas in children, especially Ewing's sarcoma and osteosarcoma.

In the chronic phase of osteomyelitis a localised abscess can become walled off in the bone. This is called a Brodie's abscess. The Brodie's abscess appears as a localized lucency in the metaphysis with sclerotic borders (fig 24.3).

Fig 24.1
Child with acute osteitis demonstrating periosteal reaction, cortical destruction, and permeative lytic destruction of the right femur.

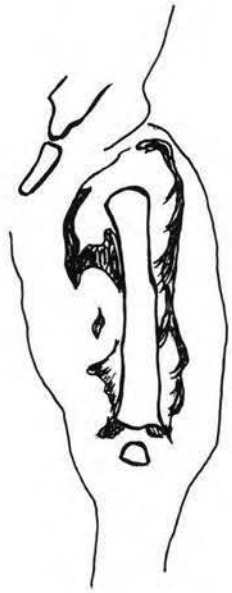

Fig 24.2
Infant with chronic osteitis of the femur with extensive new bone formation (involucrum).

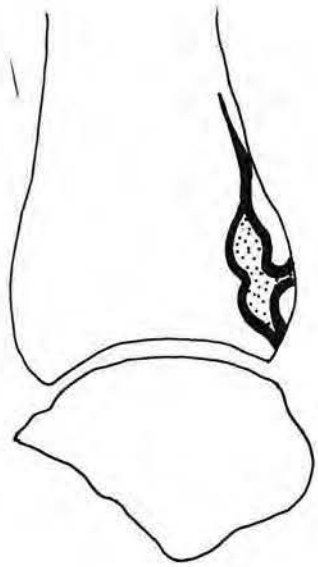

Fig 24.3
Adult with a Brodie's abscess of the distal tibial metaphysis and epiphysis demonstrating a well-defined cavity within the bone and sclerotic borders.

Septic arthritis

Septic arthritis is a very important diagnosis to make in children where the hip and knee joints are most commonly affected. Delayed diagnosis will result in a destroyed joint and life long disability. The infection is usually due to staphylococcus aureus or haemophilius influenzae. Spread is usually blood borne to the synovial lining of the joint and then into the synovial fluid and cartilaginous epiphysis. Infection rapidly destroys the epiphyseal cartilage. On radiographs soft tissue swelling around the joint is noted initially with a joint effusion (fig 24.4). As the cartilage is destroyed there is joint space narrowing and articular erosions. There is usually an associated osteitis. In the chronic phase bony ankylosis will be noted.

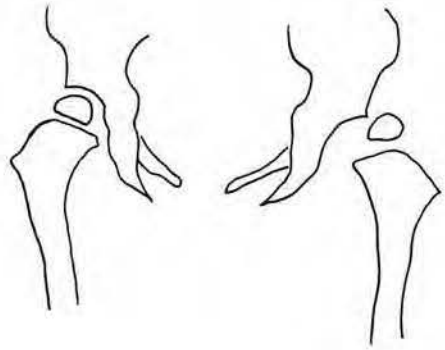

Fig 24.4
Infant with septic arthritis of the left hip joint demonstrates lateral displacement of the femur with dislocation of the femoral head to pus within the joint.

Tuberculous arthritis

Tuberculous arthritis occurs in large joints especially the hip joint, but also in the sacroiliac joints. Granulomatous infection starts in the synovium. Initially focal osteopaenia (decreased bone density compared to the opposite normal hip) and soft tissue thickening around the joint are detected on plain radiographs. As the disease progresses, articular cartilage destruction occurs with joint space narrowing and irregularity of the joint margins (fig 24.5). The sacro iliac joints are commonly involved with erosion of the joint margins and joint space widening (fig 24.6). In children a cystic form is not uncommon involving the metaphyses of long bones. Dactylitis (spina

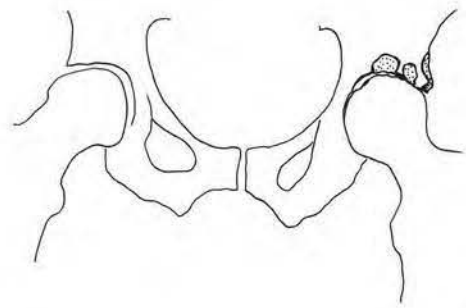

a

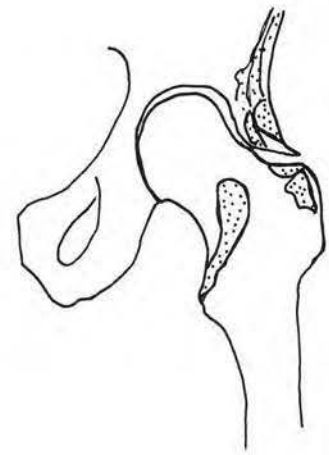

b

Fig 24.5a & 24.5b *Adult with tuberculous arthritis of the left hip joint demonstrates focal osteopaenia with joint space narrowing and erosions of the joint margins.*

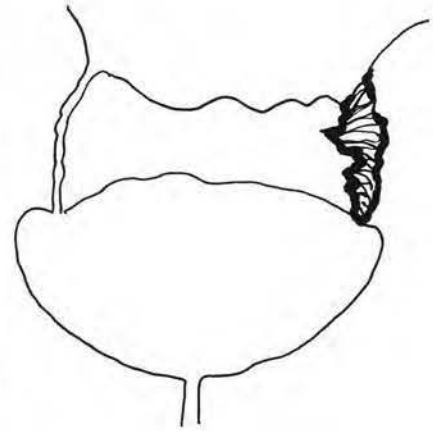

Fig 24.6 *Adult with tuberculous involvement of the left sacroiliac joint demonstrating joint space widening and erosions.*

ventosa) occurs in childhood with fusiform swelling of the phalanges with periostitis. With AIDS patients multifocal skeletal involvement is common.

Infective spondylitis

The clinical diagnosis of spinal inflammatory disease is often delayed as the symptoms and signs are non-specific. Imaging therefore has an important role in diagnosis.

Pyogenic discitis and spondylitis

Pyogenic infections, especially staphylococcus aureus, spread via the blood from other foci of infection in the body such as the skin to the vertebral body end plates and the intervertebral discs (in children). Intervertebral discs are well vascularised in children and are far more susceptible to infection than in adults. There may be a history of a

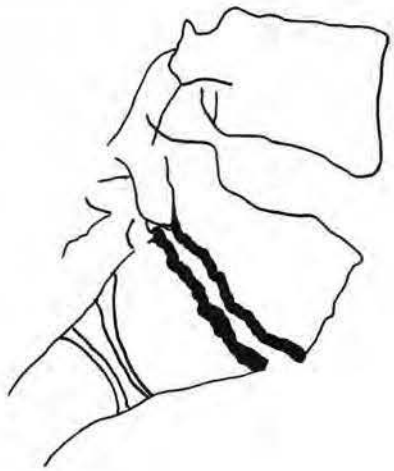

Fig 24.7
Adult with pyogenic spondylitis from Staph. aureus infection of L5/S1 intervertebral disc demomnstrating disc space narowing, end plate erosions and surrounding sclerosis.

recent surgical procedure in adults, such as cystoscopy, particularly if gram negative organisms such as E coli, pseudomonas or proteus are detected. Diabetics and patients who are immunosuppressed (HIV, on steroids) are more susceptible to infection. Clinical symptoms of non-specific backache and fever may be present.

Initially the radiographs are normal for the first week, although Tc99m isotope bone scans are positive. In the second and third week erosion of the subchondral bone and destruction of the disc occurs with loss of disc height (fig 24.7). There may be paraspinal soft tissue swelling or rarely an abscess. After 2 to 3 months regenerative osteoblastic response occurs and sclerosis dominates. Isolated intervertebral disc involvement in children is not uncommon and although the infected disc does not often culture any organisms, staphylococcus aureus is the most likely cause.

Tuberculous spondylitis

Spinal tuberculosis is extremely common in sub-Saharan Africa and is endemic in South Asia. It represents 50% of all bone and joint cases of TB. The common sites of involvement are the thoraco lumbar spine, followed by the cervical spine and lower lumbar spine. Infection starts in the anterior subchondral region of the vertebral body end plate where there is initial lysis and erosion of the cortical margin. The intervertebral disc is infected relatively late compared to pyogenic infection of the disc. The anterior and posterior longitudinal ligaments are displaced by abscess produced by the infection resulting in spread of infection to adjacent vertebral bodies. Pus spreads posteriorly to displace the dura in the extradural space with resultant spinal cord compression. Plain radiographs demonstrates bony erosion of the vertebral end plates, followed by disc space narrowing (fig 24.8). As the longitudinal ligaments become involved angulation and gibbus formation occurs. Posterior element involvement is uncommon, occurring in approximately 10% of patients. With patients with HIV infection, multifocal spinal tuberculosis is often found together with foci in other organs.

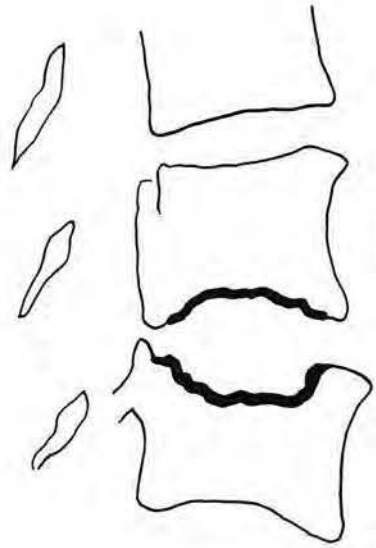

Fig 24.8 *Adult with tuberculous spondylitis demonstrates vertebral end-plate erosions at the L3 and L4 levels.*

Brucellosis

Brucellosis is an important cause of spondylitis especially in the Middle East. The cause is brucella melitensis which is an intracellular infection and very difficult to culture or to detect on biopsy. The lower lumbar spine and sacroiliac joints are commonly involved. Infections start in the vertebral end-plates with contiguous disc destruction. Plain radiographs demonstrate vertebral end plate erosion, sclerosis with prominent anterior osteophytes in the healing phase. Soft tissue paravertebral abscess formation is uncommon unlike tuberculosis.

LEARNING POINTS: BONE INFECTION

- Osteomyelitis common involves the metaphyses of long bones of children
- Radiographs are normal for the first three days following infection
- Early signs of osteomyelitis are soft tissue swelling and loss of tissue planes
- Periosteal reactions are detected at 7 days
- Brodie's abscess is a localised osteitis
- Septic arthritis is common in the hip and knee joints of infants
- Joint space widening and dispalced tisse fat planes are the first sign of septic arthritis
- Pyogenic spondylitis is more common in diabetic and immunosuppressed patients
- Tuberculous spondylitis is more common in the vertebral end-plates of the thoracolumbar spine
- Multifocal tuberculous involvement is common in patients with AIDS

PART 4

GASTROINTESTINAL AND URINARY TRACT PATTERNS

CHAPTER 25

Plain abdominal radiographs

Peter Corr

Interpretation of plain abdominal radiographs is often difficult, but as with reading chest radiographs, a systematic approach is helpful. A good knowledge of the radiographic anatomy is essential.

Radiographic anatomy (fig 25.1)

The abdomen extents from the diaphragm to the pelvis. Only the stomach and colon normally have intraluminal air. The small bowel normally does not have any air within it. Air fluid levels are normal in the stomach, duodenum and colon however it is unusual to have air fluid levels in the small bowel. The liver, gall bladder and spleen are intraperitoneal solid organs that are located in the right and left subcostal regions respectively. The retroperitoneum contains the kidneys and perirenal fascia, the adrenal glands, lymph nodes, the pancreas, the aorta, inferior vena cava, and psoas muscles.

Fig 25.1
Normal supine AP abdomen.

Interpretation of the abdominal radiograph

With the application of ultrasound and CT scanning, investigation of the abdomen has become much easier. However the plain abdominal radiograph remains an extremely useful imaging investigation especially in patients presenting with an acute abdomen.

- **Assess quality**: correct patient name, good exposure, without rotation and anatomical marker (L or R) on the film. An abdominal series will include a supine (AP) radiograph. To detect fluid levels a decubitus abdomen or an erect abdomen is required. To detect free intraperitoneal air an erect chest is useful or a left side down decubitus abdomen.
- **Assess bowel gas pattern**: normally the stomach and large bowel contain gas. The only normal fluid level is in the stomach and occasionally in the proximal duodenum.
- **Determine position of the stomach in the left upper quadrant and the colon "frames' the edges of the abdomen in the supine film.** In the erect film, colon is attached by the hepatocolonic and phrenicocolic ligaments at the hepatic and splenic flexures respectively that are constant.

If there is gas in the small bowel or small bowel dilatation is suspected a **decubitus or erect film of the abdomen** to demonstrate fluid levels is recommended.

The jejunum is dilated if >3.5 cm diameter, mid small bowel if >3 cm diameter and the

ileum if >2.5 cm diameter. Dilated jejunum has valvulae coniventes or folds transversely across the diameter of the jejunum.

If the colon appears dilated check for the presence of haustra to confirm that it is the colon dilated. Haustra interdigitate and do not cross the diameter of the colon unlike the valvulae coniventes in the jejunum. The colon is dilated if the transverse colon diameter >5.5 cm or the caecal diameter at its base >8 cm.

Check the psoas outlines bilaterally: should be symmetrical with slightly concave lateral borders.

Check the renal outlines that should normally be 10–12 cm long or 3.5 vertebrae in longitudinal length.

Check the outline of the liver and spleen. The inferior border of the liver is well defined especially laterally.

Check for free intraperitoneal fluid or collections. The properitoneal fat line is displaced laterally by free fluid.

Look for radiopaque calculi and calcification in the region of the gall bladder, kidneys and ureters. Beware of pelvic vein phleboliths that may be confused with calculi. Phleboliths are oval, smooth and have a small internal lucency. Calculi appear dense with irregular margins. Pancreatic calcification is stippled and crosses the midline in an oblique axis. Vascular calcification is commonly seen in the aorta of older patients, diabetics and patients with aortitis from takayashu's disease.

Look for soft tissue masses and extraluminal gas.

CHAPTER 26

The acute abdomen

Peter Corr

The supine AP abdomen and erect chest radiographs are the best imaging investigation of the acute abdomen. The erect abdomen is used for detecting fluid levels, although it can be replaced by a decubitus view if the patient is too ill to stand. **Plain radiographs are useful in detecting:**

free intraperitoneal air

retroperitoneal and intramural gas

small and large bowel obstruction

radiopaque calculi

detect soft tissue masses and free fluid

Free intraperitoneal air pattern (figs 26.1a & 26.1b)

The erect chest radiograph and left side down decubitus abdomen radidograph are very sensitive for detecting small volumes of free intraperitoneal air (<5 mls). The commonest causes are: bowel perforation from penetrating ulcers or trauma, and bowel wall infarction.

On the erect chest a crescent of air is noted under the hemidiaphragm. It is important not to confuse subdiaphragmatic air with subpulmonic pneumothorax. If you are unsure whether there is free intraperitoneal air, a left side down decubitus view of the upper abdomen will demonstrate free air as a low density crescent lateral to the lateral margin of the right lobe of the liver. On the supine abdomen detection of free air can be difficult. There are two signs that can help: Rigler's sign of gas on either side of the

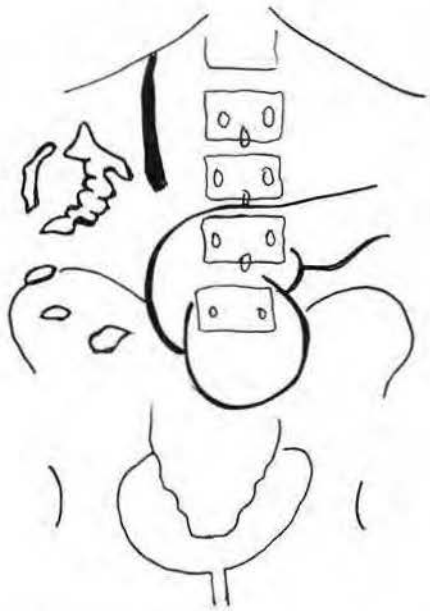

Fig 26.1a
Supine abdomen demonstrates free intraperitoneal air. Note the falciform ligament in the right upper quadrant, and the visualization of both sides of the bowel wall centrally.

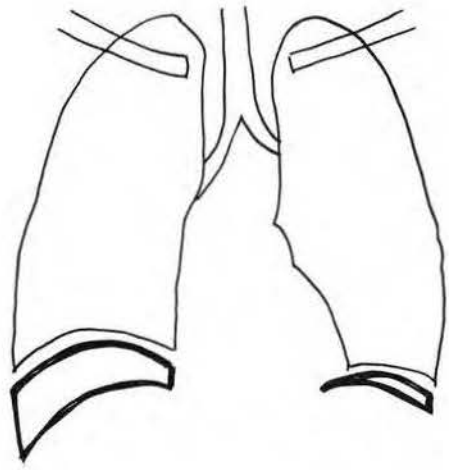

Fig 26.1b *confirms subdiaphragmatic free air on the erect chest radiograph.*

bowel wall, and the sign of outlining the falciform ligament of the liver in the right upper quadrant by free air.

Intramural gas pattern (fig 26.2)

Gas in the bowel wall appears as linear lucencies within the wall. It is usually from bowel wall infarction. In premature babies intramural gas is detected in nectrotising entercolitis (NEC). Often these neonates also have gas in the portal veins.

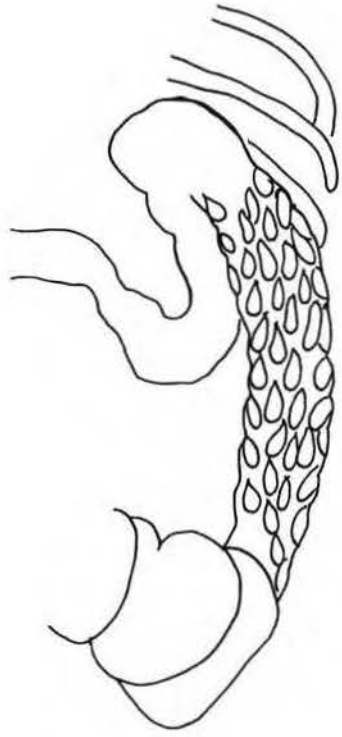

Fig 26.2 *Localised view of the colon of a premature baby demonstrates intramual air from necrotising enterocolitis.*

Gas outside the bowel (fig 26.3)

Gas may be detected in the wall of the gall bladder in emphysematous cholecystitis and in the gall bladder lumen if there is a fistula with the bowel or if there has been an anastomosis with the biliary tree.

Gas in the renal parenchyma is caused by empysematous pyelonephritis. This is usually due to a severe E coli infection of the kidneys in diabetics.

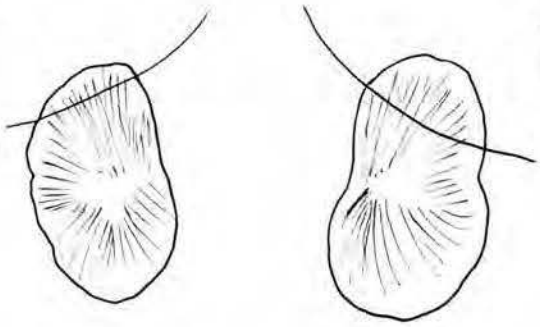

Fig 26.3
Free perirenal and renal gas in a diabetic patient with E coli renal infection.

Bowel obstruction pattern

The diagnosis of bowel obstruction is made clinically and confirmed by plain film radiographs. Supine, erect or decubitus abdomen views are usually required. With small bowel obstruction, the commonest causes are adhesions from previous surgery or peritonitis, followed by small bowel tuberculosis, appendicitis and tumours. Normally the small bowel is not visualised and there are no fluid levels present. With obstruction there is dilatation of the bowel with fluid and gas- the jejunum has valvulae conviventes while the ileum is featureless (fig 26.4a). On the erect or decubitus radiograph multiple fluid levels are present. Occasionally the obstructed bowel contains only fluid and no gas and the diagnosis can be missed. In such cases give the patient 50 mls of diluted water-soluble contrast agent orally. This will opacify dilated bowel and confirm the diagnosis (fig 26.4b).

In large bowel obstruction, the commonest cause is carcinoma of the colon, followed by inflammatory strictures and sigmoid volvulus. The colon can be identified because the haustra do not cross the lumen like valvulae coniventes of the jejunum. Usually the level of obstruction can be detected on decubitus films or a single contrast barium enema. In sigmoid volvulus there is disproportionate dilatation of the sigmoid colon with a twist (volvulus) at the rectosigmoid junction. On barium enema there is " bird of prey" appearance to the obstruction (figs 26.5a & 26.5b).

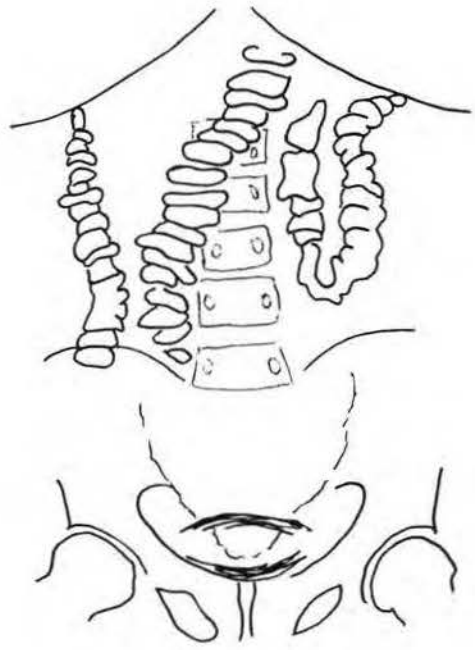

Fig 26.4a
Small bowel obstruction from adhesions. Note dilated jejunum with valvulae coniventes centrally. Calcification of the bladder noted from schistosomiasis.

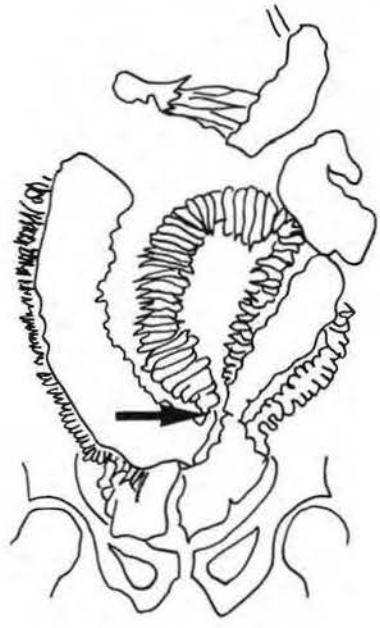

Fig 26.4b
Small bowel study confirms the site of the adhesive obstruction (arrow).

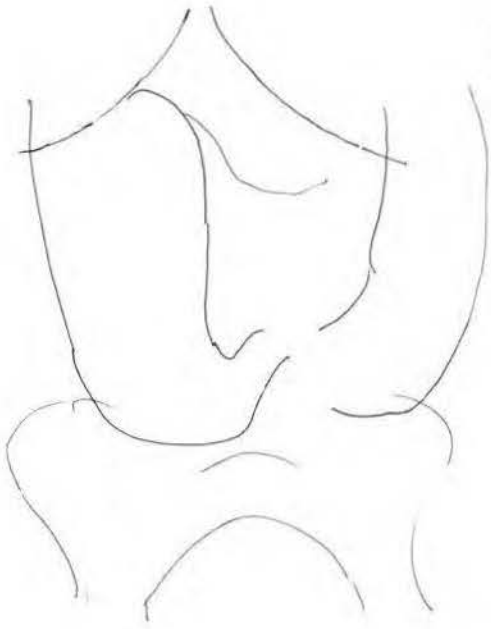

Fig 26.5a
Patient with a sigmoid volvulus. Note the disproportionate dilatation of the colon.

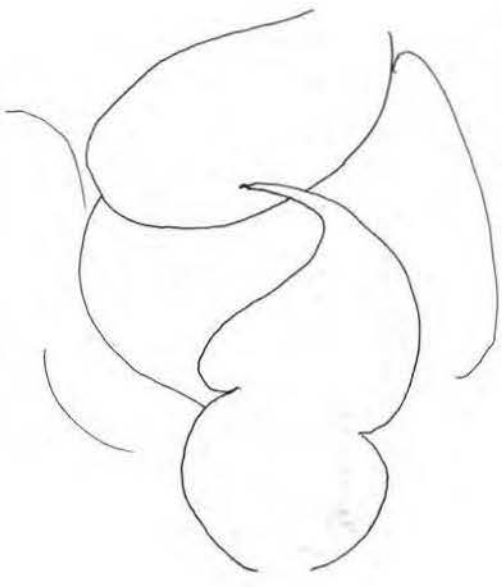

Fig 26.5b
Single contrast barium enema confirms the volvulus in the sigmoid colon.

Paralytic ileus

Paralytic ileus is generalised bowel dilatation with multiple fluid levels. Paralytic ileus is found post abdominal surgery, trauma, infection, metabolic states and certain drugs. It is particularly common in children following severe gastroenteritis.

Cholecystitis

Acute inflammation of the gall bladder is usually due to calculi obstructing the cystic duct. On plain film radiographs radiopaque calculi are detected in aproximately 20% of patients (fig 26.6). Ultrasound is usually diagnostic: a distended gall bladder >4 cm diameter, gall bladder wall thickening >4 mm, fluid around the gall bladder and echoes from calculi. Non-calculous cholecystis is found in ill patients in high care settings, ICU, burns, parenteral nutrition but the cystic duct remains patent on HIDA scan.

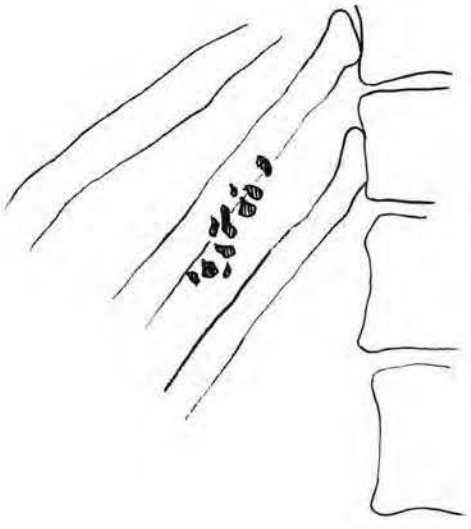

Fig 26.6
Patient with right upper quadrant pain. Localised views demonstrate multiple gallstones.

Pancreatitis

In acute pancreatitis a generalised or localised ileus is found. If there is an abscess or phlegmon a localised mass is detected. In chronic pancreatitis localised calcification is noted along the duct system of the pancreas (fig 26.7). Complications of acute pancreatitis include abscess formation, haemorrhage, pancreatic necrosis, pseudocyst formation and biliary obstruction.

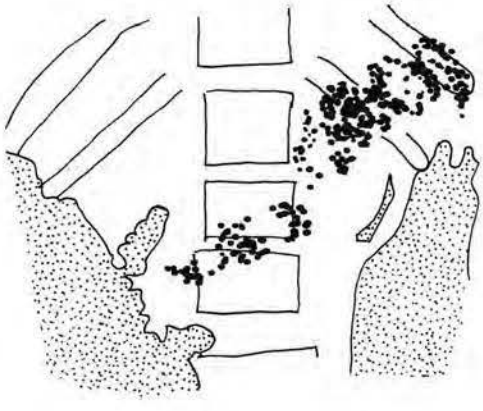

Fig 26.7
Patient with chronic pancreatitis demonstrates healvily calcified pancreas.

Abdominal collections and abscesses

Abscesses appear as soft tissue masses which may contain gas. Abscesses can be confused with the colon patterns on plain films. Both ultrasound and CT will usually establish the diagnosis. Intraperitoneal fluid and abscesses collect in the most dependent regions of the peritoneal cavity: the subphrenic spaces (fig 26.8), subhepatic space (between the right lobe of the liver and kidney) and in the pelvis in the rectovesical pouch or Pouch of Douglas (rectouterine pouch).

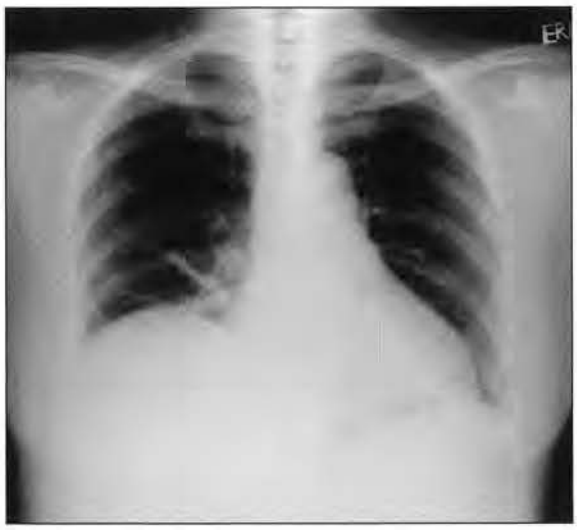

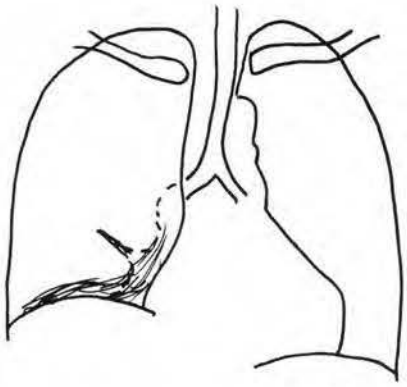

Fig 26.8
Patient with a subphrenic abscess demonstrates an elevated right hemidiaphragm with right lower lobe atelectasis.

Amoebic liver abscess

Amoebic liver abscess is common in many regions of the world. Patients present with right upper quadrant pain and marked tenderness in the intercostal spaces of the lower right ribs. Imaging is important in the diagnosis. The right hemidiaphragm is elevated and there is basal linear atelectasis in the right lower lobe because of the enlarged liver. The diagnosis is confirmed by ultrasound examination of the liver that will detect a hypoechoic lesion in the liver (fig 26.9).

Fig 26.9
Ultrasound of the right lobe of the liver demonstrates a hypoechoic solitary abscess.

Appendicitis

Appendicitis is a diagnosis that is increasingly being made in many developing countries. The classic symptoms and signs of appendicitis are not always present especially in young children and the elderly. The diagnosis may be confused with gynaecological causes in young woman. Imaging has an increasingly important role in the diagnosis. Plain radiographs may demonstrate a localised ileus in the right lower quadrant with dilated bowel loops and fluid levels, or a soft tissue mass suggesting an inflammatory mass. Very rarely will calcified appendicoliths be detected. Ultrasound will usually confirm the diagnosis. A swollen appendix with a distended lumen is detected. With patients where the appendix has perforated there is usually matted bowel loops around the appendix forming an inflammatory mass.

LEARNING POINTS: ACUTE ABDOMEN

- In suspected perforation, the supine abdomen and erect chest film or left side down decubitus abdomen are the most sensitive investigation to detect free air.
- Intramural gas usually indicates bowel wall infarction.
- Gas in the perirenal tissues and kidneys is found in acute renal infections in diabetics.
- In suspected small bowel obstruction the supine abdomen is more sensitive than the erect film. Beware of fluid filled dilated loops with no fluid levels; give the patient a water soluble contrast agent to confirm the diagnosis.
  Common causes: adhesions, inflammatory bowel disease.
- In suspected large bowel obstruction the supine abdomen and decubitus abdominal radiographs are especially sensitive. If unsure of the site of obstruction perform a dilute 1:6 single contrast barium enema to demonstrate the site of obstruction. Common causes: carcinoma, inflammatory disease, volvulus. In volvulus there is disproportionate bowel dilatation.

Reference

1. Field S. The Abdomen. In: *Diagnostic Radiology: a textbook of medical imaging*, 1997. Eds Grainger RG, Allison DJ. Publisher: Churchill Livingstone, Edinburgh.

CHAPTER 27

Gastrointestinal contrast studies

Peter Corr

Contrast media

Barium sulphate

The most common oral contrast used in the gastrointestinal tract is barium sulphate. It is an inert powder that is reconstituted into a suspension with water. Barium is safe to use for many investigations except:

- **when there is a suspicion of bowel perforation**
- **when there is a likelihood of aspiration of barium into the lungs**
- **in the presence of complete bowel obstruction**

Non-ionic water soluble contrast media

These agents are especially useful in detecting bowel perforation and when there is total oesophageal or bowel obstruction. Non-ionic constrast agents that are iso osmolar are the preferred agents in neonates and very ill infants.

Barium swallow (fig 27.1)

A barium swallow is indicated with patients with dysphagia or suspected oesophageal reflux. If total oesophageal obstruction from oesophageal cancer is suspected it is best to

Fig 27.1
Normal barium swallow.

use 5–10 mls of non-ionic water soluble contrast initially to detect the site of obstruction and so prevent aspiration of contrast into the lungs.

A swallow can be performed on a conventional erect bucky unit without fluoroscopy if you keep to the above rule. It is important to always have at least two views of the oesophagus in the AP and oblique planes. Always include the cervical oesophagus and oesophagogastric junction and stomach in the study.

Barium meal (fig 27.2)

A barium meal is performed for dyspepsia, epigastric pain or mass. It is important to give an antiperistaltic agent such as hyoscine 10–20 mg IV a few minutes before the procedure, in addition to granules that produce carbon dioxide gas to distend the stomach (ervescent fruit salts will also work!). A cup fill (250 mls) of high-density barium suspension is given orally to the patient. The patient is rotated anticlockwise to coat the stomach. Spot films of the stomach are taken using a fluorscopy table. The following views are especially important: fundus, subfundal, antrum, duodenum, and stomach body.

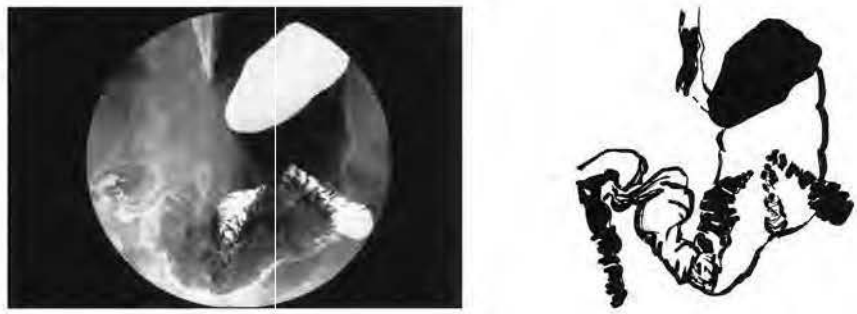

Fig 27.2 *Normal barium meal.*

Small bowel follow through (fig 27.3)

This technique is used to visualize the small bowel from the duodenojejunal junction to the ileocaecal valve. Always obtain a plain abdominal radiograph first to exclude bowel obstruction. Then give the patient a cocktail of 500 mls dilute barium suspension with

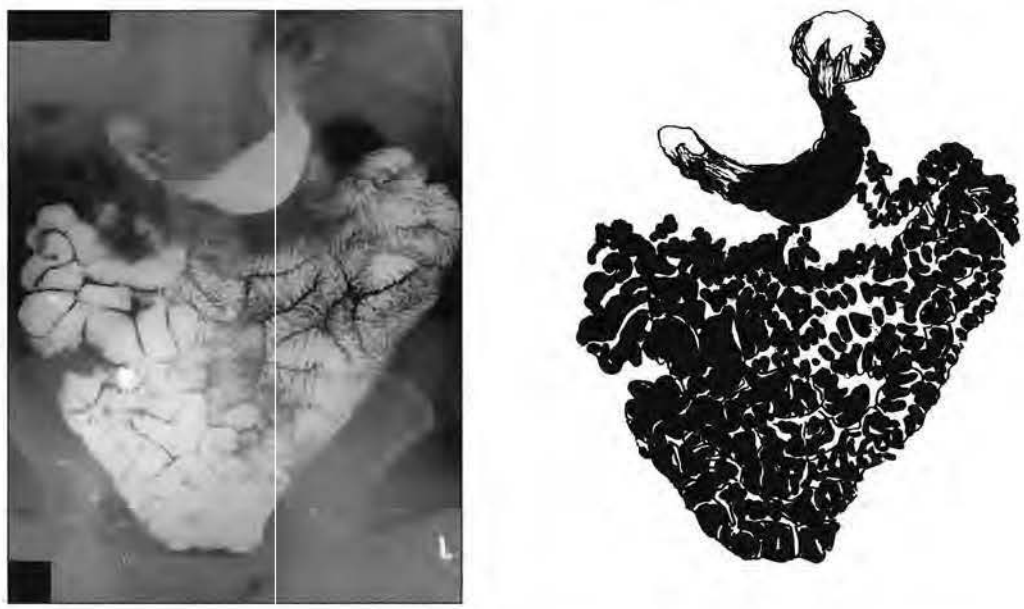

Fig 27.3 *Normal barium meal follow through examination of the small bowel.*

50 mls of water-soluble contrast medium (sodium diaztriote contrast) to drink. Lie the patient in the lateral position on their right side and take spot radiographs at 30, 60 and 90 minutes after drinking the contrast, by which time the contrast should have reached the terminal ileum. Adequate visualisation is obtained using high kv techniques (100–120 kvp).

Barium enema (fig 27.4)

Barium enema studies, using >100 kvp, are used to assess the colon for strictures, masses and polyps. The most important point is the preparation of the colon. An effective laxative must be given 24 hours before the procedure to clean the colon. Barium enemas are either single or double contrast. To detect obstruction in the presence of possible large bowel obstruction, a single contrast study is adequate. Single contrast studies involve using dilute barium sulphate (300 mls to 1800 mls of tap water). Double contrast studies require 200 mls of high-density barium and air insufflation. Double Contrast studies are used to demonstrate the mucosal surface of the colon to detect polyps or colitis.

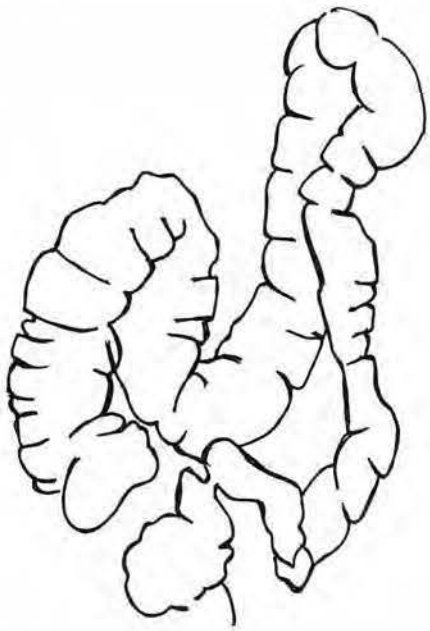

Fig 27.4
Normal barium enema.

Gastro intestinal tract patterns

THE OESOPHAGUS

The oesophagus extends from the pharynx to join the stomach at the oesophago gastric junction. In the cervical region at C3 there is an anterior impression on the lumen from a small venous plexus which must not be confused with a lesion. In the thoracic oesophagus there is a smooth impression due to the aorta and pulmonary artery. At the oesophago gastric junction there is a physiological sphincter.

OESOPHAGEAL PATTERNS

Ulcer patterns

Fold thickening and diffuse ulceration is common in monilial (candidial) infection. This is especially common in immunosuppressed patients (AIDS, patients on steroids or cytotoxic drugs) and malnourished children. Discrete longitudinal ulcers with

oedematous edges are common in herpes simplex infection. Deep punched out ulcers are found both in HIV and cytomegalovirus infections with patients with AIDS. Cytomegalovirus ulcers can be very large and perforate the oesophageal wall.

Reflux oesophagitis pattern (fig 27.5)

Peptic oesophagitis results from oesophageal reflux of gastric contents and may or may not be associated with a sliding hiatus hernia. There are often fine mucosal ulcers and if severe, can result in smooth stricturing of the distal oesophagus. **Patterns of oesophageal narrowing:**

- **oesophageal webs:** these are smooth webs in the anterior wall of cervical oesophagus. They are associated with patients with iron deficiency anaemia.
- **carcinoma:** these are irregular strictures, usually with proximal shouldering, most commonly in the middle third of the thoracic oesophagus (figs 27.6a & 27.6b).
- **benign stricture:** following reflux oesophagitis-these are usually smooth strictures in the lower third of the thoracic oesophagus (fig 27.5).
- **corrosive strictures:** particularly from caustic soda ingestion.
- **extrinsic compression:** from mediastinal lymph nodes, mediastinal tumours and aneurysms

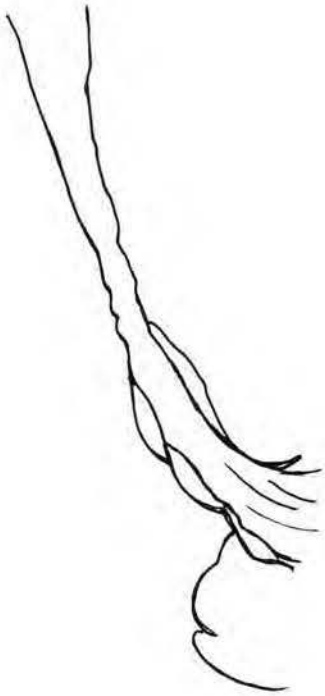

Fig 27.5
Barium swallow in a patient with a benign peptic stricture of the lower oesophagus.

Fig 27.6a
Lateral barium swallow in a patient with an extensive oesophageal carcinoma with proximal obstruction.

Fig 27.6b
Barium swallow in a patient with an oesophageal tracheal fistula from an oesophageal carcinoma.

Carcinoma of oesophagus (figs 27.6a & 27.6b)

Most carcinomas are common in the middle third of the thoracic oesophagus, followed by the lower third and then the upper third. Complications are common and must be searched for. Complications include: total obstruction, perforation and fistula formation into the tracheobronchial tree (fig 27.6b). A barium swallow will confirm the diagnosis of oesophageal carcinoma. Always give the patient a tablespoon full (15 mls) of barium to swallow first. This is to prevent aspiration of barium into the lungsin the present of severe obstruction. Usually the level of obstruction is evident on fluoroscopy. If fluoroscopy is unavailable, take erect PA and lateral chest radiographs after each swallow of barium.

Oesophageal varices (fig 27.7)

Today the diagnosis of oesophageal varices is established by endoscopy. However a barium swallow with the patient in a prone position on a fluoroscopy table will demonstrate multiple vertical serpiginious mucosal filling defects due to varices. It is important to search for varices in the undistended empty oesophagus as they can easily be compressed and be undetectable during if the oesophagus is distended by air or barium bolus.

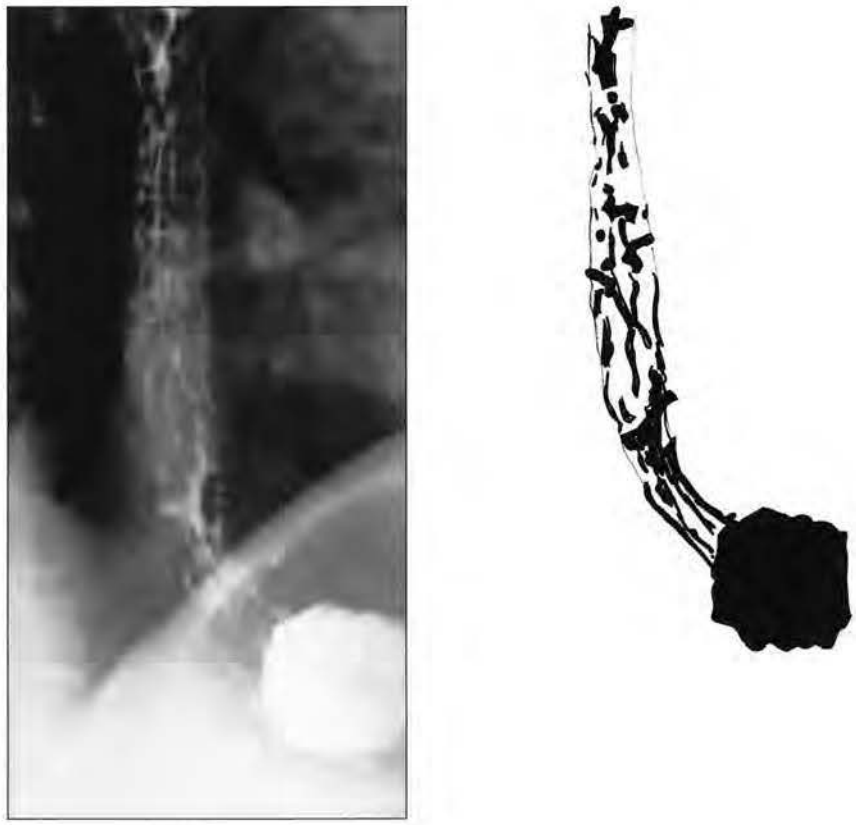

Fig 27.7
Barium swallow of a patient with oesophageal varices.

Oesophageal web (fig 27.8)

Webs are a cause of dysphagia in the cervicial oesophagus. They occur on the anterior oesophageal wall. Patients often have associated iron deficiency anaemia. They must not be confused with a small submucosal venous plexus on the anterior wall.

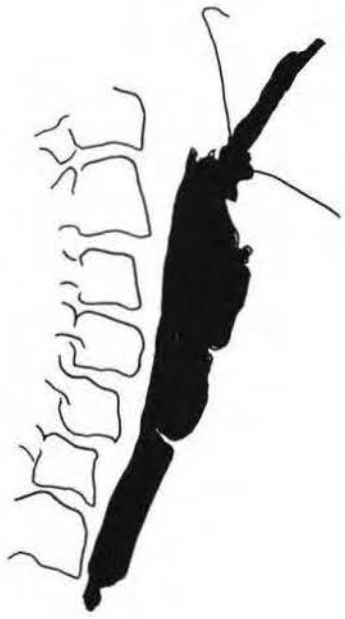

Fig 27.8
Oesophageal web on the anterior border of the cervical oesophagus at the C5 level.

Hiatus hernia (fig 27.9)

Hiatus hernia is a common finding of herniation of the stomach through the oesophageal hiatus (sliding). It may be associated with oesophageal reflux in some patients. It is best demonstrated by placing the patient in a prone oblique position and

Fig 27.9
Barium meal of a sliding hiatus hernia.

asking the patient to take a deep inspiration after swallowing a mouthful of barium. Sliding hiatus hernia can be complicated by ulceration and bleeding. A rolling or para oesophageal hernia is where the oesophago-gastric junction remains in its normal anatomical position however a cuff of stomach wall herniates around the sphincter into the chest. It is important to detect as incarceration can occur in rolling hernias but is rare in the more common sliding variety.

STOMACH

The stomach mucosa and lumen are well visualized by barium meal. By rotating the patient on the fluoroscopy table, you will achieve a double contrast effect of the mucosa from the barium and carbon dioxide gas. Remember to achieve maximum distension of the stomach lumen with carbon dioxide gas powder or tablets after the patient has swallowed the barium.

STOMACH MASS LESIONS PATTERNS

Single gastric mass (figs 27.10, 27.11, 27.12)

A mass can originate from the stomach muscle layer, submucosa, mucosa or in the lumen of the stomach or be due a mass extrinsic or invading the stomach. Masses are

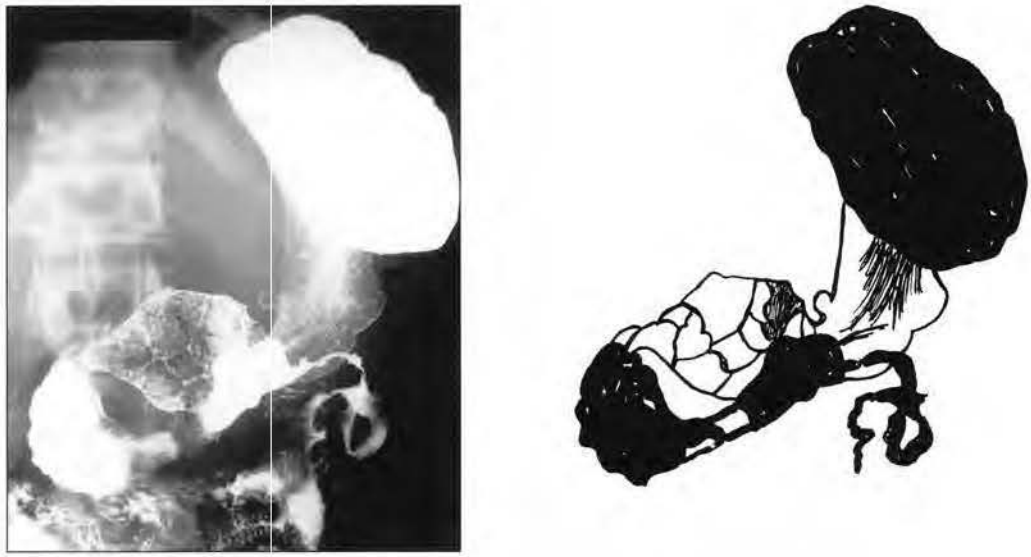

Fig 27.10 *Barium meal of a patient with linitis plastica of the stomach.*

Fig 27.11 *Barium meal of a patient with carcinoma of the stomach demonstrating concentric narrowing of the body and antrum of the stomach.*

Fig 27.12
Patient with a leiomyoma of the stomach on barium meal.

identified as filling defects on barium meal or soft tissue densities. **Common causes of solitary mass in the stomach are:**

- Polyp: adenomatous or carcinoma (primary or secondary)
- Leiomyoma or leiomyosarcoma (fig 27.12)
- Bezoar
- Extrinsic tumour: pancreas adenocarcinoma

Multiple gastric masses

- polyps
- fundal varices (fig 27.14)
- gastric cancer
- lymphomas
- Kaposi's sarcoma (fig 27.13)

  —metastases

Early stomach cancer may be difficult to detect if is plaque-like. With all masses it is important to determine the cancer's extent, especially to determine whether the oesophagogastric junction and duodenal cap are involved which may preclude gastrectomy. With antral tumours you must mention whether there is any gastric outlet obstruction. Multiple masses are common in lymphoma, metastases and Kaposi's sarcoma (fig 27.13).

Fundal varices are seen after splenic vein thrombosis and appear as serpinginous filling defects in the fundus (fig 27.14). Varices change size on changing position from supine to erect and decrease with distension of the stomach with gas. It is important not to confuse them with a mass as inadvertent biopsy of fundal varices can be fatal.

Fig 27.13 *Barium meal of an AIDS patient with Kaposi's sarcoma of the stomach. Note the polypoid masses in the body of the stomach.*

Fig 27.14 *Patient with gastric varices in the body and fundus on barium meal.*

Thickened stomach folds

The rugae or stomach folds are especially prominent along the greater curvature and body of the stomach. Rugae that are greater than 1 cm in diameter are considered to be enlarged or thickened. **Causes of rugal thickening include:**

- inflammatory: gastritis, Zollinger Ellison syndrome
- tumours: lymphoma, adenocarcinoma
- Menetrier's disease

Linitis plastica pattern ("bald stomach") (fig 27.10)

The stomach appears contracted with a featureless flat mucosal surface. This is called linitis plastica or "water bottle" stomach. Important causes for this are: adenocarcinoma, lymphoma, breast metastases, battery acid ingestion (fig 27.15), tuberculosis, Crohn's disease, and eosinophilic gastroenteritis.

Fig 27.15
Barium meal of a patient who swallowed battery acid demonstrates gastric outlet obstruction from a small stomach without rugae.

The main causes in Africa are primary stomach cancer and battery acid ingestion. With adenocarcinoma, it may be very difficult to get a positive biopsy of the stomach as the cancer spreads in the deep submucosa and the overlying mucosa is often normal. There is usually a bald stomach pattern with gastric outlet obstruction from antral stenosis and swollen mucosal folds in the small bowel (fig 27.15).

Ulcers

Stomach ulcers are common on the lesser curve and antrum. They appear as collections of barium outside the line of the stomach lumen (fig 27.16). You cannot differentiate between a benign or malignant ulcer on barium meal alone. However ulcers on the greater curvature are invariably benign. Duodenal ulcers appear as irregular deformed duodenal caps. Normally the first part of the duodenum has a triangular appearance but after ulceration the cap becomes deformed (fig 27.17). It is impossible to decide on a barium meal whether an ulcer is active or inactive without assessing the patient for clinical signs of ulcer activity first. Complications of ulcers are bleeding and perforation. Barium studies play no role in the diagnosis of gastrointestinal haemorrhage, the diagnosis is made usually by endoscopy and barium will only interfere with the endoscopic study.

Fig 27.16
Large penetrating ulcer on the lesser curve of the stomach.

Fig 27.17 *Penetrating duodenal ulcer on barium meal.*

SMALL BOWEL PATTERNS

There are only three patterns of small bowel disease: strictures or narrowing, mucosal fold thickening or multiple nodules or masses.

Small bowel stricture pattern

Strictures can be single or multiple. **Causes of small bowel strictures are:**

- fibrous adhesions from previous abdominal surgery or peritonitis are the commonest cause
- inflammatory: tuberculosis and Crohn's disease
- neoplastic: adenocarcinoma, lymphoma
- radiation strictures especially following irradiation of pelvic cancer

To detect the level of the stricture and its extent, a barium follow through examination is the best investigation. Always take a control supine abdomen radiograph first as this may demonstrate dilated small bowel and give you an idea where the stricture is. Often it is difficult to differentiate between the various causes however both TB and Crohn's disease tend to occur more commonly in the ileocaecal region.

Terminal ileum

Strictures here are common in two inflammatory conditions that are radiological indistiguishable: Crohn's disease and tuberculosis. Tuberculosis usually causes stricturing of the caecum as well as the terminal ileum which becomes small and conical with the terminal ileum becoming straight and vertical at the level of the ileocaecal valve (figs 27.18 & 27.19).

Fig 27.18
Barium enema of a patient with ileocaecal tuberculosis demonstrates deep ulcers in the terminal ileum and caecum with circumferential narrowing.

Fig 27.19
Barium enema of a patient with tuberculosis of the colon demonstrates multiple apthoid ulcers throughout the colon.

Small bowel fold thickening

Fold thickening is best visualized on barium follow through studies. There are many causes:

- ischaemia: acute from mesenteric infarction
- ischaemia: chronic from vasculitis or radiation injury
- oedema: hyproteinaemia
- inflammatory: TB, Crohn's
- venous-: Budd Chiari, cirrhosis

- lymphatic obstruction
- infiltration: lymphoma, carcinoma, metastases, eosinophilic enteritis.

The causes can be divided into two groups: **focal** and **diffuse** fold thickening.

Focal causes include ischaemia, inflammatory, and tumours while diffuse causes include oedema, lymphatic obstruction and infiltrative processes.

Nodular small bowel pattern

This usually represents an infiltrative process either inflammatory or neoplastic. Nodular lymphoid hyperplasia is a hyperplasia of the Peyer's patches in the ileum and can be a normal variant. Multiple nodules are found in small bowel lymphoma, metastases, and eosinophilic enteritis.

THE COLON

Barium enema examination remains the easiest method of imaging the colon. It is important to tailor the examination to the patient and the suspected pathology. In young patients it is usually possible to obtain good mucosal coating of the colon with a double contrast study while in older patients who have suspected large bowel obstruction a more limited single contrast study will determine the site of obstruction.

Colon stricture pattern

Colon stricture is an important pattern to identify on barium enema. There is a focal narrowing of the colon with proximal dilatation of the normal colon. If there is "shouldering" at either end of the stricture a carcinoma must be suspected ("apple core" lesion) (fig 27.20). Assessing the mucosa for destruction is very inaccurate hence it is best to consider all strictures to be malignant until proved otherwise. Inflammatory lesions tend to be longer than malignant strictures and may have fistulae present in diverticular disease. It is important to appreciate that a malignant and inflammatory stricture can coexist in diverticular disease. **Common causes for colon stricture are:**

- neoplastic: adenocarcinoma, lymphoma
- inflammatory: diverticular disease, ulcerative colitis, Crohn's, amoebiasis,
- tuberculosis
- radiation
- ischaemia
- extrinsic compression from tumours or inflammatory masses

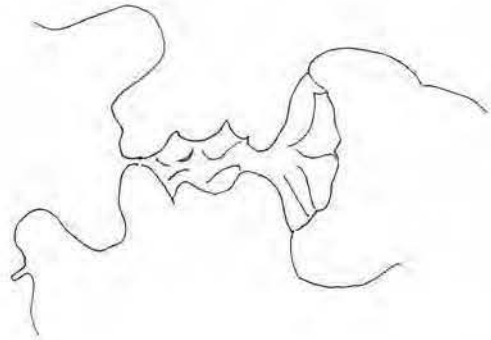

Fig 27.20
Barium enema of a patient with a transverse colon carcinoma demonstrates an "apple core" circumferential narrowing of the transverse colon from a carcinoma.

Colonic masses pattern

Focal masses or polyps appear as filling defects on a single contrast enema or as soft tissue densities on double contrast studies (fig 27.21). Polyps than are more than 2 cm in diameter should be removed because of the risk of malignancy. If multiple polyps are present in the colon polyposis coli is a possible cause (fig 27.22). This is an autosomal dominant condition, which will lead to multifocal carcinoma by the 4th decade. It is important to screen other members of the family for polyps. Inflammatory polyps are

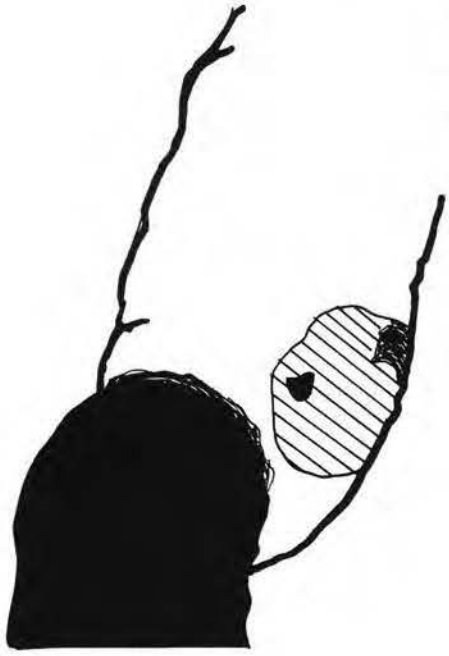

Fig 27.21
Barium enema of a patient with rectal bleeding demonstrates an ulcerated polyp in the sigmoid colon.

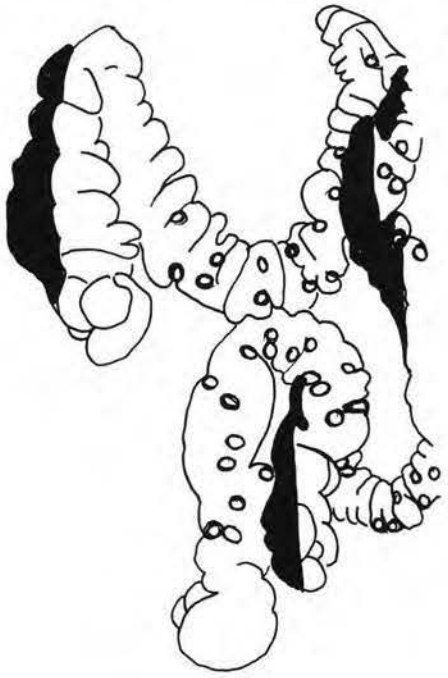

Fig 27.22
Barium enema of a patient with multiple polyposis coli. Note multiple small polyps through out the colon.

detected after colitis either amoebiasis or ulcerative colitis, they tend to be filiform in appearance. **Causes of polyps:**

- polyps: adenomas, hamartomas
- carcinoma
- lymphoma
- post inflammatory following colitis

Carcinoma of the colon (figs 27.23a & 27.23b)

This diagnosis can be made with double contrast barium enema with a sensitivity of 76%. Patients with caecal or ascending colon cancers present with chronic blood loss

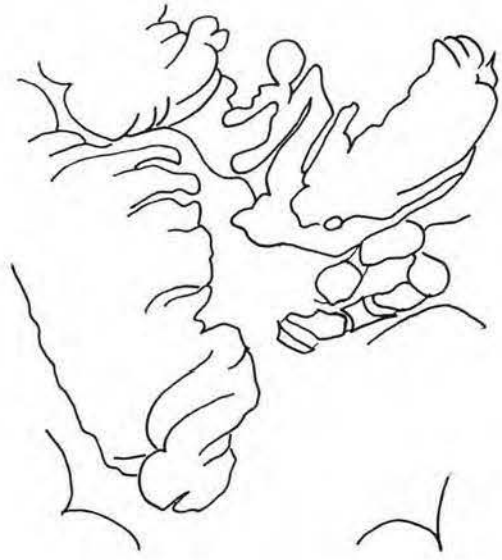

Fig 27.23a *Patient presenting with large bowel obstruction. Note large bowel dilatation.*

Fig 27.23b *Single contrast barium enema demonstrates total obstruction in the sigmoid colon from a carcinoma.*

and anaemia while patients with descending colon and sigmoid colon cancers present with symptoms of obstruction. Important points to remember are that 15% of patients will have a second tumour at presentation, so that you must be able to clearly visualize the whole colon especially the caecum ansd sigmoid colon where most cancers occur. Cancers present either as a mass or polyp or focal circumferential narrowing ("apple core" lesion). Polyps appear as a filling defect in a pool of barium or as soft tissue mass density if coated by barium. It is important to distinguish a polyp from faecal residue: faeces generally tend to have irregular sharp edges while polyps are smooth. Any polyp that is more than 2 cm diameter at the base should be viewed with suspicion as possibly malignant and removed by endoscopy.

Colonic "thumb printing" pattern (fig 27.24)

Thumb printing is an important observation on both plain radiographs and barium enema. Thumb printing usually represents odematous or ischaemic colonic mucosa. **It is found in:**

- Amoebiasis
- Ischaemic colitis
- Crohns disease
- Ulcerative colitis

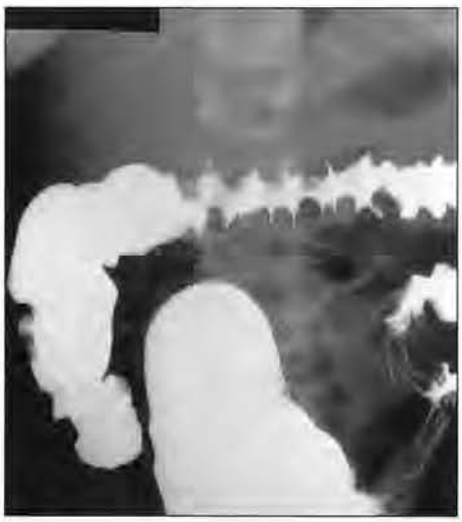

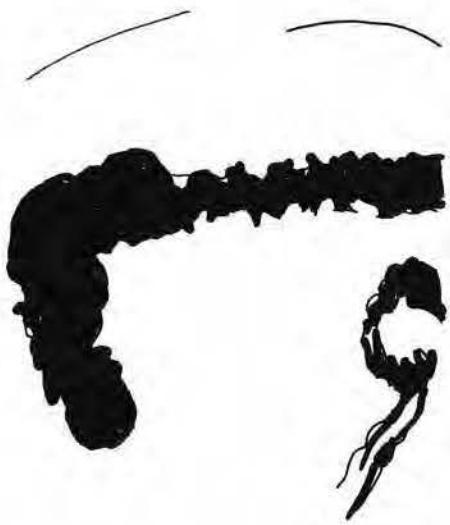

Fig 27.24
Barium enema of a patient with amoebic colitis. Note "thumbprinting" appearance to the colon.

Colitis pattern (fig 27.24)

Colitis is an inflammation of the colonic mucosa. On barium enema it appears either as discrete ulcers or diffuse ulceration. The most important colitis in many developing countries is amoebic dysentery. Amoebic colitis is often indistinguishable from ulcerative colitis. In severe cases there may be thumb-printing of the colon, megacolon and colon perforation with intraperitoneal abscess formation. Crohn's colitis and tuberculous colitis appear similar with discrete deep asymmetrical ulcers, often with fistulas and stricture formation.

Megacolon

Megacolon occurs when the diameter of the transverse colon exceeds 5.5 cm. Causes are: colon obstruction, colon pseudo obstruction, severe colitis, ischaemic colitis, and amoebiasis. When there is associated thumb-printing and the patient is ill it is termed toxic megacolon. In severe colitis this may be a precursor of colonic perforation. Serial supine abdominal radiographs are required to detect gas in the bowel wall or free intraperitoneal gas to indicate perforation.

Diverticular disease (fig 27.25)

Diverticula are out pouches of the mucosa and submucosa through hypertrophied smooth muscle in the wall of the colon. Although considered uncommon in developing countries, there is an increasing incidence from a change in diet from unrefined to refined carbohydrates. Patients may be asymptomatic, but if the diverticula become infected, form abscesses and or fistula in the sigmoid colon. Ascending diverticula may be a cause of active large bowel bleeding. The pattern is easy to recognise, however beware of confusing polyps for diverticula. Polyps have increased soft tissue density.

Fig 27.25 *Barium enema in a patient with extensive diverticular of the sigmoid and descending colon.*

LEARNING POINTS: GASTROINTESTINAL CONTRAST STUDIES

- Common oesophageal strictures are from oesophageal carcinoma and following peptic oesophagitis
- Complications of oesophageal carcinoma are: tracheal oseophageal fistula, perforation with mediastinitis, aspiration and total obstruction
- Important causes of oesophagitis in AIDS patients are monilial oesophagitis, herpes simplex, CMV and HIV infections
- Causes of a solitary gastric mass are: polyps- adenomas, carcinomas, leiomyomas or sarcomas, bezoars,and extrinsic tumours (pancreas) invading the wall
- Causes of multiple gastric masses are: polyps, fundal varices, adenocarcinoma, lymphomas, Kaposi's sarcoma and metastases.
- Causes of gastric fold thickening: gastritis, Zollinger Ellison syndrome, lymphoma, Menetrier's disease
- Causes of a "bald stomach" linitis plastica; adenocarcinoma, lymphoma, metastases, battery acid ingestion
- Causes of small bowel strictures: fibrous adhesions, inflammatorty-TB, Crohn's, tumours-adenocarcinoma, lymphoma, ischaemic/radiation damage
- Causes of colon strictures are: tumours-adenocarcinoma, lymphoma, metastases, inflammatory-diverticular, amoebiasis Crohn's, TB, ulcerative colitis, ischaemia/radiation, extrinsic compression by tumours
- Causes of colon polyps: adenomas, hamartomas, carcinoma, lymphoma, post inflammatory
- Causes of "thumb printing" of the colon: amoebiasis, ischaemic colitis, Crohn's, ulceratice colitis

Reference

1. Chapman S, Nakielny R. *Aids to Radiological Differential Diagnosis*. 1995, Saunders, London.

CHAPTER 28

Paediatric abdomen

Laurence Hadley & Peter Corr

Neonatal abdomen

Imaging the ill newborn infant requires that radiographs are taken with a mobile X-ray unit while the neonate is in the incubator. Often only the supine chest and abdomen radiograph are all that is required to make a diagnosis. When further studies are required it is very important to keep the baby warm throughout the procedure and to return the baby to the incubator immediately after the procedure.

Oesophageal atresia (fig 28.1)

Usually there is a history from the mother of sucking difficulties from birth and a nasogastric tube cannot be passed more than 11–12 cm. Babies present with bubbly saliva on their lips because they cannot swallow. It is extremely important not to give this neonate any oral contrast as this will be aspirated immediately into the lungs. Air in the distended upper oesophagus, to the level of the atresia with the nasogastric tube stopping at this site is diagnostic. There is usually no air in the stomach in pure oesophageal atresia, however in 85% of babies there is an associated tracheo oesophageal fisula which allows air into the stomach with each breath. Associated rib and vertebral anomalies are commonly detected.

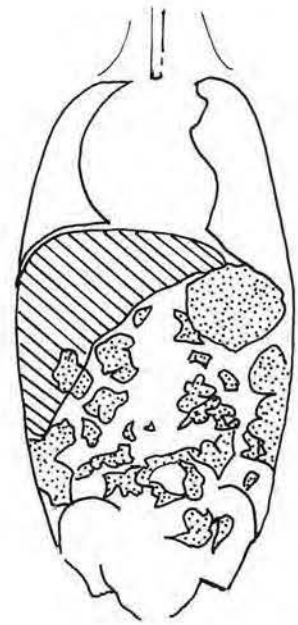

Fig 28.1 *Child with oesophageal atresia demonstrates a dilated air filled proximal oesophagus with a nasogastric tube coiled up in it.*

Neonatal bowel obstruction (figs 28.2a & 28.2b)

Bile stained vomiting in the newborn is indicative of intestinal obstruction. A supine chest and abdomen film will define the site of obstruction. Upper intestinal obstruction is characterised by a few fluid levels on the abdominal radiograph. In duodenal obstruction there are usually only two fluid levels called the double bubble sign. Duodenal obstruction is due to midgut volvulus until proved otherwise and it is extremely important not to miss this life threatening condition. Mid gut volvulus results from the small bowel twisting on itself. A non-ionic water soluble contrast agent such as iohexol will identify the volvulus. The critically important observation to make is whether the duodenum has a normal C shape with the duodenojejunal junction to the left of the midline which is found in normal babies or whether the duodenojejunal junction to the right of the spine as seen in mid gut malrotation. With mid gut volvulus there is often a "cork screw" appearance to the mid-gut. Jejunal and ileal atresia will present with distended featureless bowel loops with multiple fluid levels. It is impossible to distinguish between small and large bowel radiologically in neonates.

Fig 28.2a
Barium meal of an infant with malrotation of the duodenum. Note the inverted "C" of the duodenum.

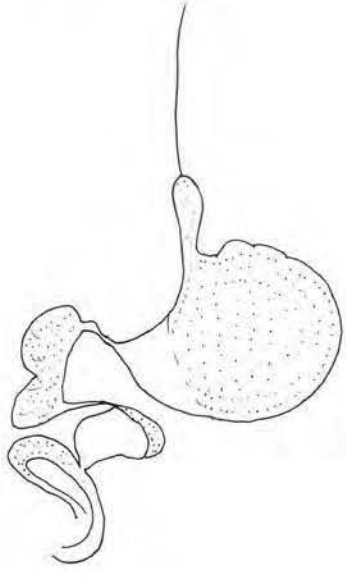

Fig 28.2b
Barium meal of a child with bile stained vomiting demonstrating mid gut volvulus with a "cork screw" appearance to the duodenum.

Anorectal malformations

The diagnosis of anorectal malformation is made by examining the child's perineum. The treatment depends on the level of the malformation. In females the level can be assessed by visual inspection but this is impossible in males to determine whether the abnormality is above or below the levator muscle. Babies should be placed in the genu pectroral position and left in this position for several minutes. This will allow gas to rest in the distal bowel and outline the malformation. A lateral shoot through abdomen film allows one to identify low malformations below the pubococcygeal line.

Nectrotising enterocolitis (NEC)

This condition, found in very ill premature babies, results in bowel wall ischaemia and infarction. Linear lucencies are noted in the bowel wall with gas in the portal vein branches of the liver. The diagnosis is made by carefully looking daily for the streaky lucencies in the bowel wall on the supine abdominal film.

Acute abdomen in infants

Abdominal radiographs are essential for the diadnosis of intestinal obstruction in children, although it is important to remember that gastroeneteritis, hypokalaemia can cause multiple fluid levels due to paralytic ileus.

Intussusception (figs 28.3a & 28.3b)

Acute abdominal pain in infants has many causes. It is important to establish whether there is bowel obstruction. Intussusception is common in infants who present with episodes of colicky abdominal pain and bloody diarrhoea. The diagnosis should be considered on supine abdomen radiographs with bowel dilatation and in some patients a soft tissue mass from the intussuception. Usually the diagnosis is more easily made by ultrasound where a "doughnut" or "target" mass is detected. An air enema is used to

Fig 28.3a *Abdominal radiograph of a child with an intersussception demonstrating non specific small bowel dilatation.*

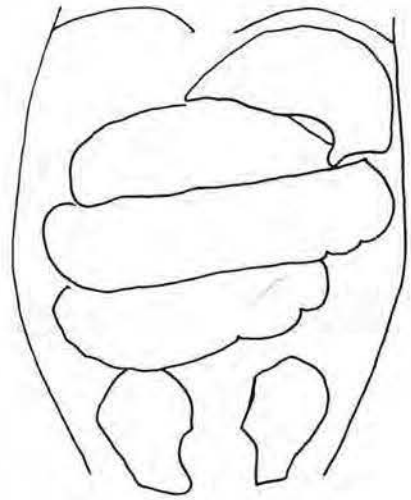

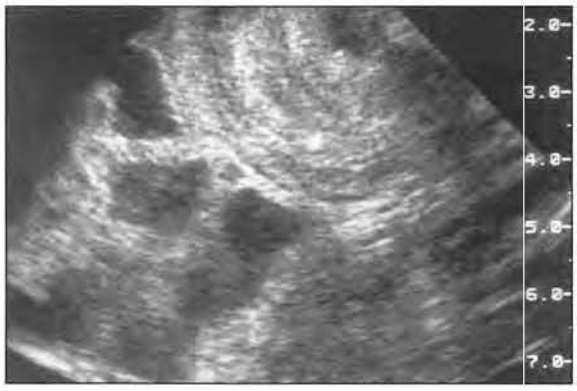

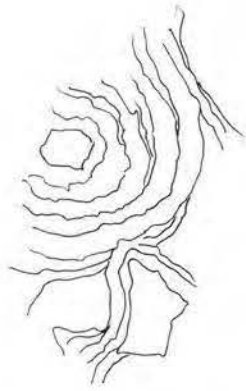

Fig 28.3b
Ultrasound demonstrated a multilayered mass in the right iliac fossa typical of an intersusception.

detect the intussusception and can also be used to reduce it at the same time. It is important to perform this procedure only if the child is well sedated, and fully resuscitated, and the history is less than 48 hours.

Worm bolus obstruction (figs 28.4a & 28.4b)

Ascaris worm boluses are a common cause of small bowel obstruction in patients in many developing countries. The child presents with severe colicky abdominal pain and vomiting. Often the abdominal radiograph will demonstrates a mass of worm bodies

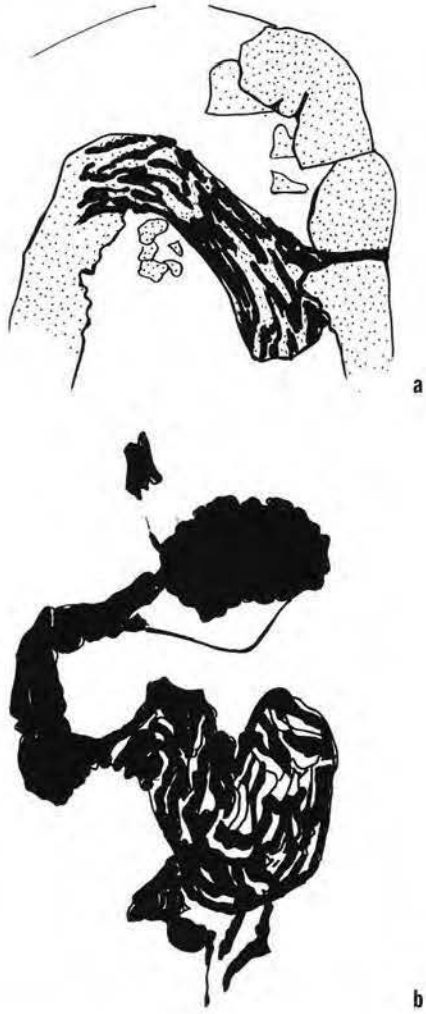

Fig 28.4a
*Plain abdomen of a child presenting with colic demonstrates a "worm bolus" and multiple fluid levels from bowel obstruction. This is confirmed on the barium meal (**28.4b**).*

with bowel dilatation and fluid levels proximal to the obstruction. The worms also ascend the common bile duct and cause cholangitis and liver abscess. The diagnosis is usually established by ultrasound, where the worm bodies are seen as echogenic masses in the bile duct.

LEARNING POINTS

- Bile stained vomiting in neonates is indicative of intestinal obstruction
- Malrotation of the mid gut is diagnosed if the DJ flexure is to the right of the spine and the doudenum C-loop is not formed
- Midgut volvulus is diagnosed in the presence of malrotation and a "cork screw" appearance of the duodenum
- Oesophageal atresia is diagnosed by a dilated proximal oesophagus with the nasogastric tube at the level of the atresia
- Never feed oral contrast media to a baby with oesophageal atresia
- Fluid levels are commonly seen in gastroenteritis
- Ascaris infestation is a common cause of bowel obstruction. The diagnosis is made by detecting the worm bolus on the plain radiograph
- Intussusception can be diagnosed on plain films and ultrasound and confirmed by an air enema that can be used to reduce it
- It is good practice to minimise radiation to the child during procedures
- It is always good practice to minimise radiation dose during procedures

CHAPTER 29

Urinary tract imaging

Malai Muttarak, Peter Corr & Wilfred C.G. Peh

Introduction

The main imaging methods for investigation of the urinary tract are radiography, intravenous urography (IVU), micturating (or voiding) cystography (MCU) and ultrasonography (US) of the kidneys and bladder.

Anatomy

An understanding of the normal anatomy and normal anatomical variants of the kidneys and collecting systems is essential to interpret imaging (fig 29.1). The kidneys are situated in the retroperitoneum with the hila located at the level of L1 vertebra. In adults, both kidneys measure 10–12 cm long from pole to pole. Kidneys are approximately 5.5 cm in length in the neonate, and grow to reach adult size by 8 years of age. The adult renal parenchyma should measure at least 2 cm in thickness. It is important to understand the position and orientation of the kidneys. The upper poles are deviated medially, and the lower poles are deviated laterally at an angle of 30 degrees from the vertical axis. Due to their anterior location relative to the psoas muscle, the upper poles are more posteriorly located poles. Each renal hilum contains the renal vein, renal artery, renal pelvis and proximal ureter. The ureters descend along

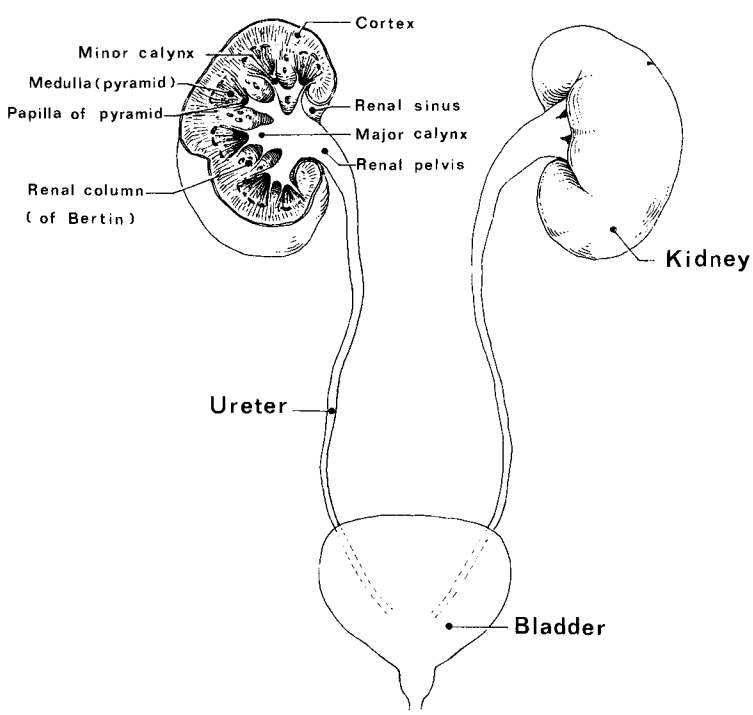

Fig 29.1
Diagram of the normal urinary tract.

a line linking the tips of the transverse processes of the lumbar vertebrae, and insert into the bladder at the ureterovesical junctions. The bladder is an extraperitoneal pelvic organ situated anterior to the uterus in females and to the rectum in males. The male urethra is divided, from proximally to distally, into prostatic, membranous and bulbar portions. The female urethra is a much shorter structure. Due to the complex embryology of the urinary tract, there are a number of normal anatomical variants, which should not be confused with pathological conditions. Recognition of these variants is therefore important (table I).

Table I. *Variants and developmental anomalies of the urinary tract*

Anomalies in number
–Renal agenesis (single kidney)
–Supernumerary kidney
Anomalies in size
–Hypoplasia
–Hyperplasia
Fusion anomalies
–Horseshoe kidney
–Cross ectopy with fusion
Anomalies in position
–Ectopic kidney (sacral or pelvic kidney)
–Cross ectopy without fusion
Other anomalies
–Foetal lobulation
–Large column of Bertin
–Ureteropelvic obstruction
–Duplication of renal pelvis and ureter
–Retrocaval ureter
–Ureterocoele
–Aberrant renal arteries

"KUB" film

The imaging examination of the urinary tract should start with a conventional radiograph of the kidney, ureter and bladder, which is commonly called a "KUB" film. It is essential the KUB film be taken before any intravenous contrast agent is injected so as not to obscure calcified structures.

Technique

Careful radiographic technique in obtaining a KUB is important. The patient is placed in a supine position. The radiograph should be exposed soon after the patient has voided and at the end of full expiration. Upper margins of the radiograph should include the suprarenal area, while the lower margin should include the pubic rami (fig 29.2). For good visualisation of the renal outlines exposure factors of 70–80 Kvp for an adult patient are required.

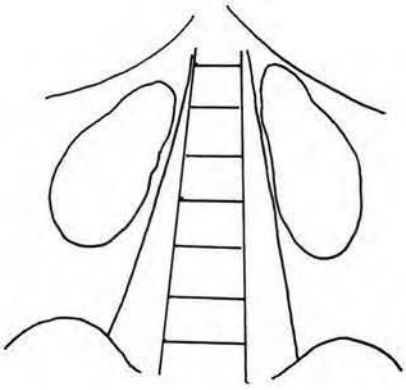

Fig 29.2
Normal KUB radiograph.

Normal KUB

The renal outlines should be seen unless they are obscured by overlying bowel gas. The size, shape and position of the kidneys should be noted. The ureter is not visualized but if a radiopaque calculus is present it may be seen along the course of the ureter (fig 29.3). The presence of vertebral scoliosis or obliteration of normal psoas shadows may suggest the possibility of renal or perirenal inflammation.

- The renal size is normally 3–4 lumbar vertebral bodies in length (12–14 cm long, 5–7 cm wide)

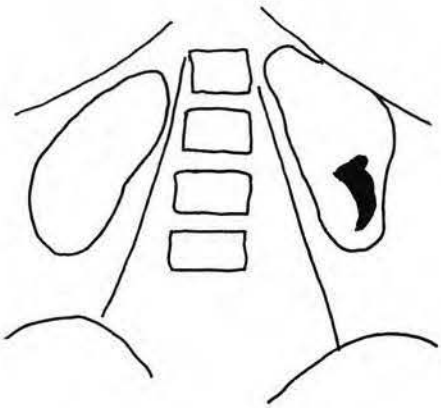

Fig 29.3
Staghorn calculus in the lower pole of the left kidney.

- Differences between the right and left renal sizes should not be more than 1 cm
- The right kidney is usually 1–2 cm more caudally located than the left kidney
- The renal axis should be parallel to the axis of the psoas muscle

Intravenous urography (IVU)

Although IVU has been replaced by spiral computed tomography and ultrasound (US) for certain indications, it remains an important imaging investigation and is able to provide a general overview of the whole urinary tract. Patient preparation is important, as is the technique of performing the IVU.

Patient preparation

- One day before examination: castor oil at 6 pm
- Nothing by mouth 6–12 hours before the examination
- Day of examination: one dulcolax suppository at 6 am

For children no preparation is required although for children under 2 years a drink of a "fizzy" cool drink before the IVU will distend the stomach and improve visualisation of the kidneys.

IVU technique

1. KUB: To detect radio-opaque renal and or ureteric calculi
2. Injection of 300–350 mg Iodine (I)/ml contrast agent
   —Dosage for adult is usually 50 ml
   —Dosage of child is 1.5 ml/kg body weight (300 mgI/ml)
3. 1 minute coned radiograph of both kidneys to show the "nephrogram" phase of contrast opacification. Gonads to be shielded by lead strips.
4. 5 minute coned radiograph of both kidneys to show the pelvicalyceal system. Distension of the upper collecting system can be achieved by compression of the mid-abdomen by a compressor band (fig 29.4).
5. 15 minute full length "release" radiograph to show the ureters and the bladder. This is obtained following release of the compressor band. The entire length of the ureters may not be seen in a single radiograph due to peristalsis (fig 29.5).
6. 30 minute coned radiograph of the opacified bladder

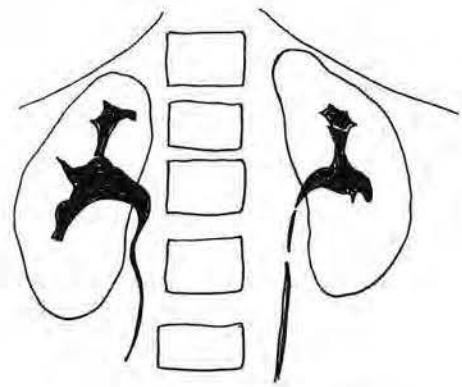

Fig 29.4
Normal 5 minutes coned nephrogram.

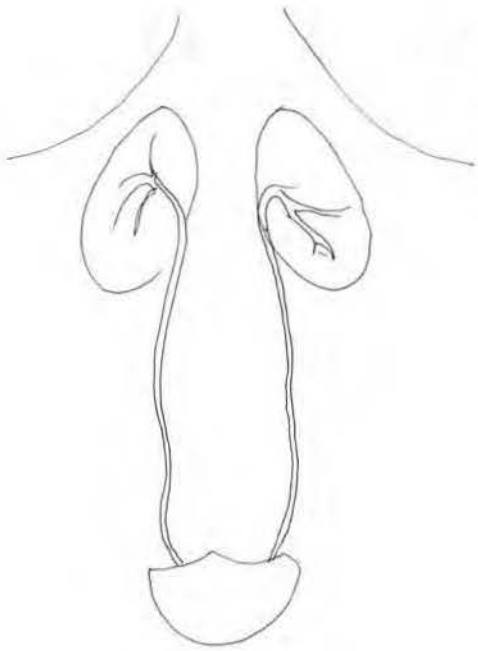

Fig 29.5
Normal 15 minutes "post release" KUB demonstrating the ureters.

7. Post-micturition full length radiograph to show the kidneys, ureter and fully or partially emptied bladder.

Indications

1. Suspected congenital anomalies
2. Persistent urinary tract infection
3. Renal colic
4. Haematuria
5. Renal trauma
6. Renal, ureteric or pelvic tumours

Contraindications

1. Renal failure. This is a relative contraindication as renal excretion of contrast is delayed.
2. Hypersensitivity or allergy to contrast agent

NEPHROGRAPHIC PATTERNS

Unilateral small smooth kidney (fig 29.6)

The kidney is similar in shape and outline to a normal one. However, it is more than 2 cm shorter in length compared to the normal contralateral kidney (table II). In renal artery stenosis, the collecting system is normal; while a dilated collecting system is seen in post-obstructive atrophy.

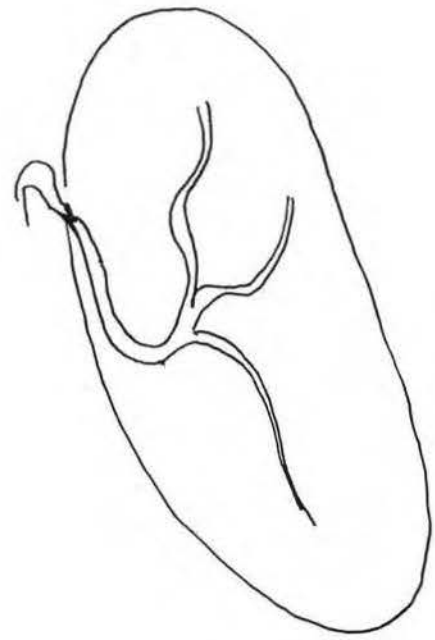

Fig 29.6 *Small unilateral smooth kidney in a patient with renal artery stenosis.*

Table II. *Causes of unilateral small smooth kidney*

Renal infarction
Radiation nephritis
Congenital hypoplasia
Post-obstructive atrophy
Post-inflammatory atrophy

Unilateral small irregular kidney (fig 29.7)

Focal scarring in a small kidney is due to reflux nephropathy and recurrent renal infection (table III). The upper pole is usually involved. Tuberculosis is a common

Fig 29.7 *Small irregular right kidney with focal calcification from renal tuberculosis.*

Table III. *Unilateral small irregular kidney*

Reflux nephropathy
Lobar infarction

cause of renal infection in many developing countries. In tuberculosis, focal calcification may be seen on the KUB film.

Bilateral small kidneys (fig 29.8)

Bilateral small smooth kidneys are usually due to post-obstructive atrophy, chronic glomerulonephritis, chronic papillary necrosis and chronic arteriosclerosis due to ageing (table IV). Bilateral small irregular kidneys are due to bilateral reflux nephropathy or chronic renal infection.

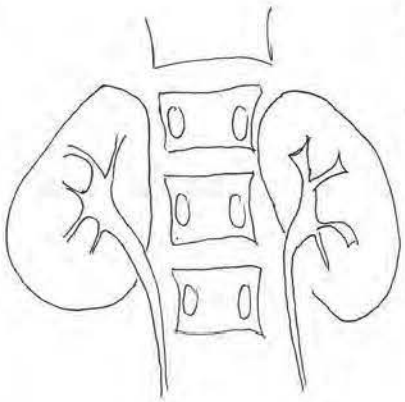

Fig 29.8
Small bilateral kidneys in a patient with chronic glomerulonephritis.

Table IV. *Bilateral small kidneys*

Chronic arteriosclerosis
Chronic renal infection
Chronic glomerulonephritis
Chronic papillary necrosis
Post obstructive atrophy
Hereditary nephropathies

Bilateral large smooth kidneys (fig 29.9)

The most common cause is bilateral hydronephrosis. Acute glomerulonephritis, acute tubular necrosis and AIDS focal glomerulonephritis are also important causes (table V).

Table V. *Bilateral large smooth kidneys*

Bilateral hydronephrosis
Acute glomerulonephritis
Acute tubular necrosis
Acute cortical necrosis
Infiltrative renal diseases
–leukaemia
–lymphoma
–amyloidosis
–multiple myeloma

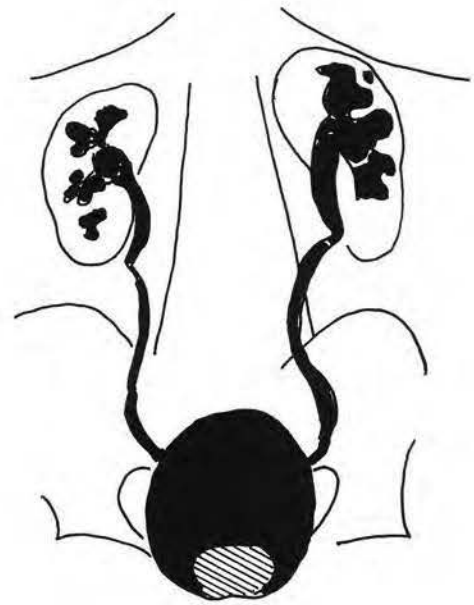

Fig 29.9 *Bilateral hydronephrosis from bladder outlet obstruction from prostate enlargement. Note prominent prostate impression on the bladder.*

Unilateral large smooth kidney (fig 29.10)

The commonest cause is unilateral hydronephrosis in which the renal pelvis and calyces are dilated. Acute pyelonephritis manifests as a swollen inlarged kidney with decreased opacification (table VI). Congenital anomalies may mimic a large smooth kidney, and conditions to consider include incomplete duplex kidney and or crossed-fused ectopia.

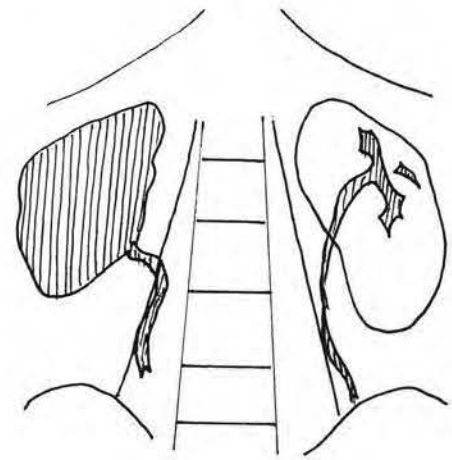

Fig 29.10 *Enlarged right kidney with a persistent nephrogram due to complete obstruction of the right ureter by a calculus.*

Table VI. *Unilateral large smooth kidney*

Hydronephrosis
Renal vein thrombosis
Acute pyelonephritis
Compensatory hypertrophy
Duplicated pelvicalyceal system

Renal masses (fig 29.11)

These may be divided into unilateral and bilateral renal masses (tables VII and VIII). Focal calcification is present in 15% of patients with hypernephroma. Tuberculosis may produce an inflammatory mass. A congenital cause of focal renal mass is obstruction of the upper moiety of a duplex kidney.

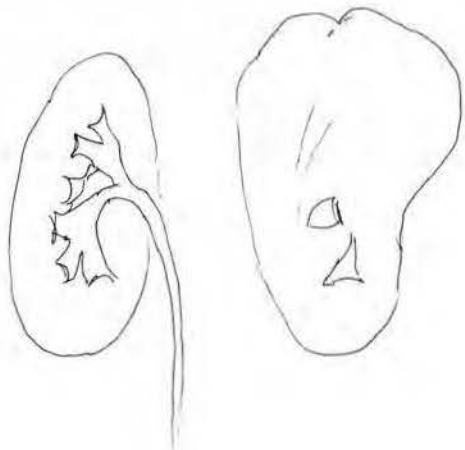

Fig 29.11 *Hypernephroma involving the upper pole of the left kidney.*

Table VII. *Unilateral renal mass*

Benign and malignant solid renal tumours
Simple cyst
Inflammatory mass (abscess)
Focal hydronephrosis

Table VIII. *Bilateral renal masses*

Polycystic kidney disease
Acquired cystic kidney disease
Lymphoma
Metastases

PELVICALYCEAL PATTERNS

Hydronephrosis

This refers to gross dilatation of the renal pelvis and calyces. A negative pyelogram is often detected in an enlarged kidney. Supplementary US, if available, is useful to demonstrate the dilated pelvicalyceal system, and whether the obstruction is proximal or distal. Causes of proximal obstruction include pelviureteric junction obstruction, calculus, tuberculosis and tumour. Distal obstruction may be due to schistosomiasis, calculus, and tumours such as carcinomas of the uterine cervix and bladder.

Ulcers (fig 29.12)

Ulcers are found in early tuberculosis and papillary necrosis.

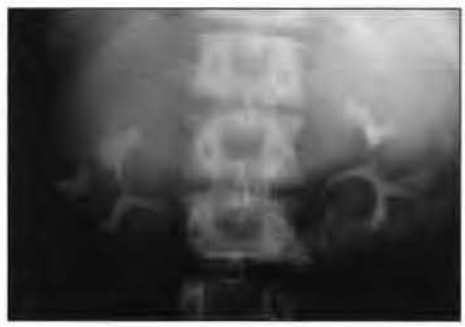

Fig 29.12 *Tuberculous pelvicalyceal ulceration.*

Clubbing (fig 29.13)

Clubbing is found in hydronephrosis where it is usually generalised and resembles "mickey mouse ears". Localised clubbing is found in reflux nephropathy or chronic pyelonephritis where there is associated focal cortical scarring, usually located at the upper pole.

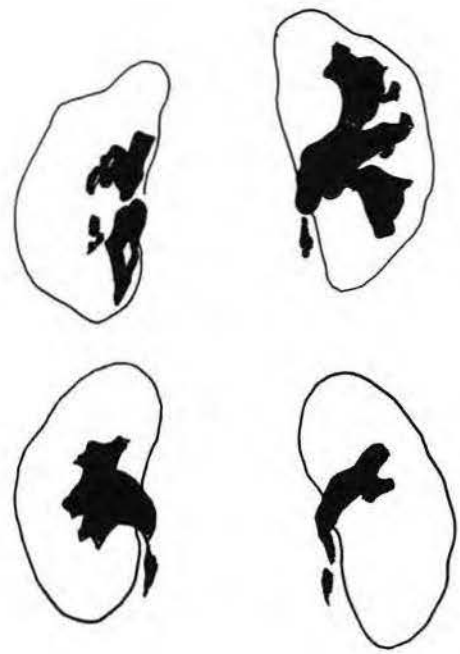

Fig 29.13 *Clubbed calyces of the right kidney following infection and pelvicalyceal calculi.*

Displacement (fig 29.14)

The pelvicalyceal system may be displaced by a mass lesion within the renal pelvis or by an adjacent mass.

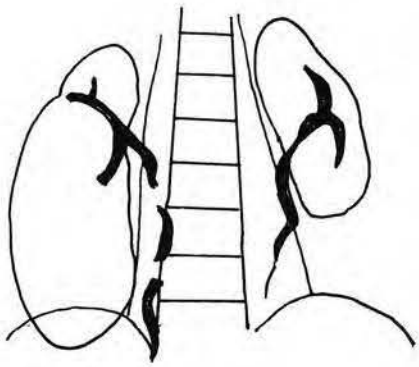

Fig 29.14
Displaced splayed right pelvicalyceal system from a large lower pole renal cyst.

Filling defects (fig 29.15)

In the differential diagnosis of a pelvicalyceal filling defect, lesions to consider include carcinoma, calculus and blood clot. Radio-opaque calculi are usually visible on the preliminary control KUB film. Some extrinsic impressions, such as those caused by vessels, may simulate the appearance of filling defects.

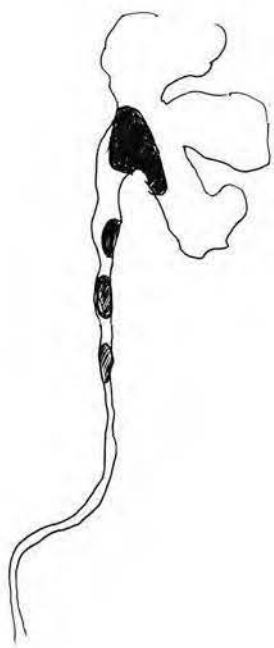

Fig 29.15
Filling defects in the pelvis and ureters from transitional cell carcinoma.

Ureter patterns (figs 29.16 & 29.17)

Ureteric obstruction may be due to intraluminal, mural, and extramural causes. The commonest intraluminal cause is calculus, with occasional causes being blood clot and sloughed papilla. Mural causes include tuberculosis, schistomiasis and ureterocoele.

Fig 29.16
Extensive multifocal narrowing of the ureters with "fish hooking" of the distal ureters from tuberculosis.

Fig 29.17
Dilated right ureter from a distal ureteric ureterocoele.

Extramural causes are usually due to pelvic tumours such as carcinoma of the uterine cervix. In acute obstruction, there is an increasingly dense nephrogram and delayed contrast opacification of the collecting system. The level of obstruction is best evaluated on delayed films taken at 60 or at 120 minutes intervals. The level of obstruction may give a clue to the cause. Displacement of the ureters is seen with retroperitoneal masses and aneurysms.

BLADDER PATTERNS

In a normal urinary bladder, a uterine impression on the bladder vertex may be seen. A small or contracted bladder may be seen in neurogenic bladder (fig 29.18), tuberculous cystitis and schistosomiasis. Prostatic enlargement may produce an elevated bladder base, superior bladder diverticula, trabeculation due to thickening of the bladder wall muscle, dilated ureters due to back pressure,and large post-micturition residue. Bladder filling defects may be due to calculus, blood clot, tumour and inflammatory polyp (fig 29.19).

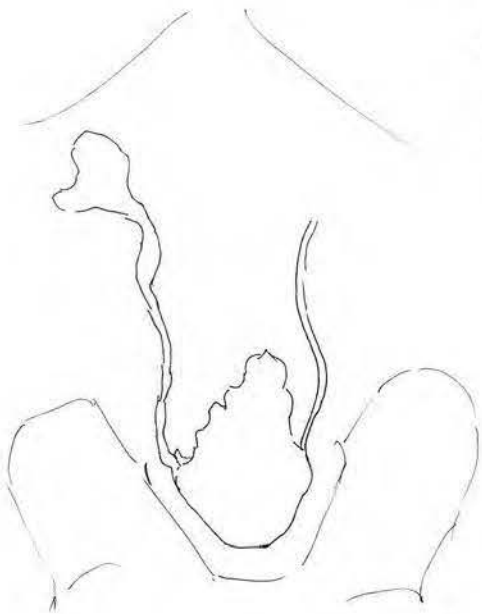

Fig 29.18
Triangular trabeculated small volume neurogenic bladder.

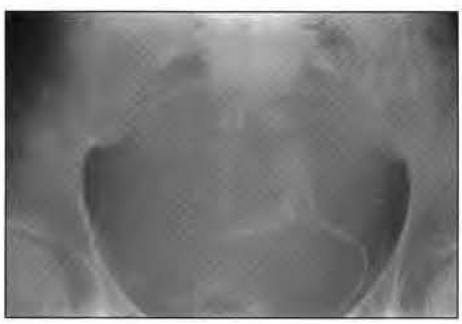

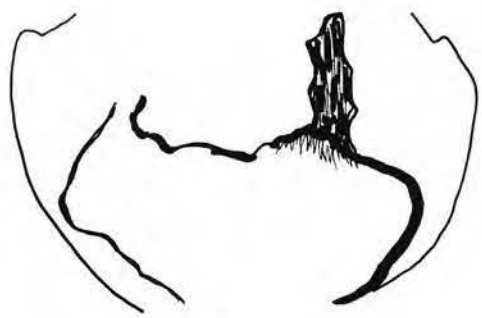

Fig 29.19a
Calcified bladder wall and left distal ureter from chronic schistosomiasis.

Fig 29.19b
Post micturition cystogram demonstrated multiple submucosal granulomas from Schistosoma haematobium (bilharziasis).

Renal ultrasonography

Technique

A 3.5 MHz transducer is generally used to scan the adult kidney. The liver and spleen act as acoustic windows for evaluation of the right kidney and left kidney, respectively. The kidneys are scanned in all planes. The patient should be in placed in the supine or decubitus position.

Indications

1. Renal mass.
2. Haematuria.
3. Flank pain.
4. Elevation of blood urea.
5. Poor or non-functioning kidney on IVU.
6. To guide biopsy and interventional techniques.

Normal anatomy (fig 29.20)

The normal kidney is easily recognised as an organ with a smooth outer contour surrounded by reflective fat. The normal renal cortical echogenicity is usually less than that of the liver and spleen. The renal medulla consists of hypoechoic triangular pyramids, separated by bands of intervening parenchyma that extend toward the renal sinus. These bands of intervening parenchyma, called "columns of Bertin", may be prominent and hence simulate a tumour. The renal sinus is composed of fibrous tissue, fat, lymphatic vessels, and renal vessels. It is seen as hyperechoic structures in the centre of the kidney. The normal ureter is not visualised on US. The bladder is seen as an ovoid fluid-filled structure in the longitudinal plane and rectangular in the transverse plane (fig 29.21). For accuate evaluation of the bladder, it should be adequately distended and the patient may need to drink additional water.

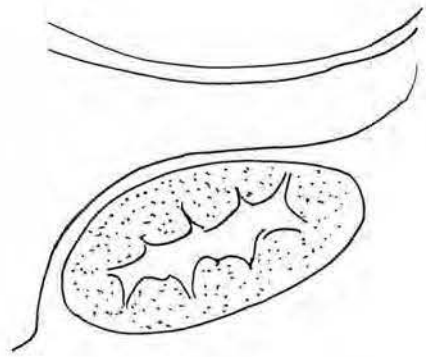

Fig 29.20 *Longitudinal ultrasound of the right kidney.*

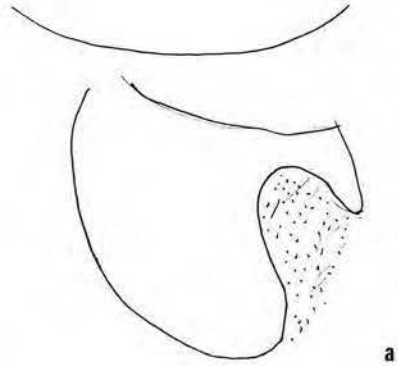

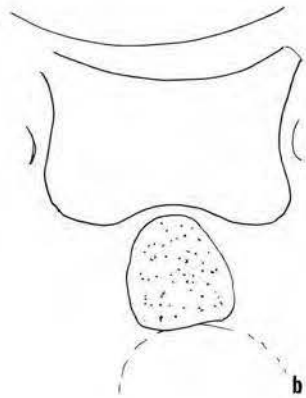

Fig 29.21a & 29.21b
Longitudinal and transverse ultrasounds of the full bladders of a 65 year old and 20 year old man. The prostate is enlarged in the longitudinal view and is normal in the transverse view.

US PATTERNS

Hydronephrosis (fig 29.22)

Obstruction of the urinary tract leads to dilatation of collecting system, which may be generalised or localised depending on the site of obstruction. The hyperechoic renal sinus is displaced around the dilated renal pelvis. In severe obstruction, there may be associated cortical thinning.

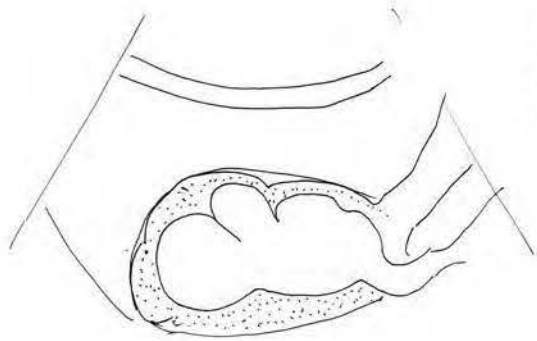

Fig 29.22
Marked hydronephrosis and hydroureter of the right kidney.

Pitfalls

1. An overdistended urinary bladder can produce dilatation of a normal pelvicalyceal system. One should make sure that the bladder is empty before making a diagnosis of hydronephrosis.

2. A prominent extrarenal pelvis, a parapelvic cyst, a renal artery aneurysm, reflux and congenital megacalyces may mimic hydronephrosis.

Renal stone (fig 29.23)

A stone is seen as a hyperechogenic focus with acoustic shadowing.

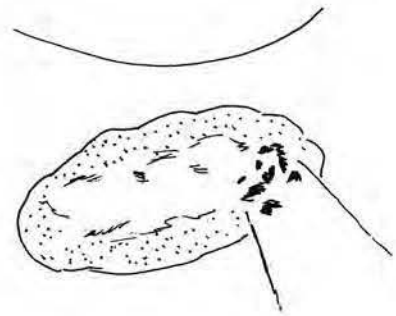

Fig 29.23 *Longitudinal ultrasound demonstrates echogenic calculi in the lower pole of the kidney causing an acoustic shadow posteriorly from the reflected sound waves.*

Pyonephrosis

Hydronephrotic fluid that is either infected or replaced with pus is known as pyonephrosis. The pus-filled renal pelvis is seen as fluid with various degrees of reflectivity within the dilated pelvicalyceal system. Debris may layer in the dependant portion and appears as a fluid-fluid level.

Renal mass (fig 29.24)

US is the investigation of choice for evaluation of a renal mass detected on IVU. It is highly sensitive for differentiating cystic from solid lesions, and has a reported accuracy rate of as high as 97%.

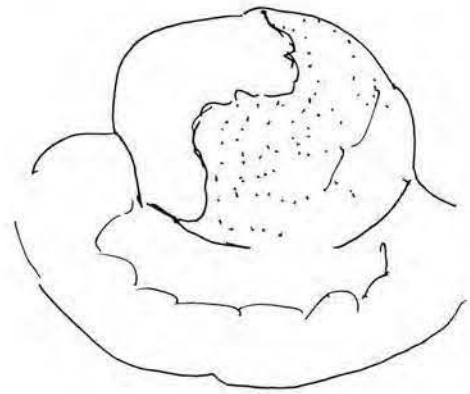

Fig 29.24 *A longitudinal ultrasound of the kidney demonstrates an inhomogeneous mass in the mid pole region which was confirmed to be a renal angiomyolipoma.*

Simple renal cyst (fig 29.25)

Simple renal cysts are common in elderly patients. The US features of cysts are similar to cysts elsewhere in the body. They are typically well-defined, have a smooth outline, are round or oval in shape, anechoic and produces acoustic enhancement. They may be single or multiple.

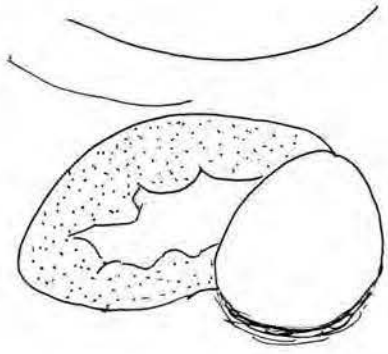

Fig 29.25
Longitudinal ultrasound of the kidney demonstrates a simple cyst of the lower pole.

Polycystic disease (fig 29.26)

Adult polycystic disease is transmitted as an autosomal dominant trait. There are multiple cysts of various size scattered throughout the renal parenchyma. IVU shows enlarged kidneys, round radiolucent nephrogram defects and irregular distorted collecting systems. On US the kidneys are enlarged with multiple cysts.

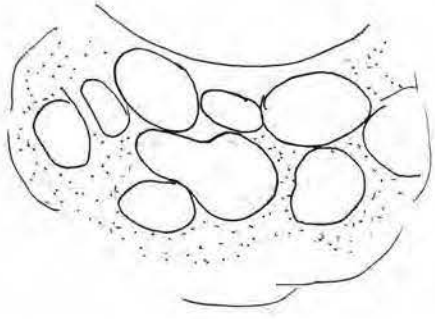

Fig 29.26
Longitudinal ultrasound of the kidney demonstrates multiple cysts replacing the parenchyma in a patient with adult polycystic disease.

Renal abscess

An abscess appears on US as a focal mass with varying internal echoes. An early abscess is seen as a slightly hypoechoic area. Eventually, the abscess becomes markedly hypoechoic to anechoic, with variable acoustic shadows.

Renal angiomyolipoma

Angiomyolipoma (AML) is a benign tumour composed of varying amount of fat, muscle and blood vessel. It may be seen on the KUB film if it is large and contains a significant amount of fat. On US, it is seen as a well-defined hyperechoic mass.

Malignant renal tumour (fig 29.24)

Hypernephroma or renal adenocarcinoma is the most common malignant tumour of the adult kidney. The characteristic US features of the tumour are based on its solid nature. The echogenicity of the tumour may vary from being hyperechoic to anechoic, in comparison to the renal parenchyma.

Lymphoma

Renal involvement mainly occurs with non-Hodgkin lymphoma. The tumours usually appear as solitary or multiple hypoechoic masses with poor sound transmission.

Increased renal parenchymal echogenicity (fig 29.27)

Hyperechoic renal parenchyma is due to chronic renal processes such as chronic glomerulonephritis and end-stage renal diseases from any cause. The kidney is usually small and may be almost impossible to visualise.

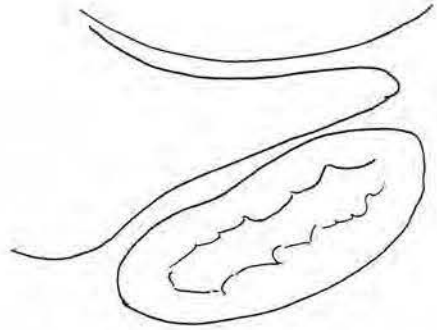

Fig 29.27 *Echogenic kidney in a patient with acute tubular necrosis. Note loss of differentiation between the cortex and echogenic fat around the pelvicalyceal system.*

Bladder ultrasonography

Technique

The patient is scanned in the supine position using a 3.5 MHz transducer. A full bladder is necessary for the study.

Indications

1. Determination of residual urine volume
2. Detection of bladder tumour and intravesical masses
3. Detection of bladder wall lesions

US PATTERNS

Normal pattern

The urinary bladder lies posterior to the pubic symphysis when empty and high in the pelvic cavity when full. Its size and shape varies with the amount of filling by urine. The urinary bladder appears round to nearly square in shape on the transverse scan, and round to oval shape on the longitudinal scan. The mucosal lining is smooth and stretched when it is full (fig 29.21).

Bladder tumour

Ninety-five percent of bladder tumours are of urothelial origin. Transitional cell carcinoma (TCC) is the most common type of malignant bladder tumour. Painless haematuria is the most common presenting symptom. The tumour appears as a smooth or irregular homogeneous or inhomogeneous mass (fig 29.28). The mass is adherent to the wall. Invasion through the bladder wall muscle may be seen if there is interruption of the sharply-defined echogenic bladder wall. However staging of bladder tumours is more accurately achieved by CT or magnetic resonance imaging. The US appearance of TCC is not specific and must be differentiated from benign papilloma, adherent blood

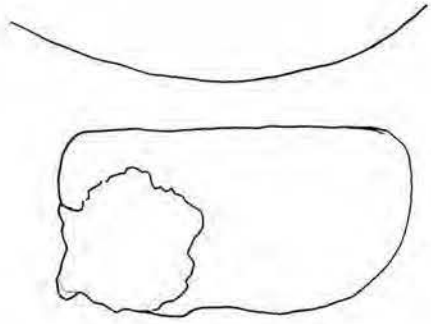

Fig 29.28 *Transverse ultrasound of the bladder demonstrates a transitional carcinoma invadind the right bladder wall.*

clot, adherent stone, invasive carcinoma of the prostate, cystitis and wall thickening secondary to chronic bladder outlet obstruction.

Diverticulum

Bladder diverticula are sac-like protrusions from the bladder wall. They are urine-filled and most are acquired in association with long-standing bladder outlet obstruction.

Cystitis

Cystitis occurs more commonly in female than in male patients. Acute cystitis is usually caused by gram negative organisms such as E. Coli, Proteus and klebsiella and most of the cases show no abnormality on US. However, with severe cystitis the bladder wall becomes thickened, either focally or diffusely, and may mimic a tumour. The US appearances of cystitis are similar whether the cause is infection, irradiation or secondary to cyclophosphamide therapy.

Schistosoma haematobium causes cystitis and ureteritis. It is characterised by granulomas, superficial mucosal ulcerations and formation of polypoid masses. With chronicity, the bladder becomes fibrosed with reduced capacity. There is an increased risk of development of bladder carcinoma.

Micturating cystography (MCU)

MCU is performed by filling the bladder with contrast agent introduced via a urethral catheter. It is important to have fluoroscopy available to perform this study if possible. 250 ml of contrast usually used in an adult patient, or until the patient feels the need to void urgently. A preliminary film is always recommended for detection of calcifications or calculi. Following filling of the bladder to capacity, spot radiographs in the anteroposterior and lateral projections are taken (fig 29.29). MCU is useful for detection of vesicoureteric reflux and bladder rupture. To detect reflux, the patient should micturate during fluoroscopy as reflux may be intermittent (fig 29.30). In suspected

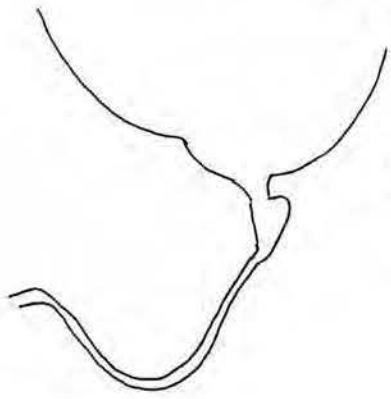

Fig 29.29a *Micturating cystourethrogram in a young male demonstrates a normal descending urethrogram.*

29.29b *normal ascending urethrogram in the same patient.*

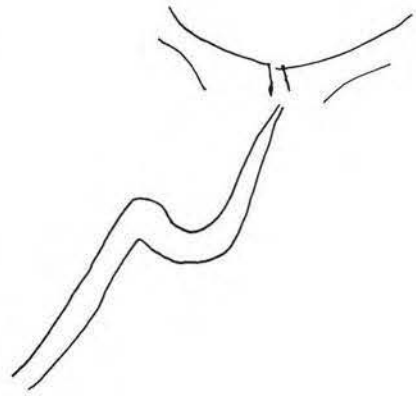

Fig 29.30a *MCUG in an infant male demonstrates urethral valves in the proximal urethra causing proximal dilatation. B-there is severe reflux up the right ureter to the right renal pelvis.*

a

b

Fig 29.31 *Cystogram demonstrates extraperitoneal rupture of the bladder with extravasation of contrast at the bladder base. Normal cystogram for comparison.*

bladder trauma, fluoroscopy should be performed and early spot radiographs should be obtained after instillation of 50 ml of contrast in order to detect early extravasation (fig 29.31).

Cystogram patterns

- **Normal appearance**: note uterine impression on the vertex of the bladder.
- **Small bladder**—seen in neurogenic bladder, tuberculous cystitis, schistosomiasis
- **Large bladder** with irregular outline-neurogenic bladder
- **Prostate enlargement** causes elevated bladder base with a convex superior border, bladder diverticula, trabeculation (due to thickening of the bladder muscle), dilated ureters from back pressure, large post micturition residue.
- **Filling defects** are due to calculi, blood clot, tumour, inflammatory polyps

Urethrography

The urethra may be visualised as part of a MCU or by ascending urethrography. The main indications are trauma and stricture following gonococcus urethritis. Urethritis produces strictures in the bulbar urethra while traumatic strictures are found in the membranous urethra (fig 29.32). In infants, congenital valves can be seen during MCU, particularly on the lateral projection (fig 29.30).

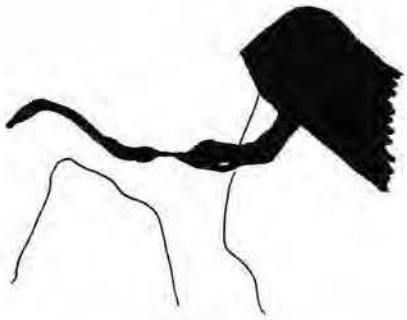

Fig 29.32 *Ascending urethrogram demonstrates a gonococcal stricture of the proximal bulbar urethra.*

LEARNING POINTS: URORADIOLOGY

- Always remember to ask for a control KUB before an IVU or cystogram study to detect radiopaque calculi.
- Congenital anomalies of the kidneys and ureters are common.
- Adult kidney size is from 12-14 cm in length.
- Kidneys are considered small if less than 9 cm in length in adults.
- More than 2 cm difference in longitudinal height between both kidneys is significant.
- Always consider renovascular disease if one kidney is 2 cm smaller than the other and the contour is smooth.
- A small kidney with an irregular border is usually due to reflux nephropathy or tuberculosis.
- Bilateral small kidneys are due to chronic renal disease such as chronic glomerulonephritis, papillary necrosis or chronic arteriosclerotic disease.
- Commonest cause for a large unilateral kidney is hydronephrosis or acute pyelonephritis. Ultrasound will confirm hydronephrosis.
- Common causes of renal "masses" are renal cysts, hypernephromas, renal abscess or inflammatory masses.
- Common causes of ureteric obstruction are-calculi, tuberculosis, pelvic tumours especially carcinoma of the cervix.
- A small contracted bladder is seen in neurogenic lesions, tuberculosis and schistosomiasis.
- Bladder filling defects are due to calculi, blood clot, tumour or inflammatory polyps.
- Commonest cause of a urethral stricture is gonococcocal urethritis and pelvic trauma.

Acknowledgements

Thank you to Leonie Munro for proof reading and Marianne Singh for organizing the manuscript.

This book was prepared by a group of international experts in diagnostic imaging who work specifically with problems encountered in small and mid-size hospitals and clinics with limited technical and human resources. It is part of a series of WHO documents being developed under the umbrella of the Global Steering Group for Education and Training in Diagnostic Imaging.

The Global Steering Group for Education and Training in Diagnostic Imaging was initiated and established by the World Health Organization (WHO) in Geneva 1999. Among the members are the major international and regional scientific societies involved in diagnostic imaging. The Group is co-chaired by WHO and the International Commission for Radiological Education (ICRE) of the International Society of Radiology (ISR).

The main objective of the Global Steering Group for Education and Training in Diagnostic Imaging is to assist countries in improving diagnostic imaging services as integrated parts of their national health systems by:

- identifying needs for education and training
- coordinating existing and planned educational activities
- suggesting, advocating, producing, and implementing specific educational material and activities according to local needs
- evaluating outcome of such activities.

The book is written primarily for radiographers and radiological technologists, but may also prove valuable for other medical professionals referring patients to diagnostic imaging and eventually also performing and interpreting X-ray examinations. It focuses on how to perform such examinations, why they are needed, and how to judge and interpret some of the most common medical conditions. The book may prove valuable both for self study and when looking for specific information. It does, however, not substitute standard textbooks in radiology, and should not be regarded as such.

For further information, please contact:

Team of Diagnostic Imaging and Laboratory Technology
World Health Organization
20 Avenue Appia
CH-1211 Geneva 27
Switzerland

Fax: +41 22 791 4836
e-mail: ingolfsdottirg@who.int

ISBN 92-4-154632-8
9 789241 546324